UNIVERSIDAD DE EXTREMADURA

TESIS DOCTORAL

ANÁLISIS BIOMECÁNICO Y CARACTERIZACIÓN DE LA INTERVENCIÓN MUSCULAR Y LA CALIDAD DE CONTROL MOTOR EN EL CONTEXTO DE LA MANIPULACIÓN MANUAL DE CARGAS

ANDREAS SKIADOPOULOS

DPTO. DE DIDÁCTICA DE LA EXPRESIÓN MUSICAL, PLÁSTICA Y CORPORAL

Conformidad de los directores:

Fdo: Kostas Gianikellis

Fdo: Marcos Gutiérrez Dávila

2015

To my daughter

“muscle moves the world”
Ragnar Granit

Resumen

La Agencia Europea de Seguridad y Salud en el Trabajo define el levantamiento manual de cargas como uno de los factores de riesgo más importantes para la aparición de patologías músculo-esqueléticas en la zona dorsolumbar. Las trastornos dorsolumbares de origen laboral surgen como consecuencia de la exposición repetitiva de las estructuras, elementos y tejidos de la columna vertebral a las cargas mecánicas que se desarrollan durante la ejecución de tareas laborales. Las cargas mecánicas se desarrollan principalmente por la (co)activación de los músculos del tronco en respuesta a la carga externa. El nivel de riesgo que suponen las cargas mecánicas depende no solo de la magnitud de la activación muscular sino también de la coordinación de los músculos que intervienen. Actualmente, los trabajos científicos se centran en cómo el diseño de trabajo influye en la magnitud de la intervención múscular siendo una método indirecto de medir las cargas mecánicas desarrolladas en la columna vertebral. Sin embargo, no existen trabajos científicos sobre la influencia del diseño del trabajo en la coordinación muscular. Cualquier error en la coordinación muscular aumenta el riesgo de padecer lesiones y trastornos músculo-esqueléticos. El gran número de músculos que el sistema motor debe controlar aumenta la dificultad en la coordinación. En este sentido, se ha propuesto que el sistema motor forma sinergias musculares para poder controlar los excesivos grados de libertad presentes en el sistema. En este sentido, el presente trabajo tiene como objetivo investigar la influencia de la intervención ergonomica basada en el protocolo NIOSH en la coordinación de los numerosos grados de libertad—i.e., la coordinación de los músculos del tronco. Para poder caracterizar el nivel de riesgo que comporta la manipulación manual de cargas para el usuario en la elevación, el National Institute of Occupational Safety and Health ha desarrollado un protocolo exclusivo para estas tareas, que se conoce como protocolo NIOSH. El protocolo se basa en una combinación de criterios y permite establecer el peso límite recomendado y el índice de levantamiento para caracterizar el nivel de riesgo que supone una tarea específica de manipulación manual de cargas. Los resultados confirman que los músculos del tronco forman grupos musculares (sinergias musculares) cuya coordinación estabiliza variables mecánicas importantes para el proceso de levantamiento de cargas dando lugar a la técnica concreta e individual de manipulación manual de cargas como respuesta. La manipulación de los parametros del protocolo NIOSH influye también en el indice de la sinergia muscular. Se propone que la intevención ergonomica en la manipulación manual de cargas basada en el protocolo NIOSH debe incorporar el indice de la sinergia muscular.

Contents

List of Figures

List of Tables

List of Abbreviations and Nomenclature

Abbreviations

3DSSPP University of Michigan 3D Static Strength Prediction Program

ACGIH TLV American Conference of Governmental Industrial Hygienists Lifting Threshold Limit Values

ANOVA Analysis of Variance

BMI body mass index

CI 95% confidence interval

CNS central nervous system

COG$_B$ box's center of gravity

COM centre of mass

COP centre of pressure

COP$_{AP}$ centre of pressure in anterior-posterior direction

COP$_{ML}$ centre of pressure in medial-lateral direction

DALY disability adjusted life year

DOE design of experiment

DOF degrees-of-freedom

EFA Exploratory Factor Analysis

EMG Electromyography

EU European Union

EU-OSHA European Agency for Safety and Health at Work

IASP International Association for the Study of Pain

ILO International Labour Organization

GBD Global Burden Disease

GHR Global Health Risk

GRF ground reaction force

GUM Guide to the Expression of Uncertainty of Measurement

ICF International Classification of Functioning, Disability, and Health

iLBP idiopathic low back pain

iLMM industrial Lumbar Motion Monitor

K1 Kaiser's criterion

L5/S1 lumbosacral intervertebral disk

LBD low back disorders

LBP low back pain

M-mode muscle-modes

M_1-mode first muscle-mode

M_2-mode second muscle-mode

M_3-mode third muscle-mode

MMH manual material handling

MSA measurement system analysis

MSD musculoskeletal disorders

NIOSH U.S. National Institute for Occupational Safety and Health

NRC-IOM U.S. National Research Council (NRC) and the Institute of Medicine (IOM)

OSHA U.S. Occupational Safety and Health Administration

OSS video-based optoelectronic stereophotogrammetric system

OSU/BWC Ohio State University/Bureau of Workers' Compensation

PA Horn's Parallel Analysis

PC Principal Component

PCA Principal Components Analysis

PV performance variable

QC quality control

R&R Gage Repeatability and Reproducibility

$U_{95\%}$ expanded measurement uncertainty

UCM uncontrolled manifold

WHO World Health Organization

WRLBD work-related low back disorders

WRLBP work-related low back pain

WRMSD work-related musculoskeletal disorders

WRULD work-related upper-limb disorders

VAF variance accounted for

Nomenclature

ρ radial displacement

z vertical displacement

θ transversal displacement

a_ρ radial acceleration

a_z vertical acceleration

a_θ transversal acceleration

v_ρ radial velocity

v_z vertical velocity

v_θ transversal velocity

$\dot{\omega}_{flex}$ flexion-extension joint angular acceleration

$\dot{\omega}_{tilt}$ lateral bending joint angular acceleration

$\dot{\omega}_{axial}$ axial rotation joint angular acceleration

θ_{flex} flexion-extension joint angle

θ_{tilt}	lateral bending joint angle
θ_{axial}	axial rotation joint angle
ω_{flex}	flexion-extension joint angular velocity
ω_{tilt}	lateral bending joint angular velocity
ω_{axial}	axial rotation joint angular velocity

1

Background and Literature Review

1.1. Background

Manual material lifting and lowering tasks are the primarily risk factors for development of work-related low back disorders (WRLBD) (Op de Beek and Hermans, 2000). WRLBD causation is primarily based on the mechanical disruption of spinal support structures, where the integrity of the connective tissue is violated and its mechanical order perturbed due to spine loading (Adams and Roughley, 2006; Marras, 2008). Since spine loading is mainly imposed by trunk muscles (co)activity in response to external loading, the magnitude of the myoelectric activity of trunk musculature during lifting and lowering tasks has been investigated extensively. However, there is lack of investigation regarding the ability of the "neural controller" to coordinate the many trunk muscles necessary to stabilize the spine during lifting or lowering tasks and whether this ability is stressed by work-design factors. Previous studies have shown that the constraints imposed by work-design factors influence not only the (I) magnitude of kinematic, kinetic, and myoelectric variability among participants who perform identical lifting tasks in terms of load weight and origin-destination state in both realistic condition and in control laboratory environments (isokinetic, isometric, isoinertial) (Granata, Marras, and Davis, 1999; Mirka and Marras, 1993; Mirka and Baker, 1996), but also (II) their spatiotemporal interjoint coordination and local dynamic stability of their coordinative movements (Burgess-Limerick et al., 2001; Graham and Brown, 2012; Graham, Sadler, and Stevenson, 2012; Graham et al., 2011; Scholz, 1993a,b). Regarding the former, variability was associated with a high probability of identifying a risky lifting task healthy, since ergonomics assessment tools are based on mean values; regarding the latter, variability was associated with an increased risk for development of low back disorders (LBD) due to trunk accelerations following sudden biomechanical and neuromuscular perturbations.

LBD are associated with accelerations that undergoes the spine as a result of trunk muscles activity in response to the loading or in response of postural reactions to balance disturbances (Butler et al., 1993; Commissaris and Toussaint, 1997; De Looze et al., 2000; Van der Burg, Kingma, and Van Dieën, 2003, 2004; Van der Burg and Van Dieën, 2001b; Van der Burg, Van Dieën, and Toussaint, 2000; Van Dieën and Looze, 1999). Previous studies postulated that certain combinations of postural perturbations and voluntary movements during lifting tasks could require different

functions of the same muscle or muscle group simultaneously. If muscle activations patterns that underlying the switching from one task demand to the other are different, this could create a disruption of the ongoing task, and such conflict may lead to motor errors, increasing postural instability and subsequent risk for development of LBD (Ebenbichler et al., 2001; Kollmitzer et al., 2002; Oddsson et al., 1999).

1.2. Low Back Anatomy

The trunk skeletal system is comprised of the pelvis, the vertebral column and the rib cage. The vertebral column is composed of 24 vertebrae, the sacrum and the coccyx. Vertebrae are connected to form the vertebral column by articulations that are formed by two adjacent vertebrae, which are interconnected by ligaments and are separated by the intervertebral disk. The intervertebral articulation is formed of two joints, one between vertebral bodies and the zygapophyseal joint. The nature of the intervertebral disk allows each vertebra to move in 6 degrees-of-freedom (DOF), which take place by compressing and stretching the disk. The zygapophyseal joints guide spine movement in particular planes and prevent movements in other planes. The movement of the vertebrae is coupled, and any spine movement combines the concurrent translation and rotation of the vertebrae, that gives to the whole spine a great range of motion. Rib cage comprises the 12 thoracic vertebrae with the corresponding ribs and the sternum. Rib cage provides attachment points for many of the muscles supporting the back. The sacrum articulates inferiorly with the coccyx, laterally with the two ossa coxae (hip bones) and together these bones form the pelvis (McKinley and O'loughlin, 2006).

The muscles of the low back can be divided into local and global systems according to their architecture (Figs. 1.1 and 1.2). Local system comprises the deep muscles that act on lumbar spine and deep portions of some muscles that have their attachment onto the lumbar vertebrae, either the insertion or origin, or both. Global system comprises the large, superficial muscles that tranfer load directly between the thorasic cage and the pelvis (Bergmark, 1989). The muscles of the local system contribute to spinal mechanical stability by controlling muscle stiffness and spine curvature (intersegmental motion). However, local muscles cannot control spinal orientation and thus local system alone cannot stabilizes the spine system effectivelly (Hodges, 2004). The global muscle system contribute to trunk movements and its mechanical role is to balance external loads applied to trunk in order the residual force transfered to the lumbar spine can be handled by the local system. Although global muscles can attenuate the force applied on the lumbar spine and control trunk orientation, they cannot fine-tune control intervertebral motion (Hodges, 2004). Activation patterns of local system muscles are mostly determined by the posture of the lumbar spine and the magnitude of the external load, whereas activation patterns of global system muscles are also dependent on the distribution of the external load (Bergmark, 1989). Regarding WRLBD, global muscles control intervertebral motion only by augmented activations, resulting in co-contractions, higher spine loads and reduced normal movement of the spine (Hodges, 2004). Therefore, the activity of the global muscles was used as a measurable compensation for poor passive or active (by local muscles) segmental support (Cholewicki, Panjabi, and Khachatryan, 1997).

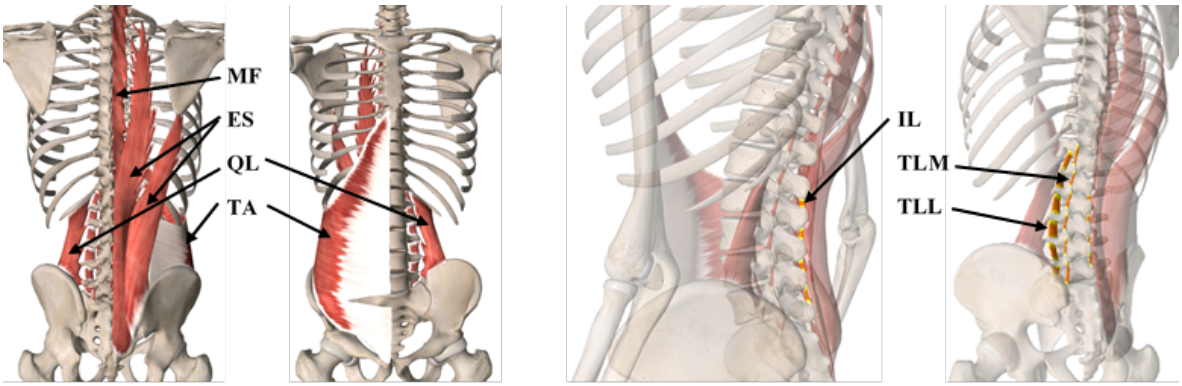

Figure 1.1 The local muscle system comprises muscles that their origin or insertion is attached to the vertebrae except of psoas (TLL: intertransversarii lumborum lateralis, TLM: intertransversarii lumborum medialis, IL: interspinalis lumborum, MF: multifidus, ES: erector spinae (lumbar part of longissimus thoracis, lumbar part of iliocostalis), QL: medial fibers of quadratus lumborum, TA: tranversus abdominis) (Ess. Anatomy 3, 3D4Medical).

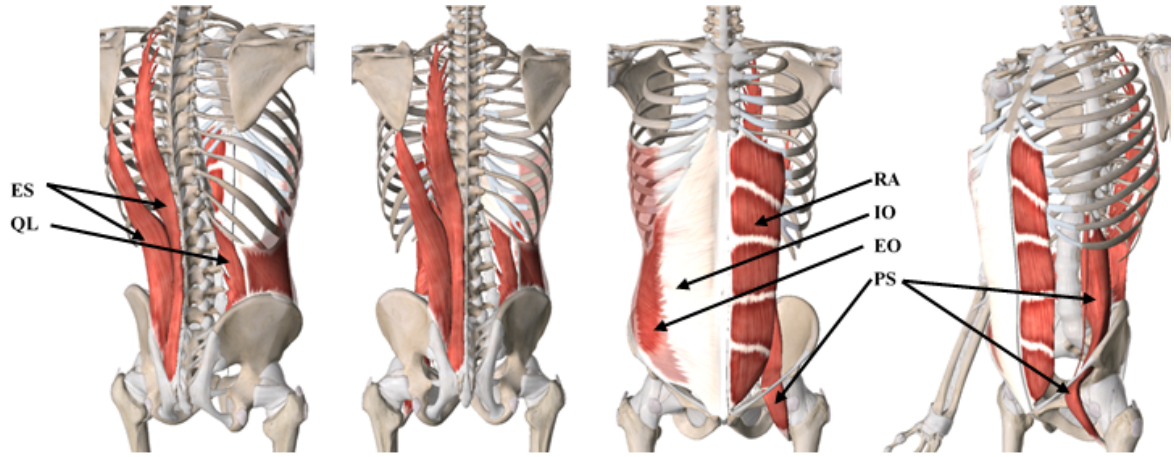

Figure 1.2 The global muscle system comprises the muscles that are not attached to the vertebrae with the addition of psoas (ES: erector spinae (thoracic part of longissimus thoracis and thoracic part of iliocastalis lumborum), QL: lateral fibers of quadratus lumborum, EO: external oblique, IO: internal oblique, RA: rectus abdominis) (Ess. Anatomy 3, 3D4Medical).

1.3. Definitions of Work-Related Musculoskeletal Disorders

The term musculoskeletal disorders (MSD) is not a diagnosis, but stands as an umbrella term covering a broad range of inflammatory and degenerative disorders of the locomotor system that develop as a result of repetitive movements, awkward postures, sustained force and other risk factors (Yassi, 1997). The term work-related musculoskeletal disorders (WRMSD), by definition, are a subset of MSD that arise out of occupational exposures (Forde, Punnett, and Wegnar, 2002). They affect both women and men and all sectors of occupational activity and are a major financial cost to businesses and society at large (Parent-Thirion et al., 2007).

The U.S. National Institute for Occupational Safety and Health (NIOSH) (1997), defines MSD as the “disorders of the muscles, nerves, tendons, ligaments, joints, cartilage, or spinal discs that are not typically the result of any instantaneous or acute event but reflect a more gradual or

chronic development. They are disorders diagnosed by a medical history, physical examination, or other medical tests that can range in severity from mild and intermittent to debilitating and chronic, and with several distinct features as well as disorders defined primarily by the location of the pain". The definitions of others governmental agencies and organizations mirror the definition proposed by NIOSH, however, with some changes. U.S. Occupational Safety and Health Administration (OSHA) (2010), dissociates MSD from the motor vehicle accidents or other similar accidents and cites also some examples. The European Agency for Safety and Health at Work (EU-OSHA) adds to the affected tissues the vascular system (Schneider and Irastorza, 2010). World Health Organization (WHO) mirrors the above definitions (Luttmann et al., 2003). The NIOSH and OSHA, by excluding explicitly from their definitions the disorders caused by certain instantaneous or acute events and by incorporating specific examples, have added substantial clarity as to what disorders are not to be denoted as MSD.

Even though WRMSD were described systematically for the first time more than two centuries ago by B. Ramazzini (Franco, 1999), it does not exist yet a single definition about them on the scientific literature. This is because its definition largely depends upon the organizations, authoritative agencies and national institutes from which it has been promulgated (WHO, 1985). Therefore, different definitions have been used and proposed. According to the definition used by EU-OSHA, WRMSD are MSD that are caused or aggravated primarily by the performance of work and by the effects of the immediate environment where the work is carried out. Most of them are cumulative disorders, resulting from repeated exposures to high – or low – intensity loads over a long period of time. The symptoms may vary from discomfort and pain to decreased body function and disability (Podniece et al., 2007, 2008). Definitions used by others authorities mirror that of EU-OSHA (ANSI, 2007; NIOSH, 1997; Swedish Work Environment Authority, 1998).

Therefore, by definition, WRMSD are an heterogenous group of MSD, which are supposed to be caused, accelerated, exacerbated or aggravated by exposure to ergonomic physical, physiological and psychosocial risk factors, and their occupational exposure profile depends on which organ or tissue level the underlying pathophysiological mechanism acts (Barbe and Barr, 2006; Forde, Punnett, and Wegnar, 2002; Hagberg et al., 1995). In contrast to occupational diseases, where there is a direct exposure-response relationship between hazard and disease (e.g., asbestos → asbestosis), WRMSD do not involve always an objective pathologic condition (WHO, 1985). On one hand, there are WRMSD for which a diagnosis can be deduced from specific symptoms and where work related exposures are coherent with the development of the disorder (e.g., carpal tunnel syndrome) and on the other hand, there are work related symptoms for which it is impossible to identify reliably the pathology (e.g., iLBP) (Balagué et al., 2007; Boocock et al., 2009; Hagberg et al., 1995; Op de Beek and Hermans, 2000; Van Dieën and Van der Beek, 2009; Visser and Van Dieën, 2006).

Frequently, others synonymous terms have also been used internationally to describe WRMSD or a group of them: work-related upper-limb disorders (WRULD), cumulative trauma disorders (mostly in U.S.), repetitive motion injuries, occupational cervicobrachial diseases (mostly in Japan and Sweden), repetitive strain injuries (mostly in Australia, U.K. and Canada), occupational overuse syndromes (mostly in Australia), occupational overexertion syndromes, activity related soft tissue

disorders, complaints of the arm, neck and/or shoulder, occupational cervico-brachial disorders, upper extremity disorders, upper limb disorders, work-related upper extremity disorders, MSD and ergonomic injuries (Boocock et al., 2009; Hagberg et al., 1995; OSHA, 2010; Yassi, 1997). Nowadays the term that is used commonly worldwide is WRMSD because it precludes the use of words that are related with possible causations (repetition, cumulative, injury, etc) that may or may not be the real cause of a particular disorder (Hagberg et al., 1995).

1.4. Extent of Work-Related Low Back Disorders

1.4.1. Prevalence

The term LBD cover both low back pain (LBP) and low back injuries (Op de Beek and Hermans, 2000), because low back disorders (LBD) almost always lead to LBP (Bogduk, 2005; McGill, 2007). However, both terms have been used interchangeably. Sometimes, despite of being a symptom, the term LBP was used as a diagnosis instead (Negrini et al., 2008).

Despite the difficulty to make direct comparisons between epidemiologic studies with different methodological designs that used different case definitions of MSD or LBP, the scientific literature is rather convinced in supporting that MSD, and primarily LBP, are very prevalent among the general population and moreover with a rising tendency. The available extrapolated data about the magnitude of MSD on the general population comes primarily from European Union (EU), North America and Scandinavian countries and mainly are based on individual self-report in surveys. The overwhelming thrust of the data revealed that MSD and especially LBP, are very prevalent among the population of the western industrialized countries and constitute a serious health problem with great socioeconomic impact (NRC-IOM, 2001; Shekelle, 1997). The U.S. National Ambulatory Medical Care Survey on 1989 ranked MSD second after respiratory conditions as the most common reason for seeking health care (NRC-IOM, 2001). The prevalence of impairment from MSD for the entire U.S. population was estimated at 15% on 1988, and at 13.9% on 1995, with an estimation of 18.4% or 59.4 million people by the year 2020 due to changes in the demographics of U.S. society and the workforce (Lawrence et al., 1998; Praemer, Furner, and Rice, 1999) (cited in NRC-IOM, 2001).

LBP has been reported as the most prevalent and costly MSD in many studies (Burton, 2005; Krismer and Van Tulder, 2007; Negrini et al., 2008; NRC-IOM, 2001; Praemer, Furner, and Rice, 1999; Shekelle, 1997). Hoy et al. (2012), undertook a systematic review and meta-analysis on 165 cross-sectional studies published between 1980-2009 to assess the global prevalence of LBP. The results of their study revealed that the global prevalence of LBP increased very slightly over the past 3 decades and it was most prevalent among females and persons ages 40-80 years. Most epidemiological studies on LBP are prevalence studies because is difficult to estimate the incidence of LBP due to its cumulative origin (Hoy et al., 2010). The point prevalence for LBP in the adult population in the industrialized countries ranges from 10% to over 50%, the 1-month prevalence from 19% to 43%, the annual prevalence for any LBP is 53%; for frequently or persisted LBP ranges from 10% to 18%; for herniated disc diagnosed by a physician is 2.1 %, and the lifetime prevalence for any LBP ranges from 14% up to 90%, while for frequently or persisted

pain is 14% (Nachemson, 2004; NRC-IOM, 2001; Schneider and Irastorza, 2010; Shekelle, 1997). Other surveys have estimated that LBP has an annual incidence in the adult population in the industrialized countries that ranges from about 1.4 to 4.9% (Op de Beek and Hermans, 2000; Shekelle, 1997) or between 19% and 56% (NRC-IOM, 2001). The NRC-IOM (2001) reported that the National Health Interview Survey estimated at 17.6% (or 22.4 million people) the prevalence of suffer from LBP the entire U.S. population on 1988, while for the U.K. it was estimated at 39% on 1999 and for the Netherlands it was found to be 46% for men and 52% for women on 1999 (Op de Beek and Hermans, 2000).

A comparative analytical report compiled by Eurofound, based on national surveys and European Working Conditions Surveys carried out by Eurostat, showed that WRMSD are the major source of occupational morbidity in EU accounting for the majority of the occupational diseases, with an estimated prevalence rate of over 2.5% among employees, the equivalent of more than four million employees (Giaccone, 2007), with work-related low back pain (WRLBP) the most prevalent. Even if in practice it is often impossible to distinguish between WRLBP and that of uncertain origin (Op de Beek and Hermans, 2000) or between WRMSD and MSD as there is not a comparative estimates of the incidence in the non-working general population (NRC-IOM, 2001), surveys among the EU workers reported that millions of workers across EU are affected by WRMSD throughout their labour tasks, a fact that designate WRMSD as the major source ($\sim$39%) of occupational morbidity within EU member states, with the WRLBP (24.7% of the workers) and myalgia (22.8% of the workers) to be the most prevalent (Parent-Thirion et al., 2007).

Besides the health concern, the WRMSD have also a great financial cost to society, which for the U.S. in 1995 it was estimated that had been yielded to $215 billion (Praemer, Furner, and Rice, 1999) and for the Europe up to 2% of the gross domestic product annually with a total cost due to sickness absence of about £254 billion (Bevan et al., 2007; Lancet, 2009). The European annual cost of WRLBP is about € 12 billion (Bevan et al., 2007) and for the U.S, a conservative cost estimation is about $50 billion annually in work-related costs (NRC-IOM, 2001).

1.4.2. Global Burden

It seems that the global burden of LBP has been underestimated in the Global Burden Disease (GBD) reports compiled previously to 2010 due to methodological issues of the measurements (Hoy et al., 2010). By using disability adjusted life year (DALY) metric as a measure to quantify the burden of disease from morbidity, where one DALY equals one lost year of healthy life from mortality and disability (Fig. 1.3), the last GBD released in 2010 reported that MSD and LBP are among the non-communicable diseases that most increased between 1990-2010. The high ranking of LBP (Fig. 1.4) is partly due to the undertaken method that took into consideration the functional loss and disability that is caused by LBP, contrary to previous GBD reports where prevalence estimations of LBP were based on case definitions that correlated poorly with functional disability and also limited the available data of the epidemiologic studies that were aligned with the used definition (Hoy et al., 2010). The 2010 GBD report estimated LBP as the seventh cause of disability worldwide (Fig. 1.5a), while neck pain and other MSD also listed in the top-25 ranking. For the western industrialized countries LBP ranks as second cause of disability (Fig. 1.5b), while other

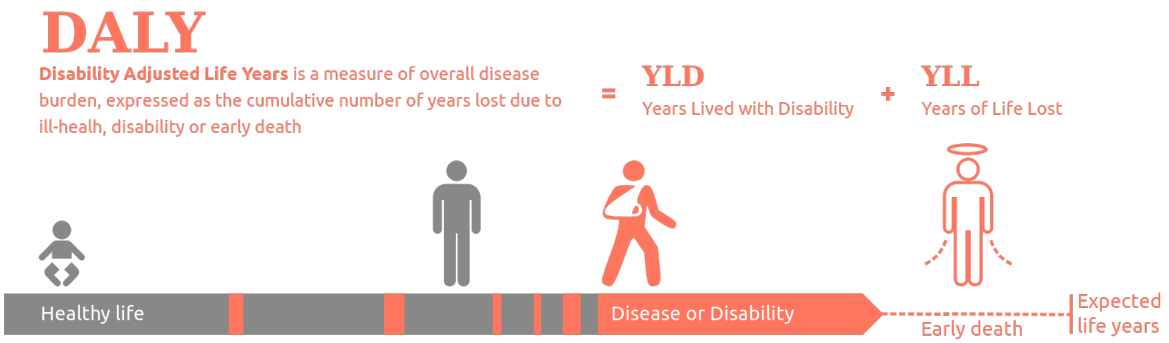

Figure 1.3 Disability-Adjusted Life Year (DALY) metrics to quantify the burden of disease from morbidity. DALY = YLD + YLL, where YLD = number of cases × duration till remission or death × disability weight, and YLL = number of deaths × life expectancy at the age of death (Devleesschauwer et al., 2014) (reprinted from wikipedia).

MSD and neck pain listed ranked in high places as well (Institute for Health Metrics and Evaluation, 2013a).

With a peak onset at an age between 45-49 (over 15 millions DALY - 11.6% of total DALY), MSD (including LBP) shared the sixth largest number of years that people lived with disability worldwide (6.7% of total DALY), while LBP alone shows a peak onset at an age between 40-44 (over 7 millions DALY - 5.7% of total DALY). The study reported that the global health burden of MSD was increased from ∼114 millions DALY (4.6% of total DALY) in 1990 to ∼166 millions DALY (6.7% of total DALY) in 2010 (↑45.5%). Within MSD, LBP contributed ∼56 millions DALY (2.3% of total) in 1990 and ∼81 millions DALY (3.2% of total) in 2010 (↑43%) and nowadays ranked seventh of the world causes of disability (Fig. 1.4a). In developed countries the burden of LBP is ranked third with an increase of 16% in DALY since 1990.

LBP is so common among workers that it may almost be considered an occupational disease (WHO, 1985). WRLBP contributed ∼18 millions DALY (0.7% of total DALY) in 1990 and ∼22 millions DALY (0.9% of total DALY) in 2010 (↑22%) and nowadays ranked 21^{th} of the world risks of disability with a peak onset at an age between 40-44 (2.7 millions DALY - 2.1% of total DALY). However, in the developed countries there is a decrease trend, ∼3.32 millions DALY (0.9% of total DALY) in 1990 and ∼3.26 millions DALY (0.8% of total DALY) in 2010, while in the developing an increase trend, ∼14.5 millions DALY (0.7% of total DALY) in 1990 and ∼18.9 millions DALY (0.9% of total DALY) in 2010. In 1990 it was estimated that a ∼31% of the global LBP is deemed attributable to occupational risk factors (Institute for Health Metrics and Evaluation, 2013a). In 2010 it was estimated at ∼26-37 % of the global LBP (measured in DALY) (Institute for Health Metrics and Evaluation, 2013a; Mathers, Stevens, and Mascarenhas, 2009; Punnett et al., 2005).

Conceptually, the "disability" term used in DALY calculation is not the same with the definition provided by the International Classification of Functioning, Disability, and Health (ICF) and adopted by WHO (Grosse et al., 2009). The GBD study use "disability weights" to convert the years lived in states of less than full health to equivalent number of lost years of full health, while ICF defines disability as an interaction between health conditions and contextual factors and does not assume

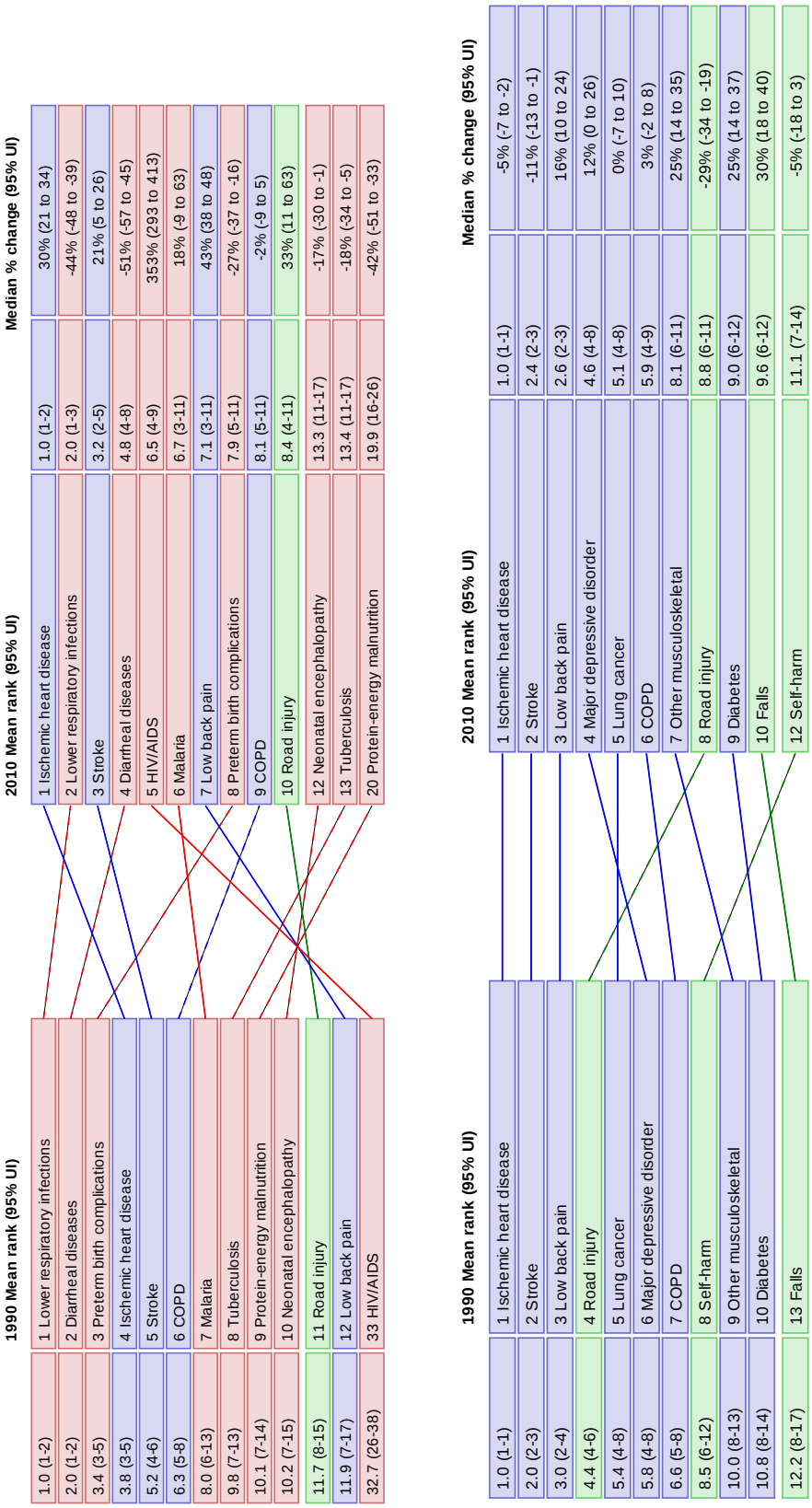

(a) Global DALY ranking.

(b) Developed countries DALY ranking.

Figure 1.4 Ranking of causes of disability based on DALY, 1990 - 2010 (reprinted from Institute for Health Metrics and Evaluation, 2013a).

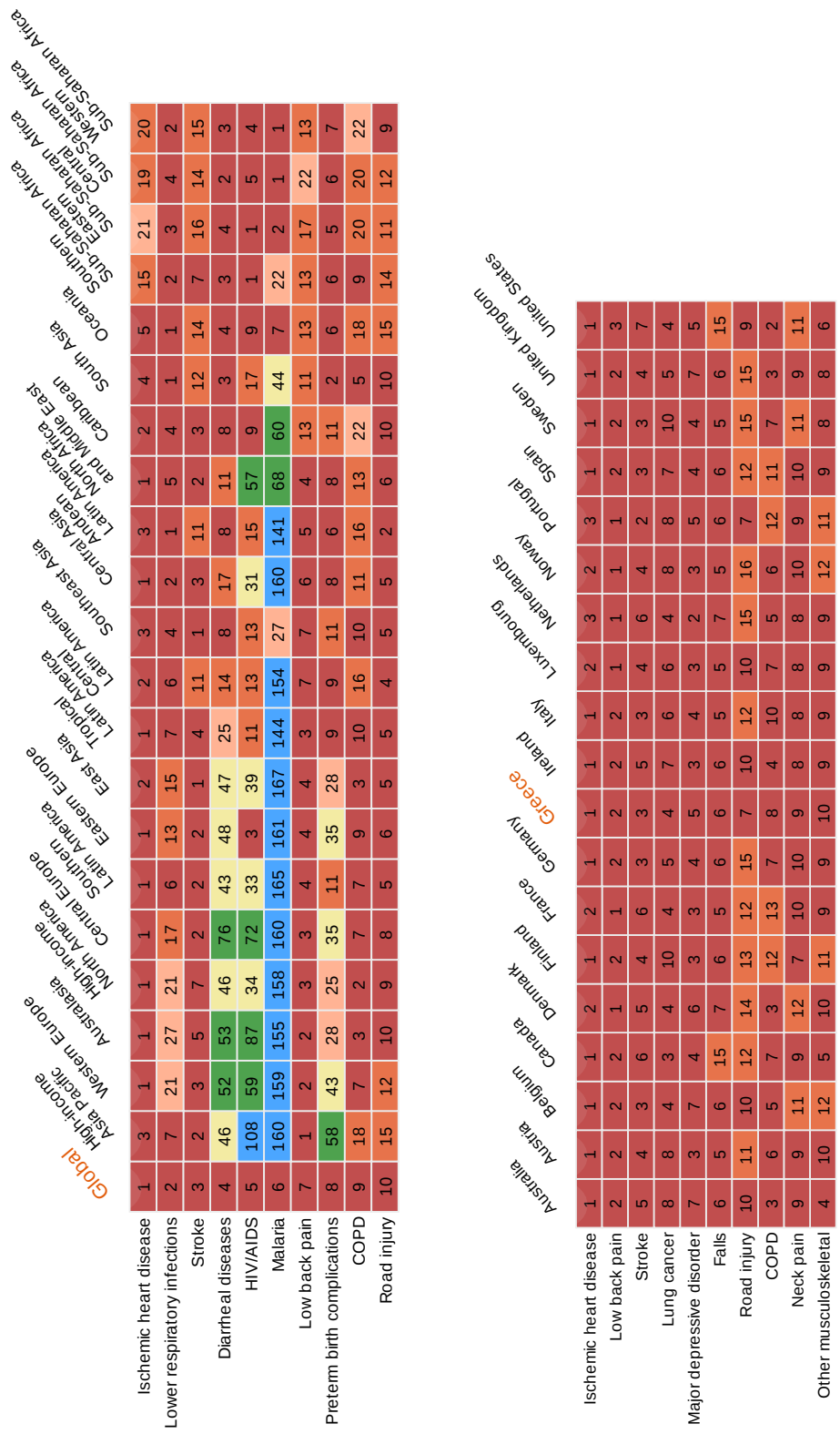

(a) Global ranking and comparison of causes of disability based on DALY.

(b) Ranking and comparison of causes of disability based on DALY. Greece's ranking compared with the others western industrialized countries based on DALY.

Figure 1.5 Rankings of leading causes of disability by geographical zone and country (reprinted from Institute for Health Metrics and Evaluation, 2013a).

a causal link between injury or disease and disability. Taking into considerations the previous criticisms, the last GBD study has improved the "disability weights" values (Hoy et al., 2010). Moreover, it is reported that "disability weights" are very consistent among different cultural environments (Salomon et al., 2013).

WRLBP causes considerable morbidity and it is a major cause of work absenteeism, resulting in economic and productivity loss. According to the rationale of disability adjusted life year (DALY), the so far prevention policies of WRMSD were not effective to reduce work disability (Institute for Health Metrics and Evaluation, 2013b). The Institute for Health Metrics and Evaluation (2013b) argues, that demographic changes, longevity and prior health policies changed the global view of health loss. The risk factors for health loss shifted from communicable to non-communicable diseases and from fatality to disability, whereas the objective consists to live longer, free of disease and with less disability (Institute for Health Metrics and Evaluation, 2013b).

1.5. Work-Related Risk Factors and Causality for Low Back Pain

Figure 1.6 shows the conceptual framework of physiological pathways and factors that potentially contribute to the development of WRLBD as adopted by EU-OSHA and NRC-IOM. It is centered on the load-tolerance relationship (Radwin, Marras, and Lavender, 2002), whereas "load" was defined as the physical stresses acting on the body, or on anatomical structure within the body, and are developed by (I) mechanical loads of kinetic and kinematic origin, (II) heat loss and (III) transmission of vibrations, resulted either from the external environment or internally from the neuromusculoskeletal system, and "tolerance" was defined as the capacity of physiological and physical responses of the tissues to the loading (Radwin, Marras, and Lavender, 2002). The conceptual model can be devided into two periods following nomenclature of previous generic exposure-outcome models (Armstrong et al., 1993; Hagberg et al., 1995), (A) the prepathogenesis period, which includes the workplace features and the individuals risk factors, and (B) the pathogenesis period, which comprises the pathophysiology (biomechanical loading and internal tolerances) and the outcomes (pain, discomfort, impairment, disability).

1.5.1. Work-Related Risk Factors for Low Back Pain

According to the conceptual model of Fig. 1.6, at the prepathogenesis period, the worker is exposed to risk factors that are induced by the work environment and which may trigger a pathological condition. The occupational risk factors that are potentially precursors of triggering a pathological condition resulting to MSD are divided into physical, psychosocial, organizational and individual factors. The prepathogenesis period is a conceptual scheme of the invloved pathways to LBP based on epidemiological and critical analyses evidence. Many epidemiological studies have been performed in order to identify occupational factors that are associated either negatively or positively with the development of WRMSD. Critical reviews of the epidemiologic evidence associated with WRMSD and pattern of evidence analyses performed from different organizations, authoritative agencies and national institutes (WHO, EU-OSHA, NRC-IOM, NIOSH, etc.) reported that there is a strong evidence of work-relatedness of LBP that supports its relation with the physical and

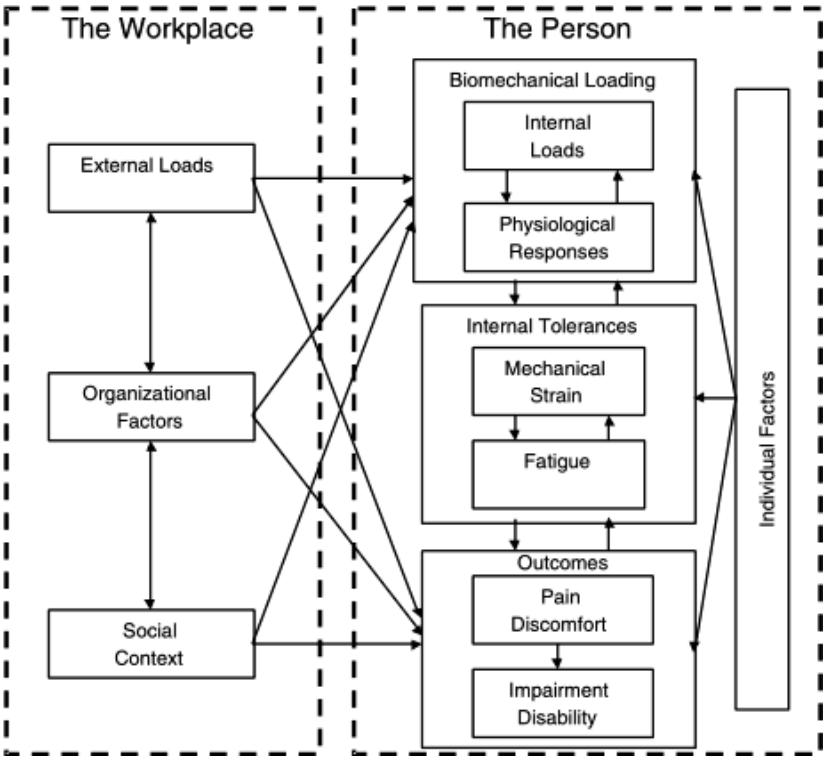

Figure 1.6 A conceptual framework for the development of WRLBD (reprinted from NRC-IOM, 2001).

psychosocial aspects of work, and especially with exposures to physical heavy work including lifting heavy loads (Hagberg et al., 1995; Mathers, Stevens, and Mascarenhas, 2009; NIOSH, 1981, 1997; NRC-IOM, 2001; Op de Beek and Hermans, 2000).

Table 1.1 provides the occupational risk factors that are associated with LBP and their scientific evidence. According to the Global Health Risk (GHR) report (2009), physical risk factors with strong scientific evidence that are reported at Table 1.1 are also considered by WHO, under the term ergonomic stressors, as the major causes of WRLBP worldwide. Hence, according to WHO (Mathers, Stevens, and Mascarenhas, 2009), the following biomechanical risk factors are recognized as global risk factors for disease burden because of the considerable global work disability and work absenteeism that LBP provokes, and because of the economic and productivity loss: (I) lifting and carrying heavy loads, (II) demanding physical work, (III) frequent bending, and (IV) twisting and awkward postures.

However, there are epidemiological studies where occupational mechanical factors, included the global risk factors, were reported as non-causative factors of LBP (Roffey et al., 2010a,b,c,d,e; Wai et al., 2010a,b,c), and systematic reviews where occupational mechanical risks associated with lifting, bending and other body actions have been reported as not effective to prevent LBP (Balagué et al., 2012). The epidemiological approach to MSD (observational studies) has been criticized that due to the multifactorial nature of occupational risk factors is not able to identify single causal factors on LBP (Dagenais et al., 2012; Kuijer et al., 2012; Marras, 2000; Marras et al., 1995). Therefore, it can be said that these studies have only recognised the strong interaction

between potential occupational risk factors.

Table 1.1 Work related risk factors for development of LBP (adapted from Op de Beek and Hermans, 2000).

Category of risk factor	Risk factor	Evidence
Physical factors		
	Manual material handling (lifting loads ≥ 3 kg)	+++
	Whole-body-vibration	+++
	Awkward postures	++
	Heavy manual labour (incl. lifting heavy loads)	++
	Slipping and falling	+
	Static work	+/0
Psychosocial factors		
	Social support	+++
	Job dissatisfaction	+++
	Job content	+/0
	Job control	+/0
	Work/time pressure	+/0
Individual factors		
	Medical history	+++
	Socio-economic status	+++
	Smoking	++
	Age	+/0
	Anthropometry	+/0
	Gender	+/0
	Physical activity	+/0

$^{+++}$ Strong evidence of work-relatedness
$^{++}$ Sufficient evidence
$^{+/0}$ Insufficient evidence

1.5.1.1. Manual Material Lifting and Lowering Tasks

For industrial workers who perform manual lifting or lowering tasks a high risk exist for suffering LBD (EU-OSHA, 2000; Mathers, Stevens, and Mascarenhas, 2009; NIOSH, 1981; Op de Beek and Hermans, 2000; Podniece et al., 2008). The ISO 11228-1 (2003) standard, defines manual material lifting and lowering task as the action to move an object with a moderate mass of 3 kg or more (included people or animals) from its initial position upwards/downwards without mechanical assistance. Workers who perform lifting tasks constitute a high risk group for suffering WRLBD resulting to LBP (EU-OSHA, 2000; Mathers, Stevens, and Mascarenhas, 2009; NIOSH, 1981; Op de Beek and Hermans, 2000; Podniece et al., 2008). As early as 1911, Middleton and Teacher (1911) (cited by Lancet, 1911) postulated, that possible intervertebral disk injury during lifting heavy loads is due to the high muscular effort, and may be fatal.

Although epidemiological studies have be used to identify occupational risk factors leading to the development of WRLBD, an inherent problem is that it is difficult to determine the level or magnitude at which the presence of a risk factor becomes problematic (Marras, 2000; Marras et al., 1993). Marras et al. (1993), performed a cross-sectional study in order to understand the relationship between risk factors for WRLBD and biomechanical variables. The study reported that the most significant variables associated with WRLBD in *repetitive* lifting tasks are (I) lifting frequency, (II) maximum load moment, (III) maximum trunk lateral velocity, (IV) mean trunk

twisting velocity, and (V) maximum trunk sagittal angle. A multivariate logistic model (the industrial Lumbar Motion Monitor (iLMM) risk assessment model) consisting of the above five risk factors were able to predict the probability of high-risk group membership (odds ratio of 10.7).

Another model that is used to rate lifting tasks in terms of risk for development of LBD is the NIOSH lifting equation (Waters et al., 1993), which implies the following factors: (I) lifting frequency, (II) box weight, and (III) horizontal distance, (IV) vertical height and (V) vertical displacement of the box's center of gravity (COG_B) with respect to the mid-point between the inner-ankle bones. A comparison between iLMM and NIOSH risk assessment models showed that the multivariate logistic model consisting of five risk factors implied by the NIOSH lifting equation yielded less odds ratios than the iLMM dynamic model (Marras et al., 1993)—odds ratios of 3.5 when the average values were used and 4.6 when the maximum factors of the workplace factors were used. It was postulated that NIOSH lifting equation cannot identify low- and medium-risk jobs well and may require the changing of jobs that do not necessarily place workers at risk (Marras et al., 1999). NIOSH revised equation relied principally on biomechanical studies of static lifting tasks, whereas the contribution of lifting load dynamics to injury risk was relied mostly on physiological and psychophysical studies. Therefore, NIOSH equation was limited to assess mainly smooth and slow lifting tasks. It can be said, that with the development of the iLMM risk assessment model (Marras et al., 1993) it was recognized the importance of trunk kinematics as a conditioning parameter that increases the risk factor for development of WRLBD during lifting tasks.

A common limitation of the above settings is that they cannot be applied for handling unstable (liquid) loads. They are limited mainly for manufacturing or industrial settings where loads do not present any instability. Although there is some epidemiological evidence that workers who handle liquid loads have higher incidence of LBD compared to others with similar lifting demands (McGlothlin, 1996; Personick and Harthun, 1992), and moreover the unstable factor is considered by the agencies a parameter that increases the risk for the development of WRLBD (NIOSH, 1981, 1994, 1997), the workers who handle liquid loads are assessed with the same parameters that are used for assessing stable loads, however, with an additional but subjective stressor added by the specialist.

1.5.2. Low Back Pain Causality

As showed the conceptual model of Fig. 1.6, at the pathogenesis period, which comprises the pathophysiology and the outcomes, the mechanical, physiological, and psychological risk factors influence the causal factor for development of WRLBP – the internal loading to the tissues – which in turns provoke biological reactions. The pathophysiological mechanisms underlying these pathways may have not been known yet. However, different biological hypotheses have been put forward with respect to the pathways structure in order to associate the responses of the tissues and cells to an etiologic agent coherent with occupational exposure (Forde, Punnett, and Wegnar, 2002). Several models and hypotheses have been presented in order to describe the assumed causal pathway(s) between putative work environment risk factors and symptoms of MSD (Armstrong et al., 1993; Hagberg et al., 1995; Marras et al., 2009; NRC-IOM, 2001; Op de Beek and Hermans, 2000; WHO, 1985). However, the diagnosis of LBP is challenging.

LBP has many possible etiologies (Merskey and Bogduk, 1994) and its diagnosis is made by exclusion (Negrini et al., 2008). In 85-95% of the cases the etiology of the LBP is unclear and therefore is termed as idiopathic low back pain (iLBP) or nonspecific LBP (Krismer and Van Tulder, 2007; Op de Beek and Hermans, 2000; Snook, 2004), which is defined as LBP not attributed to recognisable, known specific pathology (Burton et al., 2006). Balagué et al. (2012), stated that for the iLBP pathogenesis, epidemiologically and etiologically, there are limits of knowledge of causal responsibility. Only for the resting 5-15% there is a diagnosis determined via clinical examination (X-ray, MRI imaging, CT scan) and related to discogenic, neurological, structural, muscular or ligamentous origin, and therefore is termed as traumatic (Marras, 2008; McGill, 1997; Op de Beek and Hermans, 2000). According to Waddell (1998), less than 1% of LBP is a serious disease such as cancer and less than 1% is inflammatory disease (cited in Snook, 2004).

1.5.2.1. Definition of Pain

Despite the subjectiveness of pain perception, the International Association for the Study of Pain (IASP) defines pain as un unpleasant sensory and emotional experience associated with actual or potential tissue damage, or described in terms of such damage. Moreover, it recognises psychological reasons as pain source. The psychological dimension of the pain becomes very relevant in chronic LBP[1] (Balagué et al., 2012). However, IASP does not recognise explicitly LBP as it does with lumbar spinal pain and sacral spinal pain (Merskey and Bogduk, 1994). Therefore, LBP can be defined as pain *perceived* as arising from the lumbar or sacral areas or a combination of both with or without referred pain[2] (Bogduk, 2005). It is localized within a region bounded laterally by the lateral borders of the erector spinae muscles and the imaginary vertical lines through the posterior superior-to-posterior inferior iliac spines, superiorly by an imaginary transverse line through the 12^{th} thoracic spinous process, and inferiorly by a transverse line through the posterior sacrococcygeal joints, (Bogduk, 2005; Merskey and Bogduk, 1994). Following the topographically definition of LBP with the help of the IASP lumbar spinal pain and sacral spinal pain definitions, it is deduced that the origin of LBP may or may not arise from these spine regions as it is based on the subjective opinion of the patients about where they perceived the source of the pain. Similarly, the European guidelines for prevention in LBP defines it as pain and discomfort localized below the costal margin and above the inferior gluteal folds, with or without leg pain (Burton et al., 2006).

1.5.3. Low Back Pain Pathways

LBP implies a somatic origin for the pain, therefore, only the tissues of the lumbar spine can be candidates for LBP (Bogduk, 2005). Bogduk (2005), postulated that in order for a spinal element to be a candidate for a possible source of LBP, it should be evaluated by adopting criteria analogous to Koch's postulates for bacterial diseases. Therefore, for any structure to be deemed a cause of LBP it should (I) be innervated, (II) exist biological plausibility of causing pain, (III) be susceptible to diseases or injuries that are known to be painful, and (IV) have been shown to be a source of pain in patients using diagnostic techniques of known reliability and validity.

[1] Chronic pain lasts more than three months or occurs episodically within a 6 month period.
[2] Pain which perceived at an other location than its origin.

Accordingly, two pathways that are in accordance with the criteria postulated by Bogduk (2005) have been deemed as a cause to develop LBP (Fig. 1.8). LBP is based primarily (I) on the mechanical disruption of the spine support structures (tendons, nerves, muscles, bones, ligaments, discs), where the integrity of the tissues is violated and their mechanical order perturbed either by exposure to high or to repeated and prolonged relative low stresses (load-tolerance mismatch), and (II) on muscle function disruption, where trunk muscles functioning and "balance" between muscles' intensities are disrupted by physiological, biochemical or mechanical mechanisms (Bogduk, 2005; Kumar, 2001; Marras, 2008; McGill, 2007; Roy and DeLuca, 1996; Solomonow, 2004, 2009; Zernicke and Whiting, 2000).

1.5.3.1. Tissues' Mechanical Disruption

Body movements are powered and controlled by the force produced by the contractions of the skeletal muscles that is transmitted via its associated tendons to the skeleton to produce a musculotendinous moment of force at the joint axes modulated by the length and velocity of each motor unit, and by the interaction of the musculotendinous moment of force with the external forces that are transmitted to the body from the environment (Winter, 2009). The external forces, and the forces that are generated internally by muscle contractions and by the passive reactions of tendons, ligaments and fascia to muscle and/or external forces, also act on spine's supporting structures, either directly like in the musculotendinous union, or indirectly transmitted through other tissues like the compression and shear stresses developed in the intervertebral disks during trunk bending (McGill, 2007).

LBP related to the spine's supporting structures can be developed in two different ways both arising within the load-tolerance framework of Fig. 1.6 (Ayoub and Woldstad, 1999; Chaffin, Andersson, and Martin, 2006; Kumar, 1999, 2001; Marras, 2008; McGill, 1997, 2007; NRC-IOM, 2001; Op de Beek and Hermans, 2000; Pećina and Bojanić, 2004; Radwin, Marras, and Lavender, 2002). This is because the tissue load can exceed the tissue tolerance in two ways: (I) the load can increase or (II) the tolerance can decrease (Fig. 1.7). On one hand, it is the acute trauma injury, arising from a single and identified event where the load exceeds the failure tolerance of the tissue or the ability of the support structure to withstand the load, and on the other hand, it is the time-varying cumulative disorder, which result from the accumulated effect of transient external loads that, in isolation, are insufficient to exceed tissues tolerances, but when repeated or sustained loads are applied for a prolonged time the internal tolerances of the tissues or the ability of the structure to withstand the load are eventually exceeded (Radwin, Marras, and Lavender, 2002).

Cumulative disorders are caused by a repeated micro-trauma caused by continuous exposure to mechanical strain that overwhelms the tissue's ability to repair itself from the micro-damages and therefore biological adaptation cannot take place (Kumar, 2001; Pećina and Bojanić, 2004). This is because micro-damages depend on viscoelastic characteristics of biological tissues where the repeated or sustained application of load to a tissue tends to wear it down, thus, lowering its mechanical tolerance to the point where the tolerance is exceeded through a reduction of the tolerance limit (Marras, 2006). When micro-damages occur, the tissue undergoes an inflammatory process necessary to initiate a healing process and biological adaptation. If the natural cycle of

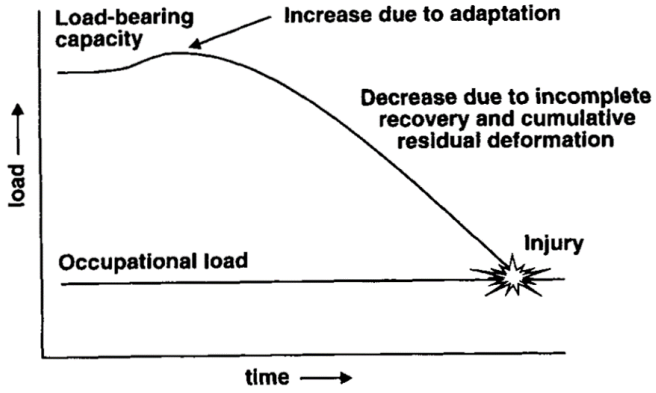

Figure 1.7 Load-tolerance capacity and LBP. When tissue biological adaptation is disturbed it is lowering its stress bearing capacity and raising the injury potential (adapted from Kumar, 2001).

healing process is interrupted it results to MSD of cumulative origin and functional disability (Barbe and Barr, 2006; Barr and Barbe, 2004; Kumar, 2001; Marras, 2006; Pećina and Bojanić, 2004).

Tolerance limit is further influenced by individuals factors (anthropometric characteristics, strength, endurance, age, leisure time, genetic makeup, etc) (see Fig. 1.6) and improper muscle rectruitment patterns due to (I) muscle fatigue, (II) co-contractions, or (III) *motor control errors* . Co-contraction of antagonist muscles increase the mechanical loads (compression, shear and torsion) or change the nature of the mechanical loads placed on the body's articulations and tissues during an exertion or motion (Radwin, Marras, and Lavender, 2002). Localized muscle fatigue is failure of the fiber to contract in response to continuing a motor neuron stimulation. The EU-OSHA defines localized muscle fatigue as a potential precursor to WRMSD (Buckle and Devereux, 1999; Op de Beek and Hermans, 2000). Localized muscle fatigue changes the loadings experienced by the supported spinal structures. While the fatigued fibers are not themselves permanently damaged, they can put other motor units at risk of structural damage due to inappropriate recruitment or excessive strain from external loads (NRC-IOM, 2001; Radwin, Marras, and Lavender, 2002). Moreover, localized muscle fatigue may result in ballistic motions and exertions in which loads are poorly controlled and rapidly accelerated indicating that there are large impulse forces within muscles and connective tissues (NRC-IOM, 2001; Radwin, Marras, and Lavender, 2002).

McGill (1997), reported that improper muscle activation patterns or trunk force magnitudes provoked single vertabra rotation resulting in pain. As joint stiffness that is needed to maintain mechanical stability of spine depends on the relative activation of the muscles spanning the joints and muscle strength capability, inappropriate muscle activation patterns may reduce the stiffness needed for spine mechanical instability provoking spine buckling. The *in vitro* buckling of ligamentous lumbar spine under compressive forces lesser than bodyweight (80 N) (Crisco and Panjabi, 1992; Crisco et al., 1992), highlights the importance of the "neural controller" to control the forces of trunk musculature that stiffen the spine. NIOSH (1981), pointed out the difficulty that is supposed to be for the worker to control dynamic actions that result to high inertial forces. Furthermore, NIOSH (1981) is aware that in the fast movements, the ability of the "neural

controller" to coordinate the necessary trunk muscles for stabilizing the spinal column is stressed.

Regarding the trunk muscles activation patterns, it was showed that local and global muscles are affected in an opposite manner in the presence of LBP (Hodges, 2004). Global muscles control intervertebral motion only by augmented activations, resulting in co-contractions, higher spine loads and reduced normal movement of the spine (Hodges, 2004). Therefore, the activity of the global muscles was used as a measurable compensation for poor passive or active (local muscles) segmental support (Cholewicki, Panjabi, and Khachatryan, 1997).

1.5.3.2. Muscle Function Disruption

LBP related to the muscle function disruption is well documented to the scientific literature, however, the question is what kind of disorders can effect back muscles (Bogduk, 2005). Bogduk (2005), postulated that there is a lack of direct evidence of the responsible lesion. Therefore, (A) according to the "Cinderella" hypothesis there are low-threshold motor units (type I) that are always recruited as soon as the muscle is activated and stay active until total muscular relaxation face energy crisis at the membrane level, which may lead to degenerative processes, necrosis, and pain (Hagg, 2000). If the load condition remains the same, the next motor units on the recruitment pyramid get affected (Henneman, Somjen, and Carpenter, 1965). Localized muscle fatigue can also occur in low-level long-lasting static contractions where the "Cinderella" fibers are always recruited (Hagg, 2000; NRC-IOM, 2001; Radwin, Marras, and Lavender, 2002; Sjogaard, 1985; Sjogaard and Jensen, 2006). (B) Constant muscle tension can decrease blood flow and oxygenation in muscles and its nerves resulting in ischaemic muscle pain (Bogduk, 2005; Marras, 2008). (C) Myofascial trigger points represent areas of hypercontracted muscle cells that deplete local energy stores and impair the function of calcium pumps, thereby perpetuating the contraction. Pain is said to occur as a result of obstruction of local blood flow and the accumulation of algogenic metabolites such as bradykinin. Myofascial trigger points are believed to arise as a result of acute or chronic repetitive strain of the affected muscle or 'reflexily' as a result of underlying joint disease (Bogduk, 2005; Marras, 2008). (D) In eccentric contractions the mechanical load that is applied on the muscle exceeds the force developed by the muscle. The muscle is doing negative work and absorbs mechanical energy. The use of the absorbed energy is task depended. Therefore, it can be dissipated as heat, in which case the muscle is functioning as a damper and attenuates impact forces, or the energy is recovered at the concentric phase of the stretch-shortening cycle, hence potentiates the power output. Muscle strain injuries occur as a response to excessive load or stretch and are most common during eccentric contractions in muscles that span two or more joints. Workplace factors like repetition, range of motion, work-rest cycle, and age influence effects the susceptibility of injuries (Bogduk, 2005; Cutlip et al., 2009; Marras, 2008; Roy and DeLuca, 1996).

1.5.4. Theories for MSD Causation

Kumar (2001), proposed four models about the development of MSD, where he took into consideration that localized muscle fatigue can provoke either fatigue of motor units or skeletal fiber damage. Regarding the latter, fatigue may decrease the tolerance to stress and therefore

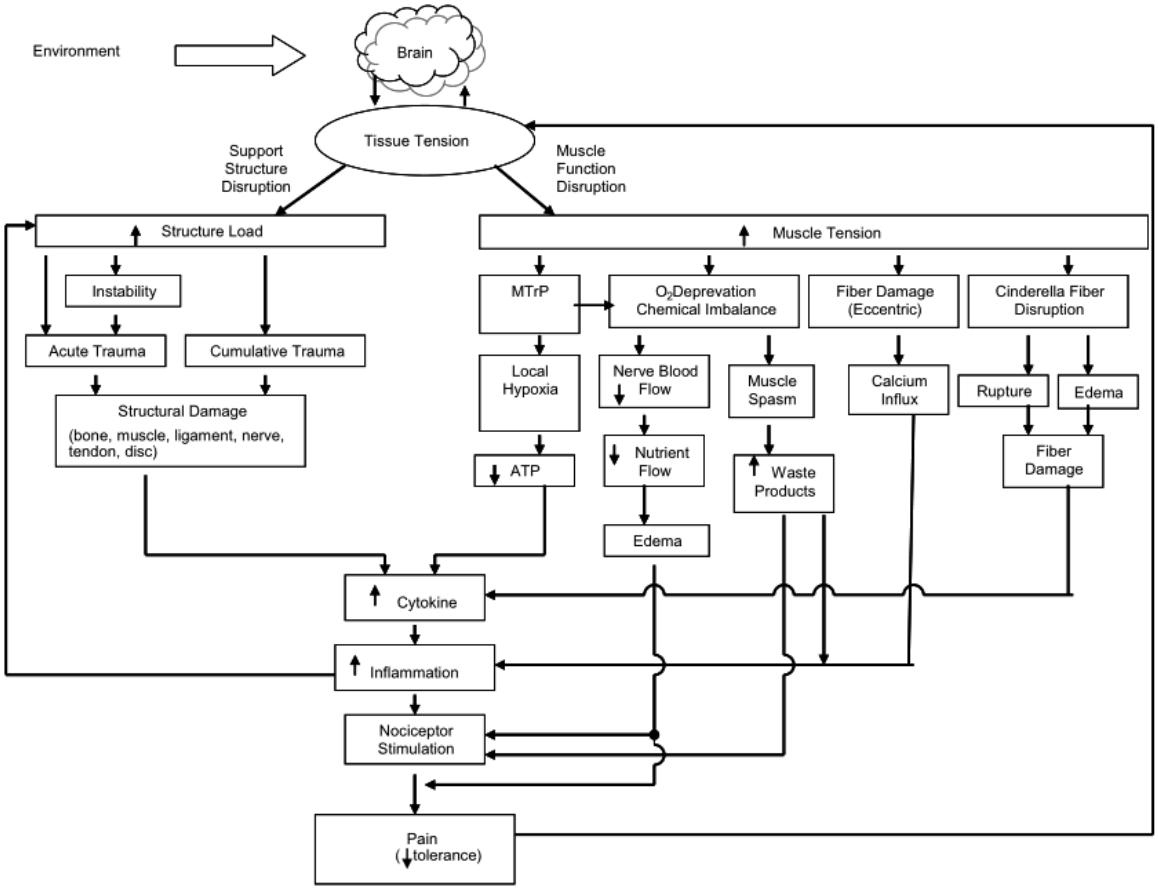

Figure 1.8 Pathways for the development of LBP. The common link connecting all LBP pathways is motor control (adapted from Marras, 2008).

result in microtrauma to the muscle fibers; regarding the former, while the fatigued fibers are not themselves permanently damaged, they can put other motor units or connective tissues and supported structures at risk of structural damage due to inappropriate recruitment or excessive strain from external loads. The first model of Kumar (2001), is the multivariate interaction theory of musculoskeletal injury precipitation which opines that a precipitation of MSD is an interactive process between individual genetic makeup, morphological characteristics, psychosocial profile and mechanical stresses upon biological tissues. By definition exertion is task dependent and upon the components that it is based is the force of exertion, its duration, and job range of motion. The second is the differential fatigue theory in which different joints and muscles are differentially loaded by unbalanced and asymmetric activities, where probably the muscles are not load proportional to their individual capabilities. In prolonged and/or repeated loading the develop of localized muscle fatigue alters the muscle tension that is transmitted via its associated tendons to the skeleton to produce a musculotendinous moment of force at the joint axis, and subsequently, taking into consideration that the rate that muscles are fatigued is different and furthermore connective tissues in joints may be disproportionately deformed due to prolonged performance with unequal loads, it can leads in changes in human kinematic chain that may result in joint kinematics and load patterns different from the desired, thereby altering the joint

stability. The third is the cumulative load theory, which states that because all biological tissues have viscoelastic properties with its individual characteristics, repeated and prolonged usage leads to slow mechanical degradation and reduction of their stress-bearing capacity, rendering the tissues more vulnerable to injuries at lower tolerance levels, which are product of load magnitude and frequency. Herein, localized muscle fatigue favors biological safety by preventing cumulative load from rising rapidly as the maximum voluntary contraction for level can neither be held for a long time, and nor can it be repeated in quick succession. The fourth is the overexertion theory, which is similar to the cumulative load theory except that the injury is acute or rather momentary in time because the exertion exceeds the tolerance limits of the system, or the ability of the structure to withstand the load, or it exceeds the tolerable strain rate. An overexertion injury precipitation can also occur in a situation when the combination of exertion and repetition does not allow adequate recovery and leads to overexertion. Herein, localized muscle fatigue in combination with inadequate recovery can leads to overexertion and muscle fibers damage. Overexertion by definition is a function of internal stresses magnitude, duration, frequency, adopted posture and motion and it addresses only the internal physical factors. Direct trauma is excluded.

1.6. Prevention of Work-Related Low Back Disorders

1.6.1. Ergonomic Intervention

In seeking to cope with WRMSD and to foster safer work environments, an ergonomic intervention is required to eliminate the occupational risk factors for MSD (WHO, 1985). In 1962, the International Labour Organization (ILO) (cited by NIOSH, 1981) suggested limits for occasional weight lifting based on inspection of injury and illness statistics, which depicted manual material handling (MMH) as contributing to about threefold of increase in spinal injuries among others. From a biomechanical standpoint, if MMH activities cannot be avoided in the workplace, at least, they should be ergonomically well designed as they are a potential precursor of LBP (WHO, 1985).

Based on systematic review of the epidemiologic evidence, the European Guidelines for Prevention in LBP does not recommend standalone physical ergonomics interventions programs, but multidimensional interventions that include physical ergonomics interventions for reduction of the prevalence and severity of occupational LBP. However, it recognizes the fundamental role of physical ergonomics in order to redesign the workspace for early return to work (Burton, 2005). In many circumstances where manual lifting and lowering tasks are unavoidable, work redesign may carry on in order to decrease the mechanical loads on the joints at acceptable individual levels for each worker by reducing the exposure to dangerous loading conditions and/or to stressful body movements and thus to ensure that musculoskeletal system cannot be overloaded and fail when workers perform various MMH activities in the workplace.

An optimal ergonomic intervention is achieved by an engineering control approach and preferably through task automation or mechanization. However, in some cases where such mechanical aids are not feasible and consequently manual lifting tasks cannot be avoided, handling devices can be used to simplify the problem of handling an object. Engineering controls are the preferred method of risk control because they permanently reduce or eliminate the biomechanical risk

factors. However, there are many cases in job (re)design where the engineering control approach cannot eliminate all of the hazards account for LBD. Therefore, administrative control approaches are used as a secondary option or in parallel to organize the structure of the labour, and also, to inform the workers how to seek for a correct work technique for protecting their backs from injury. Workers who manipulate handling devices (cobots) also seek information about the correct use of the devices, especially in the presence of accelerations (Chaffin, Andersson, and Martin, 2006; Lavender, 2006; Op de Beek and Hermans, 2000). All these collaborative robotic systems extent workers' physical capability. However, these devices need to take into account worker's biomechanics and motor control in order to be used effectively. Description of the biomechanics alone cannot explain whether the natural limits of worker's motor and sense system capabilities are being reached during the manipulation.

1.6.2. Manual Material Lifting and Lowering Work-Technique

The training of workers to recognize, evaluate and manage occupational risk factors is incorporated into the prevention strategy of the EU-OSHA (Op de Beek and Hermans, 2000) and NIOSH (Cohen et al., 1997) as a proactive action to cope with WRMSD. On the other hand, the European Guidelines for Prevention in LBP does not recommend information, advice or instruction on biomechanics or lifting techniques for prevention in LBP, but it rather recommends secondary intervention, like the prevention of recurrence and of the disability from LBP (Burton, 2005) that seems to be more realistic and feasible than primary intervention (Balagué et al., 2012; Snook, 2004).

The technique of lifting and lowering objects at work is determined by assessing worker neuro-musculoskeletal performance limits, as well as the constraints imposed by the physical demands of the workplace, which include the handled load and the specificity of the work task, under the framework that any mismatch leads to WRLBD (Bloswick and Hinckley, 2004; Chaffin, Andersson, and Martin, 2006; Jones and Kumar, 2004). The ISO 11228-1 (2003) standard, makes reference to the association of the manual-handling injuries with the (I) individual physical capabilities of the workers, like the decreased lifting strength in women, the (II) less skilled actions in young workers, and (III) the age-related alterations of the viscoelastic properties of the biological tissues. However, the aforementioned imposed constraints cannot define unambiguously which motor patterns the workers can execute during lifting and lowering tasks.

Motor redundancy at the kinematic level, which is arose by the numerous DOF of the human locomotor apparatus compared with the substantially lower anatomical constraints that are imposed by the structure of the musculoskeletal system at joints' level, gives to the workers the possibility to adopt an infinite number of postures during lifting or lowering tasks, and consequently the ability to execute a countless voluntary motor patterns in order to accomplish their labor activities. This phenomenon, of the accomplishment of the same task using different body configurations and environmental means is referred to as "motor equivalence" (Berkinblit, Feldman, and Fukson, 1986; Bernstein, 1967; Hebb, 2002; Lashley, 1930; Tunik et al., 2003). Besides that, it seems coherent that similar muscle activation patterns cannot be presented always among workers or in the same worker who performs replications of the same lifting or lowering task in terms of

origin-destination state (motor equivalence), as it is known that similar motor patterns can be achieved by different muscle activation patterns, unconcernedly task's complexity (Bernstein, 1967; Levin et al., 2003; Mattos et al., 2013). Therefore, the biomechanical rationalization of lifting objects at work has to take into account the abundance of the DOF at the neuromotor level, and lifting tasks have to be treated as a motor control problem, where the neural controller is trying to identify a physiologically feasible motor complex solution (neural constraint) in order to achieve a goal with minimal physical effort and discomfort on the part of the worker (Aruin and Bernstein, 2002; Bernstein, 1930, 1967, 1996; Delleman, 2004).

Nowadays, work-technique for lifting or lowering tasks is generally perceived as an implementation of good practices that are focused to reduce the risk of LBD within the lumbar disks from tasks where the same load is handled repetitively in similar manner throughout the work. Therefore, it is mainly regarded under an "educational" framework, where workers are learning stereotyped behaviours of how to avoid or minimize the biomechanical risk factors during the lifting tasks (NIOSH, 1981). Accordingly, a classical and simultaneously oversimplified approach to characterize the work-technique in manual material lifting tasks is in terms of the method that the worker uses to carry it out (liftstyle), which is deduced to the elemental concept of identifying the posture adopted by the worker just prior to the lift. Thus, three methods have been considered widely for accomplishing lifting tasks, namely: the stoop, the squat, and the semi-squat methods.

However, controversy persists in the scientific literature as to which of the aforementioned methods come to the fore as the most efficient in terms of optimization of the mechanical workload on the spine (Burgess-Limerick, 2003; Sedgwick and Gormley, 1998; Straker, 2003). In general, squat lifting is recognized widely as the "correct" method, however it seems that is superior to stoop only when is limited to lift loads from positions between the knees (Straker, 2003). It was postulated that there is not biomechanical evidence in support of advocating the squat lifting technique over the stoop one to prevent low back pain, mainly because of the unavoidable *variability* on the work-task, workplace, workers' morphology, and of the undesired adaptation of the method to workers' habits (Burgess-Limerick, Abernethy, and Neal, 1995; Van Dieën, Hoozemans, and Toussaint, 1999). However, the U.S. National Health Service Centre for Reviews and Dissemination (2001) cautioned that the review by van Dieen and coworkers (1999) contained methodological flaws that affected the authors' conclusions, and supports the use of the squat lift. On the other hand, Gagnon (2005) questioned the effectiveness of these liftstyles to reduce LBD in long-term. Likewise, the EU-OSHA underlines that there are scientific evidence that focusing only on the position of the back during lifting is not sufficient, and furthermore, modifying the liftstyle is not eliminate the inherent risk when the job requirements are physically stressful (Op de Beek and Hermans, 2000). In accordance with the aforementioned, work-technique training during manual material lifting and lowering tasks is limited to learn the workers how to adopt a posture or execute a movement that minimize the mechanical load on the spine structure based on an educational model approach.

However, the performance of lifting or lowering tasks requires the resolution of potentially motor control conflicts where any misleading may results to a high risk of tissue injury (Ebenbichler et al., 2001). Therefore, in order to reduce the incidences of LBD during lifting or lowering tasks

it is suggested that ergonomic prevention have to be focused on the characterization of the work-technique and especially on the interaction between motor patterns performance and the imposed perturbations by the handling load, load's weight and load's spatiotemporal variables, rather to focus only on the reduction of the biomechanical risk factors based on the recommended risk levels (i.e, NIOSH) (Scholz, 1993a; Scholz and McMillan, 1995; Scholz, Millford, and McMillan, 1995). For example, Oddsson et al., 1999, postulated that when the hip strategy of the postural control mechanism get into action to correct exogenous postural perturbations during the lift of a load, there is a a motor control conflict where different function of the same muscle is required (erector spinae). Therefore, the erector spinae muscle is activated eccentrically after a silence period of postural correction, and the concurrent risk to suffer an acute soft tissue injury is extremely high.

Thus, by the aforementioned it can be deduced that the execution of lifting and lowering tasks have to be approximated as the "optimum" biomechanical solution to the motor problem encountered during the task. In this sense, McGill (2007, pp.: 135) proposed that in order to reduced LBD it is probably required to "change the worker to fit the task", comparing workers' technique during lifting tasks with that of elite weightlifters. Similarly, Sedgwick and Gormley (1998) have underlined that work-technique of lifting tasks should adapt the same principles that rule weightlifters' technique. Lavender (2006), in agreement with the latter, added that lifting tasks have to be thought and taught as a complex motor skill, reinforced by the use of feedback performance tools and provide peer-review means to maintain the desired motor behavior. Jarus and Ratzon (2005), proposed a prevention model inspired by a behavioral psychology theory of motor learning (Schmidt and Lee, 1998) in order to facilitate workers' acquisition of correct motor patterns. A limitation is that generalized motor programs cannot solve the question of how motor programs can be learned or how a learned motor pattern can be applied to a variety of contexts or how a new motor skill can be learned immediatelly. Moreover, biomechanical and environmental constraints played little role (if not none) in the formation of that programs.

1.6.3. Ergonomic Workplace Design

Prevention of WRLBD in MMH tasks refers to (re)design the workplace focused on the reduction of the work-related risk factors. Several ergonomic assessment tools can be used to make useful inferences about workers behaviour on a given job in order to identify potential precursors of developing LBD before workers develop symptoms severe enough to require medical treatment and to lead to work absenteeism and work disability. Nevertheless, if these tools cannot be used proactively, when a workstation is designed, they have to be used reactively during work in order to determine which specific workspace parameters or worker actions are most likely to be the cause of LBD and therefore redesign ergonomically unacceptable workstations (Cohen et al., 1997). The basic idea behind every ergonomic assessment tool is that work physical demands should not exceed worker's physical capacity, because any mismatch of human physical capacities and human manual performance requirements in industry may produce or exacerbate LBD (Chaffin, Andersson, and Martin, 2006). A drawback is that all these ergonomic assessment tools assumed that a *correct work technique is presented always*, unconcernedly if lifting tasks are made under ideal ergonomics conditions or not.

1.6.3.1. Physical Ergonomic Assessement Tools

In ergonomics, lifting and lowering tasks can be categorized according to their risk level of suffering WRLBD. Physical demands assessment tools were used proactively or reactively to make useful inferences about workers behaviour on manual material lifting or lowering tasks in manufacturing environments in order to identify potential precursors of developing WRLBD before workers develop symptoms severe enough to require medical treatment and to lead to work absenteeism and work disability (Cohen et al., 1997). Frequently ergonomic assessment tools for lifting tasks are: (I) the revised NIOSH lifting equation (Waters et al., 1993; Waters, 2006) and its modifications (Grieco et al., 1997; Hidalgo et al., 1997; Shoaf et al., 1997) and standards (EN 1005-2; ISO 11228-1) that are used to estimate relative magnitude of physical stresses for lifting tasks[3], (II) the ACGIH TLV guideline (Marras and Hamrick, 2006), which estimates threshold limit values under which workers may be repeatedly exposed without developing WRLBD associated with repetitive lifting tasks and the OSU/BWC guideline (Hamrick, 2006) that extent the threshold limit values for workers currently experiencing LBP, (III) the low back disorder model (Marras et al., 1993, 2000), which uses trunk kinematics data recorded by the iLMM to estimate the likehood of a repetitive lifting task without job rotation to be considered high or low risk for development of WRLBD, and (IV) the University of Michigan 3D Static Strength Prediction Program (3DSSPP) that predicts the percentage of workers who have sufficient strength to perform a lifting task, together with an estimation of spine load (compression and shear forces) (Chaffin, 1997). Each of the above outlined models have strengths and limitations, though they share complementary information (Mirka et al., 2000). Differences have been found between risk assessment tools (Lavender et al., 1999; Marras et al., 1993; Russell et al., 2007). The main difference is their ability to quantify acute or cumulative risk level.

The NIOSH lifting equation (Fig. 1.9) was developed to assist safety and health practitioners evaluate lifting demands in order to prevent or reduce the occurrence of occupational LBDs (NIOSH, 1981, 1994; Waters et al., 1993). It is used in the decision-making process of (re)designing a job that contains repeated lifting (or lowering) tasks. An additional benefit of this equation is also the potential to reduce other WRMSD associated with some lifting tasks such as shoulder or arm pain (Waters et al., 1993). The 1991 revised lifting equation (Waters et al., 1993) has been introduced to upgrade the 1981 Work Practices Guide for Manual Lifting (NIOSH, 1981) by including the possibility to evaluate those jobs that are violating the sagitally symmetric lifting assumption of the old version and by introducing corrections for the reduced physical strength of the disabled/rehabilitated worker.

The equation estimates the recommended weight limit (RWL) by taking into consideration the weight of the load plus several other factors of the lifting tasks that contribute to the risk of injury. These factors are 'weighted' according to biomechanical, physiological and psychophysical criteria (the most conservative load limit allowed by any individual criterion is chosen) and then are used as multiplicative factors in the Equation (1.1) (e.g., HM is the horizontal multiplier, etc.) (NIOSH, 1994; Waters et al., 1993):

[3] NIOSH equation and its modications cannot predict the magnitude of the risk for a given individual and the exact percentage of the work population who would be at an elevated risk for development of WRLBD.

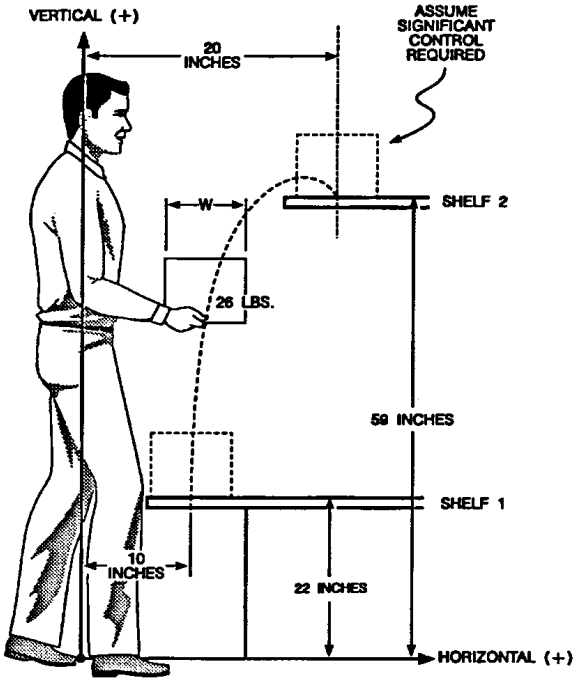

Figure 1.9 Lifting assessment with NIOSH lifting equation. Controlling the stressors related to a lifting task using NIOSH lifting equation RWL parameter (adapted from Waters et al., 1993).

$$RWL = LC \times \overbrace{\left(\frac{25}{H}\right)}^{HM} \times \overbrace{(1-(0.003 \times |V-75|))}^{VM} \times \overbrace{(0.82+\left(\frac{4.5}{D}\right))}^{DM} \times (FM) \times \overbrace{(1-(0.0032 \times A))}^{AM} \times (CM) \quad (1.1)$$

where LC is a mass constant (23 kg) that corresponds to the maximum recommended load weight that almost all healthy workers (75% of the females and 90% of the males workers) should be able to lift under ideal conditions, H is the horizontal distance of hands from the midpoint between the ankles at the origin and the destination of the lifting load (25 cm $\leq$ H $\leq$ 63 cm), V is the vertical height of the hands from floor at the origin and the destination of the lifting load (V $\leq$ 175 cm), D is the vertical displacement between the origin and destination of the lift (25 cm $\leq$ D $\leq$ 175 cm), FM is the frequency and duration of lifting, A is the angle that is formed between the line passing from the midpoint of the ankles to the point of projection of the midpoint between the hands on the floor, and the sagittal line at the origin and the destination of the lifting load (0°$\leq$ A $\leq$ 135°), and CM is the quality of the hand to object grasping (good - fair - poor).

The RWL represents the weight in kilograms that the 90% of the healthy workers can lift/low under task specific conditions without increased risk of task related LBDs. To assess the relative risk of a lifting task the lifting index (LI) which is the ratio between the actual load weight to the RWL is used. When the LI is greater than 1.0 there is an increased risk of injury for some fraction of the workforce. When LI is greater than 3.0 then many of the workers would be at risk and

changes on the work design should be held. This procedure is extended also to multi-task manual lifting jobs by calculating the overall LI (Composite Lifting Index - CLI) (NIOSH, 1994).

The lifting model proposed by Hidalgo et al. (1997), is a multiplicative model based on the revised NIOSH equation (Waters et al., 1993) using for lifting tasks. The equation estimates the personal lifting capacit (PLC) and the general lifting capacity (GLC) by taking into consideration several additional multipliers:

$$LC = (W_B) \times (H) \times (V) \times (D) \times (F) \times (TD) \times (T) \times (C) \times (HS) \times (AG) \times (BW) \tag{1.2}$$

where AG is the age factor (yrs), HS is the heat stress (wet bulb globe temperature), TD is the task duration (hrs), W_B is the maximum load acceptable to different percentages of worker population (kg), BW is the body weight (kg), and H = HM, V = VM, D = DM, T = AM, F = FM, C = CM (see Eq. (1.1)). The multipliers have been adjusted in order to accommodate others percentiles more than the 75% of the females and 90% of the males workers that NIOSH lifting equation assume. New multipliers have been introduced in order to be gender-, age-, and fitness-based specific. The authors argued that the model is adequate to be used also for back-to-work decisions.

The EN 1005-2 (2009) standard, applies to the manual handling of machinery, components parts of machinery and objects processed by the machine (input/output) of 3 kg or more. Like in the NIOSH approach it provides a risk index (R_I) which is calculated as the ratio between the actual mass to the recommended mass limit (R_{ML}). The recommended mass limit is estimated by an equation which is based to Eq. (1.1) where three more multipliers have been added:

$$RML = RWL \times (OM) \times (PM) \times (AT)$$

where O_M is the one handed multiplier (if true $O_M = 0.6$, otherwise $O_M = 1$), P_M is the two person multiplier (if true $P_M = 0.85$, otherwise $P_M = 1$) and A_T is the additional task multiplier (if true $A_T = 0.8$, otherwise $A_T = 1$). If the risk index is lesser than 0.85 the risk may be regarded as tolerable. When $0.85 < R_I < 1.0$ there is a significant risk of injury to the operator(s) and it is recommended the redesign of the machinery or to ensure that the risk is tolerable. If $R_I \geq 1$ it means that redesign is necessary, so the design can be improved by changing the multipliers.

Grieco et al. (1997), modified the multipliers of the NIOSH lifting equation in order to contemplate a large number of possible major risk factors (Fig. 1.10) many of which are listed in the Annex to EC Directive 90/629 (1990). The model uses the NIOSH lifting equation but it includes a further discount of 0.6 for one-arm-lifting and 0.85 for more than one operator lifting. Moreover, there is a discount for workers who have WRLBD according to their gender (Fig. 1.10).

Since the other multiplicative models mentioned above can used only for lifting tasks, Shoaf et al. (1997) proposed a multiplicative model similar to NIOSH lifting model but for evaluating lowering tasks in combination with pushing, pulling, and carrying tasks. The model is an adaptation of Snook and Ciriello (1991) psychophysical tables but incorporating biomechanical and physiological sources of stress. The equation estimates the lowering capacity (LOC) as:

- SKOLIOSIS: 20° COBB AND TORSION SCORE 2
  30° COBB AND TORSION SCORE 1+
- BAASTRUP'S SYNDROME
- SCHEUERMAN'S DISEASE
- KLIPPEL-FEIL'S SYNDROME
- SPONDYLOLISTHESIS OF 1st DEGREE of SPONDYLOLISYS
- HEMI-SACRALIZATION WITH PSEUDO-ARTICULATION
- STENOSIS OF MEDULLARY CANAL
- SERIOUS LUMBAR DISCOPATHY
- INVERSION OF LUMBAR LORDOSIS WITH DISCOPATHY
- SLIGHT VERTEBRAL INSTABILITY (10-15%)

These kinds of disease must be excluded permanently from tasks with manual handling of loads higher than loads in figure.
Frequency: 1 lifting every 5 minutes for 4 hours (non-continuative task).

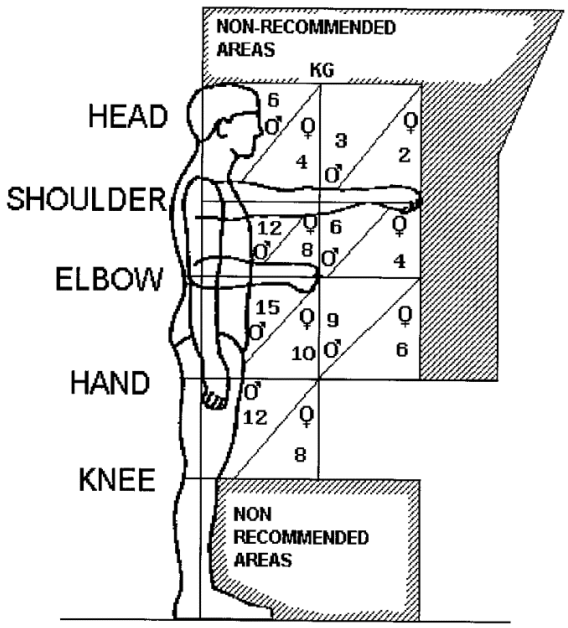

Figure 1.10 Lifting assessment with Grieco's lifting equation for workers with WRLBD (adapted from Grieco et al., 1997).

$$LOC = (W_B) \times (H) \times (V) \times (F) \times (AG) \times (TD) \times (BW)$$

where W_B is the maximum load acceptable to a specified percentage of worker population (kg) and is also a function of level of lowering height (for the other multipliers see Eqs. (1.1) and (1.2)).

The University of Michigan University of Michigan 3D Static Strength Prediction Program (3DSSPP) software (Fig. 1.11) predicts the percentile of the working population that is capable of performing the task according to the NIOSH (1981) recommended limits for percent capabilities (percent of the population with sufficient strength) (3DSSPP, 2012). The mathematic model uses the condition of static equilibrium to derive the compression and shear forces and rotating moments of force acting on the L4/L5 and L5/S1 vertebrae, the strength percent capable of the wrist, elbow, shoulder, torso, hip, knee and ankle, the moments of force due to body weight and external applied

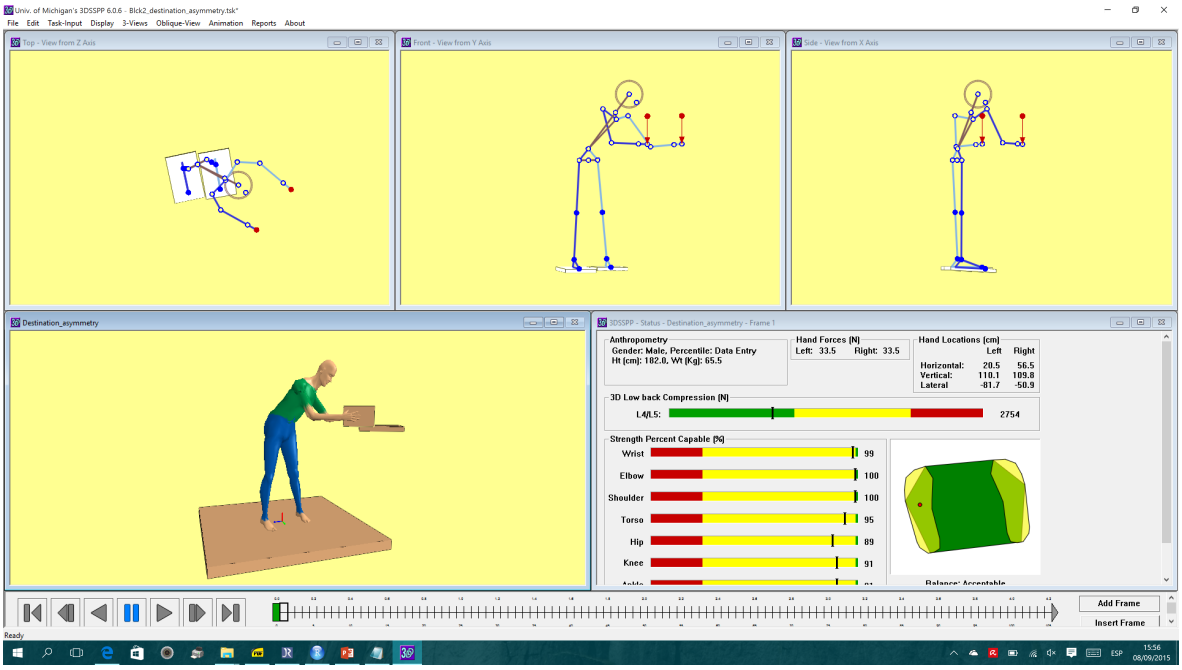

Figure 1.11 Lifting assessment with the 3DSSPP software.

loads, percent of maximum voluntary contraction of the required effort at each joint. Moreover, it predicts a balance index (the projection of the center of mass to the base of support). 3DSSPP can be used for static or slow motion lifting tasks and lowering tasks.

The ACGIH TLV guideline (Marras and Hamrick, 2006), estimates threshold limit values under which workers may be repeatedly exposed without developing WRLBD associated with repetitive lifting tasks and the OSU/BWC guideline (Hamrick, 2006) includes guidelines for workers with WRLBD. The threshold limit values are limited to tasks performed within 30°of the sagittal plane. Like the NIOSH model, it accepts only two-handed lifting tasks from one operator. However the scientific rationale was based to the most recent scientific studies. Therefore, not only includes biomechanical data from the NIOSH sources but also from studies with EMG-driven biomechanical models. Trunk kinematics have also been taken into consideration. The rationale of the guide is the load-tolerance criterion for cumulative disorders. The ACGIH TLV guideline consist of three charts that are used to determine the TLV in function of lifting duration and lifting frequency. Then, the workplace factors are included (lifting height and horizontal distance) and the TLV is calculated. Sometimes the chart cannot indicate safe limit for repetitive lifting tasks under specific conditions. The OSU/BWC guideline is based on the work of Marras et al. (2001) postulated that operators with LBD experience higher spine loading than for asymptomatic operators due to muscle coactivation. The guideline provides three charts for quick guide (Fig. 1.12). The inputs of the OSU/BWC guideline are the status of the worker (health or WRLBD), asymmetry angle, horizontal distance, vertical distance (as described by NIOSH lifting equation). Three charts are provided depended of the asymmetry angle (0-30°, 30-60°, and 60-90°).

The iLMM risk assessment model developed by (Marras et al., 1993) uses trunk kinematics data (maximum sagittal angle, average twisting velocity, maximum lateral velocity) recorded by the

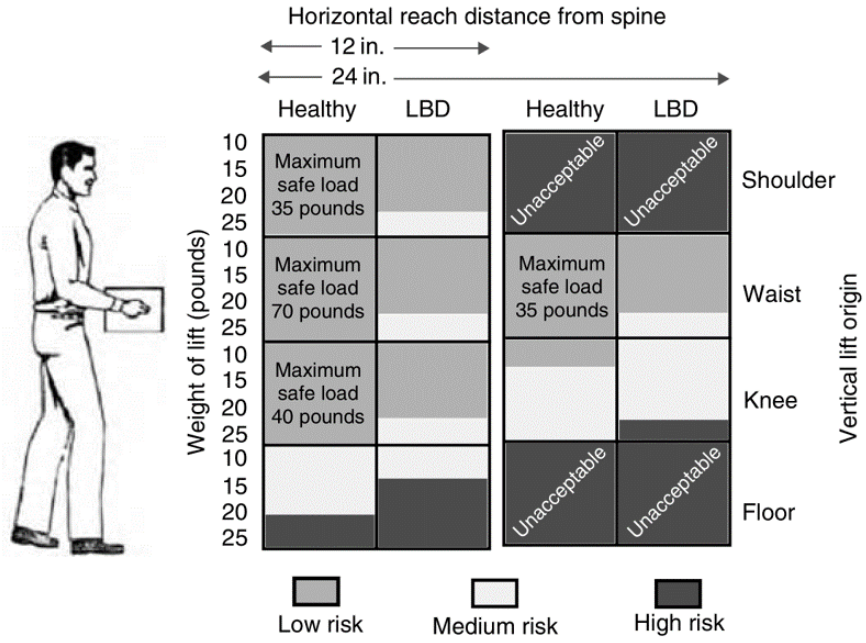

Figure 1.12 The chart of the OSU guidelines for asymmetry of 0-30°(adapted from Hamrick, 2006).

Figure 1.13 The LBD risk model together with the exoskeleton attachment iLMM.

exoskeleton attachment iLMM together with the lifting rate and maximum moment lift, to estimate the likehood of a repetitive lifting task without job rotation to be considered high or low risk for development of WRLBD. The model overcome the drawbacks imposed by the static biomechanical models used directly or indirectly in the others assessment tools, however, is limited to workers who perform repetitive jobs without rotations. Accordingly, for heavy lifting tasks in static akward postures may cannot identified the corresponding risk. The output is a risk percentage, the average probability for LBD with the individual risk values of the input factors (Fig. 1.13).

Physical demands assessment tools were used in both primary and secondary prevention under an engineering control aproach to predict the level of risk presented to a given population of workers and then to minimize or elimimate it. However, these tools cannot measure the impact of physical factors to the performace of a given worker since are not person-specific models. Among the physical demands assessment tools, the iLMM come closest to provide an individual assessment

of risk because it can account for the dynamic components of task demands in addition to the external loads the worker is exposed. The rest of the tools are unable to consider the effects of dynamic movements upon risk. Common drawbacks that share these tools are: (I) physical work factors interact with nonphysical factors (organizational, psychosocial and individual) and *influence rectruitment patterns of muscle activations*, (II) kinetic imbalance is not measured or cannot be predicted[4], and (III) mean task demands and/or mean physical capability values are used to predict risk level[5]. To overcome these drawbacks, person-specific biomechanical models of varying complexity have been developed to capture individual muscle coordination variability (Arjmand, Shirazi-Adl, and Parnianpour, 2008; Cholewicki and McGill, 1996; Grenier and McGill, 2007; Kingma et al., 2006; Marras and Sommerich, 1991a,b; McGill, 1992; McGill and Norman, 1986; Tafazzol et al., 2014; Van Dieën, Kingma, and Van der Burg, 2003). The basic difference among these biomechanical models relies on the assumptions and the mathematical approaches that had been used to estimate trunk muscle forces due to the kinetic redundancy of trunk musculoskeletal system (Ayoub and Woldstad, 1999; Jinha, Rachid, and Herzog, 2006; Kee and Chung, 1996). EMG-driven biomechanical models were used to assign the force generated by a given trunk muscle in manual material lifting and lowering conditions.

1.7. Previous Research

Previous studies of our research group (BioẼrgon, Biomechanics of Human Movement and Ergonomics Lab.), suggested that the NIOSH 1993 revised lifting equation (Waters et al., 1993) should take into consideration also aspects of movement technique (i.e., balance maintenance) when it is used to quantify the risk for development of WRLBD (Gianikellis et al., 2008). A 2^{k-1} fractional factorial design experiment with four factors (vertical displacement, horizontal displacement, asymmetry, and type of load; two level each) was ran indicating that the relative amount of muscle activity (RMS_{EMG}) and consequently of muscle effort is dependent on the levels of the above factors and their combinations. Furthermore, a correlation analysis showed significant positive pairwise correlations between individual muscles RMS_{EMG} (erector spinae and upper trapezoid), and between individual muscles RMS_{EMG} and centre of pressure (COP) parameters across lifting and lowering tasks. As COP, by definition[6], is dependent on more than one variable (i.e., muscle activation patterns) and furthermore these variables are also correlated (e.g., coactivations) (Winter et al., 1993; Winter, 2009) pairwise correlation may lose its power or show untrue linear scales. Therefore, the question that was arised by this study was how trunk muscle activation patterns covariation affect COP trayectory (and COP parameters). This question can be addressed by using the theory of uncontrolled manifold (UCM) (Scholz and Schöner, 1999) reviewed by (Latash, Scholz, and Schoner, 2007). The UCM theory uses the *nullspace* formalism to analyze coordination strategies for minimizing the influence of external or internal perturbances (Burdet, Franklin, and Milner, 2013; Latash, 2008b).

[4] In 3DSSPP, muscle activation patterns have a unique 'optimized' solution (due to kinetic redundancy) valid for all workers (or for the same worker) who perform(s) replications of the same lifting or lowering task in terms of origin-destination state and load weight.

[5] Since are not person-specific models

[6] COP is the neuromuscular response to body sway.

1.8. The Problem of Motor Redundancy on Ergonomics

Mirka and Marras (1993), showed that although muscle activity of trunk muscles varied significantly among repeated lifting trials, the changes were coordinated so that the external torque produce by the muscles together was relatively constant and have little effect on net spinal compression. Granata, Marras, and Davis (1999) showed that experience workers present higher trial-by-trial variability of spine loading than inexperiences workers during repeated lifting and lowering tasks. Moreover, workplace factors influence the kinematic, kinetic, and myoelectric variability among participants who perform identical lifting tasks in terms of load weight and origin-destination state, and consequently the spine loading magnitudes and the variability in spine loading (Granata, Marras, and Davis, 1999; Mirka and Baker, 1996).

Bernstein (1930) (cited in Aruin and Bernstein, 2002) postulated that the biomechanical rationalization of lifting tasks[7] is based on the DOF problem (Fig. 1.14). The apparently muscle redundancy offers numerous option in how trunk muscles can be rectruited to perform a task—i.e., *kinetic redundancy*. Improper muscle activation patterns influence spine loading either directly by kinetic imbalance[8] and coactivation of antagonistic trunk muscles or indirectly by tuning spine stability[9]. Kinetic redundancy represents the cornerstone of biomechanical rationalization of manual material lifting and lowering tasks because of the possibility to create kinetic imbalance and spine instability that potentiate the precipitation of WRLBD (Kumar, 2001; Marras, 2008; McGill, 1997, 2007). Moreover, motor redundancy that arises by the numerous DOF of the human locomotor apparatus compared with the substantially lower anatomical constraints that are imposed by the structure of the musculoskeletal system at joints' level, gives to the workers the possibility to adopt an infinite number of postures during lifting or lowering tasks and consequently the ability to execute a countless voluntary motor patterns in order to accomplish their labor activities—i.e., *kinematic redundancy*. However, not all of the possible postures that the worker can adopt nor all of the movement patterns that can be executed are healthy. On one hand, there are certain ones, that given the constraints imposed by (I) anthropometric characteristics, (II) the natural limits of motor and sense system capabilities, (III) work design, (IV) man-task-environment system interaction and (V) the required performance of the intended operation, cannot be adopted or executed voluntarily by the workers (Delleman, 2004; Smith et al., 2014). On the other hand, there are postures and motor patterns, that even if it is possible to be adopted and executed by the workers they have to be avoided, because the mechanical stresses that are generated on tissues can exceed tissues' stress tolerance limits and lead to mechanical disruption of spinal support structures giving rise to WRLBD (Kumar, 1999, 2001; Marras, 2000; Waters et al., 2006; Waters, 2006). Workplace layout has to take into account the ability of the "neural controller" to organize the abundant DOF of the locomotor apparatus into purposeful actions.

According to ISO 11228-1 (2003) standard, the reduction of the risk of injury, when lifting manual tasks are unavoidable, can be achieved by the (re)design of the job (task, workplace and organization), of the manipulated object and of the work environment by taking into account the

[7] The organization of a lifting task according to biomechanical principles in order to increase efficiency.
[8] Kinetic imbalance provokes jerky contractions.
[9] A trade-off exists between coactivation and spine stability.

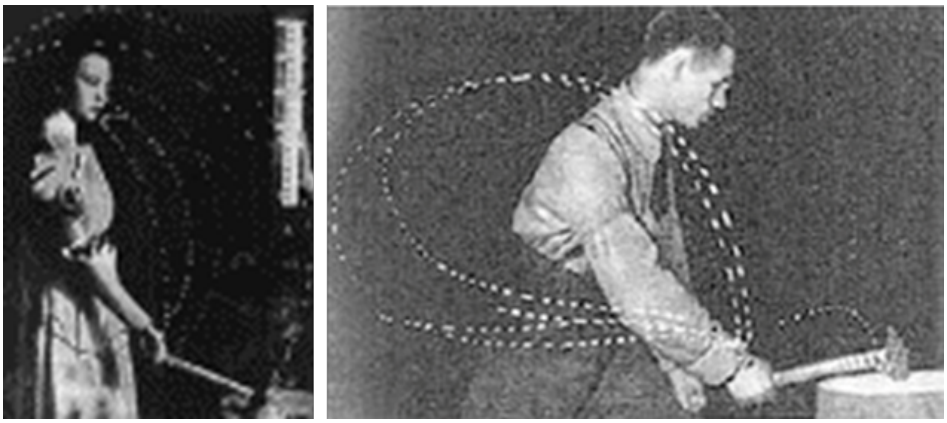

Figure 1.14 Motor learning and variability in Bernstein's *repetition without repetition* concept. Bernstein himself viewed the problem of "elimination" of redundant DOF as the central issue of motor control (Bernstein, 1967).

physical limitations and capabilities of the workers. Bernstein (1930) (cited in Aruin and Bernstein, 2002), defined this procedure of ergonomic intervention as the *normalization* of the work process or the ratio of job's demands to worker's performance capability. Moreover, Bernstein (1930) had included in his ergonomic framework the *biomechanical rationalization* of operations based on the DOF problem (reviewed in Bernstein, 1967) rather than on western scientific management of work design (Taylorism, Therbligs, etc. (reviewed in Keyserling and Chaffin, 1986)). The biomechanical rationalization of an operation process consisted in identifying a **physiologically feasible motor complex solution in order to achieve a goal with minimal effort and discomfort on the part of the worker** (Bernstein, 1930). Although the biomechanical approach is the fundamental part of physical ergonomics and workspace design, as it has an explicit hypothesis of injury mechanism linked to it (Dempsey and Mathiassen, 2006), biomechanical rationalization is linked mostly with the *motor control* process of voluntary movements and how it is influenced by work-space or task design (Bernstein, 1930).

The number of the available DOF are larger than the constraints imposed by the motor task together with the worker constraints. Therefore, the biomechanical rationalization of lifting objects at work has to take into account the abundance of DOF and to be treated as a motor control problem, where the "neural controller" is trying to identify a physiologically feasible motor complex solution in order to achieve a goal with minimal physical effort and discomfort on the part of the worker (Bernstein, 1930, 1967, 1996). Lifting and lowering technique can, therefore, be defined as the biomechanical and motor control solution of the lifting motor task problem that entails minimization of the mechanical stresses on joints, structures and of the soft tissue effort, and smoothness maximization of trunk movements and load trajectories, while synchronously balance control is maintained. Moreover, it should be *useable*, in sense that it has to be applicable to a specific restricted workplaces by most of the workers. The exploration of how the neural controller coordinates the excessive DOF during lifting and lowering tasks can help to improve worker performance and product usabilty including systems and tasks for productive, comfortable and safe human use.

The ergonomic approach that is proposed by the ISO 11228-1 (2003) standard determines whether the technique that workers used in lifting or lowering tasks is adequate or not: workers should maintain body balance and use the minimum amount of physical effort to achieve a smooth, uninterrupted and completely controlled motor activity, while they hold by two hands the load as close to the body as possible, and synchronously avoid trunk rotations and stooped postures. However, when they are lifting unstable loads, a trade-off exists between *effort minimization* and *smoothness maximization* of load trajectories and trunk movements as the co-activation of the muscles of the trunk has been interpreted as serving both movement control and trunk stability at the expense of the increased compression forces at a lumbosacral intervertebral disk (L5/S1) (Graham, Sadler, and Stevenson, 2012; Van Dieën, Kingma, and Van der Burg, 2003). Lifting unstable loads, compared to stable loads, increased muscular activity about the selected trunk musculature (Matthews et al., 2007; Pinto et al., 2013), but did not increase thoraco-lumbar kinematics (Matthews et al., 2007) or local dynamical stability of 3D lumbar angle quantified using the maximum finite-time Lyapunov exponent (Beaudette, Graham, and Brown, 2014).

Effort minimization is summarized with the criterion of *load-tolerance* and reflects the interaction between the muscular tension generated by trunk muscles, external forces and compression forces experienced by a L5/S1, and with the criterion of *muscle force capability* (NIOSH, 1981, 1994): the compression force that experienced by the L5/S1 as well as the muscular force required to perform lifting tasks cannot exceed tissues tolerance. In this sense, biomechanical modelling of low-back is used to estimate the mechanical stresses placed upon the internal structures during lifting and lowering tasks, and to obtain further insight into how these stresses are influenced by the combination of the external forces at the joints, and by the internal forces created by muscles and connective tissues due to reactions of the body to the external forces, and hence to predict, whether the mechanical stress will lead to damage of L5/S1, and moreover, whether worker's muscle strength that produces moment of force at the L5S1 equates the required muscular moment that generated at the L5/S1 (Ayoub and Woldstad, 1999; Chaffin, 1997, 2009; Marras, 2008). Biomechanical studies explored the relationship between external loads and biomechanical loading.

Smoothness maximization of load trajectories and of trunk movements can be summarized with the criterion of *smoothest discrete movement* proposed by Hogan and Sternad (2007) and reflects the problem of mastering the redundant DOF at any level of the motor control hierarchy at the presence of internal or external perturbations (motor variability) (Bernstein, 1984) and the ability of a central nervous system (CNS) to modulate the activation of the trunk muscles to ensure, on one hand, the control of movement and posture in order to maintain trunk motion at the desired path and, on the other hand, to provide the required stiffness to maintain mechanical stability of the lumbar spine system at every DOF (Hodges, 2004; Marras, 2008; McGill, 2007; Parnianpour et al., 1999; Scholz, 1993a). Spine traumatisms are related with the accelerations that undergoes the spine and the reflex responses or co-activation of trunk muscles as result of it (Cresswell, Oddsson, and Thorstensson, 1994; Oddsson et al., 1999; Santos et al., 2011; Van der Burg and Van Dieën, 2001a) and with the spine buckling when the value of the muscle stiffness that is needed to maintain mechanical stability is below an acceptable level (Bergmark, 1989).

Ergonomic intervention on manual lifting and lowering objects at work can, therefore, be regarded as a motor control problem, as well.

1.9. Assessment of Motor Redundancy: Synergies

Due to joint coupling, muscle activation on both involuntary (due to external or internal perturbations) and voluntary movements, produces moments of force not only to the joint that muscle spans but also to remote joints, therefore, other muscle activations should counterbalance the undesired moments. Therefore, muscle coordination is required to make purpuseful movements. Control motor provides tools to describe muscle coordination. Of course, this is a DOF problem as muscle space have as many DOF as the number of the skeletal muscles. On the other hand, the neural controller should be able to manage the excessive DOF in order to produce the desired movement. A current hypothesis suggests that "neural controler" simplifies control by formulating muscle synergies, a coordination group of muscles. Although NIOSH (1981) points out the difficulty that is supposed to be for the worker to control dynamic actions that result to high inertial forces, and is aware that with fast motions the ability of the "neural controller" to coordinate the many trunk muscles necessary to stabilize the spinal column is stressed , there is a lack of scientific studies that take into account the motor control of lifting and lowering tasks providing, therefore, inspiration for new man-task-environment system interaction designs, as well as more targeted ergonomics assessments.

1.9.1. Dynamical Systems Theory

The dynamical system approach to movement is a physical law-based mathematical structure describing and predicting the spatiotemporal interlimb coordination across different coupling (interaction) media involved in the coordination (Kelso and Engstrøm, 2006). The basis of the dynamical system approach to movement was introduced by Kugler, Kelso, and Turvey (1980, 1982) who linked the theoretical subfields of homeokinematic physics (Iberall, 1977), nonequilibrium thermodynamics (Morowitz, 1968; Prigogine and Nicolis, 1971), catastrophe theory (Thom, 1969), synergetics (Haken, 1977), and the theory of "well-organized" systems (Gelfand and Tsetlin, 1962, 1971) to the *redundancy* of the DOF as described by (Bernstein, 1967). The experimentally discover of spontaneous pattern formation in rhythmic intelimb movements by Kelso (1984) and the mapping of these patterns onto the concept of synergetics by Haken (1999) and Haken, Kelso, and Bunz (1985), gave rise to a phase-space reduction, where the dynamics of a lower dimensional variable (the collective variable or order parameter) of the neuromuscular system can be described in terms of nonlinear behavior (hysteresis, bifurcation, stability, intermittency). A collective parameter that is able to characterize the behavioral pattern of two rhythmically moving segments was found experimentally to be the relative phase between them, whose nonlinear dynamics can be modelled mathematically by two coupling nonlinear point oscillators. The relative phase not only reduce system's dimensionality but also incorporate information about the position and velocity of the coupled joints. The values of a system's collective parameter corresponds to its patterns or synergy. *Synergy* or coordinative structure in the dynamical systems approach

was defined as a dynamic pattern (a dissipative structure) that "expresses a stable steady state maintained by a flux of energy, that is, by metabolic processes that degrade more free energy than the drift towards equilbrium" (Kelso, 1995). Coordinative structures are functional units in the sense that the individual DOF constituting them are constrained by particular purposeful behavior goals. Control parameters are factors that are able to change the functional state of the identified pattern. When the control parameters changes its values (e.g., frequency is identified as a control parameter) the system may remain in the same basin attractor, hence, it exhibits hysteresis, or nonequilibrium phase transitions may occur and transition of the system between different atractors take place. Information, in a broad sense, is a coupling medium that can specify required coordinative relations, therefore, collective variables are of informational nature. Following the information-based ecological perception-action approach to the control of behavior (Gibson, 2014; Turvey, 1977), perception-action coupling forms coordination patterns that can be mapping them onto attractors and characterize their nonlinear dynamics (Kelso, DelColle, and Schöner, 1990). All these concepts, finally, have used to define the broadly concept of coordination dynamics, or the science of coordination, developed to describe the laws, principles, and mechanisms underlying coordination from micro-to-macro (Kelso and Engstrøm, 2006). Coordination dynamics are (I) the coordination patterns that arise in a self-organized fashion (self-organizing dynamic patterns) and (II) their spatiotemporal evolution (stability, loss of stability, etc), which is described by nonlinear dynamical laws (pattern dynamics) (Kelso and Engstrøm, 2006). Self-organization correspond to the creation of new or different patterns after transition take place.

Motor coordination in lifting and lowering tasks have been investigated experimentally under the coordination dynamics approach. Some studies identified coordination patterns (in-phase and anti-phase patterns), where other studies were focused to nonlinear dynamics of the patterns that characterize system's motor variability. Quantifying the coordinative patterns and variability of manual material lifting and lowering motor actions in terms of dynamical systems theory can be helpful to understand the working techniques that place the lifter at higher risk of developing WRLBD (Bartlett, Wheat, and Robins, 2007; Hamill, Palmer, and Emmerik, 2012; Srinivasan and Mathiassen, 2012; Stergiou and Decker, 2011).

It was showed that load weight influence spatiotemporal coordination between joint pairs, in particular lumbar spine lags further behind knee extension when lifting heavier loads (Burgess-Limerick, Abernethy, and Neal, 1991, 1993; Burgess-Limerick et al., 2001; Scholz, 1993a,b; Scholz and McMillan, 1995). Scholz (1993a), analyzed the motor variability of the individual work-technique and suggested that the increased variability of the motor patterns that were observed during lifting tasks may reflect the difficulty to maintain them stable in the face of increasing load weight, especially when such motor patterns are subservient to precise trajectory accuracy control. Lowering and lifting tasks did not showed the same coordination patterns. However, the observed coordination changes could not be characterized as phase transitions. Scholz (1993b), was investigated whether relative timing between joint movements remain invariant across load weight changes. It was supposed that the discovery of relational invariants could gain insight into coordination strategies of lifting and lowering tasks. Significant load effeccts found for relative time measures. However, the observed coordination changes could not be characterized as phase

transitions since stability stayed unchanged.

Scholz and McMillan (1995), postulated that for a safe lifting using the squat method, the 45% of the maximum lifting capacity could be considered as an adequate upper limit of load effort, as above of this limit the motor patterns are difficult to be maintained stable. It was suggested that variability of the motor patterns during the lifting tasks is caused mainly by differences on the motor control regulation rather than of the inertial effects of the load's mass (Scholz, 1993a; Scholz and McMillan, 1995). Scholz and McMillan (1995) showed that differences in the coordination among subjects appear to be at the beggining to the lifting task, at the accelerative phase.

Burgess-Limerick et al. (2001), showed that during lifting and lowering tasks, in self-selected speed, spontaneous transitions occured between stoop (anti-phase) and squat (in-phase) techniques as the lifted height was changed. In the lowering tasks, transitions from stoop to squat were observed, whereas in the lifting tasks the transitions were from squat to stoop. Control parameters were not possible to identified. It was supposed, that a trade-off between workplace factors (initial load height and lifting speed) and a trade-off between biomechanical and motor control costs and benefits of the observed movement patterns induced the phase transition from one pattern to another.

Motor variability according to the dynamical systems approach was modelled and viewed as "colored" noise (Fuchs and Kelso, 1994; Haken, 1999; Haken, Kelso, and Bunz, 1985; Schmidt and Turvey, 1995; Schöner, Haken, and Kelso, 1986). According to Haken (1999) variability (or critical fluctuations in Haken's terminology) is typical for nonequilibrium phase transitions which occurs when self-organization happens. Motor variability is obligatory in order to be formed a self-organizing system. Nonlinear tools that are used to quantify motor variability includes power frequency, Lyapunov exponents, dimensions, entropies, detrended fluctuation analysis, fractals, surrogates, etc. (Kay, 1988; Kelso and Engstrøm, 2006; Kelso, 1995; Stergiou, 2004).

Graham and Brown (2012) and Graham, Sadler, and Stevenson (2012), investigated whether spinal local stability during repetitive lifting and lowering tasks is influenced by varying the weight load and lifting speed by quantifying local dynamic stability of the lumbar spine angle time-series using finite-time Lyapunov exponent. Lyapunov exponents is a nonlinear stability parameter that represents the average exponential rate of divergence of nearest neighboors in state space, portraying how the systems responds to an extremely small perturbations. It was showed that weight load influence spinal stability in terms of reducing finite-time Lyapunov exponents indicating that it was more difficult to perturb system dynamics away from the target equilibium trajectory when heavier load is carried. However, lifting speed did not influence local stability. It was concluded that instability increased due to low task demands, which exchibits less muscular demands and less trunk stiffness. Instability, as measured by short-term finite-time Lyapunov exponents, was increased when moving up the kinematic chain (from ankle to upper back joints), indicating that ankle joint stability is used to control trunk centre of mass (COM) perturbations (Graham et al., 2011). Except work-design factors like load's weight, lift height and speed of lifting load, individual factors like work experience was showed to influence local dynamic stability of lumbar spine as well, with experienced worker to exhibit higher spinal local stability quantified

using Lyapunov exponents (Lee and Nussbaum, 2013).

Coordinated movements are expected to show two features that seem hardly compatible: Stability of performance in the presence of unavoidable unpredictable changes in the environment and within the neuromotor system, and flexibility of performance in cases of quick modifications of the task and/or major changes in external conditions. The former aspect of coordination has dominated movement studies. Correspondingly, coordination has been frequently quantified using indices that describe stability of the systems behavior. However, coordinated actions may be purposefully organized to destabilize aspects of motor behavior if the context requires quick modifications of important performance variables. Coordination may also have, as a goal, a perceptual effect(as in some sports such as figure skating and synchronized swimming) or a complex perceptual-motor effect that cannot easily be formalized (as in a stretching exercise).

1.9.2. Uncontrolled Manifold Hypothesis

According to the principle of motor abundance, which was introduced by Gelfand and Latash (1998) followed the ideas of Gelfand and Tsetlin (1962, 1971), the DOF of a neuromotor level are participated all in the voluntary motor tasks assuring both stability and flexibility by formulating synergies. Synergy has been defined as a task-specific neural organization of a set of elemental variables (DOF) that organizes (i) sharing of a task among them and (ii) ensures certain stability/flexibility features of the performance variables, whereas elemental variables have been defined as those DOF whose values can be changed by the controller while keeping the values of other DOF unchanged, and the performance variable has been defined as a particular feature of the overall output of the multi-element biological system that plays an important role for a group of tasks (Latash, Gorniak, and Zatsiorsky, 2008; Latash, 2008b; Latash, Scholz, and Schoner, 2007). Under this approach, synergies can be quantified using the framework of the UCM hypothesis (Latash, Scholz, and Schöner, 2002; Scholz and Schöner, 1999). Briefly, the UCM hypothesis maps the variance of the elemental variables onto the performance variable variance, and therefore separates the combination of solutions (elemental variables) that are equally able to solve the motor task problem (performace variable) within an acceptable margin of error for those solutions that are irrelevant of the ongoing task (Latash, Scholz, and Schöner, 2002; Scholz and Schöner, 1999). Synergies have been defined at every neuromotor level (Latash, Scholz, and Schoner, 2007).

As suggested by Bernstein (1967, 1996) and further developed by Gelfand and Tsetlin (1962, 1971) and Gelfand et al. (1971), the motor control mechanism exploits the available *synergies* in order to deal with the seemingly infinite number of neuromotor choices that it possesses and thus to assure a coordinated voluntary movement. Therefore, taking into account that all neuromotor levels are interconnected by numerous types and grades of cybernetical processes (Bernstein, 1967; Houk and Henneman, 1967; Wiener, 1985), it is hypothesized that the motor control mechanism regulates any voluntary movement by settling all the available DOF of an hierarchically lower neuromotor level into purposeful task-specific structural units in order to ensure the correct function of particular performance variables which are assigned to the structural units by the higher hierarchically neuromotor level (Gelfand and Latash, 1998; Gelfand and Tsetlin, 1971; Latash, 2010; Latash, Gorniak, and Zatsiorsky, 2008; Latash, 2008a,b; Latash, Scholz, and Schoner,

2007).

Thereby, the higher hierarchically neuromotor levels it is supposed to be responsible to set in advance the performance variables, but not in a prescriptive way as originally it was suggested by Bernstein (1967), but rather experimentally by selecting from a set of all possible combinations the ones that enable the biological system to attain its goal within an acceptable time and by means of a sufficient economy as Gelfand and Tsetlin, 1962 proposed, where the lower hierarchically neuromotor levels have to ensure its correct execution according to the *principle of minimal interaction*, which states that the interaction among elements (DOF) at the lower levels of hierarchy is organized so as to minimize the signals that the structural unit receives as a whole from the hierarchically higher neuromotor level and from the environment, and also to minimize the external inputs to each of the elements of the structural unit, as well as the interaction between them, in order to keep the elements' outcome at the lowest possible value compatible with the task (sharing pattern) (Gelfand and Latash, 1998; Gelfand and Tsetlin, 1971; Gelfand et al., 1971; Latash, 2008b).

Thus, following the principle of minimal interaction, if an element(s) introduces an error into the common output of the structural unit that it belongs to, provoked either by external or internal perturbations, another element(s) change(s) its contribution to the common output in order to minimize the error and therefore to introduce both (i) *stability* of the motor performance (error compensation in accordance with the principle of minimal interaction) and (ii) *flexibility* of the motor pattern to deal with concurrent tasks and/or possible perturbations (mechanical and/or neuromotor) that typically are caused by the unforeseeable environments where usually the voluntary movements are executed in.

Thus, it is suggested that the motor control mechanism make use of the motor abundance to solve the motor redundancy problem, and does not eliminates or freezes the excessive DOF according to certain optimization criteria as originally was suggested by Bernstein (1967). This forms the principle of motor abundance which was introduced by Gelfand and Latash (1998) followed the ideas of Gelfand and Tsetlin (1962, 1971) and which states that the DOF of a neuromotor level are never eliminated or frozen, rather they are participated all in the voluntary motor tasks assuring both stability and flexibility by formulating synergies. Therefore, *synergy* (or structural unit) has been defined as a task-specific neural organization of a set of elemental variables (DOF) that organizes (i) sharing of a task among them and (ii) ensures certain stability/flexibility features of the performance variables, whereas elemental variables have been defined as those DOF whose values can be changed by the controller while keeping the values of other DOF unchanged and the performance variable has been defined as a particular feature of the overall output of the multi-element biological system that plays an important role for a group of tasks (Latash, Gorniak, and Zatsiorsky, 2008; Latash, 2008b; Latash, Scholz, and Schoner, 2007).

Coordination is defined as the purposeful pattern of actions by a set of effectors (Latash, 2009) and is related with the DOF problem which is presented at any level of the neuromotor hierarchy. At the kinematic level coordination refers to the behavior of the spatiotemporal relationship among segments. Henceforth, a coordinate motor pattern can be viewed as a purposeful pattern of actions

by a set of elemental variables (a set of DOF) which are characterized by a certain irreducible level of neuromotor variability in their outputs. Thus, according to the principle of motor abundance, a masterful work-technique of the lifting/lowering tasks has to be a combination of solutions that are equally able to solve the motor task problem within an acceptable margin of error (Latash, 2008a,b). This combination of skilled solutions should reflected in the "good" variability (V_{UCM}) of the motor patterns when the same task is repeated. On the other hand, covariation patterns of the elemental variables that affect important characteristics of the performance variable and are irrelevant of the ongoing task are tried to be limited by the controller as they are reflected "bad" variability ($V_{\perp}$). Thereafter, motor pattern's variability according to the UCM is not regarded as a biological system's "noise", but as a direct consequence of the motor abundance (Latash, Scholz, and Schöner, 2002). It is an intrinsic feature of the established synergies which corresponds to the error compensation of their elements and to the flexibility feature that they possess. This means that neuromotor variability possesses structure, and its analysis can gain important information regarding the complex behavior of the human motor system. In this sense, the main goal of a synergy is to try to make most variability "good" (V_{UCM}). Hence, the analysis of the motor variability can be used to gain insight into the way synergies are structured and what action they are trying to accomplish (Latash, 2008b).

1.9.2.1. Muscle Synergies or Muscle-Modes

A motor primitive is an hypothetical variable at the motor control level and is defined as a network of spinal neurons that activates a particular set of muscles in order to realize a purposeful movement (Degallier and Ijspeert, 2010). Looking for a low dimensional space to regulate movement, it is hypothesized, that there is an hierarchical level on the spine where a neural organization called central pattern generator is able to produce a rhythmic activity pattern without phasic sensory feedback. Recent studies found differences between rhythmic and discrete movements at neural level suggesting that are subserved by different control mechanisms (Schaal et al., 2004). Discrete movements have been defined as those that "preceded and succeeded by postures and occupies a non-negligible duration containing no posture" (Hogan and Sternad, 2007). On the other hand, rhythmic movements are timed repetitive movements that do not have such distinguishable endpoints and can be classified into a broad categories based on their differences from a periodic sinusoidal function. Lifting and lowering tasks have been considered both as a rhythmic and discrete movements. Motor promitives are related conceptually to M-modes.

Researh suggests, that the motor control mechanism exploits the available synergies in order to deal with motor redundancy and thus to assure coordinated voluntary movements. The control of multi-muscle synergies assume a two-level hierarchy. At the lower level the muscles form groups within which the neural controller scales the activation level in parallel either in time on the course of performing an action, or in space across actions with different parameters (Alessandro et al., 2013; Bizzi and Cheung, 2013; Krishnamoorthy et al., 2003; Latash, 2012; Latash et al., 2005; Ting, 2007; Ting and Chvatal, 2011). Such muscle groups have been called muscles synergies or M-mode. At the upper level, M-mode covariation is organized in a task-specific manner to stabilize an important performance variable. M-mode variability can be mapped into task-irrelevant or

task-relevant variability. Task-relevant variability does not affect selected performance variables.

M-mode is a set of muscles within which the CNS scales the activation level in parallel either in time[10] or space[11]. Mathematically, a M-mode represents a unitary n-dimensional vector, where n is the number of the muscles formed it and each n-dimension (vector's components) represents the fixed weighted contribution of the n-muscle to the M-mode. A muscle can participate in multiple M-mode. The CNS controls the n-dimensional vector's magnitude by scaling linearly its elements, the weighting coefficients of the muscles (Latash, 2008b; Latash, 2012; Ting, 2007; Ting and Chvatal, 2011). Following Ting (2007) and according the nomenclature of Figure (1.15), the net activation pattern for any given muscle ($\mathbf{m}_{[N\times 1]}$) on the course of performing an action is a linear combination of the sum of the fixed elements of the M-modes vectors $\mathbf{W}_{1\rightarrow k}$ that are structured temporally by the scaling coefficients of the neural commands vectors $\mathbf{C}_{1\rightarrow k}$

$$\mathbf{m}_{[N\times 1]} = \sum_{i=1}^{k} \mathbf{C}_i(t_{1\rightarrow N}) \cdot w_i \tag{1.3}$$

and the activation patterns of all muscles formed the M-modes at any given instant t is

$$\mathbf{m}_{[1\times n]} = \sum_{i=1}^{k} c_i(t) \cdot \mathbf{W}_i. \tag{1.4}$$

Therefore, the activation patterns of all muscles on the course of an action is

$$\mathbf{m}_{[N\times n]} = \sum_{i=1}^{k} \mathbf{C}_i(t_{1\rightarrow N}) \cdot \mathbf{W}_i. \tag{1.5}$$

Several M-modes may form a muscle synergy, i.e., a neural organization that provides stability of a performance variable by co-varied adjustments of its elements, the M-modes (Latash, 2008b; Latash, 2012). Assuming that synergies are organized in a hierarchical control scheme, a M-mode may be viewed as a performance variable itself, stabilized by a lower level synergy that uses firing patterns of individual motor units as elements (Latash, 2008b; Latash, 2012). Assuming that the M-modes are fixed throughout certain task repetitions, whereas their scaling factors are varied (Ting and Chvatal, 2011), the low level synergy ensures that the proportion of the weighted contribution of each muscle on the M-mode does not change. This is equivalent to the notion that the low level synergy stabilizes the direction of the n-dimensional vector within the muscle activation space, and mathematically represents the angles formed between the n-dimensional vectors of the M-mode across tasks and repetitions (Fig. 1.15).

Recently, experiments showed that the organization of muscles into groups in complex whole-body tasks can differ significantly across both task variations and subjects (Danna-Dos-Santos et al., 2009; Frère et al., 2012), but either with similar temporal profiles of the gains at which the M-modes are rectruited (Frère et al., 2012), or with gains that help stabilizing important mechanical variables like COP shifts (Danna-Dos-Santos et al., 2009)—i.e., the ability to organize muscles co-variation

[10] On the course of performing an action.
[11] Across actions with different parameters.

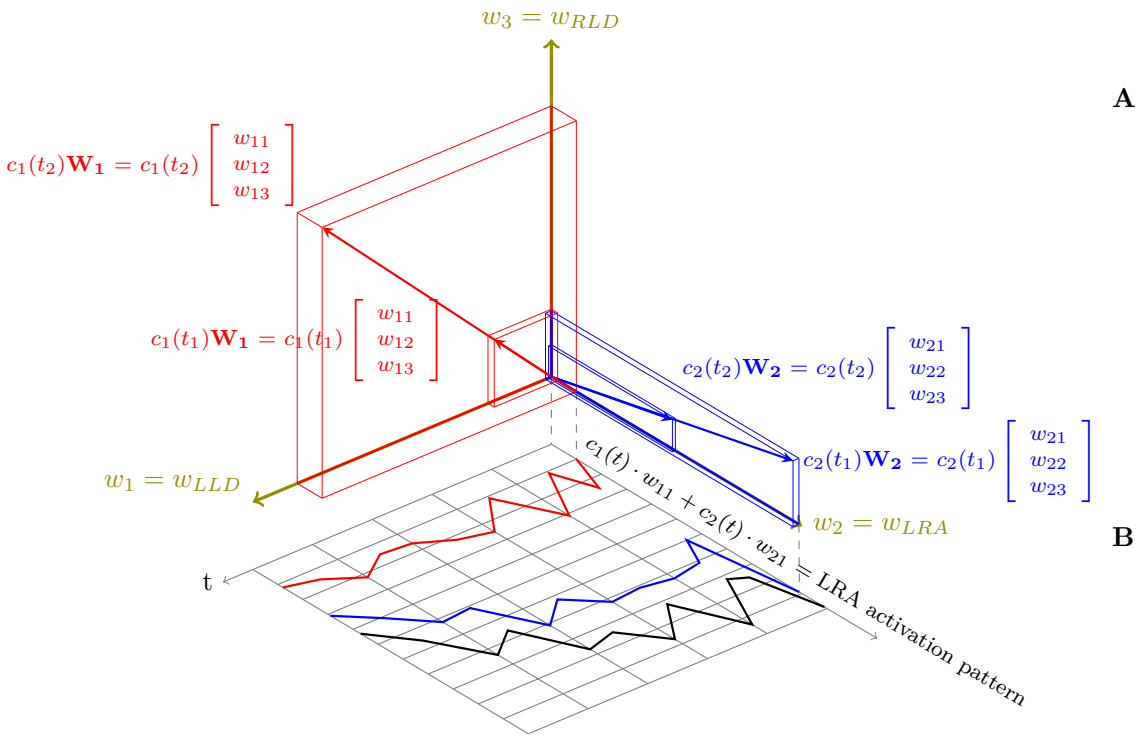

Figure 1.15 (**A**) Geometrical representation of two three-dimensional M-modes $\mathbf{W_1}$ and $\mathbf{W_2}$ (by definition $\mathbf{W_1} \perp \mathbf{W_2}$) that are modulated by two independent neural commands C_1 and C_2 respectively, at two different instants t_1 and t_2. The direction of the M-modes vectors is fixed, while their elements are co-vary linearly over time (or over space). (**B**) Therefore, the LRA muscle activation pattern over time is the combination of two signals which imply two neural commands, i.e., at time t_1 is $\text{LRA}(t_1) = c_1(t_1) \cdot w_{11} + c_2(t_1) \cdot w_{21}$ and at time t_2 is $\text{LRA}(t_2) = c_1(t_2) \cdot w_{11} + c_2(t_2) \cdot w_{21}$. The same happens for the other two muscles. Therefore, it is reduced the dimension of the neural control task to two commands, less than the number of the muscles. The orthogonality of the three dimensional muscle space and between M-modes defines their inter-independence (adapted from Ting, 2007; Ting and Chvatal, 2011).

at higher hierarchical level of motor control. However, by increasing task's complexity M-modes composition can change. It was supposed, therefore, that as the task goes more challenging there are more M-modes to be controlled by the neural controller (Danna-Dos-Santos, Degani, and Latash, 2008). This was confirmed in many studies of human standing. During voluntary body sway, where the body is modelled as a single inverted pendulum, M-modes are robust across subjects stabilizing COP shifts (Danna-Dos-Santos et al., 2007; Klous, Santos, and Latash, 2010). When trunk or arm segments accelerations are involved during body sway, M-modes are no more robust accross subjects or trials, however, there are still stibilizing COP shifts (Danna-Dos-Santos, Degani, and Latash, 2008; Danna-Dos-Santos et al., 2009).

1.10. Research Voids

The literature review revealed voids in the research.

Void I Physical demand ergonomic assessment tools take into consideration worker's biomechanics but not motor control although the common characteristic of all risk factors is their influence on trunk muscle activation patters. Biomechanics alone cannot explain whether the natural limits of workers motor and sense system capabilities are being reached during the manual handling manipulation.

Void II The litetature review revealed that LBD are associated with accelerations that undergoes the spine as a result of trunk muscles activity in response to the loading or in response of postural reactions to balance disturbances. To date, there are no published studies of the effect of external perturbations (e.g. handling liquid loads) during an ongoing voluntary lifting or lowering movement on trunk muscles activation patterns, and whether such perturbations influence the functional outcome of muscles activation patterns or not;

2

Research Questions and Hypotheses

2.1. Research Questions

The main research questions that will be addressed are:

Question I Do trunk muscle activation patterns form a modular network comprising M-modes?

Question II Does the "neural controller" stabilizes task-relevant performance variables that they can increase also the likelihood for spine loading?

Question III Does the ability of the "neural controller" to coordinate trunk muscle activation patterns remains unchanged during lifting or lowering tasks?

Question IV Do the same sets of M-modes that stabilize task-relevant performance variables could be involved also in stabilization of COP shifts?

to modulate the activation of the trunk muscles to ensure, on one hand, the control of movement and posture in order to maintain trunk motion

2.2. Research Hypotheses

It is hypothesized that trial-by-trial trunk muscle activation patterns in motor-equivalent manual material lifting and lowering tasks can be parameterized and analyzed based on the notion of M-mode. M-modes were viewed as elemental variables and was hypothesized that "neural controller" acts in the M-mode space in order to formulate muscle synergies by their combination and to modulate the gain of each M-mode in order to stabilize the time profile of selected performance variables (PVs), which have been used previously to characterize the risk level for development of WRLBD. By using the UCM framework (Latash, Scholz, and Schoner, 2007) we expected to quantify the synergestic control of M-mode for stabilizing the selected PVs, and to determine whether the risk level for development of WRLBD would affect it. Main hypotheses are:

Hypothesis I Trunk muscle activation patterns during lifting and lowering tasks can be described with a few M-modes that are consistent across participants;

Hypothesis II Trunk M-modes form the basis for multi-M-mode synergies stabilizing the time profile of selected performance variables that have been used previously to characterize the risk level for development of WRLBD;

Hypothesis III M-modes and multi-M-mode synergies will differ between lifting and lowering tasks;

Hypothesis IV Multi-M-modes synergies stabilize the shift of the COP while stabilize time-profiles of task-relevant performance variables.

3

Experiment Design and Methods

3.1. Participants

Fourteen physically active students (7 female, 7 male) who were attending under- or postgraduate programs at the Faculty of Sports Science participated voluntary in the study. Participants were excluded if there was a history of musculoskeletal problems or functional mobility impairments. All participants provided informed consent according to the procedure approved by the Review Board of the University of Extremadura (Appendix A).

The mean age, stature and mass (and standard deviation) of the participants was of 22.6 (2.1) years, 68 (9) kg, and 171 (10) cm, respectively. Table 3.1 shows descritive statistics of age and anthropometric characteristics for both genders. Male subjects' height ranged from 50^{th} to 99^{th} percentile stature for Spanish male workforce, while female subjects' height ranged from 5^{th} to 95^{th} percentile stature for Spanish female workforce. The male subjects were in the 5^{th} percentile of body mass index (BMI) for Spanish male workforce, while female subjects were on the the second quartile of BMI for Spanish female workforce, with BMI of about 23 kg/m^2 for both genders (Benjumea, 2001).

Table 3.1 Subjects' characteristics (knee, hip, and elbow height measurements made with their shoes put on).

	Age (yrs)	Mass (kg)	Stature (cm)	Knee height (cm)	Hip height (cm)	Elbow height (cm)
Female (n = 7)	23 (3)	62 (6)	164 (7)	45 (4)	84 (5)	102 (6)
Male (n = 7)	22 (1)	74 (7)	178 (6)	53 (2)	93 (3)	108 (3)

3.2. Instrumentation

The study was conducted in the Biomechanics of Human Movement and Ergonomics lab at the University of Extremadura. The lab was equipped with a video-based optoelectronic stereophotogrammetric system (OSS) (MaxPRO, Innovision Systems, Inc.), a force measurement system with two force platforms mounted on a ground-level concrete slab (Dinascan 600M, IBV, Valencia,

Spain), and a portable EMG 16-channel system (Myomonitor IV Delsys Inc., Boston, MA). Check verification was conducted in order to verify the performance specifications of the force and OSS measurement systems.

The errors specified by the manufacturers are not the actual errors the force measurement system exhibits in the field, but rather the limits of the errors that the force measurement system could have. These errors are asociated to specific properties of the measurement system and its instruments and are assessed by the manufacturer during the calibration process. For a simplified control of the performance properties of the measurement system, a verification control can be done in the laboratory. A measurement process can be thought of as a well-run production process in which measurements are the output (NIST/SEMATECH, 2012). Verification is a specific case of quality control (QC), much like QC in manufacturing, which simply reveals whether the error of a measuring process exceeds their specified limits (Rabinovich, 2013). Verification is defined as "provision or objective evidence that a given item fulfils specified requirements" (ISO-JCGM 200, 2008).

3.2.1. Force Measurement System

The presented section reports on a measurement system analysis (MSA) and on an uncertainty analysis following the Guide to the Expression of Uncertainty of Measurement framework for confirmation that a target measurement uncertainty can be met in assessing ground reaction force (GRF) and COP estimates under static loads, respectively. Two strain-gauge force platforms (Dinascan 600M, IBV, Valencia, Spain) were utilized to obtain the temporal evaluation of the components of the GRF vector and the coordinates of the COP during the experiment. A strain-gauge force platform is a robust and accurate easy-to-use force measurement device that is typically composed of four load cells each one bonded with electric resistance stain gauges that produce a resistance change that varies *linearly* with strain and which convert the magnitude of the local stretching of gauge into an electrical signal proportional to the magnitude of force that they experience. The output electrical signal from the transducers is usually processed by passing through a signal conditioner, which performs tasks such as amplification and analog filtering (anti-aliasing) of unwanted frequencies, and then it is recorded using a data acquisition system, calibrated, filtered digitally and stored for further off-line processing. The four load cells register the applied forces along each of the anterior-posterior (X), medial-lateral (Y) and vertical (Z) axes of platform's orthogonal reference system. Individual reaction forces are measured by the three components of each of the four load cells and the temporal evolution of the force components, $\mathbf{F}_x$, $\mathbf{F}_y$ and $\mathbf{F}_z$ of the ground reaction force is determined. The coordinates of the point where the resultant of the vertical GRF components intersects the support surface (centre of pressure) at every instant are calculated as a function, f, of the components of the GRF measured by each load cell, while the computation of the free moment (M) is further dependent on the COP location (Bartlett, 2007; Challis, 2008; Hunt, 1998; Lees and Lake, 2008; Medved, 2001; Winter, 2009).

In general, modern force measurement systems fulfill the performance characteristics that are necessary for the registration of any type of human activities. However, additional errors may be arose while recording and during data analysis originated by degradation of the equipment over time

from previous usage or user abuse, or from influences of installation and operation environment (Challis, 2008; Hunt, 1998; Lees and Lake, 2008). Thus, any cable malfunction, electrical and electronic faults, temperature and humidity variations, or vibrations of the supporting structure can alter spatial accuracy and precision characteristics that are provided by the manufacturer (Bartlett, 2007; Hunt, 1998; Lees and Lake, 2008; Medved, 2001). Consequently, a spot check should be conducted periodically in order to verify that either the performance specifications of the force measurement system in current laboratory conditions are in conformance with the measurement accuracy and precision stated by the manufacturer, or that the system maintains its performance characteristics during operation in the experimental procedure, or that the performance characteristics are adequate for the ongoing experiment—i.e, experimental *liability*. What is accurate for one experimental procedure might be aproximate for another.

A force measurement system includes several instruments and their performance characteristics have to be taken into consideration in order to verify whether the error of the measuring system exceeds its specified by the manufacturer limits (Bartlett, 2007; Challis, 2008; Hunt, 1998; Lees and Lake, 2008; Medved, 2001; Winter, 2009). Therefore, the entire measurement chain is considered, from force transducer to digital indicator, as uncertainty in measurement may arise not only during analog signal transportation but also from the data acquisition system and software processing (Challis, 2008; Hunt, 1998; Proakis and Manolakis, 1996). A complete check verification is always preferable as it gives the most reliable results, however it should remain as much simplified as possible (Rabinovich, 2013).

Bizzo, Ouaknine, and Gagey (2003) and Browne and O'Hare (2000), have developed QC procedures to check the performance characteristics of a force measurement system and hence to provide a general information about system's spatial *accuracy*, *precision*, and *uniformity*. Accuracy is defined as "the closeness of agreement between a measured quantity value and a true quantity value of a measurand" (ISO-JCGM 200, 2008), and is usually limited by calibration errors. The spatial accuracy of the force measurement system is affected by the electronic noise and hysteresis of the system, the nonlinearity and different offset voltages of the transducers (Browne and O'Hare, 2000). Precision is defined as the "closeness of agreement between indications or measured quantity values obtained by replicate measurements on the same or similar objects under specified conditions" (ISO-JCGM 200, 2008), and is limited mostly by the resolution of the A/D converter. The precision of force platform is affected by the repeatability and the temporal stability of the system (Browne and O'Hare, 2000).

Since a degree of uncertainty in calibration corrections is unavoidable, there are always errors that characterize system's accuracy and usually are provided by the manufacturer who performs the calibration. However, precision usually is not provided. Uniformity is the force platform's characteristic to respond equally on the same load at different coordinates. It is an accuracy characteristic. Uniformity is affected by non-linear of the transducers response to load, hysteresis, different offset voltages of the individual transducers, electronic noise in the individual components of the force platform, and deformation of the top plate (Browne and O'Hare, 2000). When uniformity is not presented, the COP measurement will be affected by the place of the feet on the top plate of the force platform and if the area of the excursion of the COP increases it will not be

Table 3.2 Technical characteristics and conditions of the force measurement system used in the study according to the manufacturer.

Sensors	OCTEC-IBV
Lowest recommended vertical force	250 N
Deadband	0 - 50 N
Maximal vertical force	15 kN
Maximal shear force	7.5 kN
Maximal force error	$< 2\%$
Cross-talk sensitivity	Null due to mechanic
Maximal error about the COP	$\pm$ 2 mm
Maximal sampling rate	1000 Hz/platform
Maximal registry time at 1000 Hz	16 sec
A/D converter	CIO-AD-16Jr, 12 bits, differential quantization
Outcome variables	GRF, M, J, COP
Top plate	CELTEC-IBV
Natural frequency of the top plate	> 400 Hz
Mounting	Concrete slab

measured accurately (Bobbert and Schamhardt, 1990; Gill and O'Connor, 1997; Schmiedmayer and Kastner, 1999).

3.2.1.1. Uncertainty in GRF Measurement

A MSA provides standard tools to qualify a measurement system for use by quantifying its short-term (precision) and long-term variability (accuracy, stability, linearity)—i.e., its *capability* to perform measurements that conform to target specifications. It gathers the data and estimates standard deviations for sources that contribute to the uncertainty of the measurement result. Thereafter, the uncertainty of GRF measurements is determined by using the experimentally determined standard uncertainty based upon the analysis methods outlined in the NIST/SEMATECH (2012) handbook. The procedure for the uncertainty on force measurements has two parts: A 'Gage Linearity and Bias' test to determine the accuracy of the measurement system throughout the expected range of the measurements, and a Gage Repeatability and Reproducibility (R&R) study to determine system's precision (Appendix B). According to NIST/SEMATECH (2012), this is a reasonable approach to take if the results are *truly* representative of the measurement process in its working environment. The goal is to provide uncertainty metrics for static loads.

The results indicate that the measurement uncertainty presented in $\mathbf{F}_z$ is comfortable with the recommendations specified by the manufacturer (Table 3.2). Table 3.3 shows the results of the uncertainty analysis for the GRF measurements. The expanded measurement uncertainty ($U_{95\%}$) at 95% confidence interval (CI) for the $\mathbf{F}_z$ of the GRF is $U_{95\%} = 6.06$ N for the force platform 1 and $U_{95\%} = 9.64$ N for the force platform 2.

3.2.1.2. Uncertainty in Center of Pressure Measurement

The COP is not measured directly with the force measurement system, rather, it is derived by the components of the GRF measured by each load cell. Since $\mathbf{F}_z$ is always dominator in the function to compute COP, when $\mathbf{F}_z$ reaches low levels a small error in it represents a large percentage error in COP (Winter, 2009). The expanded measurement uncertainty ($U_{95\%}$) for the COP was

Table 3.3 Uncertainty budget for force measurement.

Error source	Estimate type	Value FP1 (N)	Value FP2 (N)	Error distribution	Divisor	Sensitivity	Uncertainty FP1 (N)	Uncertainty FP2 (N)	df
Linearity	B	0.07	0.20	Rectangular	$\sqrt{3}$	1	0.04	0.12	∞
Bias	A	4.45	8.61	Rectangular	$\sqrt{3}$	1	1.69	4.54	199
Resolution	B	0.31	0.31	Rectangular	$\sqrt{3}$	1	0.18	0.18	∞
Repeatability	A	0.64	0.64	Gaussian	1	1	0.64	0.64	1
Reproducibility	A	1.46	1.46	Gaussian	1	1	1.46	1.46	1
t for 95% confidence		1.98		Combined uncertainty			3.03	4.82	203
Coverage factor k		2		Expanded uncertainty			6.06	9.64	

verified based upon the Guide to the Expression of Uncertainty of Measurement (GUM) framework outlined in the NIST/SEMATECH (2012) and NASA (2010) handbooks, and on the QC procedures of Bizzo, Ouaknine, and Gagey (2003) and Browne and O'Hare (2000).

Appendix B describes the structure of the uncertainty analysis covering all the details of the applied procedure. Briefly, direct measurements were made to determine whether the measurement of a series of nominal COP coordinates that obtained with the force measurememt system are within the error limits specified by the manufacturer. The quantity of interest was the COP coordinates obtained from the force measurement system within a range of ± 50 mm of the geometrical center of the top plate of the force platform along with their estimated total uncertainty. Four dead loads ($M_1 = 98\,N$, $M_2 = 196\,N$, $M_3 = 294\,N$, and $M_4 = 392\,N$) were used for the COP measurements. Table 3.4 shows the results of the uncertainty analysis. For the worst case condition, the $U_{95\%}$ in the measurement of the centre of pressure in anterior-posterior direction (COP_{AP}) is $U_{95\%} = 3.1$ mm and of the centre of pressure in medial-lateral direction (COP_{ML}) is $U_{95\%} = 2.7$ mm, for both force platforms.

3.2.2. Video-based Optoelectronic System

Videogrammetry is a subcategory of both photogrammetry and machine-vision disciplines that uses video components for image acquisition. Photogrammetry is the science and art of making *precise* and *reliable* measurements from images, whereas machine-vision refers to the broad use of digital-photogrammetry including sensor models and system aspects for computer vision (Gruen, 1997). In biomechanics of human movement, the so called digital close-range measurements involve the use of OSS to track the 3D position of retroreflective or light-emitting markers allowing the reconstruction of the 3D landmarks coordinates from digitized *noisy* video images (Chiari et al., 2005). The uncertainty in the 3D reconstructions is the propagation error originates from individual camera calibrations and from inconsistencies in the pixel coordinates used to compute 3D landmarks. Although random and systematic interacting errors inherent to the OSS and its calibration procedure can be minimized by use of appropiate calibration and digitization methodologies, all reconstruted points have some uncertainty associated with them. This error should be measured and used to create confidence intervals for measurements (Hedrick, 2008).

The performance of the OSS is the uncertainty in the 3D reconstructions originated from the

Table 3.4 Uncertainties in COP measurements at X- and Y- axes for the two force platforms (FP 1, FP 2) and for the different loads (M_{10}, M_{20} and M_{30}).

Error Source	Estimate Type	Error Distribution	X-axis						Y-axis					
			Force platform 1 (N)			Force platform 2 (N)			Force platform 1 (N)			Force platform 2 (N)		
			M_{10}	M_{20}	M_{30}	M_{10}	M_{20}	M_{30}	M_{10}	M_{20}	M_{30}	M_{10}	M_{20}	M_{30}
Resolution (u_{res})	B	Rectangular	0.03	0.03	0.03	0.03	0.03	0.03	0.03	0.03	0.03	0.03	0.03	0.03
Repeatability (u_{ran})	A	Gaussian	0.59	0.22	0.22	0.53	0.25	0.15	0.62	0.25	0.16	0.5	0.21	0.15
Uniformity (u_{unf})	B	Rectangular	0.02	0.01	0.01	0.09	0.003	0.003	0.04	0.01	0.001	0.02	0.01	0.01
Nonlinearity (u_{lnr})	B	Rectangular	0.52	0.46	0.65	0.64	0.4	0.34	0.69	0.63	0.54	0.63	0.59	0.53
Hysteresis (u_{hys})	B	Rectangular	0.89	0.7	0.84	0.69	0.47	0.35	0.92	0.68	0.47	1	0.73	0.75
Combination of uncertainties (u_{tot})			1.19	0.87	1.07	1.09	0.67	0.51	1.3	0.96	0.73	1.29	0.96	0.93
Expanded uncertainty (U) (95%)			2.38	1.74	2.14	2.18	1.33	1.02	2.61	1.92	1.46	2.57	1.92	1.87
Offset ($\hat{\beta}_0$)			−0.635	0.083	0.689	−1.415	−0.26	0.347	1.121	0.102	0.246	1.005	0.103	0.45
Slope ($\hat{\beta}_1$)			1.012	0.99	0.983	1.048	0.996	0.994	0.985	0.994	1.001	0.99	0.983	0.99
Noise (σ_{COP})			5.57	2.34	1.52	5.39	2.18	1.44	5.68	2.14	1.47	4.76	1.84	1.26
Spatiotemporal resolution criterion (Q_{ST})			1.017	0.427	0.278	0.984	0.398	0.263	1.037	0.391	0.268	0.869	0.336	0.23

random and systematic interacting errors inherent to the measurement system, its calibration procedure, the standard used to provide the known values, the measurement technique and the network layout and the care of the user in performing the calibration procedure (Chiari et al., 2005; Gruen, 1997). Therefore, an uncertainty analysis can be conducted previously to the experiment to check the performance characteristics of the OSS by estimating the resulted error in the 3D coordinates.

3.2.2.1. Uncertainty of 3D kinematics

Using the variance addition rule to combine statistically independent uncertainties from different sources, the uncertainty in the measurement error is

$$u_{3D} = \sqrt{u_{lnr}^2 + u_{bias}^2 + u_{rand}^2} = 3.41 \text{ mm}$$

The $U_{95\%}$ is reported as the combined uncertainty of measurement multiplied by the coverage factor k = 2 which for a normal distribution corresponds to a coverage probability of 95%

$$U_{3D} = k \times u_{3D} = 6.82 \text{ mm}$$

3.2.3. Electromyography System

The myoelectric signals were registered using the active sEMG sensors DE-2.3 (Delsys Inc., Boston MA). The sensors had dual, bipolar, 10 × 1 mm silver bars and an inter-electrode distance of 10 mm. The myoelectric signals were individually pre-amplified (gain up to 1000 $^{V}/_{V}$ ± 1%, a CMMR of >80 dB with an input impedance >100 $^{M}/_{\Omega}$) and band-pass filtered (20 ± 5 Hz to 450 ± 50 Hz, 20 $^{dB}/_{oct}$) prior to digitization. The analogue signals were digitized at a rate of 1 KHz using the Myomonitor IV (Delsys Inc., Boston, MA) portable EMG 16-channel system (16 bits, range ± 5 V) and the data were transmitted wireless to the receiving host computer for storage and off-line analysis using the EMGWorks 3.6 acquisition software (Delsys Inc., Boston, MA).

3.3. Experimental Task Conditions

3.3.1. Biomechanical Risk Factors based on NIOSH Recommended Risk Levels

Prior to the experiment, in order to monitor any risk of injury and to assess the percentile of the working population that is capable of performing the tasks according to the NIOSH (1981) recommended limits for percent capabilities (percent of the population with sufficient strength), the static joint moment loads and low back stresses acting on the L4/L5 and L5/S1 intervertebrae segments were predicted at the starting and at the final posture adopted by each subjects during the lifting and lowering tasks (Fig. 3.1). For the risk assessment, the 3D Static Strength Prediction Program was used (3DSSPP v6.0.6, University of Michigan, Centre for Ergonomics, 2012) (3DSSPP, 2012). Mann - Whitney test was used for gender comparisons of the estimated intervertebral disk stresses imposed on the L5/S1 and L4/L5 level of the lumbar spine at the different static postures adopted by the subjects in the experimental procedure and the percent capabilities for the major joints (Table 3.5).

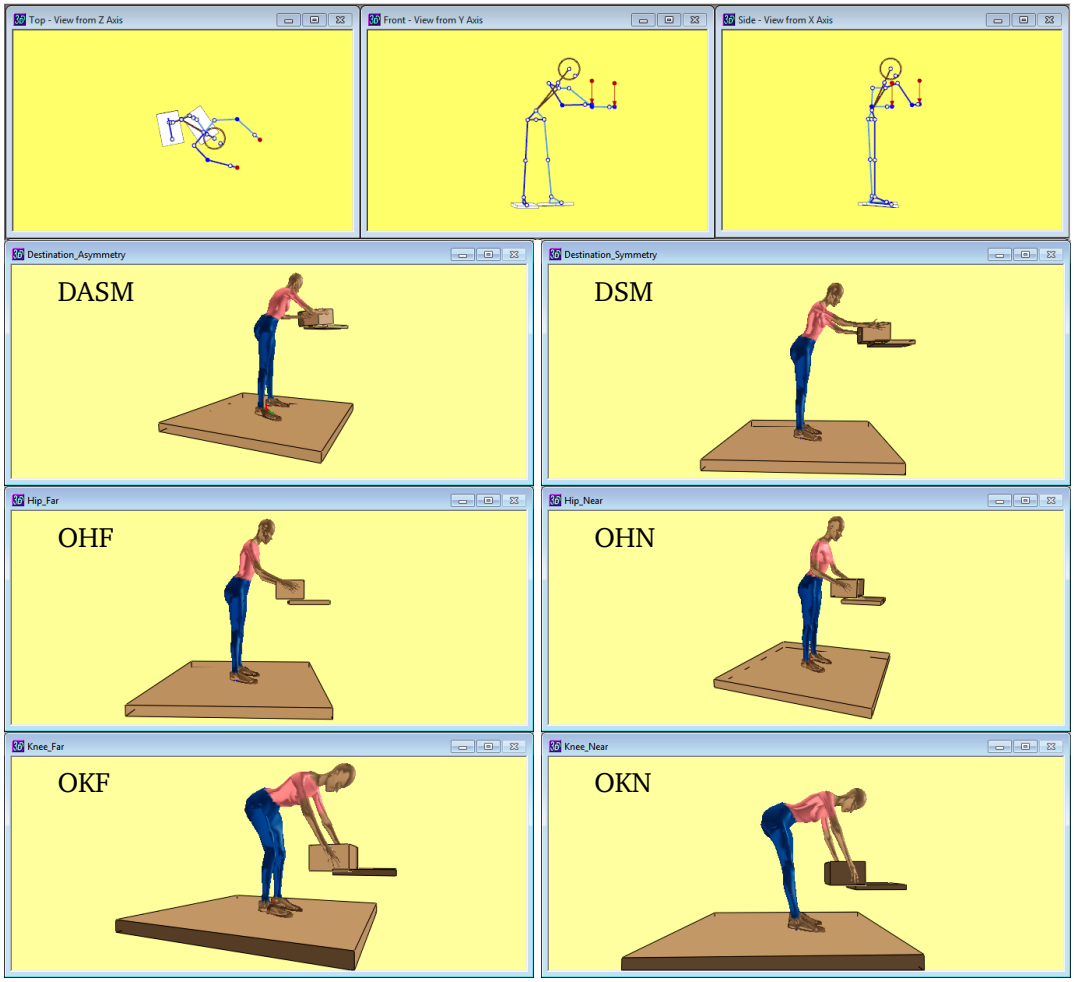

Figure 3.1 Risk assessment for the experimental task conditions. Ilustration of the posture configuration according to the 3DSSPP ® software, and the the six different postures adopted by the subjects during the experiment (DASM: Destination with Asymmetry; DSM: Destination with Symmetry; OHF: Origin (Destination for lowering tasks) levels Knee and Far; OHN: Origin (Destination for lowering tasks) levels Hip and Near; OKF: Origin (Destination for lowering tasks) levels Knee and Far; OKN: Origin (Destination for lowering tasks) levels Knee and Near).

The estimated compressive and shear stresses imposed on L5/S1 and L4/L5 intervertebral disks at the initial and final stoop posture adopted by the subjects during the experimental procedure did not suppose to be risky according to the NIOSH strength tolerance limits recommendations (Table 3.5). The compressive stress was estimated to be, for some subjects and adopted postures, near the 3400 N value, which corresponds to the action limit threshold according to NIOSH, and represents the value at which workforce under 40 years of age can begin to experience vertebrae microtrautisms (Marras, 2008). However, it is much less than the 6400 N threshold that corresponds to the value at which the 50% of the workforce is expected to suffer vertebrae microtraumatisms (Marras, 2008). The shear forces was less than 700 N, which corresponds to the recommended limits for the 90 % of the workforce for up to 1000 $^{\text{loadings}}/_{\text{day}}$ (Gallagher and Marras, 2012). For some postures the percent capability of the knee joint reached approximatelly the 50 % of the working population of the same morphological characteristics.

Table 3.5 Risk assessment for the postures adopted by the subjects in the experimental procedure.

Variable	Levels	Min	q_1	$\bar{x}$	q_3	Max	s
Compr.L5S1	Female	1136.3	1609.8	1955.5	2205.5	2720.1	390.6
	Male	1183.6	1908.1	2320.1	2747.8	3448.7	568.0
$p = 0.002$	all	1136.3	1731.2	2137.8	2494.8	3448.7	518.0
Compr.L4L5	Female	1108.7	1569.1	1983.7	2279.9	2965.1	434.2
	Male	1096.2	1809.7	2276.2	2758.7	3227.8	592.5
$p = 0.01$	all	1096.2	1667.1	2130.0	2511.5	3227.8	536.9
Shear.L5S1	Female	199.3	223.8	258.8	304.1	355.9	45.6
	Male	253.8	303.9	344.8	400.8	478.9	63.9
$p < 0.0001$	all	199.3	239.4	301.8	334.3	478.9	70.1
Shear.L4L5.AP	Female	-13.1	150.3	187.8	295.4	347.2	99.2
	Male	-206.1	182.2	218.1	398.2	484.0	206.2
$p = 0.01$	all	-206.1	154.6	202.9	301.0	484.0	161.6
Shear.L4L5.ML	Female	-161.8	1.3	-19.0	3.3	14.1	50.5
	Male	-93.8	-0.1	-13.2	-0.1	0.1	29.9
$p < 0.0001$	all	-161.8	-0.1	-16.1	2.4	14.1	41.3
Wrist	Female	97.7	98.3	98.9	99.4	99.7	0.6
	Male	98.4	98.7	99.1	99.3	99.7	0.4
$p = 0.28$	all	97.7	98.6	99.0	99.4	99.7	0.5
Elbow	Female	99.2	99.6	99.7	99.9	100.0	0.2
	Male	99.9	100.0	100.0	100.0	100.0	0.0
$p < 0.0001$	all	99.2	99.8	99.8	100.0	100.0	0.2
Shoulder	Female	88.5	93.5	96.9	99.6	99.8	3.9
	Male	98.7	99.4	99.7	99.9	100.0	0.4
$p < 0.0001$	all	88.5	99.0	98.3	99.9	100.0	3.1
Torso	Female	81.1	87.7	90.6	94.3	97.6	4.2
	Male	86.4	92.1	94.4	96.9	99.3	3.3
$p < 0.0001$	all	81.1	89.8	92.5	95.6	99.3	4.2
Hip	Female	70.4	80.4	87.1	94.8	97.7	7.8
	Male	78.8	89.0	92.1	96.2	98.4	4.9
$p = 0.0021$	all	70.4	85.6	89.6	95.4	98.4	6.9
Knee	Female	49.5	87.8	88.9	96.1	99.4	10.8
	Male	77.6	93.8	95.2	98.4	99.8	4.5
$p = 0.00014$	all	49.5	90.3	92.0	97.1	99.8	8.8
Ankle	Female	71.7	91.8	94.0	98.4	99.7	6.8
	Male	75.3	92.6	94.1	97.4	99.4	5.1
$p = 0.16$	all	71.7	92.4	94.0	98.1	99.7	6.0

3.3.2. Task Configuration Factors

Four variables were manipulated independently in the study: (I) manual handling load,(II) vertical distance, (III) origin distance (IV) asymmetry angle (Fig. 3.2).

3.3.2.1. Manual Handling Load

According to the regulations of the ISO standard 11228-1:2003, a lifting or lowering task is defined as the action to move a load with a mass of 3 kg (≡ 29.43 N) or more from its initial position upwards/downwards, without mechanical assistance. The weight of the lifting and lowering load was fixed at 67 N, which represents the value between the 50^{th} and the 75^{th} percentile of the weight distribution corresponded in real industrial lifting conditions Marras et al., 1995. Two identical rigid handy plastic storage boxes ($39 \times 27 \times 18\,cm^3$) with lock handles were used for the manual handling tasks. The coupling of the box was considered "good" according to the revised NIOSH lifting equation (Waters et al., 1993).

3.3.2.2. Vertical and Horizontal Distance and Asymmetry

A step-up wooden platform with adjustable legs and an adjustable step-up platform with rubber surface were used to standardize the tasks to each subjects' anthropometric characteristics (Fig. 3.2).

3.4. Design of Experiment

A split-plot experimental design with repeated measurements on experimental units was used in this study in order to investigate the main effects of four factors and all their interactions (Fig. 3.2), on the control of voluntary trunk movements during lifting and lowering tasks of males and females participants. Each participant was considered a block and repeated measurements made on each block under factorial treatment structure (Table 3.6). In total, there were $a = 16$ treatment combinations per block that were run in a randomly order with 112 trials totally in every block (16 treatments × 7 trials per treatment). As there were not of interest the interactions between lifting and lowering, the order of randomization between them was the same, which resulted in confounding. Therefore, the data for lifting and lowering were analyzed separately.

3.5. Procedure

The subjects adopted a stooped posture at the start of the lifting and lowering tasks (Fig. 3.3). As depicted in Fig. 3.3, the subjects were instructed to stand during the tasks with a foot on each force platform. The layout of lab's force platforms allowed participants carrying out the manual material lifting and lowering tasks while they were standing with each foot on a force platform. They did not allow to change the placement of the feet or to move the feet off the ground or to flex the knees during the tasks. The subjects stood at a self-comfort position with the projection of the midpoint of the left and right ankle onto a predefined point of the surface. The experiment was performed by randomly selecting a treatment combination and then the subjects performed the box motion, which gave result to four lifting and three lowering trials for every treatment,

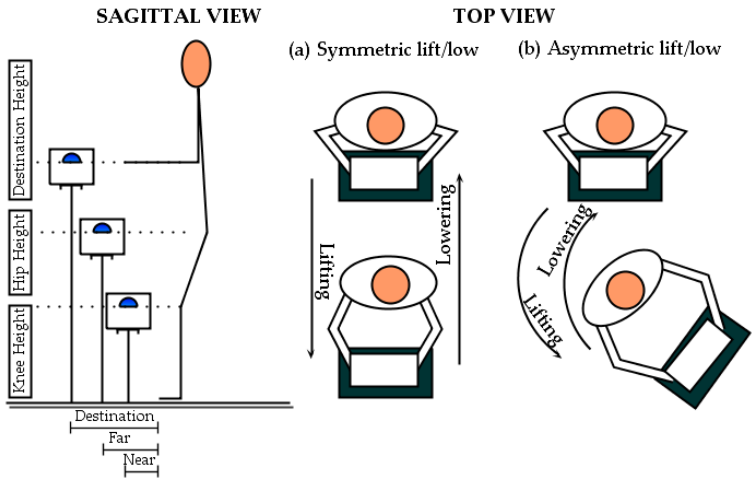

Figure 3.2 Task configuration factors. Schematic representation of a sagittal and top view of a subject performing a typical symmetric (a) and an asymmetric (b) lifting and lowering task. The independent variables of the experiment design are:

- Factor 1 (VD) = Vertical Distance (2 levels: Knee and Hip). The vertical origins of the lifting activity (vertical destination of the lowering activity) were determined according to the knee and hip heights of each subject.
- Factor 2 (HD) = Horizontal Distance (2 levels: Far and Near). The first level (Near) of the horizontal origin of the lifting activity (horizontal destination of the lowering activity) was determined as the placement of the box just in front of each subjects toes, whereas the second level (Far) as the placement of the box at a distance equal of the length of their feet from the toes.
- Factor 3 (AM) = Angle of Asymmetry (2 levels: 0° and 45°). The angles of asymmetry used in this study were 0° and 45° measured from the sagittal plane. Foot movement during lifting/lowering was not permitted.
- Factor 4 (LD) = Type of Load (2 levels: Liquid and Solid). The subjects were asked to lift/low a box that contained a liquid and a box that contained a solid material, both of the same weight.

interspersed with 5 min rest breaks between each treatment. The geometrical arrangement of the cameras of the OSS allowed tracking the landmarks affixed on participants' pelvis and trunk segments and on the handled box.

In order to simulate realistic MMH situations, the subjects allowed to move and/or rotate the pelvis during the tasks. Each trial duration was constrained at 2 sec (pace: 30 lifts per min) independently of the treatment, which was ensured by an electronic metronome. The subjects were ordered to pick up the box of size 0.39 m × 0.27 m × 0.18 m from the origin at metronome's "beeping" sound and leave it to the destination at the consecutive metronome's beat, assuming voluntary control of movement actions both at origin and destination. Then, they picked the box up from the destination at the next "beep" and left it back at the origin at the consecutive metronome's beat, and so on. Therefore, each treatment measurement (seven trials) lasted about 16 sec. The lifting destination of the box (which coincides with lowering task origin) was located vertically at subjects'

Table 3.6 Representative design of experiment matrix for one block with the randomized 2^4 full factorial treatment structure. The actual randomized run order is given in the "Treatment" column. Relative ranking of ergonomic risk assessment among treatments according to the NIOSH criteria is shown (4 = highest risk).

				FACTORS			
Block	Run	Treatment	Risk	VD	HD	AM	LD
1	1	15	2	Hip	Far	0	Liquid
1	2	7	3	Knee	Far	0	Liquid
1	3	5	1	Hip	Near	0	Liquid
1	4	2	2	Knee	Near	0	Liquid
1	5	11	3	Hip	Far	45	Liquid
1	6	4	4	Knee	Far	45	Liquid
1	7	9	2	Hip	Near	45	Liquid
1	8	1	3	Knee	Near	45	Liquid
1	9	12	1	Hip	Far	0	Solid
1	10	16	2	Knee	Far	0	Solid
1	11	13	0	Hip	Near	0	Solid
1	12	3	1	Knee	Near	0	Solid
1	13	10	2	Hip	Far	45	Solid
1	14	6	3	Knee	Far	45	Solid
1	15	14	1	Hip	Near	45	Solid
1	16	8	2	Knee	Near	45	Solid

elbow height in upright position and horizontally at subjects' extreme reach. For the extreme reach, the subjects were required to bend forward and deposit the box to a specific location onto the adjustable platform without move the feet off the ground and without lean against the box (Fig. 3.3). The origin of the box (which coincides with the destination of the lowering task) was located vertically at subjects' knee or hip height in upright position and horizontaly in front of subjects' toes or at a distance equal of the length of their feet from the toes (Fig. 3.2). A rectangular was drawn on the surface of origin and destination platforms in order the subjects to deposit the handled box always on the same place. The measurement session for each subject lasted about three hours. All subjects wore their own sports shoes.

3.6. Data Collection and Processing

3.6.1. Surface Electromyography Procedure

After saving the hair where it was necessary and cleaning the skin with 70% isopropyl alcohol pad in order to reduce skin impedance, the active sEMG sensors adhered to the skin using adhesive strips over the specific locations of the ten muscle in interest. The electrodes locations were: righ and left (1) erector spinae (RES and LES): 1/6 of the distance from the iliac crest to the spine of the 7th vertebra above the iliac crest (Zipp, 1982), (2) rectus abdomini (RRA and LRA): approximately 2 cm lateral of the umbilicus over the muscle belly (Cram, 2011), (3) external oblique (REO and LEO): lateral to the rectus abdominus directly above the anterior-superior iliac spine (ASIS),

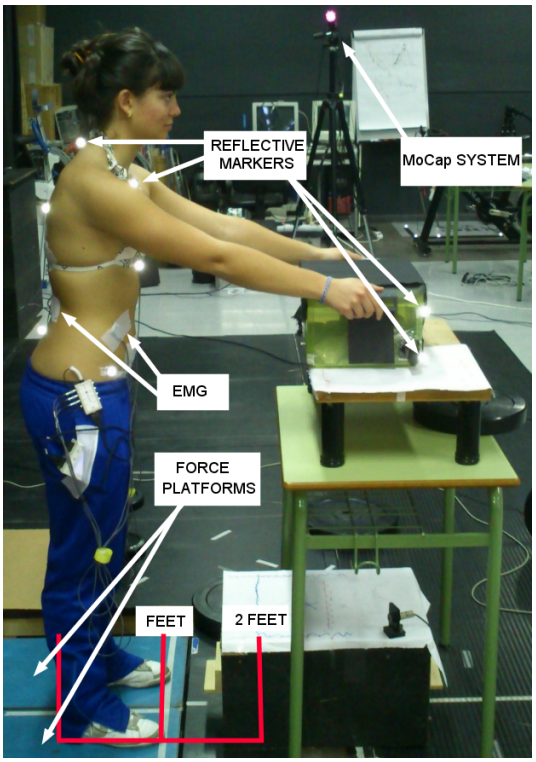

Figure 3.3 Laboratory configuration during the lifting and lowering tasks.

halfway between the iliac crest and the ribs at a slightly oblique angle (Cram, 2011), (4) internal oblique (RIO and LIO): approximately midway between ASIS and symphysis pubis, above inguinal ligament (McGill, Juker, and Kropf, 1996; Miller and Medeiros, 1987), and (5) latissimus dorsi (RLD and LLD): approximately 4 cm below the inferior tip of the scapula, half the distance between the spine and the lateral edge of torso, oriented in a slightly oblique angle of approximately 25 ° (Cram, 2011). Moreover, one sEMG sensor was placed on the heart side in order to record an ECG signal simultaneously with the EMGs. This signal was used later in order to remove ECG artifacts from the EMG signals (Hof, 2009).

Once EMG signal collected and stored, post-processing of the data by removing the ECG artifacts was performed (Hof, 2009). Then, the data were band-pass filtered using a fourth-order Butterworth filter with a corner frequency of 20 - 450 Hz (De Luca et al., 2010), demeaned and stored in ASCII files in order to parameterized it. The EMG signal is the electrical manifestation of the neuromuscular activation associated with a contracting muscle and its amplitude reflects the amount of muscle force production (Basmajian and De Luca, 1985; De Luca, 1997). In order to quantify the level of the relative amount of muscle activity and consequently of muscle effort, the root mean square value of the EMG amplitude was used (RMS_{EMG}). This parameter is preferred among others because (i) it represents the electrical power in the signal and thus has a physical meaning (Basmajian and De Luca, 1985; De Luca, 1997) and (ii) it is not affected by the cancelation caused by the superposition of motor units action potentials (MUAPs), representing, therefore, motor units behavior during muscle contraction more completely than other temporal parameters (Basmajian and De Luca, 1985). The integration was approximated by using the trapezoidal rule

over time bins of 1% of the task cycle (≃20 ms) and normalized to max $\mathrm{RMS}_{\mathrm{EMG}}$ for every subject and muscle.

3.6.2. Extraction of Muscle Modes

Matrix factorization algorithms can be used to identify M-modes and their scaling commands (Tresch, Cheung, and d'Avella, 2006). Among them, the Exploratory Factor Analysis (EFA) with varimax rotation has been used in many studies (Asaka et al., 2008; Danna-Dos-Santos et al., 2009; Ivanenko, Poppele, and Lacquaniti, 2004; Klous, Santos, and Latash, 2010; Krishnamoorthy et al., 2004; Krishnamoorthy et al., 2003; Robert, Zatsiorsky, and Latash, 2008; Wang et al., 2006). Therefore, in order to explain correlations among muscle activation patterns a EFA was used (Calvo, 1992; Everitt, 2005; Klinke and Wagner, 2008). EFA is a linear decomposition technique, which assumes that the m observed muscle activation patterns over t time bins are linked to a smaller number of n latent common factors by a linear regression model of the form

$$\mathbf{M} - \boldsymbol{\mu} = \boldsymbol{\Lambda}\mathbf{F} + \mathbf{E} \tag{3.1}$$

with $\mathbf{M} \in \mathbb{R}^{\mathrm{m}\times\,\mathrm{t}}$ being the EMG data matrix of m muscles and t the number of time bins, $\boldsymbol{\mu} \in \mathbb{R}^{\mathrm{m}}$ the vector of the mean values of the $\mathrm{RMS}_{\mathrm{EMG}}$ data of each m muscles, $\boldsymbol{\Lambda} \in \mathbb{R}^{\mathrm{m}\times\,\mathrm{n}}$ being the factor loading matrix, $\mathbf{F} \in \mathbb{R}^{\mathrm{n}\,\times\,\mathrm{t}}$ being the matrix of the underlying common factors and $\mathbf{E} \in \mathbb{R}^{\mathrm{m}\,\times\,\mathrm{t}}$ being the matrix of the unique factors (uncorrelated errors/residuals). The scores $\mathbf{F}$ on the common factors for each time bin are given by

$$\mathbf{F} = \boldsymbol{\Lambda}^{T}\mathbf{R}^{-1}\mathbf{M} \tag{3.2}$$

with $\mathbf{R} \in \mathbb{R}^{m\times m}$ being the correlation matrix of the $\mathrm{RMS}_{\mathrm{EMG}}$ data. In order to compute the linear subspace $\boldsymbol{\Lambda}\mathbf{F}$ of the muscle activation patterns (3.1), the normalized $\mathrm{RMS}_{\mathrm{EMG}}$ data were concatenated to form the $\mathbf{M}$ matrix, where the rows corresponding to the $m = 10$ muscles and the columns the $t = 4$ trials $\times\ 100\,{}^{\mathrm{bins}}/_{\mathrm{trial}} = 400$ time bins. The elements of the $\mathbf{M}$ matrix were each standardized to have unit variance and submitted to EFA with Varimax rotation where $n = 3$ Principal Components (PCs) were retained from the correlation matrix $\mathbf{R}$ by using Principal Components Analysis (PCA) and formed the component matrix $\boldsymbol{\Lambda}$.

To explore the dimensionality of the PC subspace, the Horn's Parallel Analysis (PA) (Horn, 1965) and Kaiser's criterion (K1) *ad hoc* procedures were used. PA is a Monte-Carlo based simulation method which compares the observed eigenvalues against those derived from a random data set of same sample size and number of variables, and excludes those PC whose associated eigenvalues are less than the 95th of the distribution of the random derived eigenvalues. K1 excludes the PC with eigenvalues less than one. Typically, after the first three PC the eigenvalues drop ceased and their values were less than 1. Both PA and K1 criteria supported the conclusion that the initial 10 variables can be reduced to three PC.

After obtaining factor scores (Eq. (3.2)), the standardized muscle activation patterns $\mathbf{M}_z$ were approximated according to

$$\mathbf{M}_z \approx \hat{\mathbf{M}}_z = \boldsymbol{\Lambda}\mathbf{F}$$

The goodness of the linear subspace approximation $\hat{\mathbf{M}}_z$ on the $\mathbf{M}_z$ was quantified by calculating the cosine of the angle ϕ between each vector pairs $\left(\cos(\phi) = \cos \measuredangle \left(\hat{\mathbf{M}}_z^{(m)}, \mathbf{M}_z^{(m)}\right)\right)$ in t-dimensional space as follows

$$r_{\hat{M}M}^{m} = \cos(\phi) = \frac{\hat{\mathbf{M}}_z^{(m)^T} \mathbf{M}_z^{(m)}}{||\hat{\mathbf{M}}_z^{(m)}|| ||\mathbf{M}_z^{(m)}||} \tag{3.3}$$

with $\hat{\mathbf{M}}_z^{(m)} \in \mathbb{R}^t$ and $\mathbf{M}_z^{(m)} \in \mathbb{R}^t$, and T holds for transpose. Two vectors with the same direction have $|\cos(\phi)| = 1$, whereas two orthogonal vectors have $\cos(\phi) = 0$. As the elements of $\hat{\mathbf{M}}_z^{(m)}$ and $\mathbf{M}_z^{(m)}$ vectors are standard scores, the $\cos(\phi)$ is equal to the coefficient of linear correlation $r_{\hat{\mathbf{M}}\mathbf{M}}^{(m)}$ between the *unstandardized* muscle activation pattern vector $\mathbf{M}^{(m)}$ and its approximation $\hat{\mathbf{M}}^{(m)}$ (Calvo, 1992). The squared cosine value, $\cos^2(\phi)$, corresponds to the coefficient of determination $\left(r^2 = 1 - {}^{SSE}/_{SST}\right)$, where SSE is the sum of squared residuals $\left(\sum_{i=1}^{t} \mathbf{E}_i^{(m)}\right)$ and SST is the total sum of squared residuals from the mean value of the $\mathbf{M}_z^{(m)}$ vector. A weighted mean $\overline{\cos(\phi)}$ was computed using Fisher's z - transformation across subjects and treatments, and its r^2 value was calculated as an index to describe the shape similarity between the reconstructed muscle activation patterns in the lower - dimensional space of common factors and the measured activation patterns in the higher - dimensional muscle space. The same procedure was used to compute the cosine value of the angle θ between the *unstandardized* muscle activation pattern vector $\mathbf{M}^{(m)}$ and its approximation $\hat{\mathbf{M}}^{(m)}$ $\left(\cos(\theta) = \cos \measuredangle \left(\hat{\mathbf{M}}^{(m)}, \mathbf{M}^{(m)}\right)\right)$, which is equal to the *uncentered* coefficient of linear correlation, an index that was used to describe both magnitude and shape similarity between the reconstructed muscle activation patterns and the measured activation patterns. The squared cosine value $\cos^2(\theta)$ corresponds to the variance accounted for (VAF), a related to r^2 measure where SST is taken with respect to zero (Torres-Oviedo, Macpherson, and Ting, 2006). A weighted mean $\overline{\cos(\theta)}$ was computed using Fisher's z - transformation and the VAF value was calculated. A value of $r^2 > 60\,\%$ and of VAF $> 80\,\%$ was considered to indicate a good fit with the original data (Torres-Oviedo, Macpherson, and Ting, 2006). Two - sided 95 % confidence intervals for $\overline{\cos(\theta)}$ and $\overline{\cos(\phi)}$ values calculated. Confidence intervals and Fisher's z - transformations of correlation coefficients computed using the *r.con*(), *fisherz*(), and *fisherz2r*() routines in the **psych** library (Revelle, 2015) of the statistical software R (R Core Team, 2013).

3.6.3. Statistical Verification of Muscle Modes Similarity

To test the similarity of PC vectors across subjects and on the effects of the NIOSH factors, the concept of central vector was used (Krishnamoorthy et al., 2003). A central vector $\bar{\mathbf{\Lambda}}^{(n)}$ is a PC vector for which the sum of squared distances between it and the remaining set D_n of PC vectors of the same extraction order n is minimum

$$\underset{\bar{\mathbf{\Lambda}}^{(n)}}{\operatorname{argmin}} \sum_{\mathbf{\Lambda} \in D_n} ||\mathbf{\Lambda} - \bar{\mathbf{\Lambda}}^{(n)}||^2$$

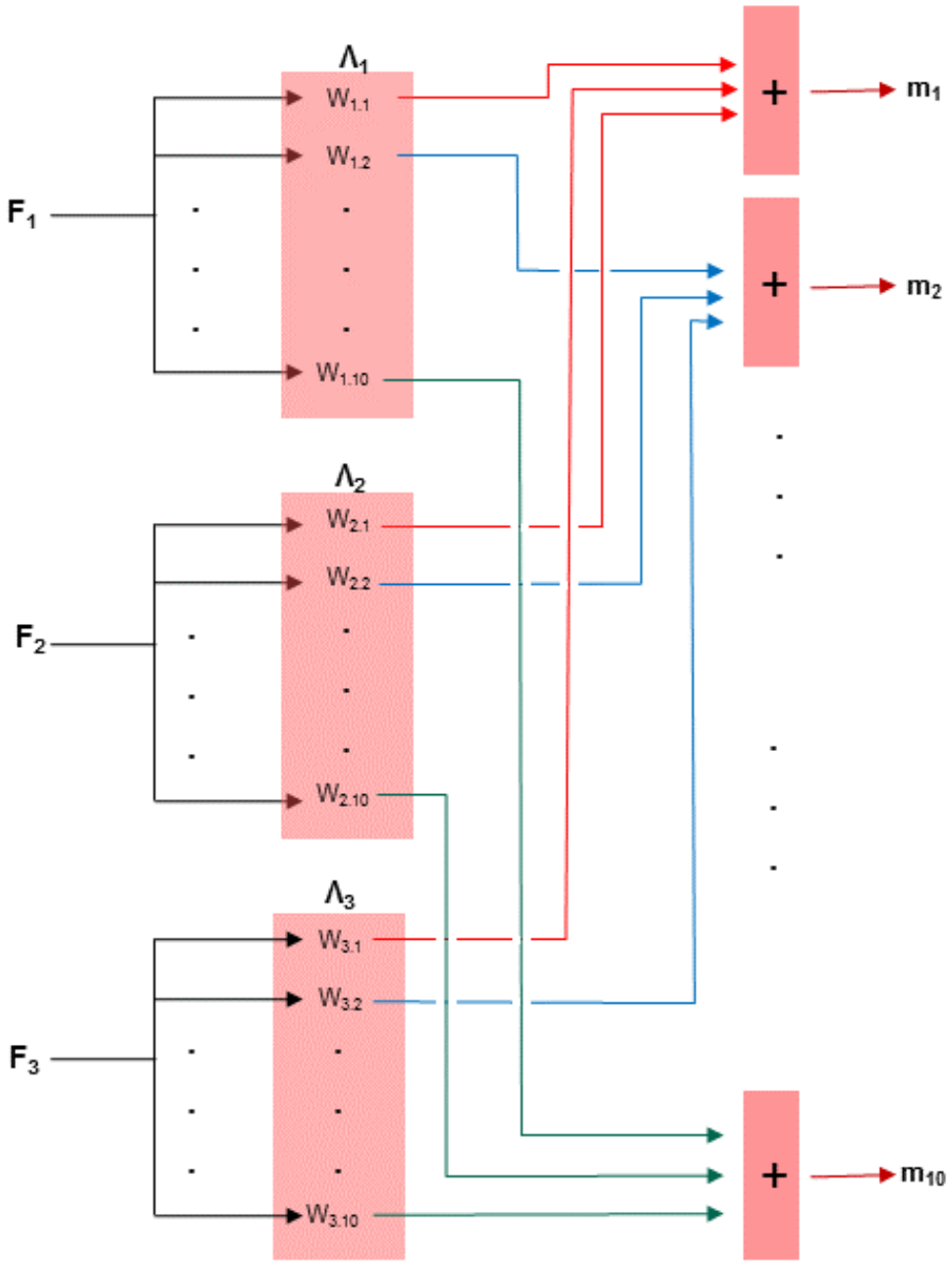

Figure 3.4 Model of the muscle synergy system. The observed EMG activity of the ten muscles is the superposition of a modular network comprising of three M-modes, where $\mathbf{F}_{1\rightarrow 3}$ represents the firing frequencies rectruiting M-modes and $\mathbf{\Lambda}_{1\rightarrow 3}$ represents the M-modes related to the synaptic weights ($\mathbf{w}_{1\rightarrow 3,1\rightarrow 10}$) from premotor neurons to different motorneuronal pools.

with $\bar{\mathbf{\Lambda}}^{(n)} \in \mathbb{R}^m$ and $D_n \subseteq \left\{\mathbf{\Lambda}_{1,1}^{(n)}, \mathbf{\Lambda}_{1,2}^{(n)}, \ldots, \mathbf{\Lambda}_{16,14}^{(n)} | \mathbf{\Lambda}_{a,s}^{(n)} \in \mathbb{R}^m\right\}$. Therefore, the $\bar{\mathbf{\Lambda}}^{(n)}$ is calculated by taking the gradient of the sum of squared distances and setting it to the zero vector

$$\nabla_{\bar{\mathbf{\Lambda}}^{(n)}} \sum_{\mathbf{\Lambda} \in D_n} \|\mathbf{\Lambda} - \bar{\mathbf{\Lambda}}^{(n)}\|^2 = -2 \sum_{\mathbf{\Lambda} \in D_n} (\mathbf{\Lambda} - \bar{\mathbf{\Lambda}}^{(n)}) = -2 \sum_{\mathbf{\Lambda} \in D_n} \mathbf{\Lambda} - 2|D|\bar{\mathbf{\Lambda}}^{(n)} = 0 \Rightarrow$$

$$\bar{\mathbf{\Lambda}}^{(n)} = \frac{1}{|D_n|} \sum_{\mathbf{\Lambda} \in D_n} \mathbf{\Lambda}$$

which proves that $\bar{\mathbf{\Lambda}}^{(n)}$ is analogous to the mean PC vector (Flach, 2012). Consequently, $n = 3$ central vectors were identified for each of the $a = 16$ treatments after averaging over subjects $\left(\left\{\bar{\mathbf{\Lambda}}_a^{(n)}\right\}\right)$. To estimate the similarity of the directions between $\mathbf{\Lambda}_{a,s}^{(n)}$ vectors and $\left\{\bar{\mathbf{\Lambda}}_a^{(n)}\right\}$ vector sets, the cosine value of the angle ξ between each vector pair, $\cos(\xi) = \cos \measuredangle \left(\mathbf{\Lambda}_{a,s}^{(n)}, \left\{\bar{\mathbf{\Lambda}}_a^{(n)}\right\}\right)$, in m-dimensional space was computed and their absolute values were transformed into z - scores using Fisher's z - transformation for statistical analyses. Herein, the absolute cosine values were used, therefore $\cos(\xi)$ values are bounded in [0,1]. By definition, the extracted PC for each subject in each treatment are pairwise orthogonal—i.e., $\mathbf{\Lambda}^{(1)} \perp \mathbf{\Lambda}^{(2)} \perp \mathbf{\Lambda}^{(3)}$. Hence, based on the same methodology described in Krishnamoorthy et al. (2003), if the PC vectors $\mathbf{\Lambda}^{(n)} \in D_n$ are collinear, then $|\cos(\xi)| = 1$ for all n = j (where $n, j = 1, 2, 3$), and $\cos(\xi) = 0$ for all $n \neq j$—i.e., for all $\mathbf{\Lambda}^{(n)} \notin D_n$. Therefore, to examine whether PC of the same extraction order are similar across subjects for each treatment, a one-way repeated measure ANOVA was run on the z - scores of the $|\cos(\xi)|$ values computed for each central vector $\bar{\mathbf{\Lambda}}_a^{(n)}$ separately. It was hypothesized that z - scores of the $\cos(\xi) = \left|\cos \measuredangle \left(\mathbf{\Lambda}_{a,s}^{(n)}, \bar{\mathbf{\Lambda}}_a^{(n)}\right)\right|$ are significantly higher if $n = j$ as compared to $n \neq j$. Paired t-tests with Benjamini-Hochberg correction were used to analyze any significant main effect. An example of the three extracted PC across subjects and the similarity procedure is depicted in Fig. 4.14.

It was assumed that directions of the $\mathbf{\Lambda}^{(n)}$ PC vectors are similar if for each $\bar{\mathbf{\Lambda}}^{(n)}$ vector the z-scores of the $\cos(\xi) = \left|\cos \measuredangle \left(\mathbf{\Lambda}^{(n)}, \bar{\mathbf{\Lambda}}^{(n)}\right)\right)$ values are significantly higher for $n = j$ as compared to $n \neq j$ (where $n, j = 1, 2, 3$). This means that the similarity of the $\mathbf{\Lambda}^{(n)}$ vectors is greater when the effects of the NIOSH factors contribute to increase significantly the difference between the z - scores of the $|\cos(\xi)|$ values for $n = j$ as compared to $n \neq j$. In order to localize the effect of the NIOSH factors and of their interactions on the similarity of the PC vectors of the same extraction order, a repeated - measures, split - plot ANOVA with factors *VD*, *HD*, *AM*, and *LD* was conducted on the differences of the z - scores of the $|\cos(\xi)|$ values calculated for the same central vector $\bar{\mathbf{\Lambda}}^{(n)}$—i.e., for $\cos(\xi)_{i-j}^{n} = \left|\cos \measuredangle \left(\mathbf{\Lambda}^{(i)}, \bar{\mathbf{\Lambda}}^{(n)}\right)\right| - \left|\cos \measuredangle \left(\mathbf{\Lambda}^{(j)}, \bar{\mathbf{\Lambda}}^{(n)}\right)\right|$, where $n, i, j = 1, 2, 3$ and $i \neq j$[1].

Moreover, the $\cos(\zeta)$ values after vectors pairs being standardized was also calculated, which corresponds to the coefficient of linear correlation r. It was considered that a pair of $\mathbf{\Lambda}_{a,s}^{(n)}$ and $\bar{\mathbf{\Lambda}}_a^{(n)}$ vectors are similar if $|\cos(\zeta)| \geq 0.765$, which corresponds to the critical value for 10 muscles at $P = 0.01$ (df= $8, r^2 = 0.585$) (Chvatal et al., 2011).

[1] n corresponds to central vectors and i, j to PC vectors.

Table 3.7 Specific marker locations and orientations.

Static and dynamic trials	
RASIS	Right anterior superior iliac spine (ASIS)
LASIS	Left anterior superior iliac spine
SACRUM	Mid point between the posterior superior iliac spines (PSIS)
BOX1	Lifted box corner 1
BOX2	Lifted box corner 2
BOX3	Lifted box corner 3
BOX4	Lifted box corner 4
Tracking only	
SJN	Suprasternale
SXS	Xiphion
C7	Spinal process of the seventh cervical vertebra
MAI	The midpoint between the most caudal points of the two scapulae
Static anatomical landmark calibration trial only	
RAC	Right acromion
LAC	Left acromion

3.6.4. Similarity Muscle Modes Gains

The similarity of time profiles of the factor scores **F** across treatments after averaging over subjects was assessed using cross-correlation analysis. To classify the cross-correlation coefficients, an hierarchical agglomerative cluster analysis carried out using the Ward's method on the dissimilarity matrix of the cross-correlation coefficients (1 - cross-correlation coefficients). The clustering obtained was represented by means of dendrograms.

3.6.5. 3D Kinematics

Nine reflective markers were adhered to the skin with hypoallergic tape and four reflective markers to the box (Table 3.7), and tracked at 60 Hz by the six-cameras (640 × 480 px, infra red lighting) motion capture system (MaxPRO, Innovision Systems, Inc.). Calibration markers were used in static trials to define the mechanical model and tracking markers for computing the movements. Some markers were used for both the segment definition and for tracking. The reconstruction, interpolation and labeling of the reflective markers were done using the MaxPRO software. The three-dimensional data were stored as .C3D files and then were processed with the Visual3D motion analysis software (C-motion, Inc., Germantown, MD, USA). Position-time "data smoothing", derivation, and interpolation at 1 KHz was carried out by quintic splines according to the "True Predicted Mean-squared Error" criterion given the known precision of the spatial coordinates previously estimated by an uncertainty analysis (Woltring, 1986).

To define the mechanical model (Fig. 3.7) five anatomical landmarks was used: RASIS, LASIS, RAC, LAC and SACRUM (Table 3.7). The box was defined by four markers in each corner of the frontal plane. Trunk and pelvis body segments were defined as solids. The torso is segmented into the pelvis that is rotated at the hips joint, and the spine, that is rotated at the L5/S1 disc, taking it

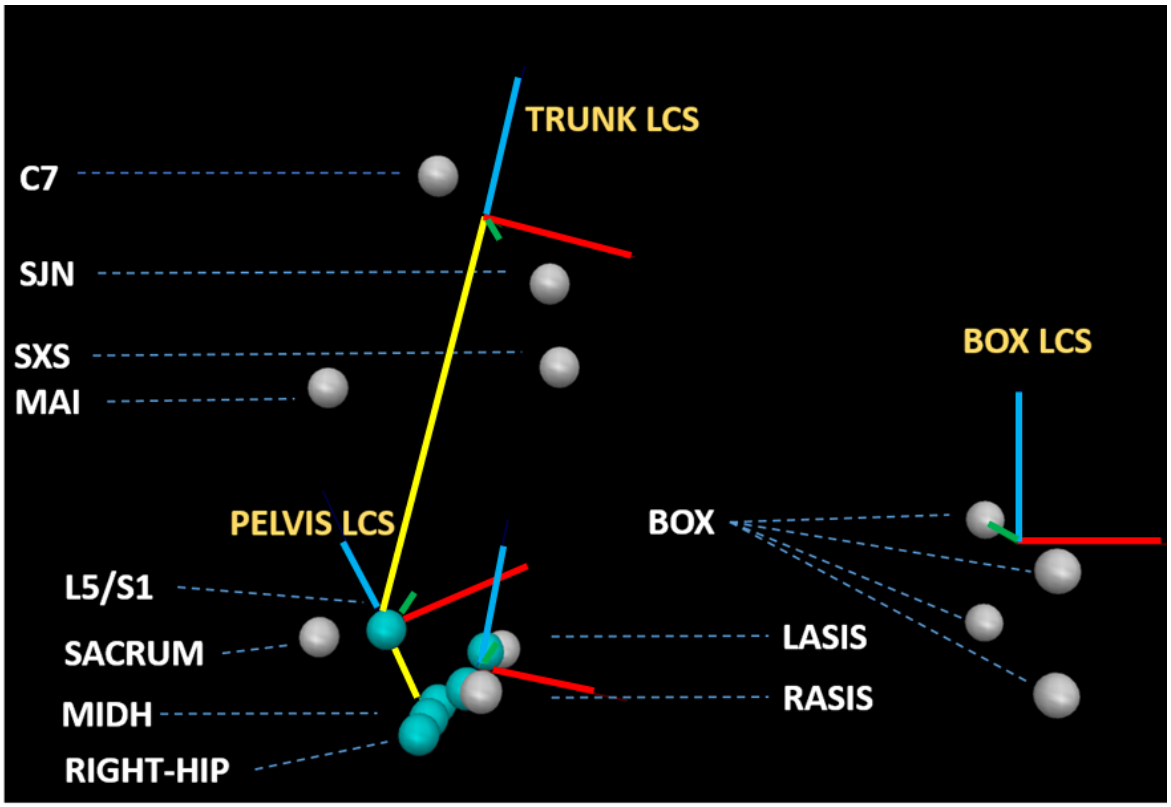

Figure 3.5 Mechanical model used in the study. Markers and virtual points location togeter with the mechanical model and the local coordinate systems (Some markers used only for the static trials do not showed). Blue points represent the virtual points. The blue axis of the local reference systems represents the axial axis, the red axis represents the anteroposterior axis,and the green axis the mediolateral axis.

as a whole. The pelvis segment was defined using the lumbosacral joint center (L5/S1) and the right and left hip joint center (RIGHT-HIP and LEFT-HIP). The RIGHT-HIP and LEFT-HIP landmark location was estimated according to Bell, Pederson, and Brand (1989, 1990) using the Visual3D software. The L5/S1 joint center was assumed to be located on 19.5 % from the point bisecting the hip joint centers (MIDH) of the distance from MIDH to midpoint between shoulder joint centers and on 34 % from the SACRUM landmark of the distance from SACRUM to the a point bisecting the line connecting the ASIS markers while standing erect (Looze et al., 1992). Hence, the trunk segment was defined using the L5/S1 and the right and left acromion (RAC and LAC, respectively).

The segments' space position and orientation (Fig. 3.7) were obtained by means of local systems of reference fixed to the body segments (Table 3.8). This process allows the measurement of the trunk-to-pelvis posture adopted by the subject in terms of clinically determined position and orientation of body segments. The posture of the trunk with respect to the pelvis in the calibration trial was defined as zero degrees about the flexion-extension, lateral bending, and axial rotation axes. The Y_P-X_T-Z_T Cardan sequence of rotations was used, which is equivalent to the Joint Coordinate System (Grood and Suntay, 1983), to obtain the flexion-extension, lateral bending, and axial rotation of the trunk. Furthermore, the trunk-to-pelvis joint angular velocity and joint angular acceleration was computed.

Table 3.8 Definitions of local coordinate systems

Pelvis	
Origin:	L5/S1 joint center.
Axial (Z_P) axis:	In direction from the MIDH to the origin
Anteroposterior (X_P) Axis:	Perpendicular to both the mediolateral axis and the plane containing LEFT-HIP, RIGHT-HIP and L5/S1 virtual landmarks.
Mediolateral(Y_P) axis:	The common axis perpendicular to the other two axes
Virtual point:	LEFT-HIP and RIGHT-HIP joint centers (Bell, Pederson, and Brand, 1989, 1990); L5/S1 joint center (Looze et al., 1992); MIDH defined as above
Trunk	
Origin:	Midpoint between LAC and RAC landmarks (MIDS)
Axial (Z_T) Axis:	In direction from the L5/S1 virtual landmark to the origin
Anteroposterior (X_T) axis:	Perpendicular to the plane containing L5/S1, RAC and LAC landmarks
Mediolateral(Y_T) axis:	The common axis perpendicular to other two axes in direction from the origin towards the LAC
Virtual point:	L5/S1 and MIDS defined as above
Box	
Origin:	CoG_B
Axial (Z_B) Axis:	The vertical common axis perpendicular to the other two axes
Anteroposterior (X_B) axis:	Perpendicular to the plane containing BOX1, BOX2, BOX3, and BOX4 landmarks in anterior direction
Mediolateral(Y_B) axis:	Perpendicular to X_B in direction from the origin towards the mid-point of BOX2 and BOX3
Virtual point:	CoG_B defined as the point where the diagonal lines of the box are crossed

3.6.6. Identification of Temporal Phases of Lifting and Lowering Tasks

The temporal phases of the lifting and lowering tasks were characterized based on the three-dimensional kinematics of the center of gravity of the box (CoG_B) with respect to the mid-point between the inner-ankle bones. In order to describe the motion of the CoG_B with respect to the mid-point between the inner ankle bones, the cylindrical coordinates have been used instead of the Cartesian (Fig. 3.6). With this transformation it was easier, on one hand, to quantify and visualize the variables that are used for the revised NIOSH equation (Waters et al., 1993), and on the other hand, to identify the temporal phases in order to characterize the lifting and lowering tasks. The parameterization according to these temporal phases had been used previously in symmetric lifting tasks (Bonato et al., 2001). In the present study its use was extended to asymmetric lifting tasks. Furthermore, it was used for the characterization of the lowering tasks.

The vertical, a_z, and radial, a_ρ, components of the acceleration of the CoG_B expressed in cylindrical coordinates were used in order to define the temporal phases of lifting and lowering tasks. The first maximum peak of the a_z (*Instant* 1) of the CoG_B corresponds to the instant when the box is lifted form the origin. The first maximum peak of the a_ρ corresponds to the instant when the box

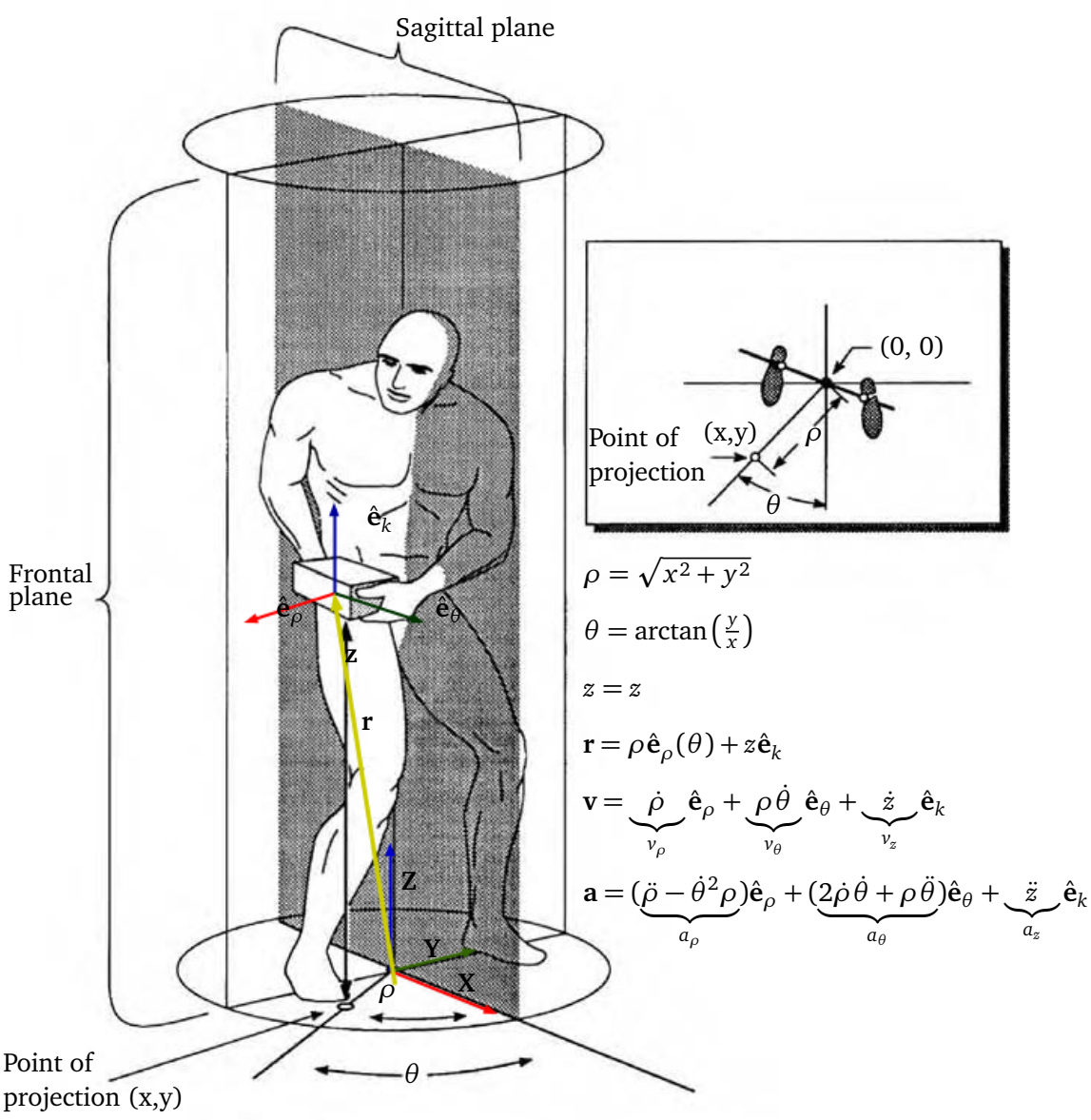

Figure 3.6 Three dimensional mapping from Cartesian to cylindrical coordinates and the corresponding unit vectors (ρ = the length of the projection of the position vector **r** onto the X-Y plane from the origin of the X-Y-Z Cartesian coordinates; θ = the counterclockwise angular displacement in radians of the projection of the position vector **r** onto the X-Y plane from the X-axis; z = the length of the projection of the position vector **r** onto the Z-axis; v_ρ = the radial velocity; v_θ = the transversal velocity; v_z = the vertical velocity; a_ρ = the radial acceleration; a_θ = the transversal acceleration; a_z = the vertical acceleration) (adapted from Waters, Putz-Anderson, and Garg, 1994).

is pushed towards the destination (*Instant* 2), and the first minimum peak of the a_ρ corresponds to the instant when the subject prepares to deposit the box on the destination self (*Instant* 3).

As the temporal evolution of the acceleration components of the CoG_B (a_z, a_ρ, and a_θ) is not the same between the lifting and lowering tasks, the followed parameterization between the lifting and lowering tasks was different. For the lifting tasks, the *Instant* 1 defines the instant of the maximum peak value of the a_z time series that is time bounded between the start of the lifting cycle and the instant of the global minimum of the a_z. *Instant* 2 defines the instant of the maximum peak value of the a_ρ time series that is time bounded between *Instant 1* and the instant of the global minimum value of the a_z. *Instant* 3 is ahead of the minimum value of the vertical acceleration. This parameterization seems to be robust for symmetric and asymmetric lifting tasks.

As with the lifting tasks, the *Instant* 1 in the lowering tasks defines the instant of the maximum peak value of the a_z time series that is time bounded between the start of the cycle and the instant of the global minimum of the a_z. However, the definition of *Instant* 2 and *instant* 3 for the parameterization of the temporal phases of the lowering tasks has to take into consideration whether the tasks are asymmetric or symmetric. For the asymmetric tasks, *Instant* 2 defines the instant of the maximum peak value of the a_ρ time series that is time bounded between the instants of the global minimum and maximum values of the tranversal acceleration (a_θ). For the symmetric tasks, *Instant* 2 defines the instant of the global maximum value of the a_ρ time series. For the asymmetric tasks, *Instant* 3 defines the instant of the minimum peak value of the a_ρ that is time bounded between the maximum peak value of the a_θ time series and the end of the cycle, whereas for the symmetric tasks *Instant* 3 defines the minimum peak value of the a_ρ time series that is time bounded between the maximum peak value of the a_ρ time series and the end of the cycle.

Therefore, using cylindrical coordinates four temporal phases are defined;

1. Lift: from beginning of cycle to *Instant* 1;
2. Pull: from *Instant* 1 to *Instant* 2;
3. Push: from *Instant* 2 to *Instant* 3;
4. Deposit: from *Instant* 3 to end of cycle.

In an ideal symmetric lifting or lowering task, the a_ρ is equivalent to the anteroposterior acceleration (Fig. 3.6) in Cartesian coordinates (Bonato et al., 2001).

3.6.6.1. Similarity of Acceleration Spatiotemporal Profiles

The similarity of acceleration spatiotemporal profiles across treatments after averaging over subjects was assessed using cross-correlation analysis. To classify the cross-correlation coefficients, an hierarchical agglomerative cluster analysis carried out using the Ward's method on the dissimilarity matrix of the cross-correlation coefficients (1 - cross-correlation coefficients). The clustering obtained was represented by means of dendrograms.

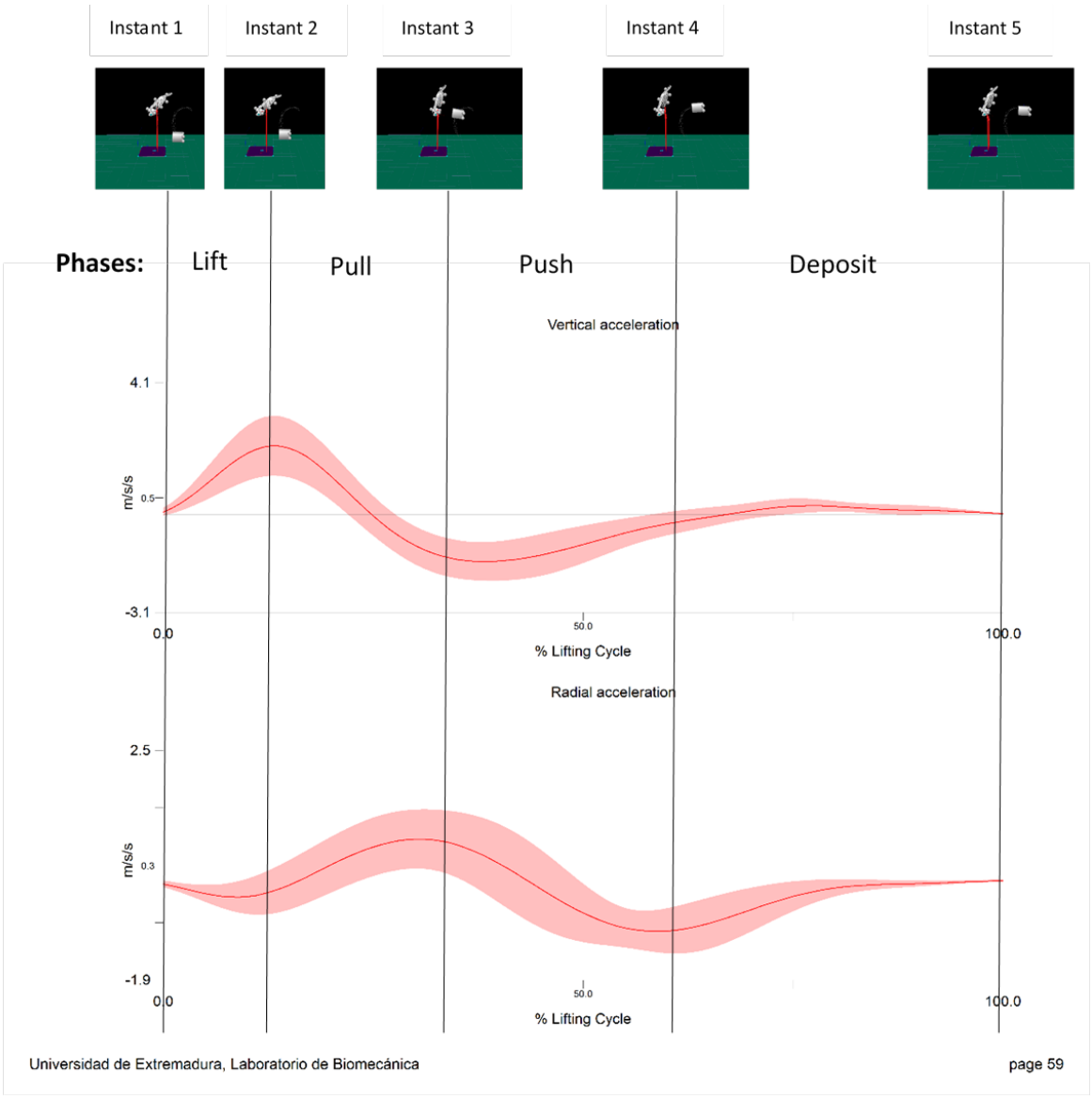

Figure 3.7 Identification of the temporal phases in lifting and lowering cycles.

3.6.6.2. Identification of Lifting and Lowering Cycle

Lifting and lowering cycle identification was manually obtained by visual inspection of the components of the acceleration of the CoG_B expressed in cylindrical coordinates. The obtained cycle intervals were then resampled on a 0-100 % basis and interpolated in order each cycle to have the same number of data in every percentage basis taking as reference the cycle with the most data. For every subject at each task (lifting or lowering) and treatment, the mean time series of the kinematic variables were calculated. The mean time series of every subject were used for further processing.

3.6.7. Force Measurement System Data

Two strain-gauge force platforms (Dinascan 600M, IBV, Valencia, Spain) were utilized to obtain the temporal evaluation of the components of the GRF vector and the coordinates of the COP

during the experiment at sampling rate of 180 Hz. Data "smoothing", derivation, and interpolation at 1 KHz was carried out by quintic splines using the GCVSPL package (Woltring, 1986). For the COP time-series a weighted matrix of the error variance estimated by an uncertainty analysis was constructed (Skiadopoulos and Gianikellis, 2014) and was used with the "True Predicted Mean-squared Error" option. Briefly, following the ISO-JCGM 100 (2010) guide, the noise in the COP signal is the uncertainty in the propagated random error resulted from the combination of the components used to compute COP (Fig. 3.8). For the GRF time-series the GCVSPL package was used by setting the smoothing parameter p a priori, extracted it from a residual analysis (Winter, 2009). The crossover frequency f_c was used to set the smoothing parameter p according to the Butterworth-filter cutoff frequency equivalence of the smoothing spline parameter p

$$\omega_c = (p\tau)^{-\frac{1}{2m}} \Rightarrow p = e^{(-2m\ln(2\pi f_c)-\ln(\tau))} \tag{3.4}$$

where m is for the order of the spline (Woltring et al., 1987) and τ the sampling rate. Under the assumption that the recorded signal is a low-pass signal with additive white noise, the smoothing spline behaves almost like an m^{th}-Butterworth filter with cutoff frequency $f_c = \frac{2\pi}{\omega_c}$ (Woltring, 1995; Woltring et al., 1987). The resultant COP (COP_{net}), either in AP or in ML directions, was calculated from the smoothed data of the two force platforms as follows:

$$COP_{net}(t) = \left[COP_1(t) \times \frac{R_{z,1}(t)}{R_{z,1}(t)+R_{z,2}(t)}\right] + \left[COP_r(t) \times \frac{R_{z,2}(t)}{R_{z,1}(t)+R_{z,2}(t)}\right]$$

where $COP_1(t)$ and $COP_2(t)$ and $R_{z,1}(t)$ and $R_{z,2}(t)$ are the COP and vertical components of the GRF registered by the two force platforms.

3.7. Data Analysis and Statistics

3.7.1. Defining the Jacobian Matrix with Multiple Regression

Performace variables (PVs) that are associated with the risk to develop WRLBD in lifting and lowering MMH tasks and related also to body balance have been investigated in order to understand whether such variables are important control variables—i.e., whether the neural controller stabilizes such variables according to the UCM hypothesis. These PVs were the vertical (z, v_z, a_z), radial (ρ, v_ρ, a_ρ), and transversal (θ, v_θ ,a_θ) components of the displacement, velocity, and acceleration of the COG_B expressed in cylindrical coordinates, and the Euler angles (θ_{flex}, θ_{tilt}, and θ_{axial}) of the trunk with respect to pelvis, together with the trunk-to-pelvis joint angular velocity (ω_{flex}, ω_{tilt}, and ω_{axial}) and joint angular acceleration ($\dot{\omega}_{flex}$, $\dot{\omega}_{tilt}$, and $\dot{\omega}_{axial}$). Except the time profile of PVs that have been associated to the development of WRLBD (Marras et al., 1993; Waters et al., 1993), the stabilization of the COP was also investigated (Winter et al., 1993). Therefore, hypotheses about the control of the COG_B movement trajectory and trunk angular displacement, as well as of their first and second derivatives, and about the COP displacement were tested.

Linear relationships were assumed between small changes in the factor scores ($\Delta\mathbf{F}$) and the change in the performance variable ($\Delta\mathbf{PV}$). **PV** was averaged over each 1% time window of the cycles in order to match **F** time bins number. After both **F** and **PV** being interpolated to 0 - 100 % basis (101

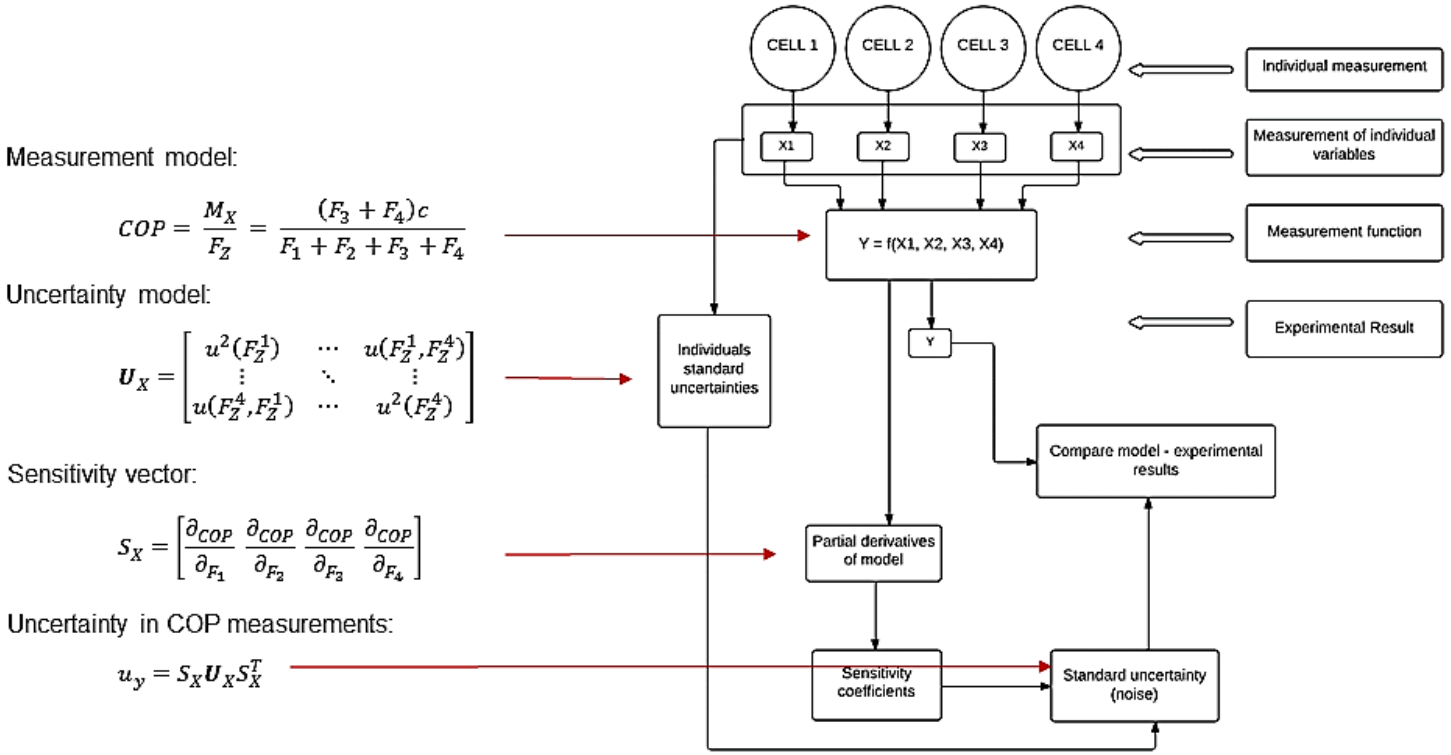

Figure 3.8 Flow chart of the general framework used to quantify uncertainty in COP measurements.

data) in order all time-series to have the same data (since trials time intervals were not exactly 2 sec) and smoothed, changes in each of the factor scores and the performance variable were computed as the successive differences of the scores of consecutive time bins—i.e., over each 1% time window of the cycles. To model the linear relationship, a multiple linear regression analysis without intercept, considering $\Delta\mathbf{F}$ as the explanatory variables and $\Delta\mathbf{PV}$ as the response variable produced a regression line of the form

$$\Delta\mathbf{PV} = \beta_1\Delta\mathbf{F}^{(1)} + \beta_2\Delta\mathbf{F}^{(2)} + \beta_3\Delta\mathbf{F}^{(3)} \tag{3.5}$$

with $\Delta\mathbf{F}^{(n)}, \Delta\mathbf{PV} \in \mathbb{R}^{t-1}$. The coefficients of the regression equation were arranged in a matrix that is a Jacobian matrix $\mathbf{J}$, reduced to this case to a 1×3 vector $\mathbf{J} = \begin{bmatrix}\beta_1 & \beta_2 & \beta_3\end{bmatrix}$. Therefore,

$$\Delta\mathbf{PV} = \mathbf{J}\Delta\mathbf{F}. \tag{3.6}$$

This analysis was used to compute $\mathbf{J}$ for each of the fourteen subjects, the sixteen treatments, and the twenty performance variables.

3.7.2. Uncontrolled Manifold Analysis

The UCM hypothesis describes a manifold in the PCs subspace on which the performance variable is reproducible from cycle to cycle. The M-modes variance that lies within the UCM subspace represents the combinations of M-modes gains that stabilize the selected performance variable—i.e., *stability* of the performance variable. The M-modes variance that lies within an orthogonal to the UCM subspace represents the combinations of the M-modes gains that destabilize the selected performance variable (Latash, Scholz, and Schoner, 2007). However, the same set of M-modes gains may be used to form different covariation patterns for different performance variables—i.e., *flexibility* of trunk muscle activations patterns. Therefore, the synergy index for each of the PVs was computed as follows in order to verify whether the system comprises all the three features (sharing pattern, stability and flexibility).

1. Computation of the UCM. The null space of the $\mathbf{J}$ matrix was computed to provide the basis vectors spanning the linearized UCM. The null space of the $\mathbf{J}$ matrix consists of all vectors $\mathbf{x}$ such that $\mathbf{Jx} = 0$. Within the three-dimensional space of all possible vectors $\mathbf{x}$, the solutions to $\mathbf{Jx} = 0$ form a two-dimensional subspace. The two basis vectors ε_1 and ε_2 defining the null space were computed with the *nullspace*() function of the package **pracma** in R environment. As the M-mode space is three-dimensional ($n = 3$), and for the one-dimensional performance variable $d = 1$ the null space is two-dimensional ($n - d = 2$), the system is redundant with respect to the task of stabilizing the performance variable.

2. Computation of deviation matrix. $\Delta\mathbf{F}$ were averaged across the trials in every time bin and the averaged vector $\overline{\Delta\mathbf{F}}$ was then subtracted from the vectors of the individual changes in the M-mode magnitudes

$$\Delta\mathbf{F}_{\mathrm{D}} = \Delta\mathbf{F} - \overline{\Delta\mathbf{F}} \tag{3.7}$$

3. Decomposition of variability. The component of the deviation matrix $\Delta\mathbf{F}_{\mathrm{D}}$ which is parallel to the UCM represents how much deviation occurs without altering the value of the performance variable and was obtained by its orthogonal projection onto the null space. To compute the projection of the $\Delta\mathbf{F}_D$ onto the UCM ($\mathbf{f}_{\mathrm{UCM}}$) and the orthogonal subspace ($\mathbf{f}_{\mathrm{ORT}}$) the projection matrix $\mathbf{Q}$ for the two-dimensional null space of R^3 spanned by the vectors $\boldsymbol{\varepsilon}_1$ and $\boldsymbol{\varepsilon}_2$ was computed

$$\mathbf{Q} = \mathbf{A}(\mathbf{A}^T\mathbf{A})^{-1}\mathbf{A}^T$$

where $\mathbf{A} = [\boldsymbol{\varepsilon}_1, \boldsymbol{\varepsilon}_1]$. Therefore,

$$\mathbf{f}_{\mathrm{UCM}} = \mathbf{Q}\Delta\mathbf{F}_D^T$$
$$\mathbf{f}_{\mathrm{ORT}} = (\mathbf{I}-\mathbf{Q})\Delta\mathbf{F}_D^T$$

where $\mathbf{I}$ is the identity matrix.

4. Computation of variance. The total trial-to-trial variance V_{TOT} as well as the variance in each of the two subspaces (V_{UCM} and V_{ORT}) normalized by the number of DOF were calculated as

$$V_{\mathrm{TOT}} = \sigma^2_{\mathrm{TOT}} = \frac{1}{3\times N}\sum_{i=1}^{N}\|\Delta\mathbf{F}_{\mathrm{D}}\|^2$$
$$V_{\mathrm{UCM}} = \sigma^2_{\mathrm{UCM}} = \frac{1}{2\times N}\sum_{i=1}^{N}\|\mathbf{f}_{\mathrm{UCM}}\|^2$$
$$V_{\mathrm{ORT}} = \sigma^2_{\mathrm{ORT}} = \frac{1}{N}\sum_{i=1}^{N}\|\mathbf{f}_{\mathrm{ORT}}\|^2.$$

5. Computation of the synergy index. A performance variable is controlled in the UCM sense when V_{UCM} is statistically higher than V_{ORT} (Latash, Scholz, and Schoner, 2007). To compare across subjects and treatments the synergy index was computed as

$$\Delta V = \frac{V_{\mathrm{UCM}} - V_{\mathrm{ORT}}}{V_{\mathrm{TOT}}}$$

which ranges between 1.5 (all variance is within UCM - a synergy) and -3 (all variance is within the orthogonal subspace - not a synergy with the current PV but probably a reflection of another synergy) (Latash, Scholz, and Schoner, 2007). A zero index means that there is not a synergy (Latash, Scholz, and Schoner, 2007). For stastisical analyses ΔV values were transformed into z-scores using Fisher's z-transformation adapted to the boundaries of ΔV (Robert, Zatsiorsky, and Latash, 2008; Verrel, 2010):

$$\Delta V_z = \frac{1}{2}\log\left(\frac{3+\Delta V}{1.5-\Delta V}\right)$$

3.8. Statistical Analysis

The experimental design was treated as a repeated-measures analysis. Prior to model analysis, parametric assumptions of normality and homogeneity of variance was examined. Furthermore,

plot by within plot interactions was assessed (Logan, 2010; Quinn and Keough, 2002). For parametric analysis, a five factor partly nested linear additive model with one between plot factor (Gender) and four within plot factors (VD, HD, AM and LD) was fitted in the data to analyze the split-plot design (Logan, 2010; Quinn and Keough, 2002). As both between-plot and within-plot factors are fixed and plot is random and moreover there is no interest of the nested term and its interactions, the replicates measurements within each combination of factor Gender, subjects and treatments for both lifting and lowering tasks were averaged after being analyzed for any outliers. Therefore, one averaged observation per cell was held for the analysis of the split-plot design. To verify the interpretation of the interaction effects simple main effects tests were performed using the *testInteractions*() routine of the **phia** library (De Rosario-Martinez, 2015).

The sphericity assumption of the repeated-measures Analysis of Variances (ANOVAs) was checked using Mauchly's test of sphericity, and when spericity assumption was violated the degrees-of-freedom was corrected using Greenhouse-Geisser (GG) estimates of sphericity. Significant main effects were analyzed with unplanned pairwise comparisons using paired *t*-tests corrected with the Benjamini-Hochberg method or with planned contrasts. For non-parametric analyses the two-way Friedman's ANOVA by ranks and post-hoc comparison carried out using the *friedman*() routine of the **agricolae** library (Mendiburu, 2015). Descriptive statistics was calculated for the dependent variables as a function of the independent variables. ANOVA carried out with the *ezANOVA*() routine of the **ez** library (Lawrence, 2013). A significance level of 0.05 was used for statistical tests. R statistical software (R Core Team, 2013) was utilized.

3.8.1. Statistical Hypotheses

The null and alternative hypotheses for the split-plot experimental design are:

For the between-plot factors (fixed):

- H_0 := there is no effect of the gender factor on the dependent variable.
- H_1 := gender factor influences the dependent variable.

For the within-plot main factors (fixed):

- H_0 := there is no effect of NIOSH factors and Liquid load factor on the dependent variable.
- H_1 := NIOSH factors and Liquid load factor influence the dependent variable.

For the within-plot interactions (fixed):

- H_0 := there is no effect of the interaction between the levels of NIOSH factors and Liquid factor on the dependent variable.
- H_1 := the interaction between the levels of the NIOSH factors and Liquid factor influence the dependent variable.

4

Results

4.1. Identification of Temporal Phases of Lifting and Lowering Tasks

The trials time intervals were controlled by an electronic metronome with pace of 2 sec (30 bpm). Ideally, each trial should last 2 sec. A one-way ANOVA revealed that there are no statistically differences among trials duration ($p = 0.61$), with mean duration of 2.31 ± 0.26 sec. Therefore, it was expected that the treatments with lift origin the *knee* level of the VD factor and/or with asymmetry would have statistically significant higher values for the distance travelled, the maximum peak linear velocity, the maximum peak linear acceleration variables and also would affect box's rotation(as compared with lift origin the *hip* level of the VD factor and/or with symmetry.)

The mean total distance travelled by the CoG_B across subjects and treatments (lifting and lowering) was 6.59 ± 1.79 m. The mean distance travelled by the CoG_B in the treatments across subjects for the lifting tasks was (0.95 ± 0.25 m) and in lowering tasks (0.96 ± 0.26 m). The total distance travelled by the CoG_B as a function of the independent variables was significant higher when the subjects picked up the box from the *knee* level (8.04 ± 0.47 m) as compared to the *hip* level (5.14 ± 0.31 m) ($F_{[1,12]} = 667.3$, $p < 0.001$), and in asymmetric (7.32 ± 0.42 m) than in symmetric (5.86 ± 0.39 m) tasks ($F_{[1,12]} = 142.3$, $p < 0.001$). Main effect of the AM factor was qualified by a significant interaction of the SEX, AM, and LD factors ($F_{[1,12]} = 5.4$, $p = 0.039$), indicating that for female subjects and in asymmetric tasks, the total distance travelled by the CoG_B decreased when the liquid load was handled (7.04 ± 0.65 m) as compared to solid load (7.36 ± 0.29 m.) A significant interaction between the HD and the LD factors ($F_{[1,12]} = 5$, $p = 0.044$) revealed that picking up the liquid load from the *near* origin (6.42 ± 0.63 m) decreased the distance travelled by the CoG_B as compared to the *far* origin (6.73 ± 0.34 m.)

Moreover, the maximum velocity of the CoG_B as a function of the independent variables was higher when the load was picked up from the *knee* level (1.01 ± 0.07 m/s) as compared to the *hip* level (0.7 ± 0.04 m/s) ($F_{[1,13]} = 330.9$, $p < 0.001$), and for asymmetric (0.95 ± 0.07 m/s) as compared to symmetric (0.75 ± 0.05 m/s) tasks ($F_{[1,13]} = 130.7$, $p < 0.001$). However, main effects for the maximum velocity variable were qualified by a significant interaction between the factors VD, AM, and LD ($F_{[1,13]} = 15.01$, $p = 0.002$), indicating a significant decrease of the maximum velocity of the CoG_B when the subjects picked up the *liquid* load from the *knee* origin (1.05 ± 0.09 m/s)

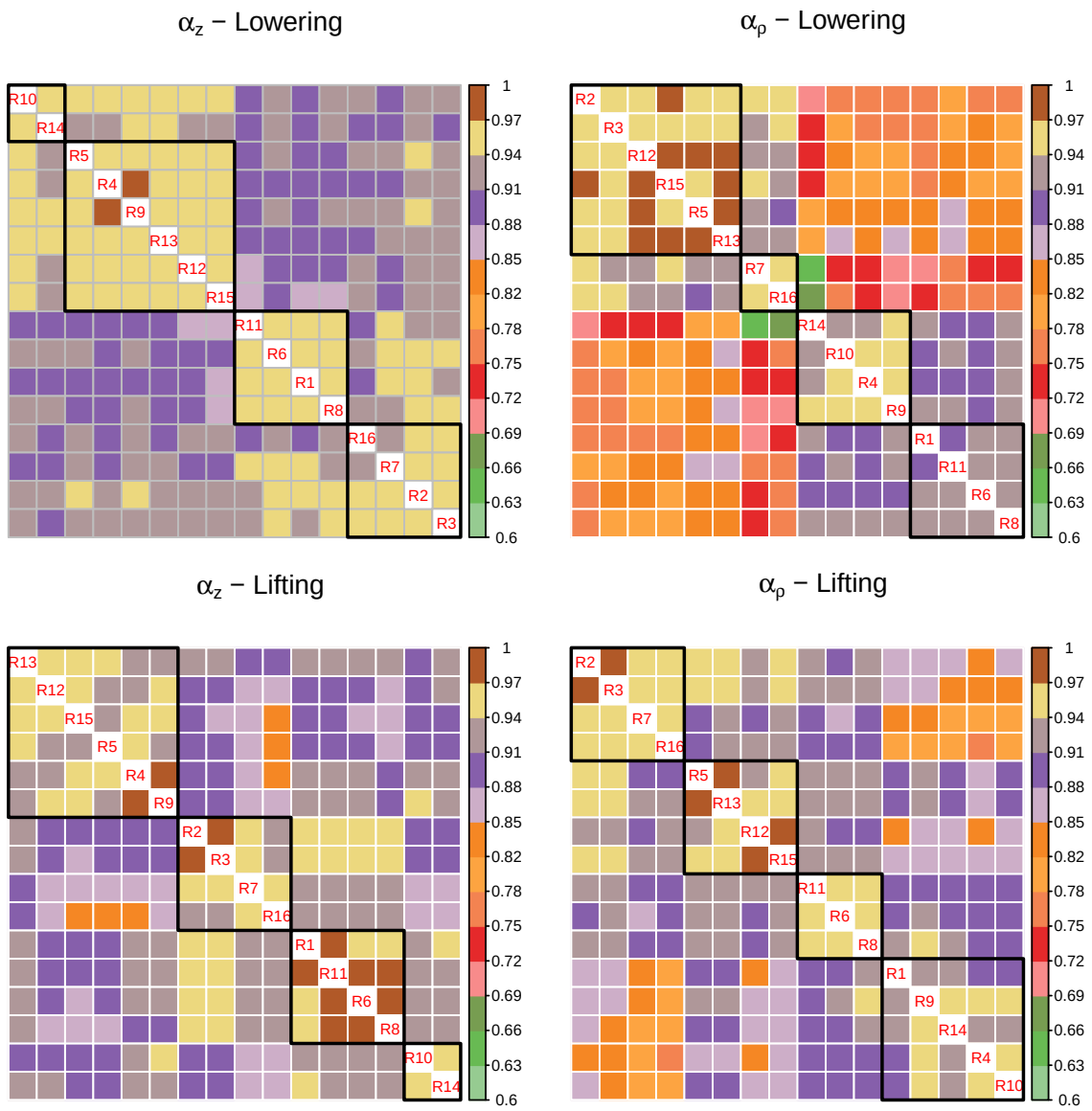

Figure 4.1 Color coded cross-correlation matrices showing paiwise collerations between the acceleration components in different treatments for the lowering and lifting task. Also, the clusters derived from the hierarchical 4 cluster grouping of the correlation coefficients values are showed.

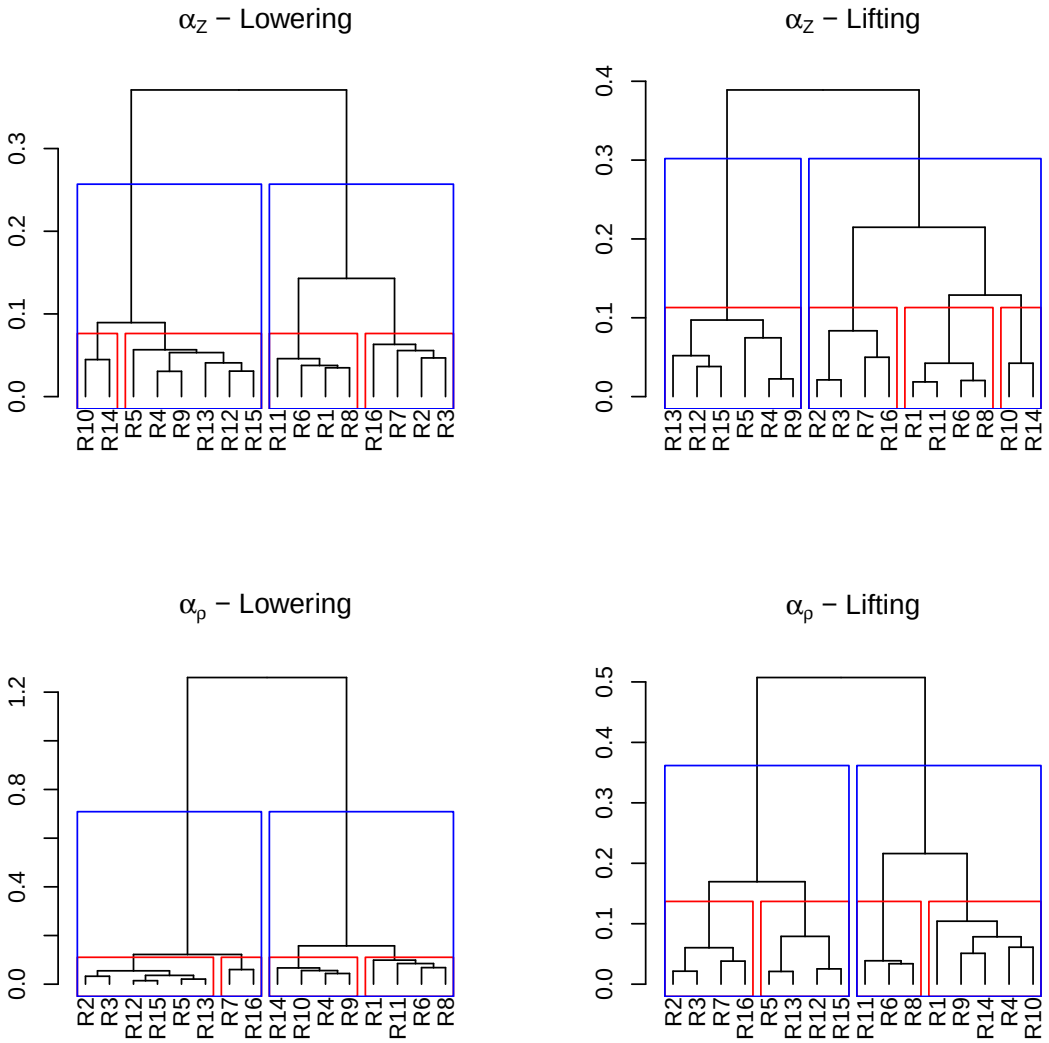

Figure 4.2 Cluster analysis dendrograms of the cross-correlation matrices of a_ρ and a_z (dissimilarity = 1 - cross-correlation values).

in asymmetric tasks as compared to the *solid* load (1.09 ± 0.09 m/s), and a significant increase when the *liquid* load was picked up from the *knee* origin for symmetric tasks (0.96 ± 0.08 m/s) as compared to the *solid* load (0.92 ± 0.1 m/s). The main effect of AM was qualified also by an interaction with factor HD ($F_{[1,13]} = 6.16$, $p = 0.028$) indicating that for the symmetric tasks maximum valocity of CoG_B is higher when the load is picked up from the *near* level of the HD factor (0.77 ± 0.05 m/s) as compared to the *far* level (0.74 ± 0.06 m/s).

The VD factor was also found to influence significantly the maximum peak linear acceleration of the CoG_B, which was higher when the load was picked up from the *knee* origin (2.94 ± 0.35 m/s^2) as compared to the *hip* origin (1.95 ± 0.24 m/s^2) ($F_{[1,13]} = 209.5$, $p < 0.001$). Moreover, the maximum acceleration of the CoG_B was higher in asymmetric (2.57 ± 0.32 m/s^2) as compared to symmetric (2.33 ± 0.24 m/s^2) tasks ($F_{[1,13]} = 25.73$, $p < 0.001$). Main effects were qualified by

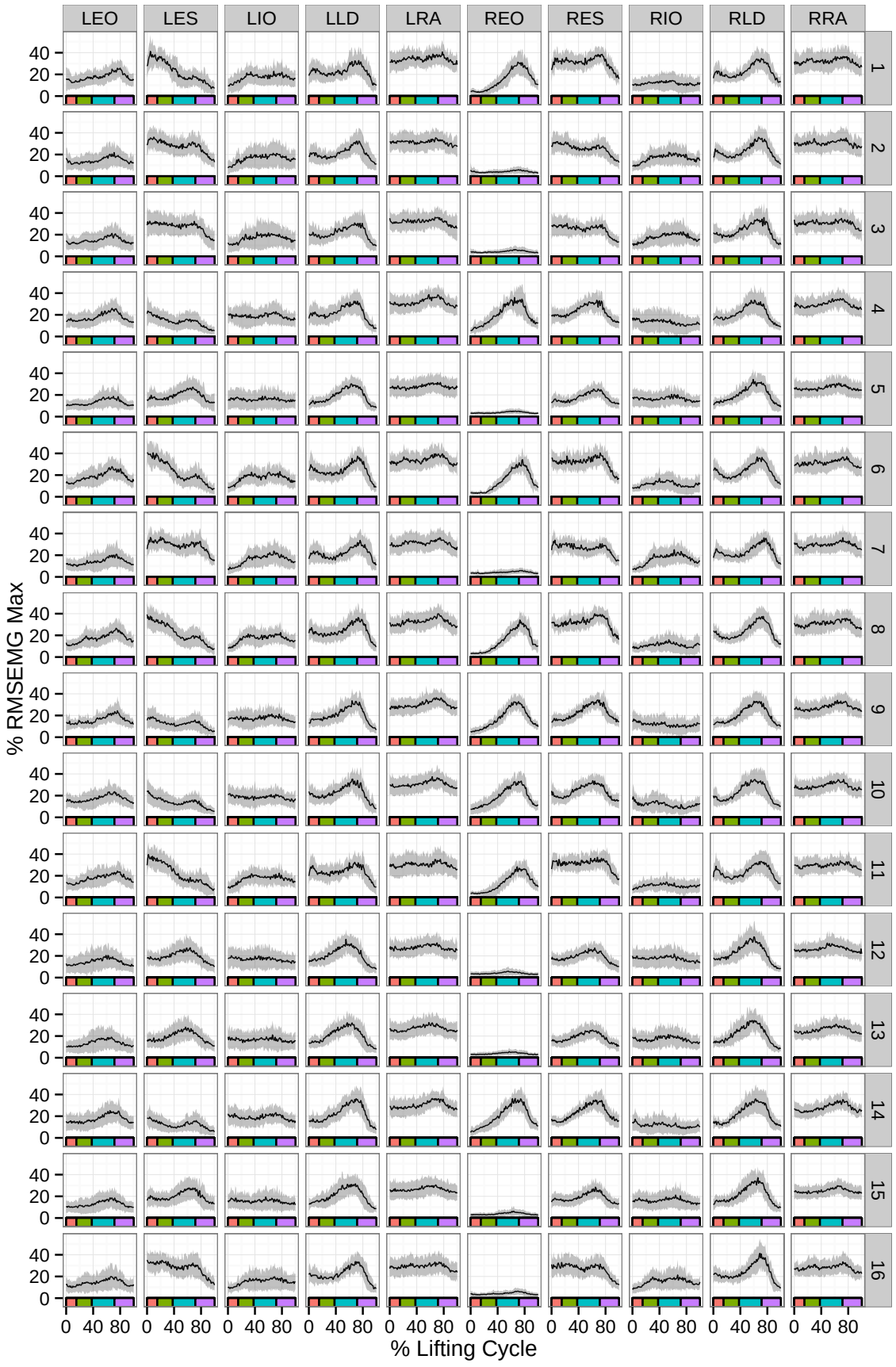

Figure 4.3 Mean EMG activity for the lifting task. The RMS of the EMG amplitude was calculated over time bins of 1% of the task cycle and normalized to the maximum value across treatments for each subject and muscle. For abbreviations see text.

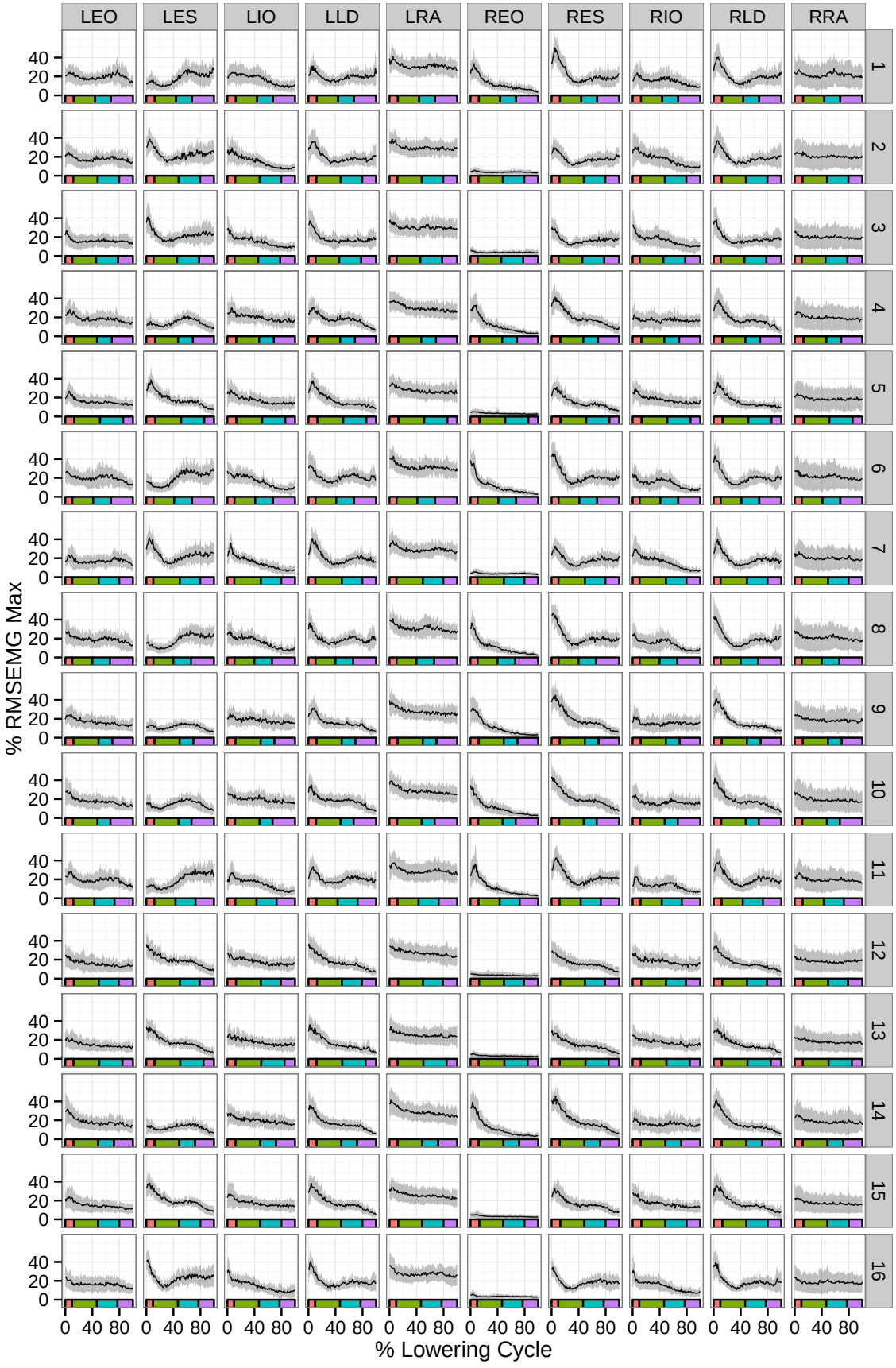

Figure 4.4 Mean EMG activity for the lowering task. The RMS of the EMG amplitude was calculated over time bins of 1% of the task cycle and normalized to the maximum value across treatments for each subject and muscle. For abbreviations see text.

a significant interaction between VD, AM, and LD factors ($F_{[1,13]} = 6.4$, $p = 0.025$) indicating a significant decrease of the maximum acceleration of the CoG_B when the subjects picked up the *liquid* load from the knee origin ($2.98 \pm 0.46\,m/s^2$) in asymmetric tasks as compared to the *solid* load ($3.12 \pm 0.4\,m/s^2$.)

Significant differences were also found for the maximum three-dimensional rotations of the box with respect to the global system of reference as a function of the independent variables. The results of the ANOVA, with the X_B rotation as dependent variable showed a significant main effect of the AM factor ($F_{[1,13]} = 570.1$, $p < 0.001$) qualified by an interaction between SEX and AM factors ($F_{[1,13]} = 6.22$, $p = 0.028$), indicating higher maximum X_B rotations for asymmetric tasks ($10.16 \pm 1.86\,°$) as compared to symmetric tasks ($3.82 \pm 1.83\,°$), and furthermore, in symmetric tasks the female subjects had significant higher maximum X_B rotations than males ($4.68 \pm 2.32\,°$ vs. $2.96 \pm 0.41\,°$, for female and male subjects, respectively.) There was a significant main effect of the AM ($F_{[1,13]} = 23.02$, $p = 4e\text{-}04$) and HD ($F_{[1,13]} = 13.62$, $p = 0.003$) factors and by their interaction ($F_{[1,13]} = 11.23$, $p = 0.006$) on the maximum Y_B rotations, indicating higher scores for symmetric ($12.87 \pm 4.42\,°$) than asymmetric tasks ($9.23 \pm 2.8\,°$), and moreover, this difference was even more pronounced for picking up the load from the *far* level (as compared to the *near* level) in symmetric lifting tasks ($14.3 \pm 5.85\,°$ vs. $11.44 \pm 3.12\,°$, for far and near levels, respectively.) Moreover, there was an interaction between the SEX, LD, and VD factors ($F_{[1,13]} = 5.04$, $p = 0.044$) indicating that for the female subjects picking up the liquid load from the hip level results to lower maximum Y_B rotations values as compared to hip level ($13.48 \pm 4.28\,°$), or as compared to solid load from both the hip ($13.19 \pm 7.65\,°$ vs. $10.41 \pm 2.79\,°$, for solid and liquid levels, respectively) or knee level ($10.41 \pm 2.79\,°$.), while for the male subjects pick uo the solid load from the knee level ($10.83 \pm 1.85\,°$) results to higher maximum Y_B rotations values as compared to the hip level ($7.97 \pm 2.2\,°$.) There was a main effect for factor AM for the maximum Z_B rotations ($F_{[1,13]} = 4436.14$, $p = 0$) qualified by a significant interaction betweeb HD, AM, and LD factors ($F_{[1,13]} = 4.83$, $p = 0.047$), indicating higher maximum Z_B rotations values for asymmetric ($54.15 \pm 1.57\,°$) than symmetric tasks ($4.65 \pm 2.02\,°$), and furthermore lower scores for the liquid load ($4.31 \pm 1\,°$) as compared to solid load ($5.94 \pm 5.91\,°$) in far level of symmetric tasks.

4.1.1. Similarity of Acceleration Spatiotemporal Profiles

All subjects were able to perform qualitatively similar time profiles of the three-dimensional kinematics of the center of gravity of the box (CoG_B) with respect to the mid-point between the inner-ankle bones. A cluster analysis on the cross-correlation matrices was performed in order to group the treatments according to the similarity of the spatiotemporal profiles of the a_z and a_ρ components of the CoG_B acceleration expressed in cylidrical coordinates. Figure 4.1 shows the cross - correlation matrices for the a_z and a_ρ time - series calculated between all pairs of the treatments for both lifting and lowering tasks. The mean correlation coefficient values across subjects for the lifting task were at 0.82 - 0.98 for the a_z, and at 0.78 - 0.98 for the a_ρ. Lowering scores ranged 0.86 - 0.97 for the a_z, and 0.63 - 0.99 for the a_ρ, respectively. The cluster analysis dendrograms (Fig. 4.2) showing that for 2 cluster grouping the cross - correlation coefficient values for the a_ρ formed 2 clusters, with the same treatments within each group for both lifting and

lowering tasks; while for the a_z time - series, the 2 cluster grouping formed also 2 clusters, but with different treatments within each group for the lifting as compared to the lowering task. Clustering analysis at a lower level grouped the correlation coefficient values of each time - series into 4 clusters. For the a_z time series, treatments within each of the 4 clusters are the same between lowering and lifting tasks; however, the order of dissimilarity among clusters for lifting as compared to the lowering task is not the same. For the a_ρ time - series, treatments within groups in 4 cluster grouping are not the same.

Regarding the association between the factorial structure of the experiment, and the clustering of the cross - correlation coefficient values, it is clear that 2 cluster grouping of a_z - lowering formed 2 clusters by grouping the correlation coefficient values between treatments of the hip vs. knee levels of the VD factor, while for the a_ρ - lowering and a_ρ - lifting, the 2 clusters formed by grouping the correlation coefficient values between asymmetry vs. symmetry treatments. Regarding the 4 cluster grouping, in most of the cases the formed clusters are grouping correlation coefficient values between treatmets with same levels of the VD, HD, and AM factors. The type of the load factor (LD: liquid vs. solid) does not form dissimilar patterns of spatiotemporal profiles of the a_ρ and a_z components of the CoG_B acceleration according the cross-correlation values.

4.2. Identification of Muscle Modes

4.2.1. Dimensionality of the Principal Component Subspace

In 56.03 % and 31.92 % of both lifting and lowering data sets the first three and two PCs, respectively, had eigenvalues over Kaiser's criterion (K1) of 1, while in the rest 10.27 % of the data sets the first four PCs had eigenvalues over 1, and in the 1.79 % of the data sets only the first PC was retained. PC5 through PC10 had eigenvalues less of 1 across all data sets. Horn's Parallel Analysis (PA) suggested that in the 52.23 % and 25.89 % of the data sets the initial 10 variables can be reduced to a two or three - dimensional PC subspaces, respectively, while in the 20.09 % of the data sets all components except the first PC were dropped, and only in the rest 1.79 % of the data sets the first four PCs were retained. Therefore, a three - dimensional PC subspace or less was suggested in the 89.74 % and 98.21 % of the data sets opposite to a two - dimensional PC subspace or less that was suggested in the 33.71 % and 72.32 % of the data sets according to K1 and PA criteria, respectively. The average dimensionality of the PC subspaces according to K1 and PA retention criteria was significant different among treatments after averaging across subjects for both lifting and lowering tasks (Friedman's $\chi^2_{[15]} \geq 103.32$, $P \leq 0.012$). The multiple - comparison analysis to the ranked data showed that the increase in the number of the retained PCs is associated with the levels of the NIOSH factors, where at least two groups were formed: *hip* vs *knee* treatments, with less dimensionality in *hip* treatments (Fig. 4.7). On average, K1 criterion suggested three PCs while PA criterion suggested two PCs for both the lifting and lowering data sets (rounding to the nearest integer). However, the convergence of K1 and PA retention criteria according to the percentage of both lifting and lowering data sets that can be explained by three PCs (89.74 % and 98.21 %, for K1 and PA respectively), supported our conclusion that the initial 10 variables can be reduced to a three - dimensional PC subspace. Using the criteria described

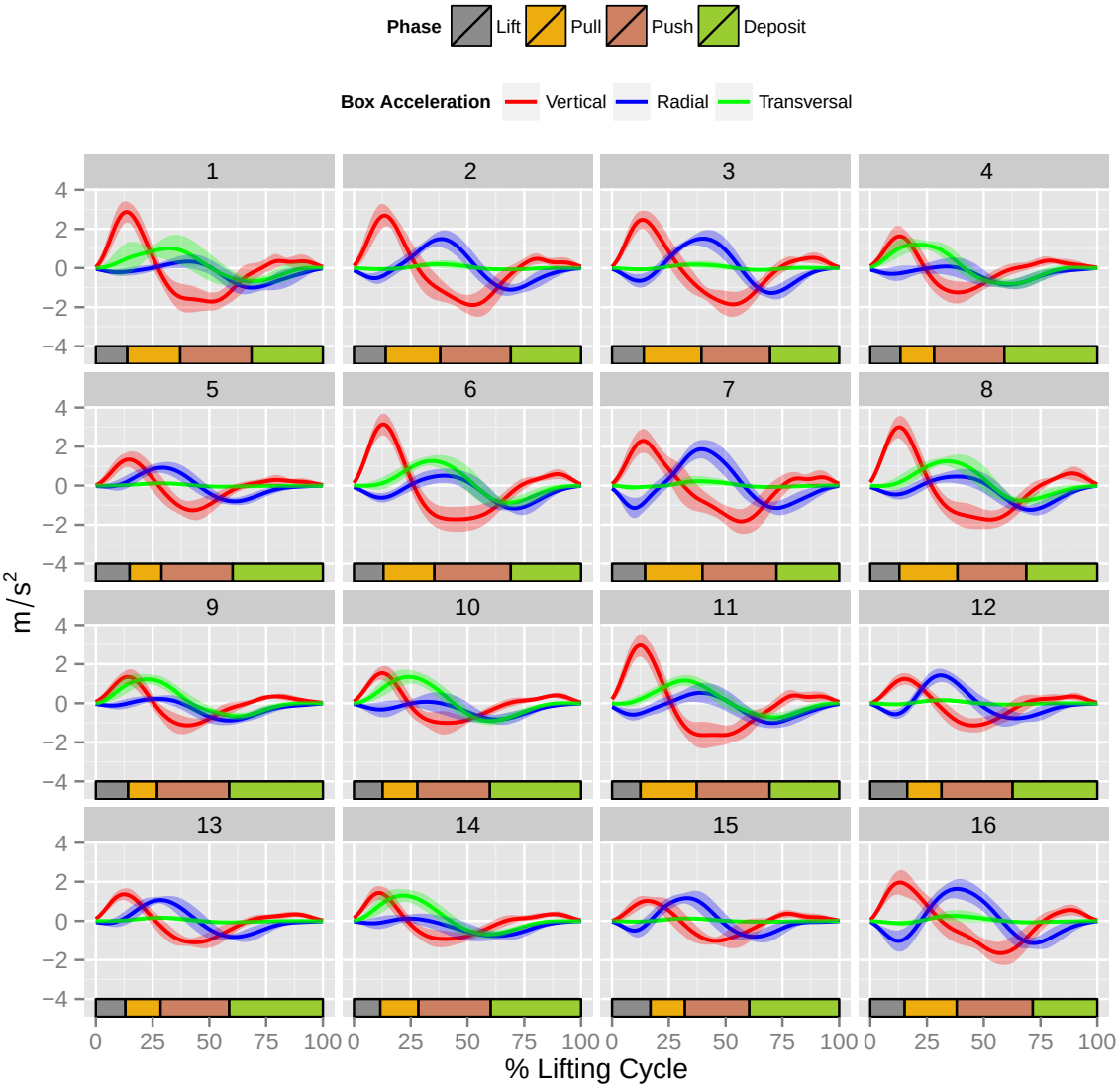

Figure 4.5 Phase definitions according to the maximum value of the vertical acceleration a_z and the maximum and minimum values of the radial acceleration a_ρ of the CoG_B. Mean values and standard deviations for the cylindrical kinematic parameters vertical acceleration, a_z, and radial acceleration, a_ρ, and mean percentage values for the phases of the lifting cycles for all subjects are shown.

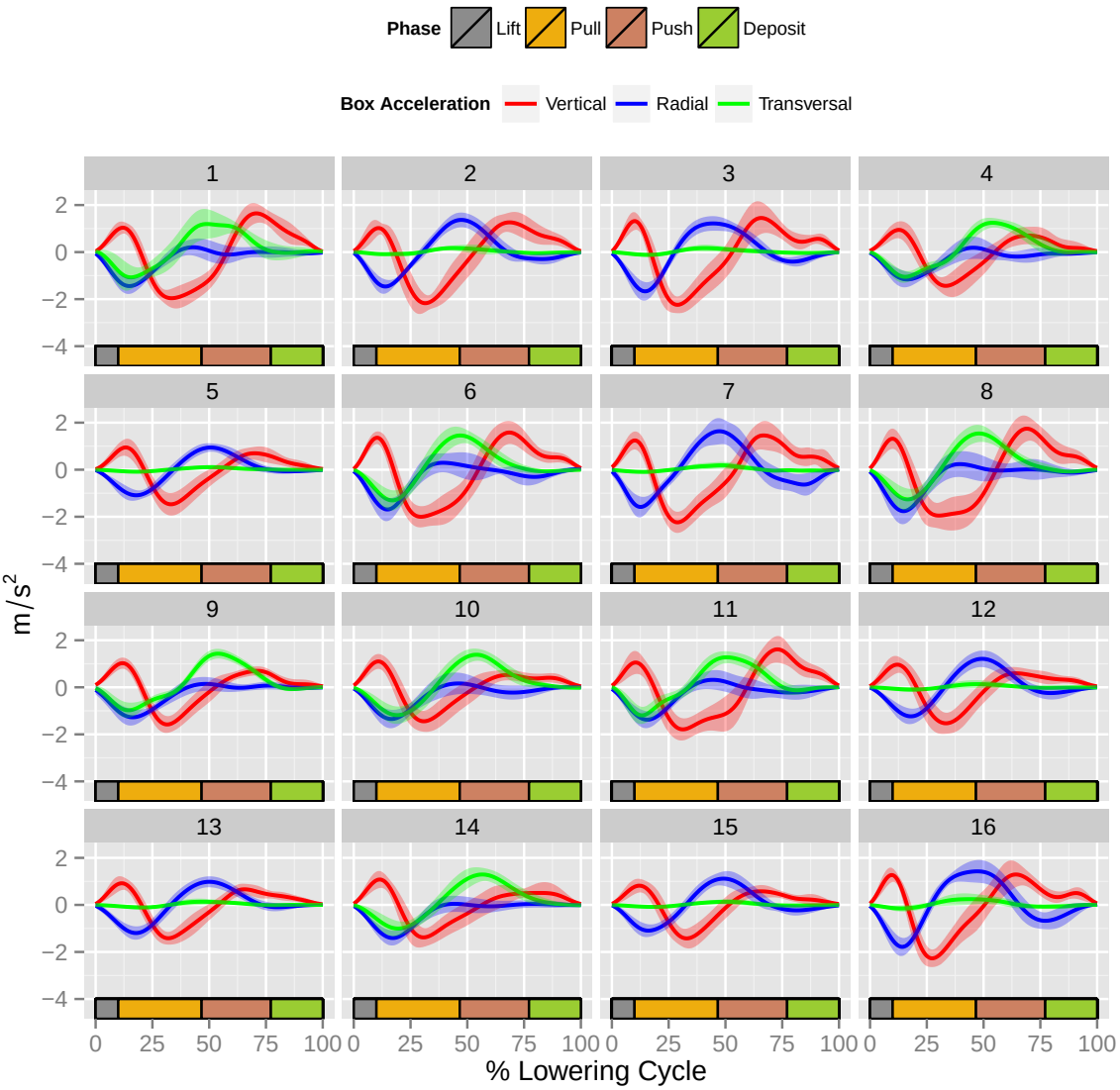

Figure 4.6 Phase definitions according to the maximum value of the vertical acceleration a_z and the maximum and minimum values of the radial acceleration a_ρ of the CoG_B. Mean values and standard deviations for the cylindrical kinematic parameters vertical acceleration, a_z, and radial acceleration, a_ρ, and mean percentage values for the phases of the lifting cycles for all subjects are shown.

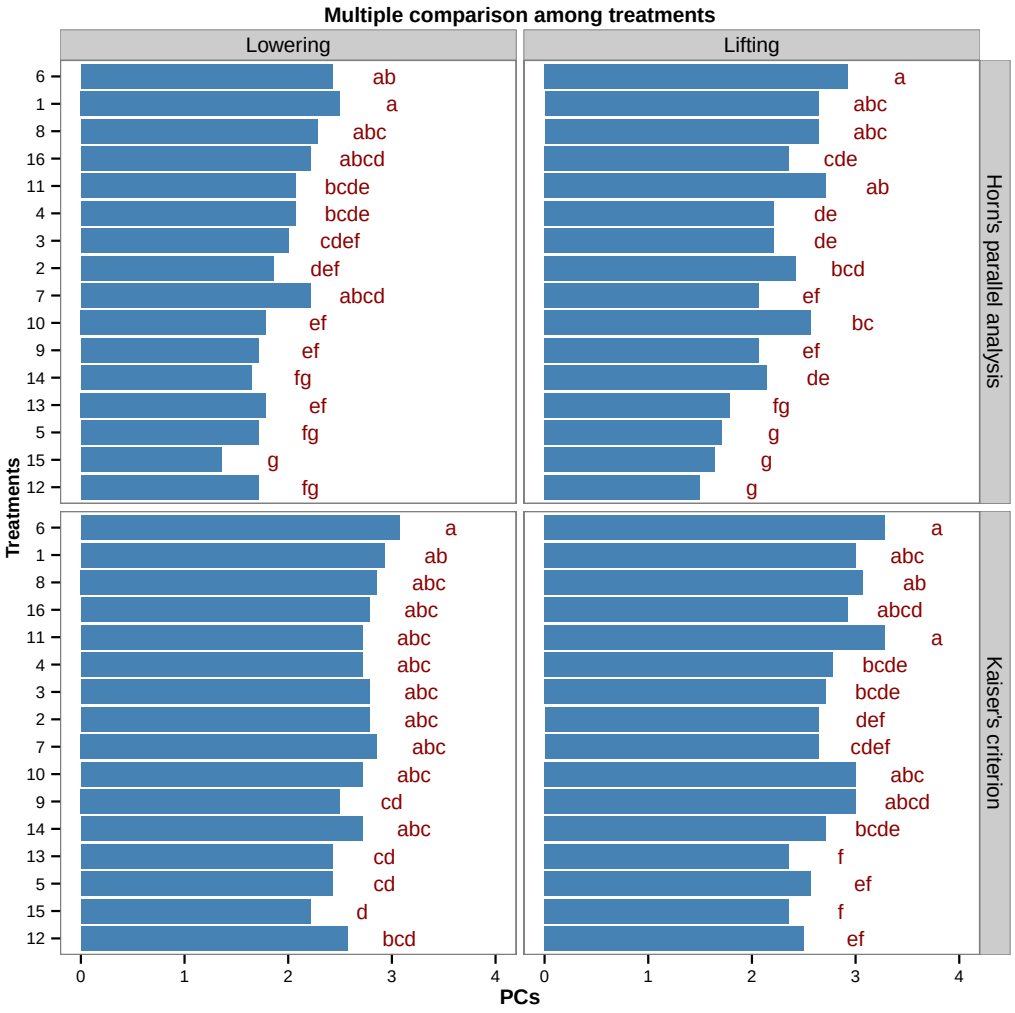

Figure 4.7 Multiple comparison analysis on the suggested number of PCs across subjects according to PA and K1 retention criteria. The Friedman ANOVA by ranks rejected the hypothesis that the suggested number of PCs are equal either across subjects or treatments. Means with the same letter are not significantly different.

previously, the first three PC were retained in each data set of both lifting and lowering tasks.

The differences in the dimensionality of the PC subspace suggested by the used retention criteria (first three PCs vs. Kaiser's criterion vs. Horn's Parallel Analysis) is reflected in the amount of the fraction of the cumulative variance explained by the sets of the retained PCs. The three retained PCs accounted, on average, for the 62.92 ± 5.67 % of the overall cumulative variance amongst the m = 10 muscles during lowering tasks ($PC1_{Low} = 37.26 \pm 8.36\,\%$; $PC2_{Low} = 15.11 \pm 3.56\,\%$; $PC3_{Low} = 10.55 \pm 1.86\,\%$), and for the 59.43 ± 5.67 % of the overall cumulative variance during lifting tasks ($PC1_{Lift} = 32.36 \pm 5.65\,\%$; $PC2_{Lift} = 15.98 \pm 3.14\,\%$; $PC3_{Lift} = 11.09 \pm 1.62\,\%$.) Figure 4.8 illustrates the average fractions of the variance accounted for by each of the first three PCs under the different treatments after averaging over subjects. In some data sets PC4 accounted for a comparable variance to that of PC3. According to K1, PC4 accounted for 10.42 ± 0.45 % of the total variance for the lowering tasks and 10.66 ± 0.59 % for the lifting tasks, while according

to PA, PC4 accounted for the 11.29 ± 0.15 % of the total variance for the lowering tasks, and 11.56 ± 0.41 % for the lifting tasks. The retained PCs according to K1 accounted, on average, for the 60.42 ± 6.03 % of the overall cumulative variance amongst the m = 10 muscles during lowering tasks, and 57.74 ± 6.49 % for the lifting tasks, while for the PA the retained PCs accounted for the 52.41 ± 8.07 % of the overall cumulative variance during lowering tasks, and the 51.49 ± 8.73 % during lifting tasks (keep in mind that K1 and PA criteria do not retained fixed number of PCs across data sets.) The results of the repeated - measures ANOVA with factor *Criterion* (PA,K1, acPC) showed significant differences of the overall cumulative variance accounted for by the retained PCs among the different retention criteria for both lifting ($F_{[2,26]} = 40.72$, $P = 0.001$, $\eta_g^2 = 0.47$) and lowering tasks ($F_{[1.21,15.72]} = 61.85$, $P_{GG} = 0.001$, $\eta_g^2 = 0.58$). For the lifting tasks, contrasts showed that the amount of overall cumulative variance explained by the three - dimensional PC subspace was comparable to that of K1 ($F_{[1,26]} = 3.21$, $P = 0.085$), but significant higher than that of PA ($F_{[1,26]} = 78.23$, $P = 0.001$). For the lowering tasks, contrasts showed that the amount of the overall cumulative variance explained by the three-dimensional PC subspace was significant higher than both K1 ($F_{[0.6,15.72]} = 7.69$, $P_{GG} = 0.024$) and PA ($F_{[0.6,15.72]} = 116$, $P_{GG} = 0.001$). The results of the repeated - measures ANOVA with factor *Treatment*, revealed that the amount of the cumulative variance explained by the three retained PCs was varied under the different treatments only during the lifting tasks ($F_{[4.58,59.6]} = 3.18$, $P_{GG} = 0.02$, $\eta_g^2 = 0.14$). Pair-wise comparisons (paired t-tests) showed that the cumulative variance explained by the three retained PCs was significant higher for treatment $a = 14$ as compared to treatments $a = 5$, 6, 7, 8, 10, 11, 13 and 15, and for treatment $a = 4$ as compared to treatments $a = 2$ and 5.

4.2.2. Goodness-of-fit of the Linear Subspace Approximation

Figure 4.9 depicts the indices of goodness of the linear subspace approximation of $\hat{\mathbf{M}}$ on $\mathbf{M}$ (VAF) and of $\hat{\mathbf{M}}_\mathbf{z}$ on $\mathbf{M}_z$ (r^2) from the PCs extracted from the 10 muscle activation patterns as a function of the number of the retained PCs. The three - dimensional PC subspace accounting for the 92 % (range = 91 - 92 %) of the total VAF and the 61 % (range = 59 - 63 %) of the total r^2 for the lifting task, and the 91 % (range = 90 - 91 %) of the total VAF and the 65 % (range = 63 - 67 %) of the total r^2 for the lowering task. For the lifting task, the reconstructed muscle activation patterns matched the original data with VAF ≥ 80 % and $r^2 \geq 60$ % in 93 % and 54 %, respectively, of all muscles activation patterns. While for the lowering task, these values were 89 % and 65 %, respectively. Figure 4.9 depicts that the mean r^2 value, after averaging across subjects and treatments, for each muscle was $r^2 \geq 60$ % for all but LRA and RRA muscles in both lifting ($r^2_{LRA} = 54$ %, range = 46 - 61 %; $r^2_{RRA} = 51$ %, range = 43 - 58 %) and lowering tasks ($r^2_{LRA} = 58$ %, range = 50 - 65 %; $R^2_{RRA} = 58$ %, range = 51 - 65 %). The mean VAF value was VAF ≥ 80 % for all muscles. Hence, by taking into consideration that the dimension of the PCs subspace must be limited in number in order to be useful in reducing the DOF to be controlled during movement (Krishnamoorthy et al., 2003; Torres-Oviedo, Macpherson, and Ting, 2006), it was considered that a three - dimensional PCs subspace can reconstruct adequately the original muscle activation patterns.

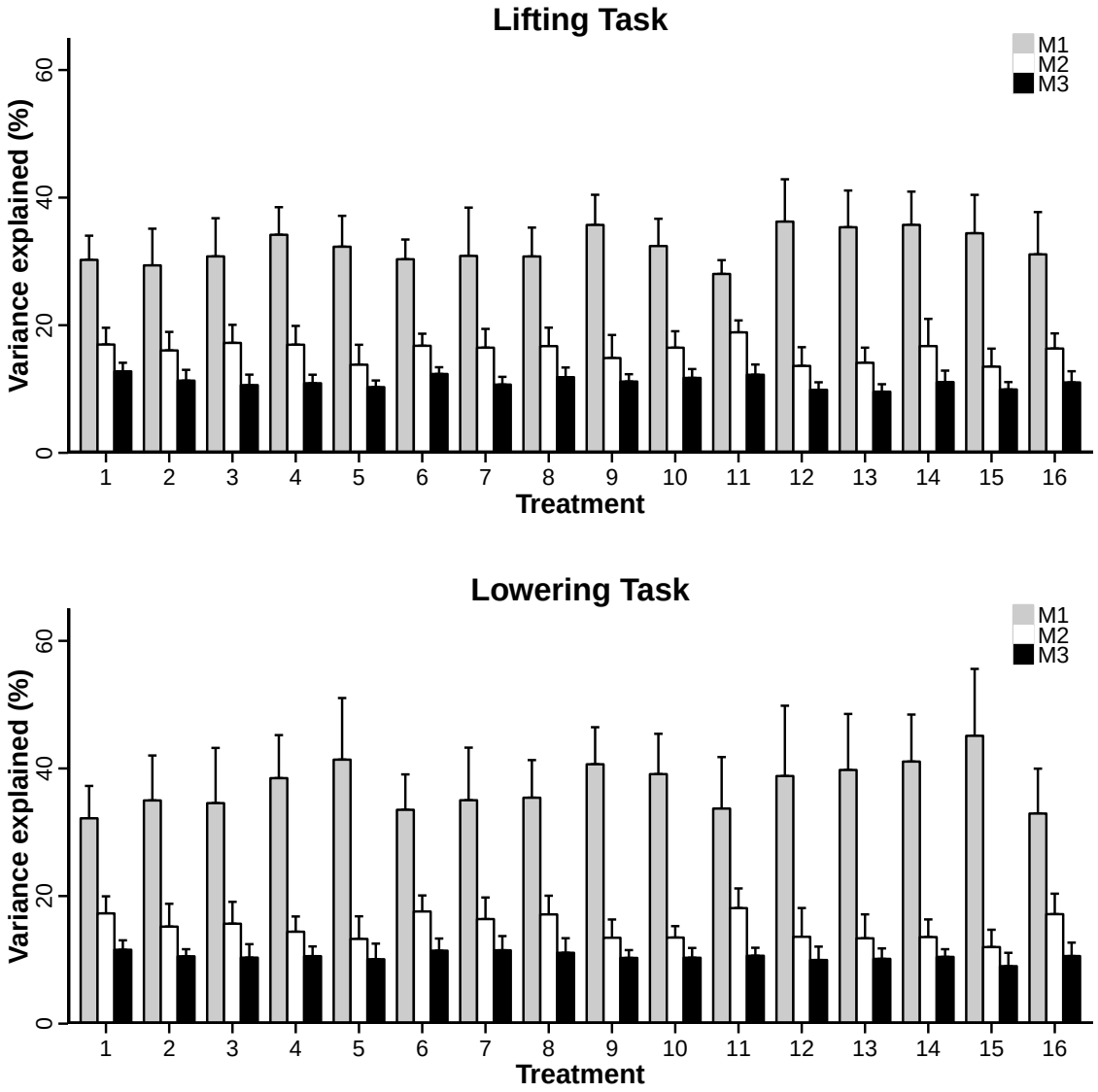

Figure 4.8 Variance explained by the M-mode averaged across subjects under each treatment, for the lowering and lifting tasks respectively.

4.2.3. Muscle Modes Composition

Three groups of muscles (PCs) whose activity was modulated in parallel during the lifting and lowering tasks were identified using EFA for every subject in each treatment and named as M-modes. There was a considerable variability across subjects and among treatments in the composition of the M-modes as it is depicted in Tables 4.1 to 4.3. We found that in the *hip* level treatments of the *VD* factor there are M-modes that share similar high loadings values of muscle activation indices across subjects. In particular, there are two types of M-modes with high loadings values of muscle activation indices concentrated in the first muscle-modes (M_1-modes) of the *hip* level treatments and separate the hip::*asymmetric* to the hip:.*symmetric* treatments:

hip::symmetric LES, RES, LLD, and RLD muscles (trunk flexion/extension M-mode)

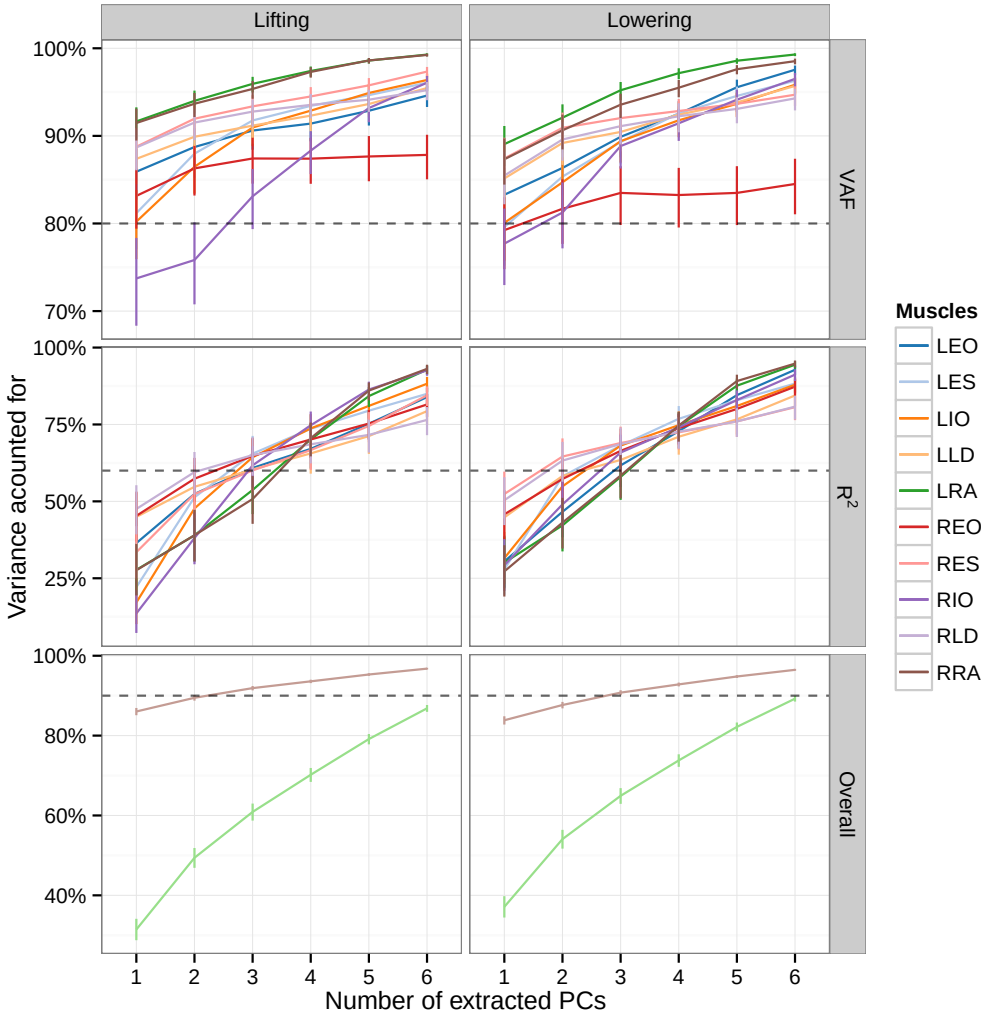

Figure 4.9 Goodness of the linear subspace approximation of $\hat{\mathbf{M}}$ on $\mathbf{M}$ and of $\hat{\mathbf{M}}_{\mathbf{z}}$ on $\mathbf{M}_z$ by the extracted PCs for both lifting and lowering tasks. The percentage of r^2 and VAF values along with their 95% confidence intervals is depicted for each muscle and over all muscles both of them across subjects and treatments as a function of the number of the extracted PCs. Dashed lines indicate the threshold values above which the approximation is adequate.

hip::asymmetric LLD, RLD, REO, and RES muscles (trunk flexion/extension and axial rotation M-mode).

Despite the variability in the significant loadings of the M-modes, the time profiles of the magnitude of the M_1-mode (factor scores) after averaging across subjects were similar among the treatments of the lifting and of the lowering tasks as depicted in Figs. 4.10 and 4.11. The time profile of the M_1-mode magnitudes during the treatments of the lifting task reach a global minimum value at (or very near to) the instant that defines the start of the deposit phase of the CoG_B. On the other hand, the time profile of the second muscle-mode (M_2-mode) and the third muscle-mode (M_3-mode) magnitudes did not show a specific trend. The time profiles of the M-mode magnitudes in the lowering tasks revealed a trend for the M_1-mode across subjects and treatments. It reaches a global minimum at (or very near to) the instant that defines the start of the pull phase of the CoG_B, but

only for the treatments where a *liquid* load was transfered. At the other treatments the time profile of the M_1-mode magnitude does not present a local minimum or maximum. A cluster analysis on the cross - correlation matrices was performed in order to group the treatments according to the similarity of the time profiles of the M-mode magnitudes. The mean correlation coefficients across subjects for the lifting task were at 0.56 - 0.89 (lag: −13.07 to 15.57) for the M_1-mode, 0.38 - 0.73 (lag: −15.57 to 22.57) for the M_2-mode, and 0.36 - 0.68 (lag: −16.93 to 18.07) for the M_3-mode. Lowering scores ranged 0.51 - 0.91 (lag: −16.14 to 12.14) for the M_1-mode, 0.41 - 0.71 (lag: −14.36 to 16.36) for the M_2-mode, and 0.36 - 0.63 (lag: −15.29 to 16.57) for the M_3-mode. The cluster analysis dendrograms (Fig. 4.12) showing that for 2 cluster grouping the cross-correlation coefficients formed two clusters (*hip* vs *knee* treatments) for the M_1-modes of the lowering tasks and for the M_3-modes of the lifting tasks. The rest two M-modes revealed a mixed grouping. Clustering analysis at a lower level grouped the correlation coefficients of M-mode modulations into 3 or 4 clusters. The order of dissimilarity among clusters for lifting as compared to the lowering task and among M-modes was not the same.

4.2.4. Statistical Verification of Muscle Modes Similarity

In each treatment and for each central vector separately (i.e., for all $\left\{\bar{\mathbf{\Lambda}}_a^{(n)}\right\}$ central vectors), a repeated - measures design ANOVA with factor *PC* $\left(\mathbf{\Lambda}^{(1)}, \mathbf{\Lambda}^{(2)}, \mathbf{\Lambda}^{(3)}\right)$ was ran on the z - scores of the $\cos(\xi)$ values across subjects. Figure 4.15 shows the *post-hoc* pairwise results for significant effects. It depicts that $\mathbf{\Lambda}^{(1)}$ PC vectors across subjects were clustered round their respective $\bar{\mathbf{\Lambda}}^{(1)}$ central vectors in all treatments but only for the lifting tasks. For the lowering tasks, $\mathbf{\Lambda}^{(1)}$ vectors were clustered mainly for the *hip* level treatments. The rest two extracted PC vectors ($\mathbf{\Lambda}^{(2)}$ and $\mathbf{\Lambda}^{(3)}$), in general, did not cluster round their respective central vectors. Moreover, the $\cos(\zeta)$ values were statistically significant ($|\cos(\zeta)| > 0.765$), mainly for the *hip* level treatments of lifting and lowering tasks (as classified by the NIOSHfactors), indicating M-mode similarity across subjects only for these treatments (Table 4.5).

4.3. Effects of NIOSH Factors on Muscle Modes

4.3.1. Effects of NIOSH Factors on Muscle Modes Composition

Since in some treatments the variance of the initial 10 variables (muscle activation patterns) can be explained by less than three or two PCs according to K1 and PA retention criteria, respectively (Fig. 4.7), it is expected, that by fixing the retention to the first three PCs, the difference in the scores of the amount of the variance accounted for by PC1 vs. PC2, PC1 vs. PC3, or PC2 vs. PC3 would be higher for these treatments (since the squared factor loading is the percentage of variance in the variable, explained by the PC). In Fig. 4.8 it is depicted the drop in the amount of the variance explained by PC1 and the increase in the amount of the variance explained by PC2 and PC3 for the treatments that retained the fewer PCs according to K1 and PA retention criteria. In relation to the associated ergonomic risk of each treatment, Fig. 4.8 depicts, that the amount of the variance accounted for by the PC1 dropped from the relatively easier to the more challenged treatments according to the NIOSH criteria (Table 3.6), while the remained PC2 and PC3 showed

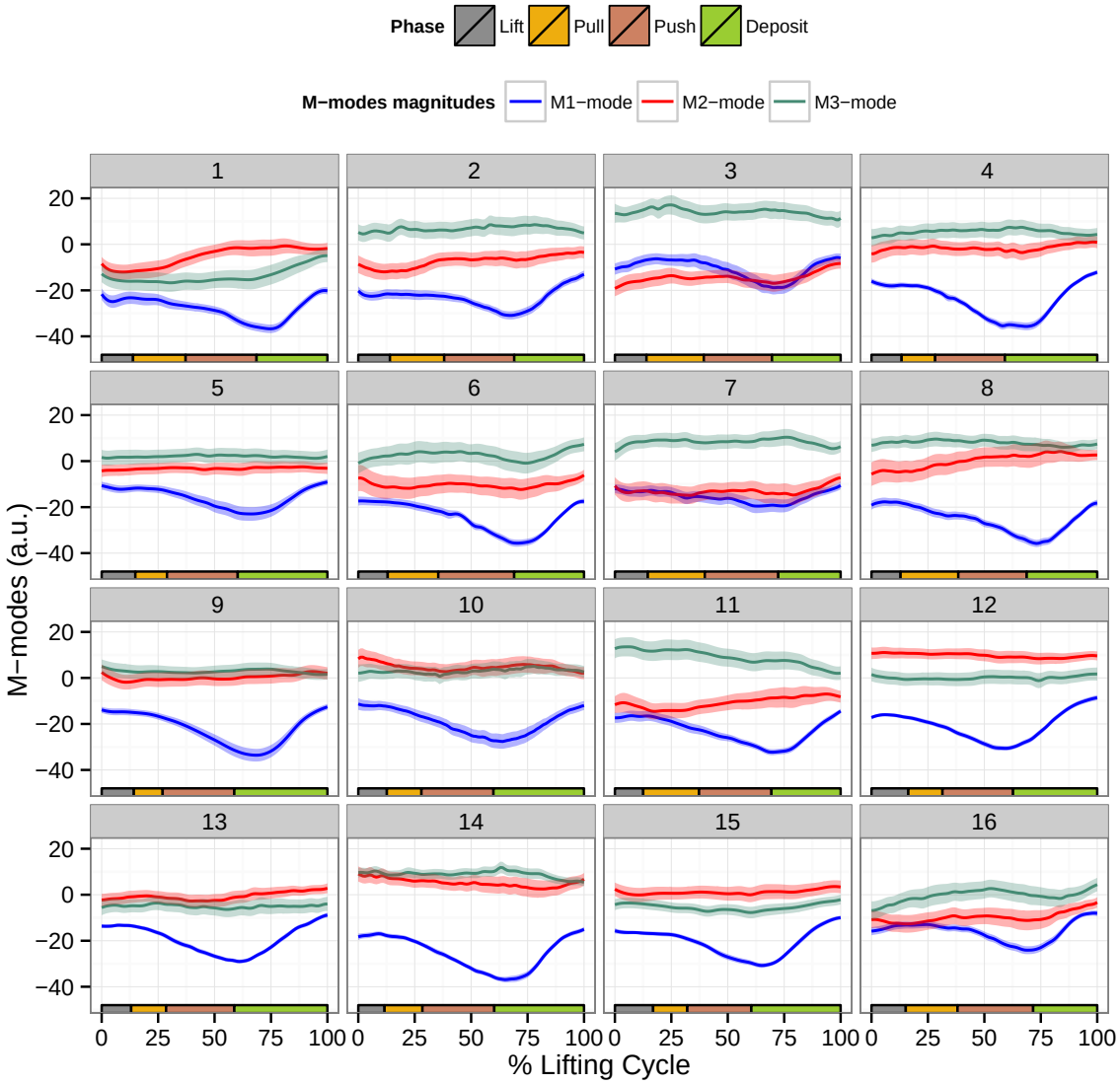

Figure 4.10 Time profiles of the three M-mode magnitudes averaged across subjects with their standard errors for the lifting tasks. M-mode magnitudes are displayed in arbitrary units and lifting cycle ia expressed in percentage of its total duration. The temporal phases of the lifting task based on the 3D kinematics of the CoG_B are shown.

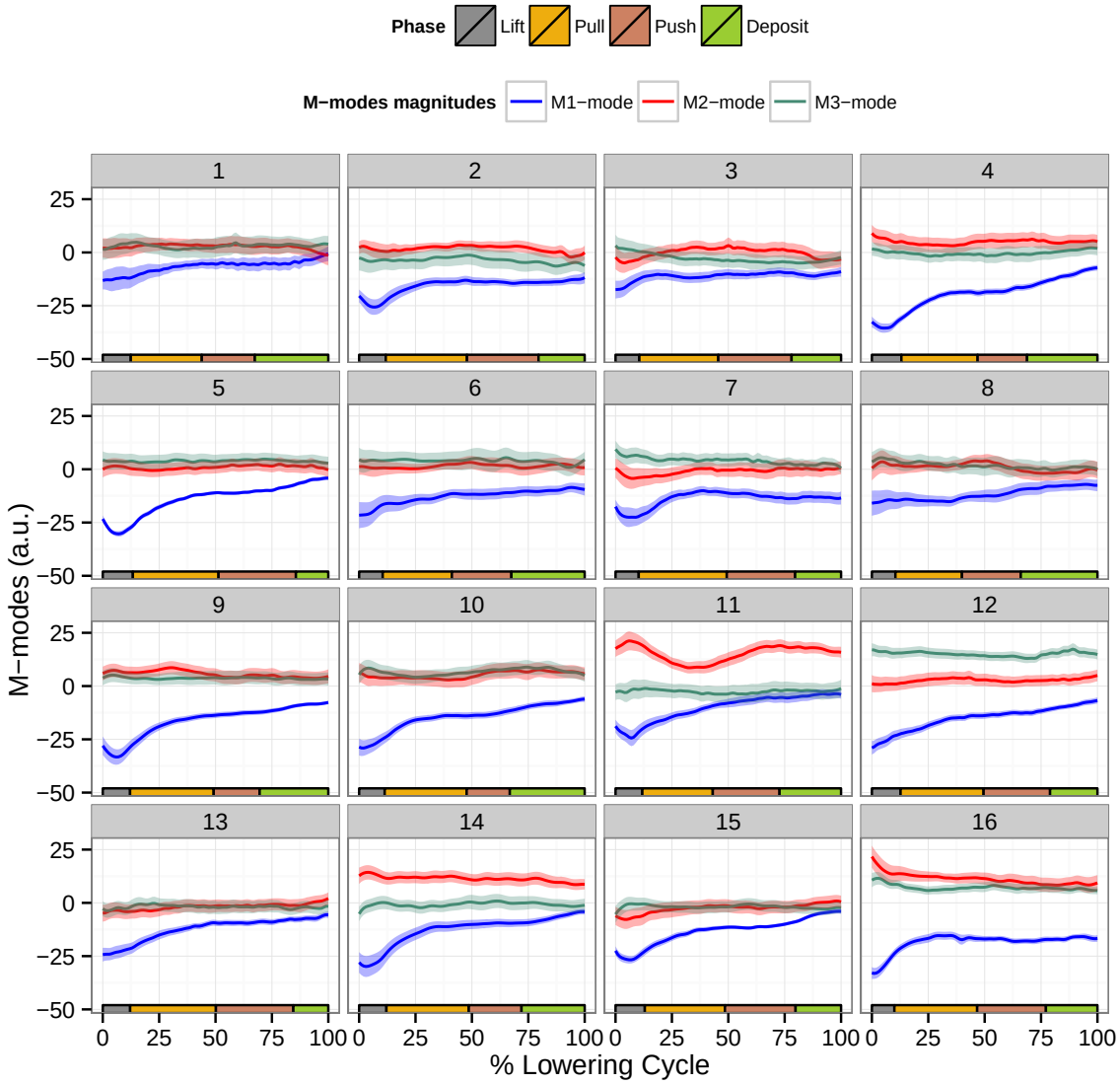

Figure 4.11 Time profiles of the three M-mode magnitudes averaged across subjects with their standard errors for the lowering tasks. M-mode magnitudes are displayed in arbitrary units and lowering cycle ia expressed in percentage of its total duration. The temporal phases of the lowering task based on the 3D kinematics of the CoG_B are shown.

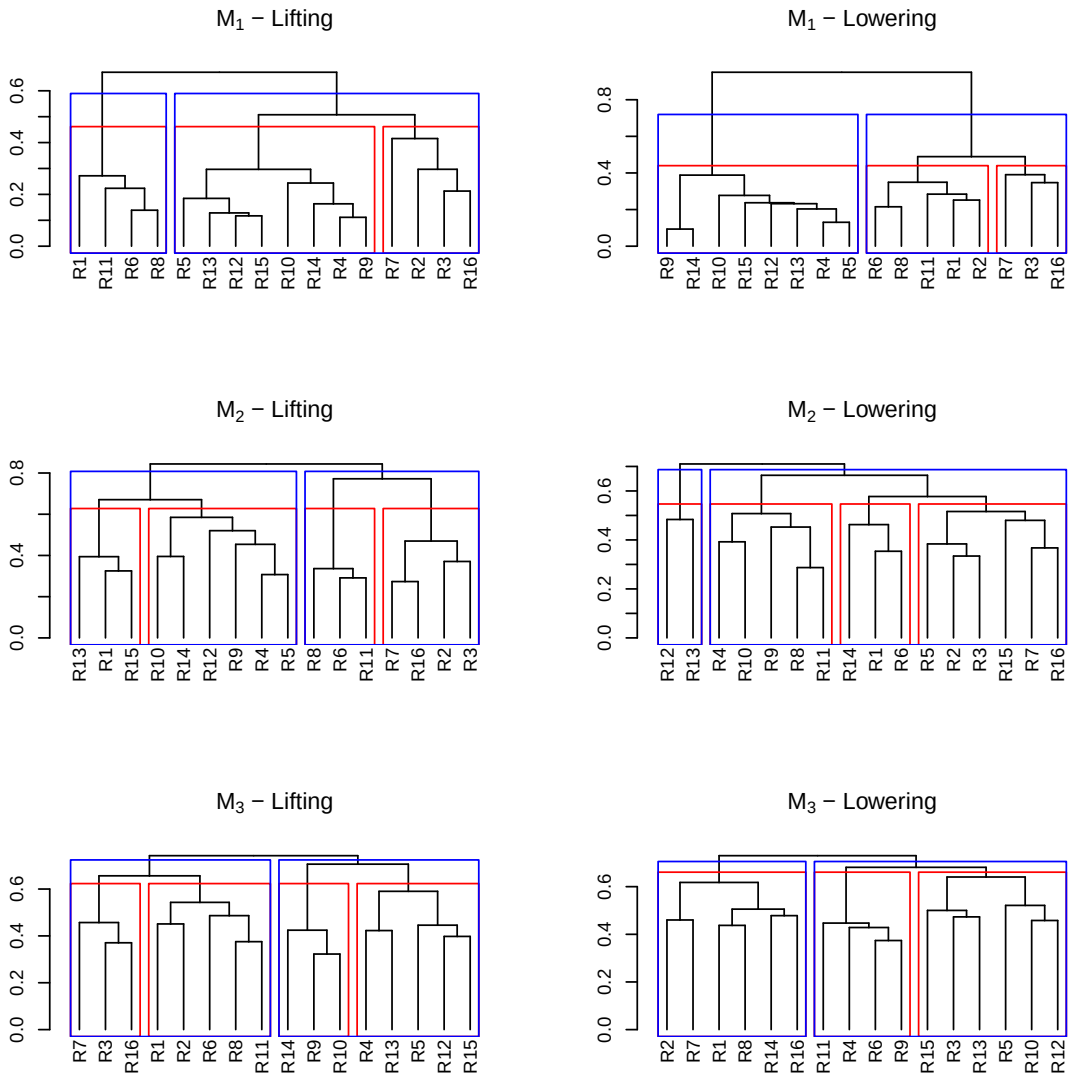

Figure 4.12 Cluster analysis dendrograms of the cross-correlation coefficients matrices of the M-mode magnitudes (dissimilarity = 1 - cross-correlation values).

an opposite trend. Figure 4.13 represents this relationship. These trends were confirmed by a two - way mixed design ANOVA with factors *Treatment* ($a_{1\rightarrow16}$) and *PC* (PC1, PC2, PC3), which revealed a significant main effect of factor *PC* for both the lifting ($F_{[2,39]} = 391.43$, $P = 0.001$, $\eta_g^2 = 0.87$) and the lowering tasks ($F_{[2,39]} = 194.09$, $P = 0.001$, $\eta_g^2 = 0.84$), qualified with a significant *PC* × *Treatment* interaction for both lifting ($F_{[7.31,142.6]} = 6.52$, $P_{GG} = 0.001$, $\eta_g^2 = 0.18$) and lowering tasks ($F_{[12.8,249.5]} = 9.03$, $P_{GG} = 0.001$, $\eta_g^2 = 0.18$.) Contrasts revealed that the amount of variance explained by PC1 was higher than that of PC2 ($F_{[1,39]} = 430.15$, $P = 0.001$ and $F_{[1,39]} = 237.02$, $P = 0.001$ for lifting and lowering tasks, respectively) and that of PC2 was higher than that of PC3 ($F_{[1,39]} = 352.71$, $P = 0.001$ and $F_{[1,39]} = 151.17$, $P = 0.001$ for lifting and lowering tasks, respectively) across all treatments. To localize these trends in relation with the NIOSH factors, a factorial repeated - measures, split - plot design ANOVA with *VD*, *HD*, *AM*,

Table 4.1 Occurrence of significant muscle loadings ($> |\pm 0.5|$) for each treatment of the lifting task. The highest occurrences are shown in bold.

(a) Treatment 1

	$\Lambda^{(1)}$	$\Lambda^{(2)}$	$\Lambda^{(3)}$
LEO	**9**	5	1
LES	3	**6**	5
LIO	**6**	4	5
LLD	**7**	3	4
LRA	**6**	1	3
REO	**7**	**7**	2
RES	4	4	**6**
RIO	3	**5**	3
RLD	**7**	3	5
RRA	**5**	3	2

(b) Treatment 2

	$\Lambda^{(1)}$	$\Lambda^{(2)}$	$\Lambda^{(3)}$
LEO	**5**	**5**	2
LES	**6**	**6**	2
LIO	4	5	**6**
LLD	**12**	1	1
LRA	**4**	3	**4**
REO	**6**	4	4
RES	**7**	6	1
RIO	**5**	3	**5**
RLD	**11**	3	2
RRA	**4**	2	**4**

(c) Treatment 3

	$\Lambda^{(1)}$	$\Lambda^{(2)}$	$\Lambda^{(3)}$
LEO	**8**	4	2
LES	5	**7**	3
LIO	3	4	**6**
LLD	**11**	3	1
LRA	3	4	**6**
REO	**8**	4	3
RES	5	**9**	0
RIO	**5**	4	4
RLD	**10**	4	0
RRA	4	1	**7**

(d) Treatment 4

	$\Lambda^{(1)}$	$\Lambda^{(2)}$	$\Lambda^{(3)}$
LEO	**7**	4	3
LES	2	**5**	**5**
LIO	3	**7**	5
LLD	**11**	3	3
LRA	**5**	1	4
REO	**12**	3	2
RES	**10**	1	3
RIO	3	**7**	4
RLD	**11**	2	2
RRA	**7**	3	3

(e) Treatment 5

	$\Lambda^{(1)}$	$\Lambda^{(2)}$	$\Lambda^{(3)}$
LEO	6	**7**	1
LES	**14**	0	0
LIO	0	**9**	6
LLD	**14**	0	0
LRA	3	4	**6**
REO	**5**	4	4
RES	**14**	0	0
RIO	0	**8**	6
RLD	**14**	0	0
RRA	0	4	**5**

(f) Treatment 6

	$\Lambda^{(1)}$	$\Lambda^{(2)}$	$\Lambda^{(3)}$
LEO	**10**	1	3
LES	3	**9**	4
LIO	**6**	2	**6**
LLD	**6**	5	2
LRA	**8**	1	4
REO	**9**	6	1
RES	1	**8**	4
RIO	4	4	**6**
RLD	**7**	4	3
RRA	**5**	2	3

(g) Treatment 7

	$\Lambda^{(1)}$	$\Lambda^{(2)}$	$\Lambda^{(3)}$
LEO	**7**	3	4
LES	3	**10**	1
LIO	**5**	4	**5**
LLD	**6**	4	4
LRA	3	2	**7**
REO	**10**	2	2
RES	3	**10**	1
RIO	**10**	3	3
RLD	**6**	**6**	3
RRA	5	1	**6**

(h) Treatment 8

	$\Lambda^{(1)}$	$\Lambda^{(2)}$	$\Lambda^{(3)}$
LEO	**10**	1	3
LES	3	**11**	3
LIO	6	1	**7**
LLD	**7**	**7**	0
LRA	**7**	3	2
REO	**10**	4	3
RES	2	**8**	1
RIO	4	2	**7**
RLD	**7**	**7**	2
RRA	**5**	2	2

(i) Treatment 9

	$\Lambda^{(1)}$	$\Lambda^{(2)}$	$\Lambda^{(3)}$
LEO	4	**5**	3
LES	2	4	**7**
LIO	2	**7**	4
LLD	**11**	1	2
LRA	**5**	4	2
REO	**11**	1	2
RES	**12**	0	1
RIO	1	**6**	5
RLD	**11**	1	1
RRA	**6**	3	2

(j) Treatment 10

	$\Lambda^{(1)}$	$\Lambda^{(2)}$	$\Lambda^{(3)}$
LEO	**7**	5	1
LES	1	**7**	**7**
LIO	3	**9**	4
LLD	**6**	4	3
LRA	**5**	3	3
REO	**11**	4	0
RES	**8**	3	3
RIO	2	3	**8**
RLD	**10**	2	3
RRA	**6**	3	2

(k) Treatment 11

	$\Lambda^{(1)}$	$\Lambda^{(2)}$	$\Lambda^{(3)}$
LEO	**7**	4	2
LES	**5**	**5**	**5**
LIO	4	3	**7**
LLD	**6**	5	3
LRA	**6**	1	4
REO	**9**	4	1
RES	2	**7**	3
RIO	2	4	**5**
RLD	**8**	5	0
RRA	**7**	2	1

(l) Treatment 12

	$\Lambda^{(1)}$	$\Lambda^{(2)}$	$\Lambda^{(3)}$
LEO	4	**7**	4
LES	**13**	1	0
LIO	0	**9**	5
LLD	**13**	0	0
LRA	2	4	**6**
REO	4	4	**6**
RES	**13**	1	0
RIO	0	4	**8**
RLD	**13**	1	0
RRA	2	1	**7**

(m) Treatment 13

	$\Lambda^{(1)}$	$\Lambda^{(2)}$	$\Lambda^{(3)}$
LEO	**7**	6	1
LES	**13**	1	0
LIO	1	**12**	1
LLD	**12**	1	0
LRA	4	3	**7**
REO	**6**	2	3
RES	**11**	1	1
RIO	1	5	**7**
RLD	**13**	1	0
RRA	**5**	4	**5**

(n) Treatment 14

	$\Lambda^{(1)}$	$\Lambda^{(2)}$	$\Lambda^{(3)}$
LEO	**8**	5	1
LES	0	5	**9**
LIO	4	**9**	1
LLD	**11**	1	2
LRA	**7**	5	1
REO	**11**	2	2
RES	**12**	2	1
RIO	3	5	**6**
RLD	**10**	3	2
RRA	**5**	4	3

(ñ) Treatment 15

	$\Lambda^{(1)}$	$\Lambda^{(2)}$	$\Lambda^{(3)}$
LEO	3	5	**6**
LES	**13**	1	0
LIO	0	**9**	4
LLD	**13**	0	1
LRA	3	**7**	4
REO	3	2	**6**
RES	**13**	1	0
RIO	0	**8**	7
RLD	**13**	1	1
RRA	**4**	2	**4**

(o) Treatment 16

	$\Lambda^{(1)}$	$\Lambda^{(2)}$	$\Lambda^{(3)}$
LEO	**6**	**6**	1
LES	2	**8**	4
LIO	4	4	**7**
LLD	**10**	2	1
LRA	3	2	**5**
REO	**9**	4	1
RES	3	**6**	5
RIO	**5**	3	**5**
RLD	**10**	4	1
RRA	2	4	**6**

and type of *LD* as within - subjects factors was conducted on the difference scores of the variance accounted for by each PC set (PC_{1-2} = PC1 - PC2; PC_{1-3} = PC1 - PC2; PC_{2-3} = PC2 - PC3).

4.3.1.1. Lifting Task

The results of the ANOVA revealed a significant main effect of the factor VD for both PC_{1-2} ($F_{[1,13]} = 30.3$, $P = 0.001$, $\eta_g^2 = 0.18$), and PC_{1-3} ($F_{[1,13]} = 46.2$, $P = 0.001$, $\eta_g^2 = 0.17$) dependent variables, and also a significant main effect and of the factor LD for both PC_{1-2} ($F_{[1,13]} = 6.9$, $P = 0.021$, $\eta_g^2 = 0.01$), and for PC_{1-3} ($F_{[1,13]} = 7.9$, $P = 0.015$, $\eta_g^2 = 0.01$) dependent variables,

Table 4.2 Occurrence of significant muscle loadings ($> |\pm 0.5|$) for each treatment of the lowering task. The highest occurrences are shown in bold.

(a) Treatment 1

	$\Lambda^{(1)}$	$\Lambda^{(2)}$	$\Lambda^{(3)}$
LEO	**5**	3	4
LES	3	**9**	2
LIO	**5**	3	4
LLD	**6**	**6**	0
LRA	3	3	**5**
REO	**8**	4	2
RES	**10**	3	2
RIO	**6**	3	5
RLD	**9**	4	1
RRA	3	1	**6**

(b) Treatment 2

	$\Lambda^{(1)}$	$\Lambda^{(2)}$	$\Lambda^{(3)}$
LEO	4	**5**	3
LES	**8**	6	0
LIO	**9**	2	3
LLD	**9**	4	2
LRA	4	1	**7**
REO	4	**5**	4
RES	**8**	6	1
RIO	**8**	2	4
RLD	**9**	4	2
RRA	**4**	3	**4**

(c) Treatment 3

	$\Lambda^{(1)}$	$\Lambda^{(2)}$	$\Lambda^{(3)}$
LEO	**6**	2	4
LES	5	**8**	1
LIO	**7**	4	3
LLD	**9**	5	1
LRA	**5**	3	3
REO	3	2	**7**
RES	5	**8**	2
RIO	**7**	4	2
RLD	**9**	5	2
RRA	**6**	1	4

(d) Treatment 4

	$\Lambda^{(1)}$	$\Lambda^{(2)}$	$\Lambda^{(3)}$
LEO	5	4	**6**
LES	3	**7**	2
LIO	4	**5**	**5**
LLD	**12**	2	0
LRA	**7**	4	2
REO	**11**	1	4
RES	**14**	0	2
RIO	2	5	**6**
RLD	**13**	0	1
RRA	**5**	4	4

(e) Treatment 5

	$\Lambda^{(1)}$	$\Lambda^{(2)}$	$\Lambda^{(3)}$
LEO	4	5	**6**
LES	**14**	0	0
LIO	2	**8**	4
LLD	**12**	2	0
LRA	2	5	**6**
REO	**7**	4	3
RES	**13**	0	1
RIO	4	3	**6**
RLD	**12**	2	0
RRA	2	**6**	4

(f) Treatment 6

	$\Lambda^{(1)}$	$\Lambda^{(2)}$	$\Lambda^{(3)}$
LEO	**5**	4	4
LES	4	**8**	2
LIO	**6**	**6**	2
LLD	4	**5**	**5**
LRA	**6**	0	4
REO	**11**	4	1
RES	**8**	3	3
RIO	**7**	3	5
RLD	**7**	5	2
RRA	4	1	**8**

(g) Treatment 7

	$\Lambda^{(1)}$	$\Lambda^{(2)}$	$\Lambda^{(3)}$
LEO	3	**6**	5
LES	**10**	4	0
LIO	**7**	5	3
LLD	**10**	5	1
LRA	4	3	**5**
REO	3	3	**6**
RES	**9**	5	0
RIO	**6**	5	4
RLD	**10**	5	0
RRA	3	**5**	**5**

(h) Treatment 8

	$\Lambda^{(1)}$	$\Lambda^{(2)}$	$\Lambda^{(3)}$
LEO	**6**	2	**6**
LES	3	**8**	4
LIO	**7**	4	3
LLD	**6**	**6**	2
LRA	**7**	1	3
REO	**9**	6	3
RES	**8**	6	0
RIO	**8**	5	4
RLD	**7**	**7**	0
RRA	**8**	3	4

(i) Treatment 9

	$\Lambda^{(1)}$	$\Lambda^{(2)}$	$\Lambda^{(3)}$
LEO	**6**	4	2
LES	2	5	**6**
LIO	**6**	2	5
LLD	**11**	2	0
LRA	**6**	2	3
REO	**12**	1	0
RES	**13**	0	0
RIO	3	**6**	3
RLD	**13**	0	0
RRA	**5**	4	3

(j) Treatment 10

	$\Lambda^{(1)}$	$\Lambda^{(2)}$	$\Lambda^{(3)}$
LEO	**7**	4	3
LES	3	**7**	3
LIO	3	**7**	4
LLD	**9**	4	1
LRA	4	4	**6**
REO	**11**	1	2
RES	**12**	3	0
RIO	4	2	**7**
RLD	**11**	2	0
RRA	**6**	4	4

(k) Treatment 11

	$\Lambda^{(1)}$	$\Lambda^{(2)}$	$\Lambda^{(3)}$
LEO	**5**	3	**5**
LES	5	**7**	3
LIO	**7**	4	3
LLD	4	**8**	2
LRA	5	1	**7**
REO	**12**	5	2
RES	**5**	**5**	3
RIO	**8**	5	3
RLD	**6**	**6**	3
RRA	**5**	3	3

(l) Treatment 12

	$\Lambda^{(1)}$	$\Lambda^{(2)}$	$\Lambda^{(3)}$
LEO	4	4	**6**
LES	**12**	1	1
LIO	2	**6**	**6**
LLD	**12**	1	2
LRA	3	5	**6**
REO	5	**6**	3
RES	**12**	0	1
RIO	1	**9**	4
RLD	**12**	1	2
RRA	3	**6**	4

(m) Treatment 13

	$\Lambda^{(1)}$	$\Lambda^{(2)}$	$\Lambda^{(3)}$
LEO	**5**	**5**	2
LES	**11**	2	1
LIO	4	**7**	3
LLD	**12**	3	0
LRA	**4**	**4**	**4**
REO	**8**	2	6
RES	**11**	2	1
RIO	2	2	**10**
RLD	**11**	3	0
RRA	2	**6**	3

(n) Treatment 14

	$\Lambda^{(1)}$	$\Lambda^{(2)}$	$\Lambda^{(3)}$
LEO	**7**	4	3
LES	2	**7**	3
LIO	3	**8**	3
LLD	**13**	0	0
LRA	**7**	**7**	1
REO	**13**	2	0
RES	**14**	0	0
RIO	3	2	**10**
RLD	**14**	0	0
RRA	**6**	3	1

(ñ) Treatment 15

	$\Lambda^{(1)}$	$\Lambda^{(2)}$	$\Lambda^{(3)}$
LEO	**7**	3	3
LES	**10**	3	1
LIO	4	**7**	4
LLD	**10**	4	0
LRA	3	**5**	**5**
REO	**7**	3	5
RES	**10**	3	1
RIO	4	3	**7**
RLD	**10**	4	0
RRA	1	3	**8**

(o) Treatment 16

	$\Lambda^{(1)}$	$\Lambda^{(2)}$	$\Lambda^{(3)}$
LEO	5	4	**6**
LES	6	**7**	1
LIO	**7**	4	3
LLD	**7**	5	2
LRA	**5**	1	**5**
REO	3	3	**5**
RES	**7**	**7**	0
RIO	**7**	4	2
RLD	**7**	**7**	2
RRA	4	2	**6**

indicating that the difference scores between the variance explained by these PCs is lower when the subjects picked up the box from the *knee* origin and when they transfered the *liquid* load. There was also a significant interaction between factors HD and AM for both the PC_{1-2} ($F_{[1,13]} = 13.2$, $P = 0.003$, $\eta_g^2 = 0.03$) and the PC_{1-3} ($F_{[1,13]} = 9.3$, $P = 0.009$, $\eta_g^2 = 0.02$) dependent variables. Simple main effects revealed that difference scores were significantly lower when subjects picked up the load from a position *far* of the body and in *asymmetric* tasks (as compared to *symmetric*) ($F_{[1,13]} = 12.1$, $P = 0.008$, and $F_{[1,13]} = 10.7$, $P = 0.012$, for PC_{1-2} and PC_{1-3}, respectively.) However, main effects of PC_{1-2} were qualified by an interaction between the factors VD, AM, and LD ($F_{[1,13]} = 6.5$, $P = 0.024$, $\eta_g^2 = 0.01$). Simple main effect tests revealed, that the decrease

Table 4.3 Results of the PCA analysis. Averaged factor loadings across subjects for each treatment of the lifting tasks. Highest factor loadings for each muscle are shown with bold.

(a) Treatment 1

	$\Lambda^{(1)}$	$\Lambda^{(2)}$	$\Lambda^{(3)}$
LEO	**-0.52**	0.21	0.10
LES	0.02	-0.35	-0.27
LIO	-0.34	0.00	-0.01
LLD	-0.49	-0.07	-0.13
LRA	**-0.50**	-0.02	-0.06
REO	-0.48	0.30	0.07
RES	-0.26	-0.16	-0.17
RIO	-0.02	-0.15	0.07
RLD	-0.47	0.06	-0.05
RRA	-0.41	-0.01	-0.01

(b) Treatment 2

	$\Lambda^{(1)}$	$\Lambda^{(2)}$	$\Lambda^{(3)}$
LEO	-0.31	0.29	-0.09
LES	-0.37	-0.28	0.01
LIO	-0.11	0.00	0.24
LLD	**-0.63**	-0.03	0.02
LRA	-0.24	0.04	0.11
REO	-0.34	0.16	-0.03
RES	-0.36	-0.25	0.02
RIO	-0.22	0.07	0.13
RLD	**-0.60**	-0.09	0.02
RRA	-0.27	-0.06	-0.03

(c) Treatment 3

	$\Lambda^{(1)}$	$\Lambda^{(2)}$	$\Lambda^{(3)}$
LEO	-0.47	0.05	0.12
LES	-0.02	-0.35	0.06
LIO	-0.13	0.08	0.14
LLD	-0.40	-0.21	0.01
LRA	-0.16	-0.05	0.16
REO	-0.49	-0.04	0.07
RES	-0.01	-0.36	0.02
RIO	-0.23	0.02	0.15
RLD	-0.38	-0.23	-0.03
RRA	-0.18	-0.08	0.22

(d) Treatment 4

	$\Lambda^{(1)}$	$\Lambda^{(2)}$	$\Lambda^{(3)}$
LEO	-0.45	0.04	-0.05
LES	-0.10	-0.13	0.13
LIO	-0.21	-0.02	-0.08
LLD	**-0.56**	-0.09	0.09
LRA	-0.43	0.02	-0.04
REO	**-0.67**	-0.01	0.13
RES	**-0.61**	-0.11	0.15
RIO	0.11	0.02	-0.15
RLD	**-0.64**	-0.15	0.16
RRA	-0.38	0.06	0.11

(e) Treatment 5

	$\Lambda^{(1)}$	$\Lambda^{(2)}$	$\Lambda^{(3)}$
LEO	-0.36	0.28	0.03
LES	**-0.50**	-0.02	0.01
LIO	0.03	-0.14	0.02
LLD	**-0.53**	0.02	0.04
LRA	-0.24	0.12	-0.15
REO	-0.31	0.16	0.09
RES	**-0.52**	0.01	0.01
RIO	-0.05	-0.12	0.09
RLD	**-0.50**	-0.01	0.04
RRA	-0.24	-0.06	0.06

(f) Treatment 6

	$\Lambda^{(1)}$	$\Lambda^{(2)}$	$\Lambda^{(3)}$
LEO	**-0.56**	0.02	-0.07
LES	0.13	-0.09	-0.11
LIO	-0.39	0.01	0.06
LLD	-0.43	-0.13	-0.16
LRA	-0.46	-0.12	0.05
REO	**-0.57**	-0.05	-0.14
RES	-0.22	-0.17	-0.14
RIO	-0.05	0.02	0.34
RLD	-0.41	-0.11	-0.10
RRA	-0.42	-0.12	0.06

(g) Treatment 7

	$\Lambda^{(1)}$	$\Lambda^{(2)}$	$\Lambda^{(3)}$
LEO	-0.43	0.13	0.05
LES	-0.13	-0.33	0.07
LIO	-0.29	0.04	0.16
LLD	-0.27	-0.08	0.15
LRA	-0.30	-0.10	0.15
REO	-0.43	0.13	-0.02
RES	-0.20	-0.33	-0.09
RIO	-0.39	0.12	0.06
RLD	-0.24	-0.10	0.05
RRA	-0.37	-0.06	0.13

(h) Treatment 8

	$\Lambda^{(1)}$	$\Lambda^{(2)}$	$\Lambda^{(3)}$
LEO	**-0.59**	0.09	0.07
LES	0.13	-0.25	0.01
LIO	-0.35	0.01	0.15
LLD	-0.41	0.01	-0.04
LRA	-0.42	-0.02	0.07
REO	**-0.55**	0.20	-0.06
RES	-0.29	-0.05	0.01
RIO	-0.00	0.02	0.21
RLD	-0.42	0.08	-0.04
RRA	-0.46	0.02	-0.03

(i) Treatment 9

	$\Lambda^{(1)}$	$\Lambda^{(2)}$	$\Lambda^{(3)}$
LEO	-0.32	0.22	0.10
LES	-0.12	-0.11	0.20
LIO	-0.14	-0.03	0.13
LLD	**-0.54**	-0.05	0.08
LRA	-0.37	-0.00	0.06
REO	**-0.54**	0.07	0.03
RES	**-0.54**	-0.02	0.09
RIO	0.10	-0.07	0.05
RLD	**-0.55**	-0.03	0.07
RRA	-0.31	0.16	0.06

(j) Treatment 10

	$\Lambda^{(1)}$	$\Lambda^{(2)}$	$\Lambda^{(3)}$
LEO	-0.47	0.09	0.04
LES	0.09	0.19	0.02
LIO	-0.09	0.14	-0.01
LLD	-0.34	0.06	0.03
LRA	-0.38	0.01	0.05
REO	**-0.54**	0.03	-0.01
RES	-0.41	0.02	0.04
RIO	0.10	-0.06	-0.08
RLD	-0.43	-0.04	0.05
RRA	-0.39	-0.03	0.14

(k) Treatment 11

	$\Lambda^{(1)}$	$\Lambda^{(2)}$	$\Lambda^{(3)}$
LEO	-0.46	-0.04	-0.06
LES	0.18	-0.22	0.29
LIO	-0.30	-0.17	-0.10
LLD	-0.41	-0.06	0.14
LRA	-0.35	-0.15	-0.04
REO	**-0.57**	0.07	-0.13
RES	-0.24	-0.15	0.18
RIO	-0.10	-0.05	-0.06
RLD	-0.46	-0.01	0.03
RRA	-0.41	-0.19	-0.01

(l) Treatment 12

	$\Lambda^{(1)}$	$\Lambda^{(2)}$	$\Lambda^{(3)}$
LEO	-0.34	0.34	-0.09
LES	**-0.70**	-0.01	0.01
LIO	0.01	0.32	0.02
LLD	**-0.73**	0.03	-0.03
LRA	-0.25	0.15	-0.02
REO	-0.40	0.17	0.12
RES	**-0.72**	-0.06	0.02
RIO	-0.06	0.15	0.06
RLD	**-0.73**	0.05	0.00
RRA	-0.32	0.12	-0.14

(m) Treatment 13

	$\Lambda^{(1)}$	$\Lambda^{(2)}$	$\Lambda^{(3)}$
LEO	-0.43	0.32	-0.09
LES	**-0.69**	-0.01	0.02
LIO	-0.02	0.20	-0.14
LLD	**-0.72**	-0.02	-0.06
LRA	-0.30	0.07	-0.20
REO	-0.47	0.10	-0.24
RES	**-0.65**	-0.04	-0.02
RIO	-0.08	-0.09	-0.23
RLD	**-0.73**	-0.06	-0.11
RRA	-0.35	0.03	-0.10

(n) Treatment 14

	$\Lambda^{(1)}$	$\Lambda^{(2)}$	$\Lambda^{(3)}$
LEO	-0.45	0.24	0.03
LES	-0.06	0.09	0.35
LIO	-0.23	0.32	0.07
LLD	**-0.64**	-0.04	0.16
LRA	-0.48	0.17	0.07
REO	**-0.61**	-0.06	-0.04
RES	**-0.62**	-0.12	0.10
RIO	0.03	0.15	0.26
RLD	**-0.59**	-0.17	0.13
RRA	-0.43	0.06	0.20

(ñ) Treatment 15

	$\Lambda^{(1)}$	$\Lambda^{(2)}$	$\Lambda^{(3)}$
LEO	-0.32	0.29	-0.27
LES	**-0.68**	-0.05	-0.04
LIO	-0.01	0.07	-0.22
LLD	**-0.70**	-0.01	-0.20
LRA	-0.26	0.17	-0.02
REO	-0.39	0.06	-0.17
RES	**-0.68**	-0.04	-0.07
RIO	-0.11	-0.20	-0.17
RLD	**-0.71**	-0.04	-0.10
RRA	-0.30	0.12	-0.04

(o) Treatment 16

	$\Lambda^{(1)}$	$\Lambda^{(2)}$	$\Lambda^{(3)}$
LEO	-0.39	0.24	0.12
LES	-0.14	-0.33	-0.16
LIO	-0.03	0.02	0.32
LLD	**-0.58**	-0.11	-0.02
LRA	-0.30	-0.02	0.16
REO	**-0.53**	0.16	0.12
RES	-0.21	-0.25	-0.21
RIO	-0.23	0.04	0.35
RLD	**-0.60**	-0.12	-0.04
RRA	-0.29	-0.12	0.18

found in difference scores when subjects picked up the load from the *knee* origin (as compared to the *hip*) was even more pronounced when the *liquid* load was handled and the lifting task was *asymmetric* (as compared to *solid* load) ($F_{[1,13]} = 10.37$, $P = 0.027$). Moreover, main effects of PC_{1-3} were qualified by an interaction between the factors AM and LD ($F_{[1,13]} = 5.5$, $P = 0.036$, $\eta_g^2 = 0.004$), indicating a decrease in the difference scores when the *liquid* load was handled by the subjects (as compared to *solid* load) only in *symmetric* lifting tasks ($F_{[1,13]} = 15.13$, $P = 0.004$). The results of the ANOVA showed also significant interactions between the factors HD and LD ($F_{[1,13]} = 11.4$, $P = 0.005$, $\eta_g^2 = 0.04$) and between the factors HD and AM ($F_{[1,13]} = 5.2$, $P = 0.04$, $\eta_g^2 = 0.01$) for the PC_{2-3} dependent variable. Simple main effects tests revealed, that

Table 4.4 Results of the PCA analysis. Averaged factor loadings across subjects for each treatment of the lowering tasks. Highest factor loadings for each muscle are shown with bold.

(a) Treatment 1

	$\Lambda^{(1)}$	$\Lambda^{(2)}$	$\Lambda^{(3)}$
LEO	-0.33	0.17	-0.14
LES	0.04	-0.11	0.15
LIO	-0.24	0.08	-0.01
LLD	-0.19	-0.04	-0.01
LRA	-0.30	0.07	0.11
REO	-0.32	0.04	-0.09
RES	-0.23	0.00	0.07
RIO	-0.20	0.08	-0.01
RLD	-0.16	0.02	0.06
RRA	-0.10	0.05	0.04

(b) Treatment 2

	$\Lambda^{(1)}$	$\Lambda^{(2)}$	$\Lambda^{(3)}$
LEO	-0.31	0.24	-0.03
LES	-0.36	-0.03	0.02
LIO	-0.31	0.12	0.06
LLD	-0.42	-0.05	-0.10
LRA	-0.28	0.07	-0.06
REO	-0.25	0.26	-0.02
RES	-0.31	-0.09	0.03
RIO	-0.31	0.13	0.07
RLD	-0.36	-0.02	-0.18
RRA	-0.27	0.26	0.02

(c) Treatment 3

	$\Lambda^{(1)}$	$\Lambda^{(2)}$	$\Lambda^{(3)}$
LEO	-0.40	-0.05	-0.02
LES	-0.18	-0.08	0.01
LIO	-0.17	0.13	0.10
LLD	-0.18	-0.22	0.08
LRA	-0.18	0.09	-0.05
REO	-0.14	0.00	0.09
RES	-0.17	-0.12	0.06
RIO	-0.20	0.02	0.09
RLD	-0.15	-0.20	0.20
RRA	-0.23	-0.07	-0.04

(d) Treatment 4

	$\Lambda^{(1)}$	$\Lambda^{(2)}$	$\Lambda^{(3)}$
LEO	-0.30	0.15	0.01
LES	-0.12	0.15	0.06
LIO	-0.27	0.01	-0.01
LLD	**-0.66**	0.06	-0.03
LRA	-0.44	0.15	-0.05
REO	**-0.67**	0.08	-0.02
RES	**-0.76**	0.05	0.07
RIO	-0.14	0.16	-0.03
RLD	**-0.74**	0.08	0.09
RRA	-0.38	0.13	0.17

(e) Treatment 5

	$\Lambda^{(1)}$	$\Lambda^{(2)}$	$\Lambda^{(3)}$
LEO	-0.34	0.30	0.03
LES	**-0.77**	-0.04	0.02
LIO	-0.29	0.15	0.04
LLD	**-0.67**	-0.04	0.02
LRA	-0.19	0.13	0.03
REO	-0.47	0.01	-0.02
RES	**-0.72**	-0.02	0.04
RIO	-0.35	-0.05	0.02
RLD	**-0.68**	-0.12	0.10
RRA	-0.21	0.00	0.16

(f) Treatment 6

	$\Lambda^{(1)}$	$\Lambda^{(2)}$	$\Lambda^{(3)}$
LEO	-0.35	0.01	-0.03
LES	0.02	0.20	0.08
LIO	-0.28	-0.13	-0.02
LLD	-0.14	0.03	0.06
LRA	-0.32	0.01	0.01
REO	-0.31	0.01	0.01
RES	-0.28	0.03	0.09
RIO	-0.26	-0.07	0.07
RLD	-0.16	-0.02	0.01
RRA	-0.29	-0.08	0.03

(g) Treatment 7

	$\Lambda^{(1)}$	$\Lambda^{(2)}$	$\Lambda^{(3)}$
LEO	-0.22	0.10	-0.01
LES	-0.33	-0.07	0.02
LIO	-0.20	-0.07	0.16
LLD	-0.42	-0.11	0.04
LRA	-0.19	0.09	0.03
REO	-0.08	0.03	0.15
RES	-0.28	-0.09	0.04
RIO	-0.23	-0.03	0.27
RLD	-0.40	-0.14	0.04
RRA	-0.11	0.09	0.28

(h) Treatment 8

	$\Lambda^{(1)}$	$\Lambda^{(2)}$	$\Lambda^{(3)}$
LEO	-0.42	0.04	-0.06
LES	0.09	-0.10	-0.03
LIO	-0.40	0.14	0.14
LLD	-0.11	-0.05	-0.09
LRA	-0.37	0.05	0.04
REO	-0.25	0.12	0.12
RES	-0.12	-0.02	0.05
RIO	-0.45	0.15	0.12
RLD	-0.05	-0.06	0.05
RRA	-0.38	0.05	-0.04

(i) Treatment 9

	$\Lambda^{(1)}$	$\Lambda^{(2)}$	$\Lambda^{(3)}$
LEO	-0.42	0.24	0.01
LES	-0.13	0.10	0.13
LIO	-0.28	-0.00	0.07
LLD	-0.49	0.10	0.10
LRA	-0.43	0.09	0.00
REO	**-0.62**	0.08	0.02
RES	**-0.64**	0.07	0.07
RIO	-0.17	-0.06	-0.00
RLD	**-0.63**	0.06	0.04
RRA	-0.35	0.13	0.11

(j) Treatment 10

	$\Lambda^{(1)}$	$\Lambda^{(2)}$	$\Lambda^{(3)}$
LEO	-0.40	0.01	0.11
LES	-0.11	0.15	0.12
LIO	-0.24	0.06	0.10
LLD	-0.45	0.02	0.10
LRA	-0.38	0.08	0.09
REO	**-0.55**	-0.07	0.02
RES	**-0.58**	-0.03	0.03
RIO	-0.24	0.02	0.03
RLD	**-0.55**	-0.08	-0.01
RRA	-0.33	-0.06	0.02

(k) Treatment 11

	$\Lambda^{(1)}$	$\Lambda^{(2)}$	$\Lambda^{(3)}$
LEO	-0.36	0.16	-0.06
LES	0.29	0.32	-0.01
LIO	-0.44	-0.13	-0.00
LLD	-0.23	0.38	0.03
LRA	-0.29	0.05	-0.12
REO	**-0.56**	0.07	-0.05
RES	-0.28	0.34	-0.05
RIO	-0.28	-0.04	-0.21
RLD	-0.27	0.38	-0.01
RRA	-0.24	0.18	-0.23

(l) Treatment 12

	$\Lambda^{(1)}$	$\Lambda^{(2)}$	$\Lambda^{(3)}$
LEO	-0.30	0.25	0.12
LES	**-0.54**	-0.10	0.11
LIO	-0.19	0.18	0.25
LLD	**-0.57**	-0.07	0.09
LRA	-0.32	-0.07	0.28
REO	-0.33	0.15	0.17
RES	**-0.59**	-0.07	0.14
RIO	-0.11	0.07	0.27
RLD	**-0.56**	-0.08	0.08
RRA	-0.19	0.03	0.21

(m) Treatment 13

	$\Lambda^{(1)}$	$\Lambda^{(2)}$	$\Lambda^{(3)}$
LEO	-0.43	0.19	-0.22
LES	**-0.53**	-0.07	-0.07
LIO	-0.31	0.07	-0.02
LLD	**-0.60**	-0.14	-0.11
LRA	-0.30	0.11	-0.04
REO	-0.40	-0.02	-0.13
RES	**-0.52**	-0.11	-0.07
RIO	-0.21	-0.07	-0.21
RLD	**-0.55**	-0.15	-0.06
RRA	-0.25	-0.06	-0.21

(n) Treatment 14

	$\Lambda^{(1)}$	$\Lambda^{(2)}$	$\Lambda^{(3)}$
LEO	-0.45	0.29	-0.11
LES	-0.19	-0.00	0.05
LIO	-0.13	0.35	0.08
LLD	**-0.53**	0.07	-0.03
LRA	-0.30	0.21	0.04
REO	**-0.58**	0.13	-0.04
RES	**-0.57**	0.05	-0.03
RIO	-0.16	0.06	-0.06
RLD	**-0.58**	-0.01	-0.03
RRA	-0.39	0.10	-0.07

(ñ) Treatment 15

	$\Lambda^{(1)}$	$\Lambda^{(2)}$	$\Lambda^{(3)}$
LEO	-0.49	0.14	-0.14
LES	**-0.60**	-0.14	-0.02
LIO	-0.27	0.16	-0.25
LLD	**-0.65**	-0.17	-0.13
LRA	-0.36	-0.16	-0.03
REO	-0.48	0.03	-0.11
RES	**-0.62**	-0.16	-0.00
RIO	-0.30	0.00	-0.10
RLD	**-0.65**	-0.21	-0.04
RRA	-0.32	0.15	-0.17

(o) Treatment 16

	$\Lambda^{(1)}$	$\Lambda^{(2)}$	$\Lambda^{(3)}$
LEO	-0.28	0.19	0.14
LES	-0.31	0.10	0.17
LIO	-0.35	0.18	0.08
LLD	-0.42	0.11	0.10
LRA	-0.29	0.21	0.04
REO	-0.27	0.20	0.18
RES	-0.37	0.11	0.07
RIO	-0.34	0.29	0.10
RLD	-0.32	0.15	0.06
RRA	-0.31	0.18	0.01

difference scores were significantly lower when subjects picked up the *liquid* load from the *near* origin (as compared to the *far* origin) ($F_{[1,13]} = 11.75$, $P = 0.009$), and when picked up the load from a position *near* to the body and in *asymmetric* tasks (as compared to *far* origin) ($F_{[1,13]} = 5.96$, $P = 0.059$.)

4.3.1.2. Lowering Task

The results of the ANOVA showed a significant main effect of factor VD for PC_{1-2} ($F_{[1,13]} = 32.7$, $P = 0.001$, $\eta_g^2 = 0.21$), PC_{1-3} ($F_{[1,13]} = 31.8$, $P = 0.001$, $\eta_g^2 = 0.14$), and PC_{2-3} ($F_{[1,13]} = 19.2$, $P = 0.001$, $\eta_g^2 = 0.15$) dependent variables, indicating lower difference scores of the variance explained

Table 4.5 Weighted means of the $\cos(\zeta)$ values across subjects for each treatment. Bold values corresponds to $|\cos(\zeta)| > 0.765$ ($P = 0.01$)—i.e., M-mode similarity across subjects.

	LIFT.PC1	LIFT.PC2	LIFT.PC3	LOW.PC1	LOW.PC2	LOW.PC3
1	0.57	0.68	0.57	0.37	0.60	0.33
2	0.56	0.68	0.52	0.50	0.62	0.35
3	0.61	**0.81**	0.55	0.39	0.63	0.33
4	**0.77**	0.46	0.60	0.76	0.35	0.29
5	**0.90**	0.45	0.53	**0.83**	0.44	0.30
6	0.66	0.59	0.66	0.51	0.60	0.38
7	0.65	**0.80**	0.35	0.65	0.50	0.43
8	0.66	0.63	0.53	0.64	0.62	0.40
9	**0.83**	0.43	0.44	**0.78**	0.39	0.47
10	**0.77**	0.39	0.34	0.65	0.41	0.36
11	0.63	0.40	0.60	0.63	0.63	0.36
12	**0.92**	0.60	0.36	**0.82**	0.47	0.45
13	**0.89**	0.56	0.50	**0.81**	0.49	0.39
14	**0.80**	0.71	0.55	0.75	0.64	0.31
15	**0.92**	0.50	0.40	**0.81**	0.55	0.36
16	0.67	0.70	0.75	0.32	0.69	0.38

by PC_{1-2} and PC_{1-3} when the subjects transfered the box to *knee* destination (as compared to *hip* destination), but an opposite trend for PC_{2-3} dependent variable—i.e., higher difference scores when the subjects deposited the box at *hip* destination as compared to that of *knee* destination. In accordance with lifting tasks, there is a downward trend in the difference of the values of the variance explained by PC1 vs PC2 or PC3 under more challenged tasks, and an opposite trend for PC2 vs PC3, however, only for the changes of the VD factor.

Overall, there is a downward trend in the difference of the values of the variance explained by PC1 vs PC2 or PC3 under more challenged tasks, and an opposite trend for PC2 vs PC3 (Fig. 4.13). These results confirmed the visual inspection on the differences in the dimensionality of the *hip* vs *knee* treatments showed on Fig. 4.7 (§ 4.2.1).

4.3.2. Effects of NIOSH Factors on Muscle Modes Similarity

4.3.2.1. Lifting Tasks

The results of the ANOVA revealed a significant main effect of the factor VD for both $\cos(\xi)^1_{1-2}$ ($F_{[1,13]} = 24.5$, $P < 0.001$, $\eta^2_g = 0.21$) and $\cos(\xi)^1_{1-3}$ ($F_{[1,13]} = 24.6$, $P < 0.001$, $\eta^2_g = 0.29$) dependent variables, indicating higher similarity of the $\mathbf{\Lambda}^{(1)}$ PC vectors across subjects when the load was lifting from the *hip* origin as compared to the *knee* origin. Moreover, a significant main effect of the factor AM for the $\cos(\xi)^1_{1-3}$ dependent variable ($F_{[1,13]} = 6$, $P = 0.03$, $\eta^2_g = 0.04$) indicated higher similarity for *symmetric* as compared to *asymmetric* tasks. However, these main effects were qualified by a significant interaction between factors VD and AM for both $\cos(\xi)^1_{1-2}$ ($F_{[1,13]} = 7.5$, $P = 0.017$, $\eta^2_g = 0.05$) and $\cos(\xi)^1_{1-3}$ ($F_{[1,13]} = 11.2$, $P = 0.005$, $\eta^2_g = 0.06$.) Simple main effect tests of the effects of factor AM at the different levels of factor VD yielded a significant

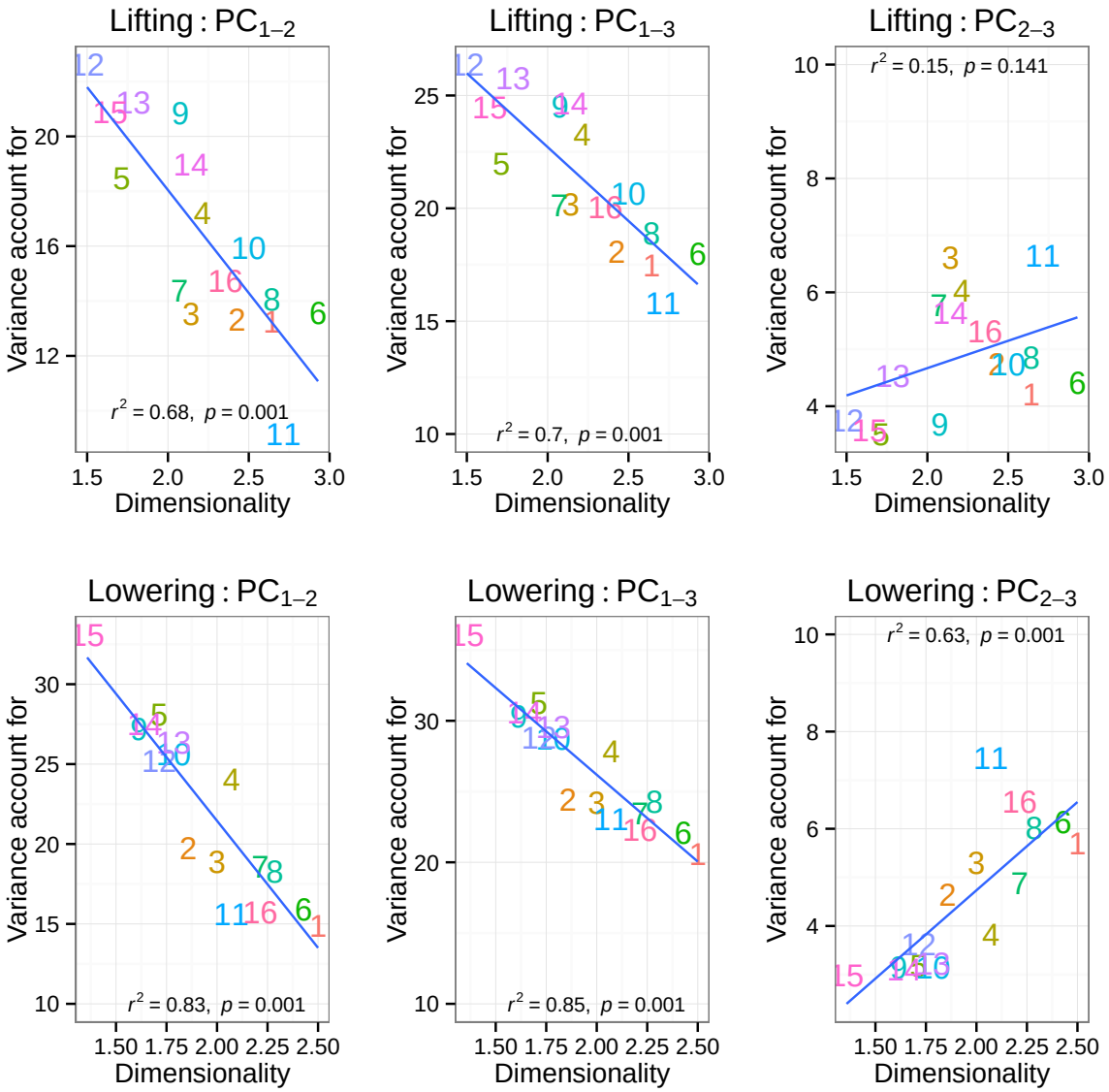

Figure 4.13 Difference in the scores of the amount of the variance accounted for by the extracted three PCs for every treatment after averaging across subjects, as a function of the suggested numbers of the PCs according to PA after averaging across subjects, for the lowering and lifting tasks, respectively (for number code see text).

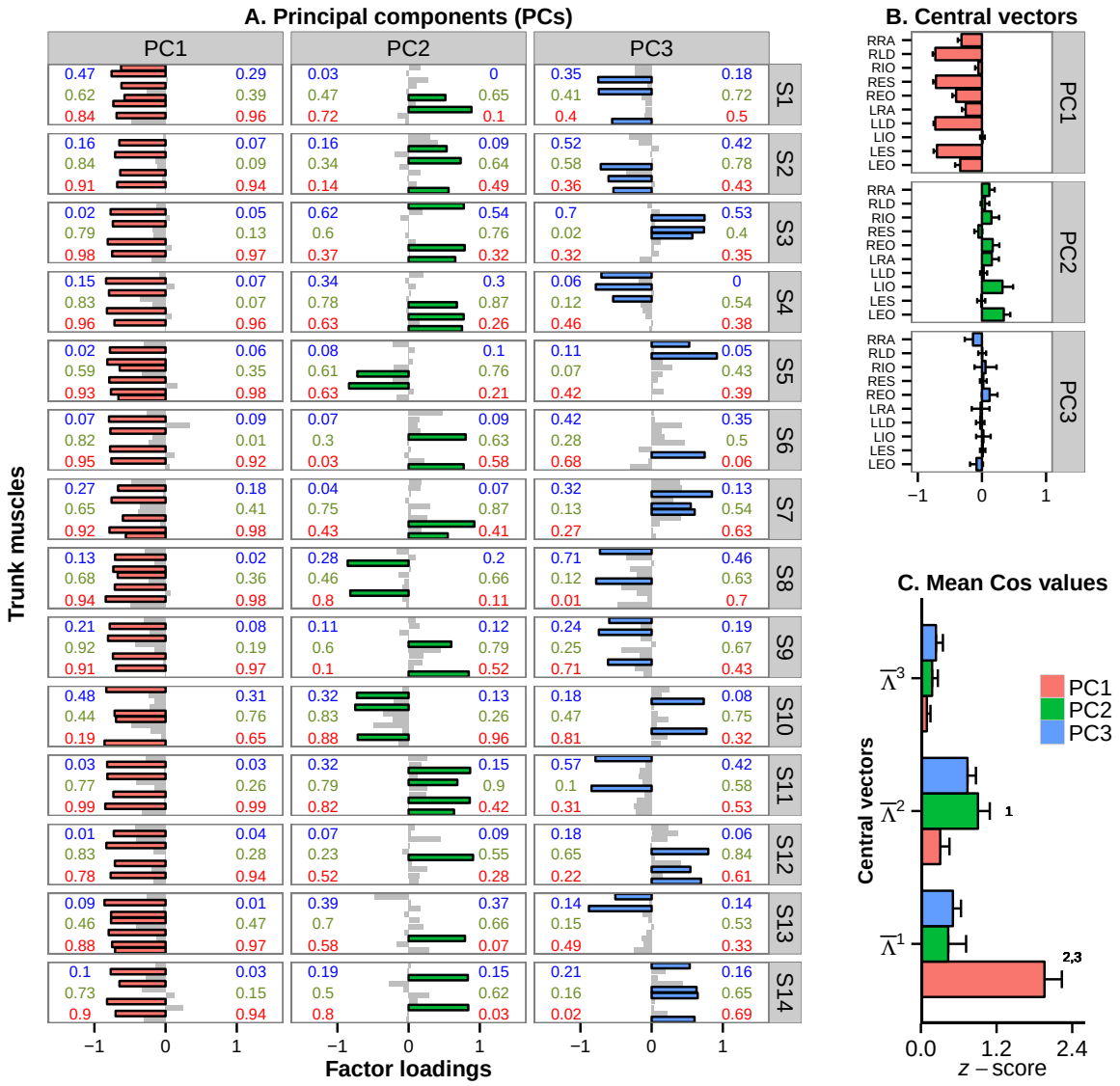

Figure 4.14 M-mode similarity across subjects for the treatment $a = 12$ of the experimental design. (**A**) Along with the factor loadings (with coloured bars the factor loadings $> |\pm 0.5|$) of each PC across subjects $S_{1\to 14}$, are showed the $|\cos(\zeta)|$ values (right), and the $|\cos(\xi)|$ values (left) as defined in Methods. The colour of the values corresponds to the cosine of the angle formed by the PC vector with the respective central vector of the same colour (red for $\bar{\mathbf{\Lambda}}^{(1)}$, green for $\bar{\mathbf{\Lambda}}^{(2)}$, and blue for $\bar{\mathbf{\Lambda}}^{(3)}$). (**B**) The central vectors are the vectors whose components are formed by the mean values of the corresponding PC across all subjects for this treatment; errors bars correspond to standard errors. (**C**) Mean values of the z-scores of the $|\cos(\xi)|$ values after being averaged across subjects along with their 95% confidence intervals. A repeated-measures design ANOVA with factor *PC* conducted separately for each central vector. Pairwise t-tests revealed that for the central vector $\bar{\mathbf{\Lambda}}^{(1)}$ the mean z-scores of the $\cos(\xi) = \left|\cos \measuredangle \left(\mathbf{\Lambda}^{(n)}, \bar{\mathbf{\Lambda}}^{(1)}\right)\right|$ were significantly higher if $n = 1$ as compared to $n \neq 1$ ($P < 0.05$); where $n = 1, 2, 3$. For the central vector $\bar{\mathbf{\Lambda}}^{(2)}$ the z-scores of the $\cos(\xi)$ was significantly higher only for $n = 2$ as compared to $n = 1$ ($P < 0.05$).

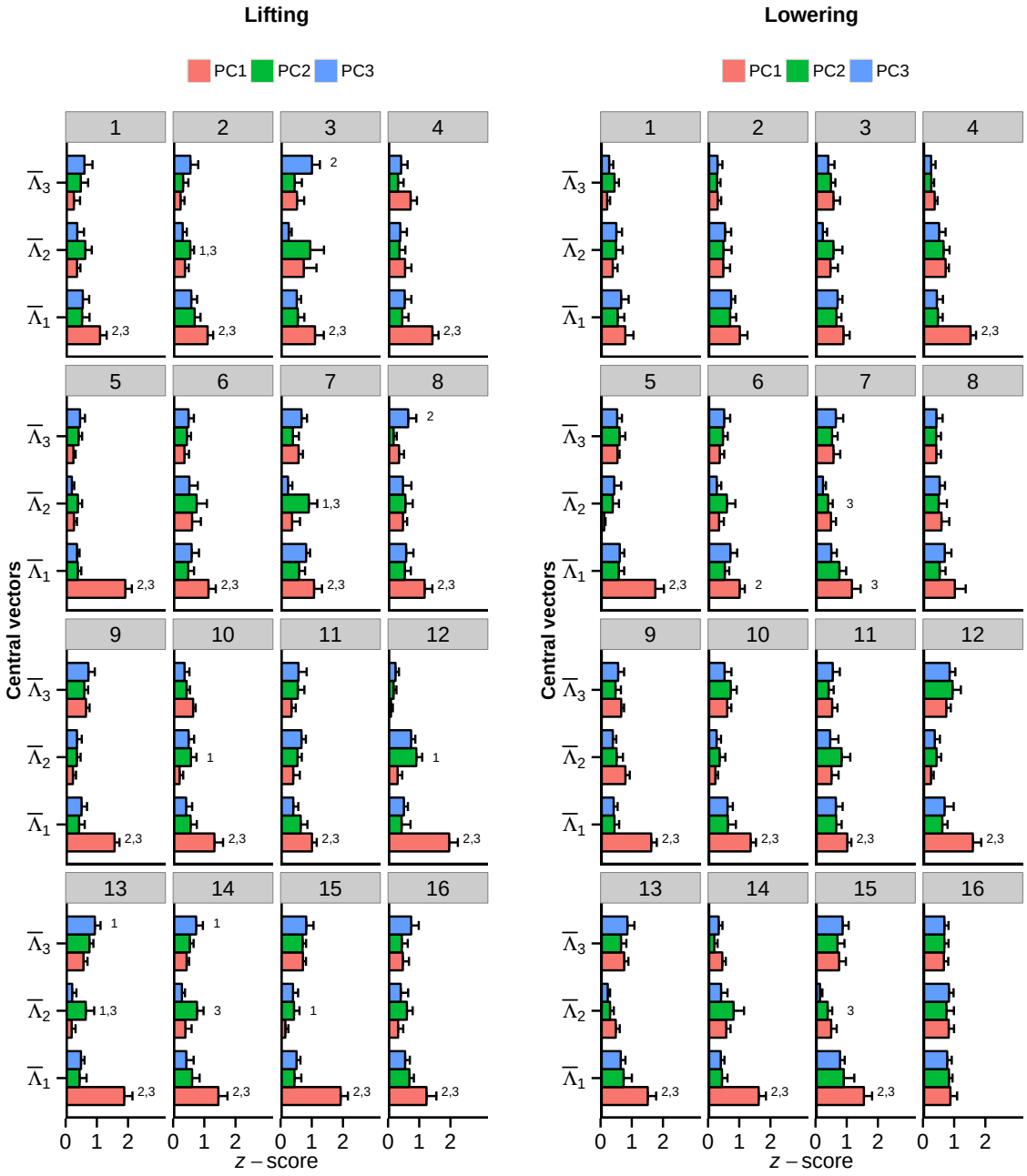

Figure 4.15 Mean values of the z-scores of the $|\cos(\xi)|$ values after being averaged across subjects along with their 95% confidence intervals. Values are shown for each treatment ($a_{1\to16}$) of the lifting and lowering tasks. Statistically significant differences of the mean z-scores of the $\cos(\xi) = \left|\cos \measuredangle \left(\mathbf{\Lambda}_a^{(n)}, \bar{\mathbf{\Lambda}}_a^{(n)}\right)\right|$ $(n = 1, 2, 3)$ are shown for each treatment ($P < 0.05$). For example, for the treatment $a = 9$ of the lifting task, the mean z-scores of the $\left|\cos \measuredangle \left(\mathbf{\Lambda}_9^{(1)}, \bar{\mathbf{\Lambda}}_9^{(1)}\right)\right|$ is statistically different from the mean z-scores of the $\left|\cos \measuredangle \left(\mathbf{\Lambda}_9^{(2)}, \bar{\mathbf{\Lambda}}_9^{(1)}\right)\right|$ and of the $\left|\cos \measuredangle \left(\mathbf{\Lambda}_9^{(3)}, \bar{\mathbf{\Lambda}}_9^{(1)}\right)\right|$ after averaging over subjects.

F-ratio for the *hip* level for both $\cos(\xi)^1_{1-2}$ ($F_{[1,13]} = 15.73$, $P = 0.003$) and $\cos(\xi)^1_{1-3}$ ($F_{[1,13]} = 13.73$, $P = 0.005$) dependent variables, indicating that the higher similarity of the $\mathbf{\Lambda}^{(1)}$ vectors found in *symmetric* tasks (as compared to *asymmetric*) for $\cos(\xi)^1_{1-3}$ holds only when the subjects pick up the load from the *hip* origin, which holds true for $\cos(\xi)^1_{1-2}$ as well. Moreover, simple main effect tests of the effects of factor VD at the different levels of factor AM yielded a significant F-ratio for both *asymmetric* and *symmetric* tasks, for both $\cos(\xi)^1_{1-2}$ ($F_{[1,13]} = 24.66$, $P = 0.001$, and $F_{[1,13]} = 5.9$, $P = 0.03$, for *asymmetric* and *symmetric* tasks, respectively) and $\cos(\xi)^1_{1-3}$ ($F_{[1,13]} = 50.6$, $P < 0.001$, and $F_{[1,13]} = 5$, $P = 0.043$, for *asymmetric* and *symmetric* tasks, respectively) dependent variables, indicating that the higher similarity of the $\mathbf{\Lambda}^{(1)}$ vectors found when subjects picked up the load from the *hip* origin (as compared to the *knee* origin) was even more pronounced in *symmetric* lifting tasks. Overall, the similarity of the $\mathbf{\Lambda}^{(1)}$ PC vectors across subjects is greater for treatments $a = 5, 12, 13$ and 15 (Table 3.6), which are those that combine *hip* origin and *symmetry*. The statistically significant $\cos(\zeta)$ values ($|\cos(\zeta)| > 0.765$) (Table 4.5) confirmed the higher similarity of the $\mathbf{\Lambda}^{(1)}$ vectors across subjects for these treatments.

The results of the ANOVA revealed a significant main effect of the factor AM for $\cos(\xi)^2_{2-3}$ ($F_{[1,13]} = 8.6$, $P = 0.012$, $\eta^2_g = 0.03$), indicating higher similarity of the $\mathbf{\Lambda}^{(2)}$ PC vector in *symmetric* tasks as compared to *asymmetric*. Moreover, there was a significant interaction between factors VD and LD for $\cos(\xi)^2_{1-2}$ dependent variable ($F_{[1,13]} = 7.1$, $P = 0.02$, $\eta^2_g = 0.03$.) Simple main effect tests of the effects of factor VD at the different levels of factor LD showed a significant F - ratio for the hip level ($F_{[1,13]} = 21.11$, $P = 0.001$), indicating higher similarity of the $\mathbf{\Lambda}^{(2)}$ PC vector across subjects when the *solid* load was picked up (as compared to the *liquid*.)

The results of the ANOVA showed also a significant main effect of the factor HD for both $\cos(\xi)^3_{1-3}$ ($F_{[1,13]} = 31.2$, $P < 0.001$, $\eta^2_g = 0.06$) and $\cos(\xi)^3_{2-3}$ ($F_{[1,13]} = 5.2$, $P < 0.001$, $\eta^2_g = 0.02$) dependent variables, indicating higher similarity of the $\mathbf{\Lambda}^{(3)}$ PC vector across subjects when the load was picked up from the *near* level as compared to the *far* level. However, for the $\cos(\xi)^3_{2-3}$ dependent variable, the main effect was qualified with a significant interaction by the factors HD and LD ($F_{[1,13]} = 7.5$, $P = 0.017$, $\eta^2_g = 0.02$). Simple main effect tests of the effects of factor LD at the different levels of factor HD yielded a significant F-ratio for the *solid* level ($F_{[1,13]} = 9.8$, $P = 0.016$), indicating higher similarity of the $\mathbf{\Lambda}^{(3)}$ PC vector across subjects when the load was picked up from the *near* level as compared to the *far* level. Simple main effect tests of the effects of factor HD at the levels of factor LD yielded a significant F-ratio for the *near* level ($F_{[1,13]} = 9.23$, $P = 0.019$), indicating higher similarity of the $\mathbf{\Lambda}^{(3)}$ PC vector across subjects when the *solid* load was picked up as compared to the *liquid* load. Moreover, the results of ANOVA showed a significant main effect of the factor VD for the $\cos(\xi)^3_{1-3}$ dependent variable ($F_{[1,13]} = 8.4$,$P = 0.013$, $\eta^2_g = 0.04$), indicating higher similarity of the $\mathbf{\Lambda}^{(3)}$ vector across subjects when the load was lifting from the *knee* origin as compared to the *hip* level.

4.3.2.2. Lowering Tasks

The results of the ANOVA revealed a significant main effect of the factor VD for both $\cos(\xi)^1_{1-2}$ ($F_{[1,13]} = 16.7$, $P = 0.001$, $\eta^2_g = 0.23$) and $\cos(\xi)^1_{1-3}$ ($F_{[1,13]} = 35.5$, $P < 0.001$, $\eta^2_g = 0.32$) dependent variables, indicating higher similarity of the $\mathbf{\Lambda}^{(1)}$ PC vectors across subjects when the

load was lowering to the *hip* destination as compared to the *knee* destination. Moreover, there was a significant main effect of the factor LD for the dependent variable $\cos(\xi)^1_{1-3}$ ($F_{[1,13]} = 11.3$, $P = 0.005$, $\eta^2_g = 0.01$), indicating higher similarity when the *liquid* load was transfered than the *solid*. However, for the $\cos(\xi)^1_{1-3}$ dependent variable, the main effect was qualified with a significant interaction by the factors VD and HD ($F_{[1,13]} = 13.5$, $P = 0.003$, $\eta^2_g = 0.03$). Simple main effect tests of the effects of factor VD at the different levels of factor HD showed a significant F - ratio for the hip level ($F_{[1,13]} = 5.99$, $P = 0.059$), indicating that the higher similarity of the $\mathbf{\Lambda}^{(1)}$ PC vector across subject found when the load was transfered to the hip level (as compared to the knee level), was even more pronounced combined it with the *near* level (as compared to the *far*.)

The results of the ANOVA revealed a significant Interaction between factors HD and AM for $\cos(\xi)^2_{1-2}$ dependent variable ($F_{[1,13]} = 5$, $P = 0.043$, $\eta^2_g = 0.01$.) Simple main effect tests of the effects of factor HD at the different levels of factor AM showed a significant F - ratio for the *far* level ($F_{[1,13]} = 6.76$, $P = 0.044$), indicating higher similarity of the $\mathbf{\Lambda}^{(2)}$ PC vector across subjects in *asymmetric* tasks (as compared to the *symmetrics*.)

4.4. Results of Multiple Linear Analyses: Jacobian matrices

4.4.1. Lifting Tasks

Multiple linear regression analysis was used to model the relationship between small changes in ΔM_1-mode, ΔM_2-mode, ΔM_3-mode magnitudes and ΔPVs by fitting a linear model to the observed data. A one-way repeated measure ANOVAs with factor *M-mode* gains (ΔM_1-mode, ΔM_2-mode, ΔM_3-mode) showed that there was a significant effect of factor *M-mode* on the regression coefficients values of the all the PVs except $\dot{\omega}_{flex}$ and $\dot{\omega}_{axial}$ ($F_{[2,45]} \geq 4.04$, $P \geq 0.024$, $\eta^2_g \geq 0.15$). Tukey's post-hoc tests revealed that for COP_{AP}, ω_{flex}, ω_{axial}, $\dot{\omega}_{tilt}$, θ_{axial}, v_ρ, θ, ρ, and z the regression coefficients for M_1-mode were significantly lower from the regression coefficients for M_3-mode and M_2-mode ($P \leq 0.05$), while for v_θ the regression coefficients for M_1-mode were significantly lower only from the regression coefficients for M_2-mode. For the COP_{ML}, ω_{tilt}, v_z, a_θ, and a_ρ the regression coefficients for M_1-mode were significantly higher from the regression coefficients for M_3-mode and M_2-mode ($P \leq 0.05$), while for the θ_{tilt}, θ_{flex} and a_z the regression coefficients for M_1-mode were significantly higher only from the regression coefficients for M_2-mode ($P \leq 0.05$). Moreover, the regression coefficients for M_2-mode were significantly higher from the regression coefficients for M_3-mode for the ω_{flex}, v_ρ, ρ, z, while for the v_z the regression coefficients for M_3-mode were significantly higher from the regression coefficients for M_2-mode.

4.4.2. Lowering Tasks

For the lowering tasks, a one-way repeated measure ANOVAs with factor *M-mode* gains (ΔM_1-mode, ΔM_2-mode, ΔM_3-mode) showed that there was a significant effect of factor *M-mode* on the regression coefficients values of the COP_{AP}, v_ρ, v_θ, a_z, ρ, θ, ω_{flex}, ω_{axial}, θ_{axial}, and θ_{tilt} ($F_{[2,45]} \geq 4.76$, $P \geq 0.013$, $\eta^2_g \geq 0.17$). Tukey's post-hoc tests revealed that for COP_{AP}, ω_{axial}, θ_{axial}, v_ρ,

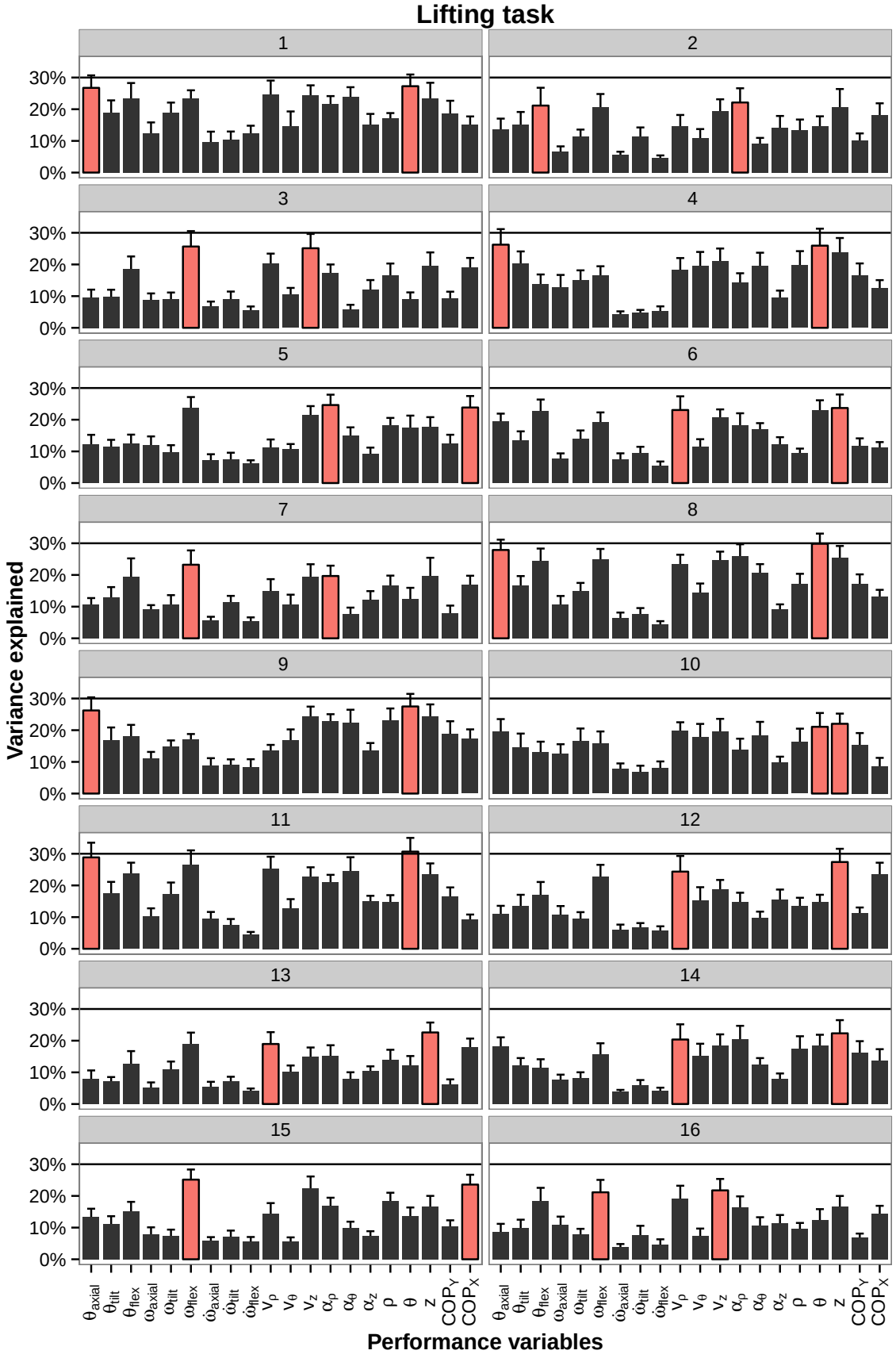

Figure 4.16 Variance explained (R^2) by the multiple linear regression analysis considering the M-modes as the explanatory variables and PV as the response variable.

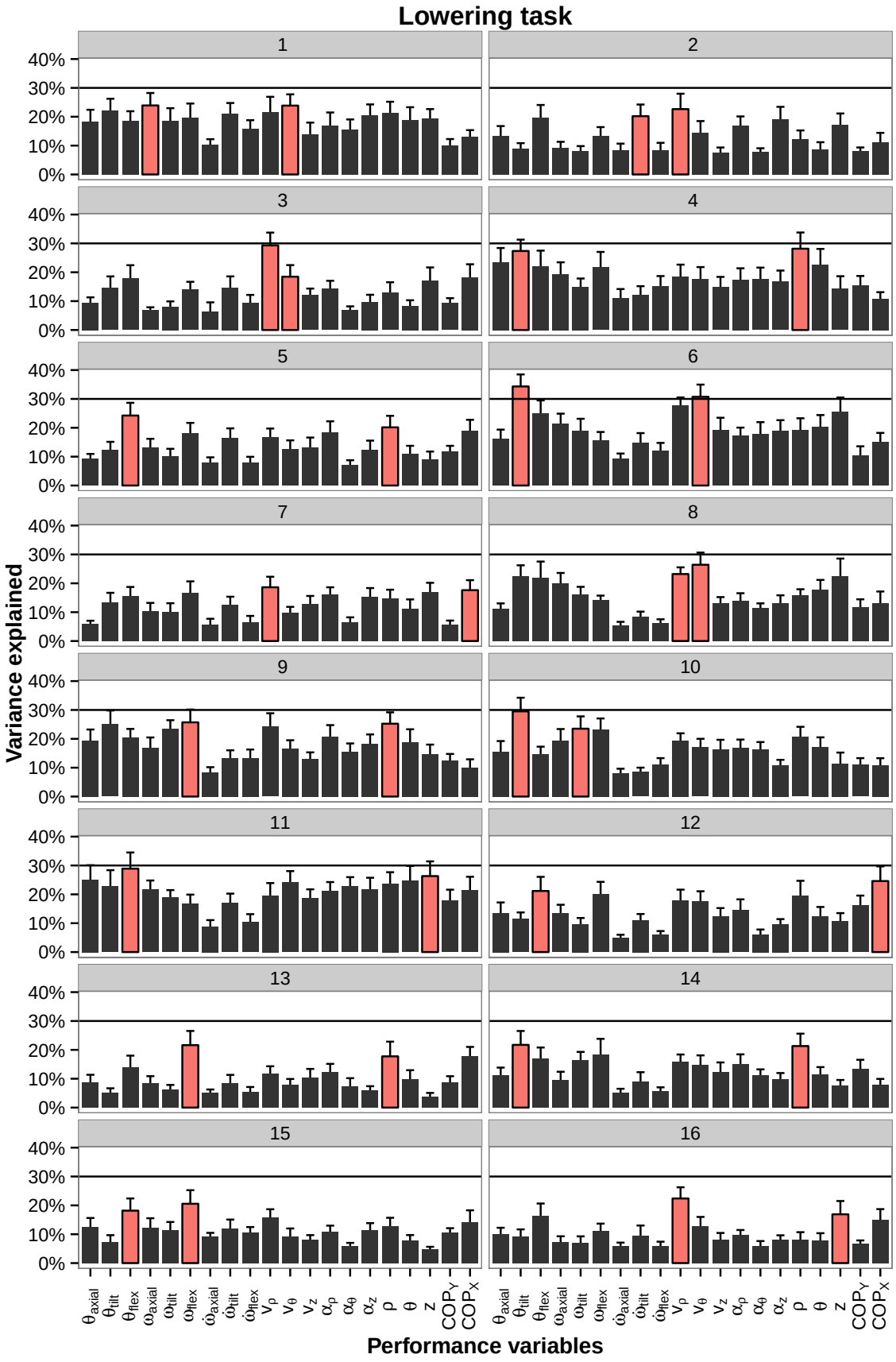

Figure 4.17 Variance explained (R^2) by the multiple linear regression analysis considering the M-modes as the explanatory variables and PV as the response variable.

a_z, θ, and ρ the regression coefficients for M_1-mode were significantly lower from the regression coefficients for M_3-mode and M_2-mode ($P \leq 0.05$), while for the θ_{tilt} the regression coefficients for M_1-mode were significantly higher from the regression coefficients for M_3-mode and M_2-mode ($P \leq 0.05$); for the ω_{flex} the regression coefficients for M_1-mode were significantly lower only from the regression coefficients for M_2-mode ($P \leq 0.05$).

Figures 4.16 and 4.17 shows the average across subjects determination coefficient (R^2) values (with standard errors). The plots show a moderate amount of variance explained by the linear regression models (maximum ≈30 %) for some PVs. The two PVs with higher R^2 values in each treatment were considered for both lifting and lowering tasks. Therefore, for the lifting task, there were considered for UCM analyses the θ_{axial}, θ_{flex}, ω_{flex}, v_ρ, v_z, a_ρ, θ, z, and COP_{AP}, while for the lowering task there were considered the θ_{tilt}, θ_{flex}, ω_{axial}, ω_{tilt}, ω_{flex}, v_ρ, v_θ, ρ, z, COP_{AP}, and $\dot{\omega}_{tilt}$. Note that there are PVs that are not presented in both lifting and lowering tasks. Lifting and lowering task share the θ_{flex}, ω_{flex}, v_ρ, z, and COP_{AP} performance variable (PV).

4.5. Uncontrolled Manifold Analysis: Synergy Index

4.5.1. Effects of Phases on Synergy Indices

A one-way ANOVA on the z-transformed values of the synergy index (ΔV) of the selected performace variables was ran to test whether the two variance components (V_{TOT}, V_{ORT}) changed similarly across the phases of the lifting and lowering cycles (*Lift*, *Pull*, *Push*, and *Deposit*). Tukey HSD *post-hoc* comparisons ran when it was appropiate. The one-way ANOVA revealed that there were no statistically significant differences among the phases of the lifting cycle for the θ_{flex} performance variable, and between the phases of the lowering cycle for the ω_{tilt}, θ_{tilt}, and ρ performace variables. Figures 4.18 and 4.19 show the ΔV indices for each of the four phases, for each of the performances variables, and for both lifting and lowering tasks, averaged across subjects. It is clear that synergy indices trend is not the same between lifting and lowering tasks. In general, lifting tasks had high mean values for lift and pull phases, while lowering tasks had high mean values for deposit and lift phases. Positive values of ΔV were interpreted to reflect a multi-M-mode synergy stabilizing the PV.

For the lifting tasks, the degree of the synergy indices decreased from lift-to-deposit phases (Fig. 4.18). Tukey's *post-hoc* tests revealed that there is either or a steep decrease of the synergy index after the lift phase (θ_{axial}, v_ρ), or a more progressive decrease (θ, z, v_z, ω_{flex}, and COP_{AP}), or a steep decrease but after the pull phase (a_ρ). Synergy indices trend for lowering tasks were not similar to those of the lifting tasks. There was, like in the lifting task, a decrease in the degree of the synergy indices but only from lift-to-pull or lift-to-push phases, followed by an increment of the synergy indices (Fig. 4.19). Tukey's post-hoc tests revealed that synergy indices were statistically recovered to initial values of the lift phase (θ_{flex}, z, v_ρ, ω_{axial}, v_θ, $\dot{\omega}_{tilt}$). Only the synergy index of ω_{flex} was not recovered. The phases with highest values of synergy indices were selected for further analysis.

To quantify if a muscle synergy is stabilizing the selected performance variables one sample student's

t tests were ran on the transformed data to check whether synergy indices were significantly different from zero ($0.5 \times \log(2)$). The results revealed that synergy indices were significantly higher from zero for all phases.

4.5.2. Effects of Risk Level on Synergy Indices

Figures 4.18 and 4.19 depict that there were not a common trend on the synergy indices across the risk level of the diferent treatments.

4.5.3. Effects of NIOSH Factors on Synergy Indices

A factorial repeated - measures, split - plot design ANOVA with VD, HD, AM, and type of LD as within - subjects factors and subjects' gender (SEX) as between-subjects factor was ran on the z-transformed values of the synergy index (ΔV) of the performace variables to test whether the two variance components (V_{TOT}, V_{ORT}) changed similarly across levels and their interaction. Only performance variables that showed statistically significant changes across phases were chosen for further analyses.

4.5.3.1. Lifting Tasks

Center of Pressure

COP$_{AP}{}^{Lift}$ The results of the ANOVA revealed a significant main effect of the SEX factor ($F_{[1,12]} = 12.3$, $P = 0.004$, $\eta_g^2 = 0.04$) indicating higher ΔV index for male subjects (0.67 ± 0.1) as compared to their female peers (0.51 ± 0.06). However, Gender effect was qualified by a significant interaction between SEX, HD and AM factors ($F_{[1,12]} = 11.3$, $P = 0.006$, $\eta_g^2 = 0.03$). Simple main effects test revealed a significant interaction of HD and AM factors for the male subjects ($F_{[1,12]} = 19.61$, $P = 0.002$). Further simple main effects test showed that in *asymmetric* tasks the synergy index was significantly higher when male subjects picked up the load from a position *near* to the body (0.92 ± 0.22) as compared to a position *far* from the body) (0.44 ± 0.18) ($F_{[1,12]} = 30.7$, $P = 0.001$).

Box's Kinematics

$\theta^{(Lift)}$ The results of the ANOVA revealed a significant main effect of *AM* factor ($F_{[4,12]} = 4.8$, $P = 0.048$, $\eta_g^2 = 0.04$), indicating higher ΔV index when subjects picked up the load in *asymmetric* (0.85 ± 0.23) as compared to *symmetric* tasks (0.67 ± 0.17).

$z^{(Lift)}$ The results of the ANOVA revealed a significant interaction between SEX and VD factors ($F_{[1,12]} = 5.6$, $P = 0.036$, $\eta_g^2 = 0.03$), qualified by a significant interaction between SEX, VD, and LD factors ($F_{[1,12]} = 8.7$, $P = 0.012$, $\eta_g^2 = 0.03$). Simple main effects test of the effects of SEX and LD factors on the difference of the levels of VD factor showed a significant F - ratio for *male*:*solid* levels ($F_{[1,12]} = 13.06$, $P = 0.014$), indicating higher synergy index across male subjects when a *solid* load was picked up from the *knee* level (0.85 ± 0.23)

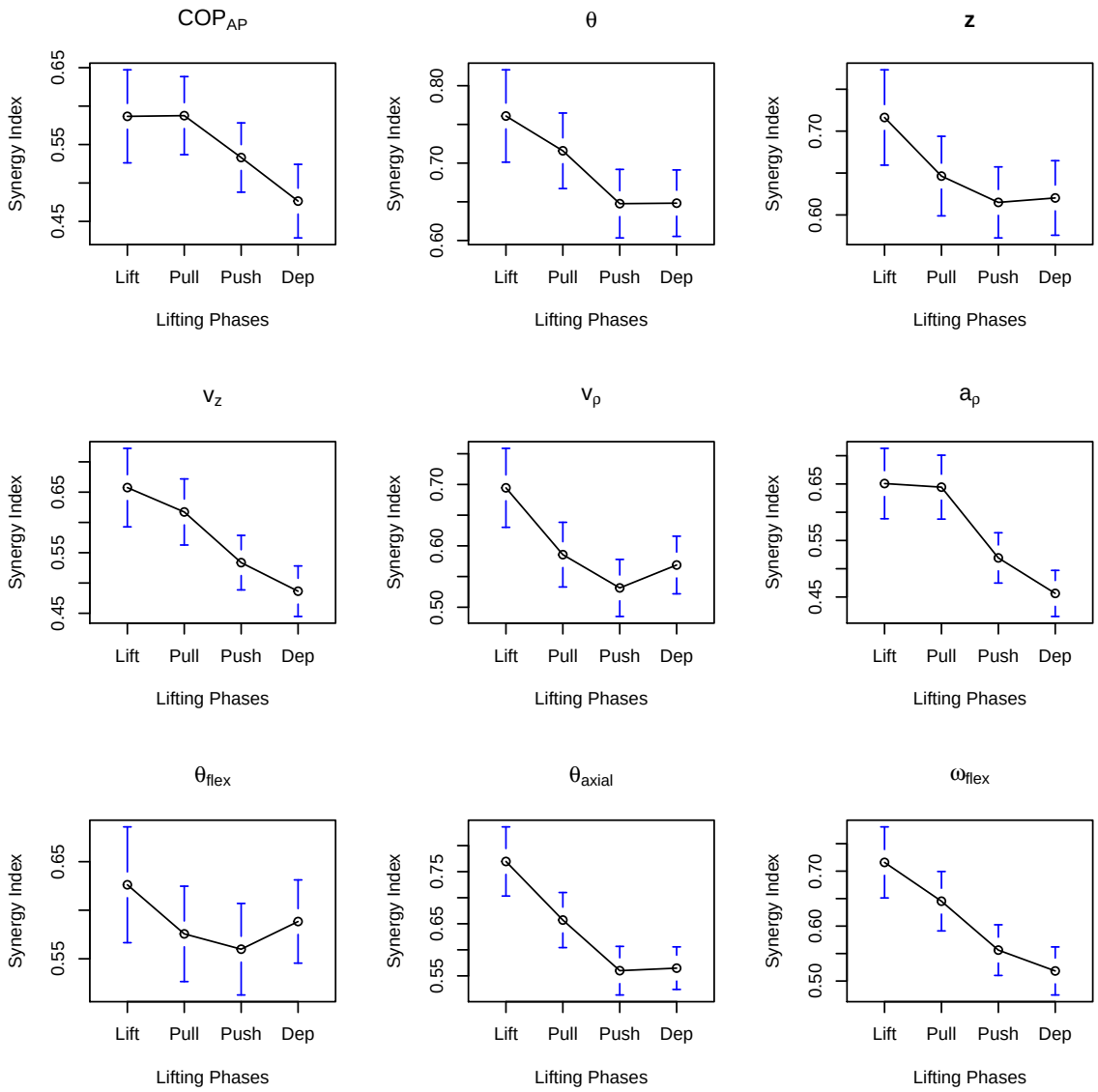

Figure 4.18 Synergy indices across subjects for each of the four phases within the lifting cycle. Mean values with 95% CI are shown.

as compared to the *hip* level (0.5 ± 0.2). Moreover,the results of the ANOVA revealed a significant Interaction between AM and LD factors ($F_{[1,12]} = 13.9$, $P = 0.003$, $\eta_g^2 = 0.03$). Simple main effect tests of the effects of factor AM at the different levels of factor LD showed a significant F-ratio for *asymmetric* tasks ($F_{[1,12]} = 4.89$, $P = 0.047$) and *symmetric* tasks ($F_{[1,12]} = 9.39$, $P = 0.02$), indicating higher synergy index when subjects picked up the *liquid* load in *asymmetric* Tasks (0.8 ± 0.22), and when the subjects picked up the *solid* load in *symmetric* tasks (0.76 ± 0.17).

$v_z^{(Lift)}$ The results of the ANOVA revealed a significant main effect of *HD* factor ($F_{[1,12]} = 4.8$, $P = 0.05$, $\eta_g^2 = 0.02$), indicating higher synergy index when subjects picked up the load from a position *near* to the body (0.72 ± 0.15) as compared to a position *far* from the body (0.6 ± 0.2). However, HD effect was qualified by a significant interaction between HD and LD

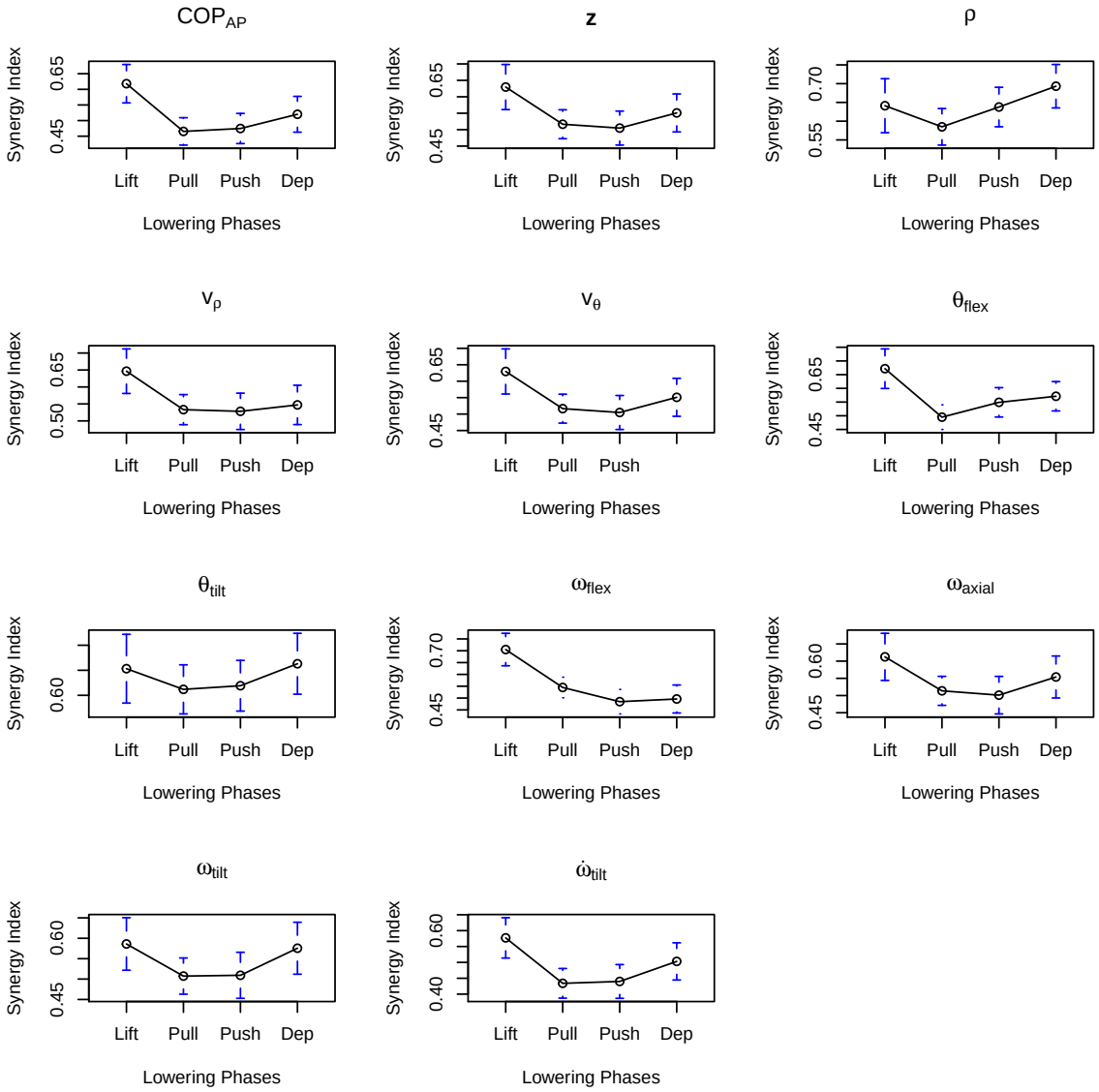

Figure 4.19 Synergy index across subjects for each of the four phases within the lowering cycle. Mean values with 95% CI are shown.

factors ($F_{[1,12]} = 4.9$, $P = 0.047$, $\eta_g^2 = 0.02$). Simple main effects test of the effects of factor LD on the levels of HD factor showed a significant F - ratio for the *solid* level ($F_{[1,12]} = 16.44$, $P = 0.003$), indicating higher synergy index when subjects picked up the solid load from a position *near* to the body (0.77 ± 0.23) as compared to a position *far* from the body (0.52 ± 0.22).

$v_\rho^{(Lift)}$ The results of the ANOVA revealed a significant main effect of *VD* factor ($F_{[1,12]} = 4.8$, $P = 0.049$, $\eta_g^2 = 0.04$), indicating higher synergy index when subjects picked up the load from the *knee* level (0.79 ± 0.24) as compared to the *hip* level (0.6 ± 0.28). VD effect was qualified by a significant interaction between SEX and VD factors ($F_{[1,12]} = 5$, $P = 0.044$, $\eta_g^2 = 0.05$). Simple main effects test of the effects of factor SEX on the levels of VD factor showed a significant F - ratio for male subjects ($F_{[1,12]} = 9.86$, $P = 0.017$), indicating higher

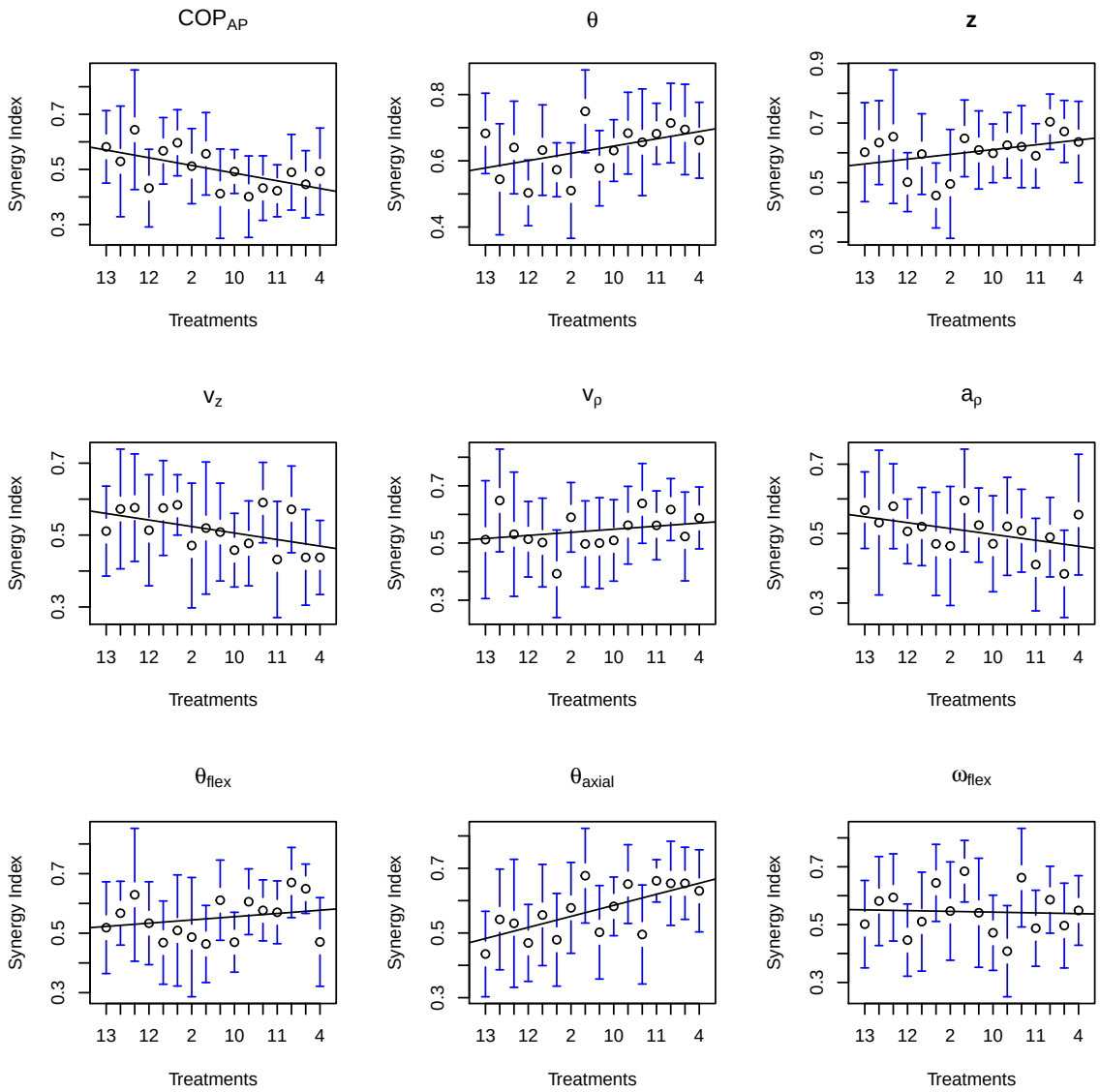

Figure 4.20 Synergy index across treatments for the lifting cycle. Mean values with 95% CI and linear regression line are shown.

synergy index when male subjects picked up the load from the *knee* level (0.8 ± 0.3) as compared to the *hip* level (0.42 ± 0.25).

$a_{\rho}^{(Lift)}$ The results of the ANOVA revealed a significant main effect of *HD* factor ($F_{[1,12]} = 13.9$, $P = 0.003$, $\eta_g^2 = 0.04$), indicating higher synergy index when subjects picked up the load from a position *near* to the body (0.74 ± 0.15) as compared to a position *far* from the body (0.56 ± 0.15). HD effect was qualified by a significant interaction between HD and AM factors ($F_{[1,12]} = 9.2$, $P = 0.01$, $\eta_g^2 = 0.04$). Simple main effects test of the effects of factor AM on the levels of HD factor showed a significant F - ratio for *asymmetric* tasks ($F_{[1,12]} = 5.14$, $P = 0.085$), indicating higher synergy index when subjects picked up the load from a position *near* to the body (0.86 ± 0.26) as compared to position *far* from the body (0.52 ± 0.24).

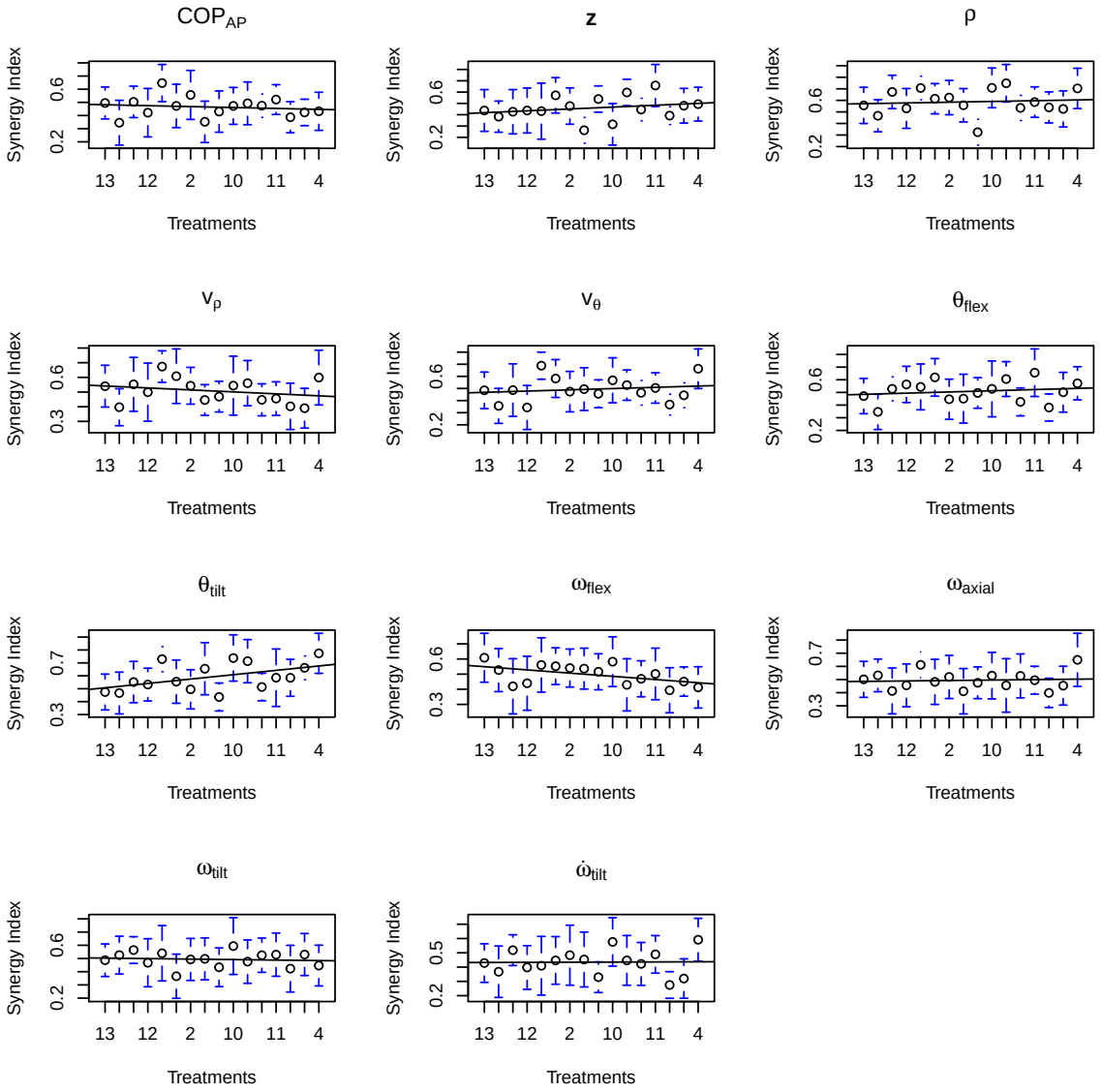

Figure 4.21 Synergy index across treatments for the lowering cycle. Mean values with 95% CI and linear regression line are shown.

Trunk Kinematics

$\theta_{flex}^{(Lift)}$ The results of the ANOVA revealed a significant interaction between SEX, AM and LD factors ($F_{[1,12]} = 7.9$, $P = 0.016$, $\eta_g^2 = 0.02$). Simple main effects test revealed a significant interaction of LD and AM factors for the female subjects ($F_{[1,12]} = 9.05$, $P = 0.022$). Further simple main effects test of the effects of LD factor on the levels of AM factor showed a significant F - ratio for the *solid* level ($F_{[1,12]} = 1.02$, $P = 0.445$) indicating higher synergy index when male subjects picked up the *solid* load in *symmetric* tasks (0.76 ± 0.19) as compared to *asymmetric* tasks (0.55 ± 0.21). Moreover, the results of the ANOVA revealed a significant interaction between VD and HD factors ($F_{[1,12]} = 13.4$, $P = 0.003$, $\eta_g^2 = 0.03$). Simple main effects test of the effects of factor HD on the levels of VD factor showed a significant F - ratio for the *far* level ($F_{[1,12]} = 7.45$, $P = 0.037$), indicating higher synergy

index when subjects picked up the load from the *knee* origin (0.71 ± 0.27) as compared to *hip* origin (0.46 ± 0.26). Simple main effects test of the effects of factor VD on the levels of HD factor showed a significant F - ratio for the *hip* level ($F_{[1,12]} = 19.09$, $P = 0.002$), indicating higher synergy index when subjects picked up the load from a position *near* to the body (0.69 ± 0.26) as compared to position *far* of the body (0.46 ± 0.26)).

$\theta_{axial}^{(Lift)}$ The results of the ANOVA revealed a significant main effect of *AM* factor for the ($F_{[1,12]} = 24.7$, $P = 3 \times 10^{-4}$, $\eta_g^2 = 0.13$) indicating higher synergy index when subjects picked up the load in *asymmetric* (0.94 ± 0.21) as compared to *symmetric* tasks (0.6 ± 0.18). However, AM effect was qualified by a significant interaction between VD and AM factors ($F_{[1,12]} = 6.2$, $P = 0.028$, $\eta_g^2 = 0.03$). Simple main effects test of the effects of factor VD on the levels of AM factor showed a significant F - ratio for the *hip* level ($F_{[1,12]} = 25.43$, $P = 0.001$), indicating higher synergy index when subjects picked up the load in *asymmetric* tasks (1.04 ± 0.28) as compared to the *symmetric* (0.54 ± 0.22).

$\omega_{flex}^{(Lift)}$ The results of the ANOVA revealed a significant main effect of *HD* factor ($F_{[1,12]} = 5.3$, $P = 0.041$, $\eta_g^2 = 0.01$) indicating higher synergy index when subjects picked up the load from a position *near* to the body (0.77 ± 0.18) as compared to a position *far* from the body (0.66 ± 0.18). HD effect was qualified by a significant interaction between HD and AM factors ($F_{[1,12]} = 6.1$, $P = 0.029$, $\eta_g^2 = 0.02$). Simple main effects test of the effects of factor AM on the levels of HD factor showed a significant F - ratio for *asymmetric* tasks ($F_{[1,12]} = 11.49$, $P = 0.011$), indicating higher synergy index when subjects picked up the load from a position *near* to the body (0.88 ± 0.25) as compared to position *far* of the body (0.66 ± 0.26).

4.5.3.2. Lowering Tasks

Box's Kinematics

$\rho^{(Lift)}$ The results of the ANOVA revealed a significant main effect of *LD* factor ($F_{[1,12]} = 5$, $P = 0.045$, $\eta_g^2 = 0.02$), indicating higher synergy index when subjects picked up the *solid* load (0.71 ± 0.24) as compared to the *liquid* load (0.57 ± 0.18). However, LD effect was qualified by a significant interaction between LD and HD factors ($F_{[1,12]} = 6.9$, $P = 0.022$, $\eta_g^2 = 0.05$). Simple main effects test of the effects of factor HD on the levels of LD factor showed a significant F - ratio for *near* level ($F_{[1,12]} = 8.69$, $P = 0.024$), indicating higher synergy index when subjects picked up the *solid* load (0.84 ± 0.44) as compared to the *liquid* load (0.48 ± 0.25). The results of the ANOVA revealed also a significant interaction between HD and AM factors ($F_{[1,12]} = 6$, $P = 0.03$, $\eta_g^2 = 0.01$). Simple main effects test of the effects of factor HD on the levels of AM factor showed a significant F - ratio for the *far* level ($F_{[1,12]} = 6.48$, $P = 0.051$), indicating higher synergy index when subjects picked up the load in *asymmetric* tasks (0.7 ± 0.24) as compared to *symmetric* tasks (0.54 ± 0.18).

$\rho^{(Dep.)}$ The results of the ANOVA revealed a significant main effect of *HD* factor ($F_{[1,12]} = 7.4$, $P = 0.018$, $\eta_g^2 = 0.02$) indicating higher synergy index when subjects picked up the load from a position *near* to the body (0.76 ± 0.18) as compared to a position *far* from the body (0.63

± 0.16). However, HD effect was qualified by a significant interaction between HD and AM factors ($F_{[1,12]} = 6.5$, $P = 0.026$, $\eta_g^2 = 0.02$). Simple main effects test of the effects of factor AM on the levels of HD factor showed a significant F - ratio for *symmetric* tasks ($F_{[1,12]} = 10.05$, $P = 0.016$), indicating higher synergy index when subjects picked up the load from a position *near* to the body (0.79 ± 0.27) as compared to position *far* from the body (0.54 ± 0.18). Further simple main effects test of the effects of factor HD on the levels of AM factor showed a significant F - ratio for the *far* level ($F_{[1,12]} = 11.99$, $P = 0.009$), indicating higher synergy index when subjects picked up the load in *asymmetric* tasks (0.71 ± 0.19) as compared to *symmetric* tasks (0.54 ± 0.18).

$Z^{(Lift)}$ The results of the ANOVA revealed a significant main effect of *VD* factor ($F_{[1,12]} = 8.2$, $P = 0.014$, $\eta_g^2 = 0.04$), indicating higher synergy index when subjects picked up the load from *knee* level (0.79 ± 0.15) as compared to *hip* level (0.6 ± 0.15). Moreover, the results of the ANOVA revealed a significant interaction between LD and HD factors ($F_{[1,12]} = 8.8$, $P = 0.012$, $\eta_g^2 = 0.01$). Simple main effects test of the effects of factor HD on the levels of LD factor showed a significant F - ratio for *far* level ($F_{[1,12]} = 8.95$, $P = 0.022$), indicating higher synergy index when subjects picked up the *liquid* load (0.83 ± 0.22) as compared to *solid* load (0.63 ± 0.21).

$V_\rho^{(Lift)}$ The results of the ANOVA revealed a significant interaction between LD and HD factors ($F_{[1,12]} = 10.5$, $P = 0.007$, $\eta_g^2 = 0.04$). Simple main effects test of the effects of factor HD on the levels of LD factor showed a significant F - ratio for the *far* level ($F_{[1,12]} = 6.88$, $P = 0.044$), indicating higher synergy index when subjects picked up the *liquid* load (0.73 ± 0.22) (as compared to the *solid* load (0.5 ± 0.23)). Further simple main effects test of the effects of factor LD on the levels of HD factor showed a significant F - ratio for the *solid* level ($F_{[1,12]} = 11.72$, $P = 0.01$), indicating higher synergy index when subjects picked up the *solid* load from a position *near* to the body (0.75 ± 0.15) as compared to lift *solid* load from a position *far* from the body (0.5 ± 0.23).

$V_\rho^{(Dep.)}$ The results of the ANOVA revealed a significant main effect of *VD* factor ($F_{[1,12]} = 17$, $P = 0.001$, $\eta_g^2 = 0.09$), indicating higher synergy index when subjects picked up the load from *hip* level (0.67 ± 0.14) as compared to *knee* level (0.43 ± 0.15). Moreover, the results of the ANOVA revealed a significant interaction between LD and AM factors ($F_{[1,12]} = 8.9$, $P = 0.011$, $\eta_g^2 = 0.03$). Simple main effects test of the effects of factor LD on the levels of AM factor showed a significant F - ratio for the *liquid* level ($F_{[1,12]} = 7.55$, $P = 0.035$), indicating higher synergy index when subjects picked up the *liquid* load in *symmetric* tasks (0.69 ± 0.23) as compared to the *asymmetric* tasks (0.51 ± 0.17).

$V_\theta^{(Lift)}$ The results of the ANOVA revealed a significant interaction betweenLD and HD factors ($F_{[1,12]} = 6.6$, $P = 0.025$, $\eta_g^2 = 0.04$). Simple main effects test of the effects of factor LD on the levels of HD factor showed a significant F - ratio for the *liquid* level ($F_{[1,12]} = 6.35$, $P = 0.054$), indicating higher synergy index when subjects picked up the *liquid* load from a position *far* from the body (0.73 ± 0.19) as compared to pick up the *liquid* load from a position *near* to the body (0.5 ± 0.33).

$V_{\theta}^{(Dep.)}$ The results of the ANOVA revealed a significant main effect of *VD* factor ($F_{[1,12]} = 19.5$, $P = 0.001$, $\eta_g^2 = 0.07$), indicating higher synergy index when subjects picked up the load from *hip* level (0.66 ± 0.23) as compared to *knee* level (0.44 ± 0.15).

Trunk Kinematics

$\theta_{flex}^{(Dep.)}$ The results of the ANOVA revealed a significant interaction between SEX and AM factors ($F_{[1,12]} = 6.3$, $P = 0.028$, $\eta_g^2 = 0.02$). Simple main effects test of the effects of factor SEX on the levels of AM factor showed a significant F - ratio for the female subjects ($F_{[1,12]} = 8.28$, $P = 0.028$), indicating higher synergy index when female subjects picked up the load in *symmetric* tasks (0.67 ± 0.11) as compared to the *asymmetric* tasks (0.51 ± 0.14).

$\theta_{tilt}^{(Dep.)}$ The results of the ANOVA revealed a significant main effect of *AM* factor ($F_{[4,12]} = 16.8$, $P = 0.001$, $\eta_g^2 = 0.06$) indicating higher ΔV index when subjects picked up the load in *asymmetric* (0.77 ± 0.13) as compared to *symmetric* tasks (0.56 ± 0.16).

$\omega_{axial}^{(Lift)}$ The results of the ANOVA revealed a significant interaction betweenLD and HD factors ($F_{[1,12]} = 8.4$, $P = 0.013$, $\eta_g^2 = 0.03$). Simple main effects test of the effects of HD factor on the levels of LD factor showed a significant F - ratio for the *far* level ($F_{[1,12]} = 11.19$, $P = 0.012$), indicating higher synergy index when subjects picked up the *liquid* load (0.71 ± 0.26) as compared to the *solid* load (0.49 ± 0.26).

$\dot{\omega}_{tilt}^{(Dep.)}$ The results of the ANOVA revealed a significant main effect of *VD* factor ($F_{[1,12]} = 8.8$, $P = 0.012$, $\eta_g^2 = 0.05$), indicating higher synergy index when subjects picked up the load from the *hip* level (0.59 ± 0.2) as compared to the *knee* level (0.41 ± 0.17).

5

Discussion

5.1. Redundancy and Ergonomics

Over the past few years, the term *physical neuroergonomics*, defined as the field of study focusing on the knowledge of human brain activity in relation to the control and design of physical tasks (Karwowski et al., 2007), has been introduced to explore the neural basis of peoples' physical performance in natural and naturalistic environments (Mehta and Parasuraman, 2013; Parasuraman and Rizzo, 2007). Physical neuroergonomics, as a branch of *neuroergonomics* described as the study of brain and behaviour at work (Parasuraman, 2003), is basically relied on neuroimaging techniques (Mehta and Parasuraman, 2013; Parasuraman and Rizzo, 2007). Recently, the term computational neuroergonomics has been introduced as the field of study focusing on the analyses of neuroimaging data for modeling perceptual-motor performance for the design and improvement of human-machine systems (Liu, Wu, and Berman, 2012). Another approach to investigate how the "neural controller" coordinates neuromotor activities during execution of voluntary movements is the so - called or muscle synergies approach (Bernstein, 1967; Bizzi and Cheung, 2013; Krishnamoorthy et al., 2003; Latash et al., 2005). It relies on the application of physical laws to the motor control of voluntary movements, and the hierarchical organization and regulation of the voluntary movements by mastering the excessive DOF formulating "synergies" (Bernstein, 1967; Gelfand and Tsetlin, 1962, 1971; Gelfand et al., 1971; Latash, Scholz, and Schoner, 2007).

According to the *principle of motor abundance*, which was introduced by Gelfand and Latash (1998) followed the ideas of Gelfand and Tsetlin (1962, 1971), the DOF of a neuromotor level are participated all in the voluntary motor tasks assuring both stability and flexibility by formulating synergies. Synergy has been defined as a task-specific neural organization of a set of elemental variables (DOF) that organizes (i) sharing of a task among them and (ii) ensures certain stability/flexibility features of the performance variables, whereas elemental variables have been defined as those DOF whose values can be changed by the controller while keeping the values of other DOF unchanged, and the performance variable has been defined as a particular feature of the overall output of the multi-element biological system that plays an important role for a group of tasks (Latash, Gorniak, and Zatsiorsky, 2008; Latash, 2008b; Latash, Scholz, and Schoner, 2007). Muscles synergies or muscle-modess (M-modes) have addressed the set of muscles within which the neural controller scales the activation level in parallel either in time on the course of performing

an action, or in space across actions with different parameters (Alessandro et al., 2013; Bizzi and Cheung, 2013; Krishnamoorthy et al., 2003; Latash, 2012; Latash et al., 2005; Ting, 2007; Ting and Chvatal, 2011). At the neuromuscular level, the spatiotemporal pattern of motoneuronal activity was quantified by applying EFA matrix factorization algorithm with varimax rotation. With this procedure, synergies can be quantified using the framework of the UCM hypothesis (Latash, Scholz, and Schöner, 2002; Scholz and Schöner, 1999). Briefly, the UCM hypothesis maps the variance of the spatiotemporal pattern of motoneuronal activity onto the performance variable variance, and therefore separates the combination of motoneuronal activities that are equally able to solve the motor task problem (performace variable) within an acceptable margin of error for those solutions that are irrelevant of the ongoing task (Latash, Scholz, and Schöner, 2002; Scholz and Schöner, 1999).

In ergonomics, lifting or lowering tasks can be categorized according to their risk level of suffering WRLBD. Injury pathways for development of LBD are based on the capacity of the "neural controler" to master the redundancy in the neuromusculoskeletal system and therefore to control the patterns of forces exerted by trunk muscles and their magnitudes that finally define spine and muscle loadings. Nevertheless, it is not known whether the risk level for development of WRLBD can be associated with the capacity of the controller to determine how to activate trunk global muscles in order to produce the desired actions in task space. Muscle activation pattens can be combined in various ways in order to perform a lifting or lowering task. Variability of muscle activation patterns allows to deal with concurrent tasks and mechanical or neuromuscular perturbations that are typically caused by the unforesseable environments where usually voluntary movements are executed in. Although this freedom can be reduced as some of these combinations are not biomechanically healthy allowing, therefore, to minimize effort or to avoid uncomfortable postures, muscle redundancy provides the capacity to control more than one performance variable at the same time and also to repeat movement patterns with little variation and coordinate the limbs in a specific way.

We hypothesized that trial-by-trial muscle activation patterns in motor-equivalent lifting and lowering tasks can be parameterized and analyzed based on the notion of M-modes. There is scientific evidence from motor control and biomechanical studies that motor equivalence can be achieved by different muscle activation patterns unconcernedly task's complexity (Gottlieb, Chen, and Corcos, 1995; Levin et al., 2003; Torres-Oviedo and Ting, 2007). Muscle space have as many DOF as the number of the skeletal muscles. Even though we could suppose that global muscles are the primarily trunk muscles for movement actions, the DOF of the movements are still less than global muscles space. Therefore, the "neural controller" has to specify how to coordinate global muscles in the space of all possible combinations. UCM hypothesis suggests that "neural controller" simplifies control by formulating muscle synergies—i.e., a coordination group of muscles. Using redundancy, it is possible to modify muscle activation patterns without changing the end effector position and orientation, which in this case is the handling load. Moreover, muscles can be involved in different movement actions—i.e., be part of different group of muscles with different activation "weights" in each. This hypothesis involves muscles' activations restricted to the *nullspace* of the Jacobian relating muscles' space to performance variable space. The variability in the nullspace

does not affect performance variable pattern.

Motor redundancy at the kinematic level, which is arose by the numerous DOF of the human locomotor apparatus compared with the substantially lower anatomical constraints that are imposed by the structure of the musculoskeletal system at joints level, gives to the workers the possibility to adopt an infinite number of postures during lifting or lowering tasks, and consequently the ability to execute a countless voluntary motor patterns in order to accomplish their labor activities. These differences in motion patterns that finally are subserving the same movement goal can be found qualitatively (the stoop and the squat liftstyle are such motion patterns) or quantitatively by implying pattern identification algorithms (Burgess-Limerick and Abernethy, 1997; Park et al., 2005; Zhang, Nussbaum, and Chaffin, 2000). Following the Bernstein's hypotheses (Aruin and Bernstein, 2002; Bernstein, 1930, 1967), repetitive lifting and lowering tasks have been seen as reaching movements, where the primary goal is the control of end-effector in order to accomplish the task effectivelly, but without accidental injuries (slips, falls, etc) or risk to develop LBD. Hence, the ergonomics approach to these tasks was to quantify the biomechanical constraints and physiological responses associated with the different joint configurations used to accomplish the same task (mainly stoop and squat) in an attempt to find the "correct" lifting technique that minimizes the risk of LBD and to provide work conditions that minimize accidents (Khanzode, Maiti, and Ray, 2012). Park et al. (2005) and Zhang, Nussbaum, and Chaffin (2000) provide indices that quantify the effects of joint space configuration to the end-effector trajectory control during lifting and lowering tasks. Although end-effector trajectory is fundamental to accomplish the tasks, other aspects of movement technique are also important, like balance maintenance, minimization of the influence of external or internal "perturbations" or attenuation of undesired movements. To date, it is not clear what variables the "neural controller" manipulates to accomplish the lifting or lowering tasks. This means that hand trajectory as the only task goal may not be sufficient to characterize movement technique (Park et al., 2005).

The accomplishment of the same task using different body configurations and environmental means is referred to as "motor equivalence". Under the UCM approach, the presence of motor equivalence can be quantified by the "internal motion" restricted to the joint linkage *nullspace*, whereas non-motor equivalent joint configurations can be quantified when motion is more in the range space than in the *nullspace*. Furthermore, joint movements can be performed using various muscle combinations (muscle redundancy). Similar muscle activation patterns cannot be presented always among workers or in the same worker who performs replications of the same lifting or lowering task in terms of origin-destination state (motor equivalence), as it is known that similar motor patterns can be achieved by different muscle activation patterns, unconcernedly tasks complexity. However, this freedom can be reduced in specific tasks by biomechanical constraints on the neuromusculoskeletal system (Kutch and Valero-Cuevas, 2012). In this study, it was supposed that redundancy provides advantages to the "neural controller" by allowing it not only to avoid biomechanically uncomfortable postures or to minimize musculoskeletal effort, but also to maintain body balance and to control kinematic variables related to task goal achievement. Moreover, it was supposed that the controlled variables can also be used to characterize the risk level for development of WRLBD. Implicity this means that when variables associated to ergonomics

stressors are manipulated (e.g., trunk velocity, box's vertical displacement, etc.) the motor control quality is also influenced.

5.2. Multi-M-modes Synergies in Lifting and Lowering Tasks

Four hypotheses have been formulated in Chapter 2. With respect to the first hypothesis, the results have provided support that muscle activation patterns during lifting or lowering tasks can be described with a set of three M-modes; however, the composition of the M-modes were not similar either across subjects or treatments or between lifting and lowering tasks. The sets of the three M-modes formed the basis for multi-M-mode synergies stabilizing the selected PVs across treatments for both lifting and lowering tasks, provided support for the second hypothesis that trunk M-modes stabilize the time profile of PVs that are being used also to characterize the risk level for development of WRLBD. In particular, we have viewed M-modes as elemental variables, hypothesized that the "neural controller" acts on the M-mode subspace in order to formulate multi-M-mode synergies by their combination and to modulate the gain of each M-mode in order to stabilize the time profile of important PVs for lifting and lowering tasks. By using the UCM theory, four PVs were found to be shared between lifting and lowering tasks: ω_{flex}, v_{ρ}, z, and COP_{AP}. Hence, we found partially evidence to support the third hypothesis: M-modes were not similar between lifting and lowering tasks, however, lifting and lowering tasks were shared some common multi-M-mode synergies. Although the hypothesis cannot be confirmed, it is worth noting that there were M-modes components (PC's eigenvectors: M_1-mode, M_2-mode, M_3-mode) that were shared among treatments. It was found that for *hip* level treatments there were M-modes components that were shared similar high loadings values of muscle activation indices across subjects for both lifting and lowering tasks. In particular, there were two types of M-modes componenets with high loadings values of muscle activation indices concentrated in M_1-mode of *hip* level treatments that separate the *hip::asymmetric* to *hip::symmetric* treatments. These M-modes are the "trunk flexion/extension" M_1-mode and the "trunk flexion/extension and axial rotation" M_1-mode, respectively.

Theses findings are similar with recent studies that showed that the organization of muscles into groups in complex whole-body tasks can differ significantly across both task variations and subjects (Danna-Dos-Santos et al., 2009; Frère et al., 2012), but either with similar temporal profiles of gains at which M-modes are rectruited (Frère et al., 2012) or with gains that help stabilizing important mechanical variables like COP shifts (Danna-Dos-Santos et al., 2009)—i.e., ability to organize muscles co-variation at higher hierarchical level of motor control. Previous studies reported that by increasing task's complexity M-modes composition and dimensionality can change. These studies have suggested that as tasks go more challenging there are more M-modes to be controlled by the neural controller (Danna-Dos-Santos, Degani, and Latash, 2008). This was confirmed in many studies of human standing: during voluntary body sway, where the body is modelled as a single inverted pendulum, M-modes were robust across subjects stabilizing COP shifts (Danna-Dos-Santos et al., 2007; Klous, Santos, and Latash, 2010), however, when trunk or arm segments accelerations were involved during body sway, M-modes were no more robust accross subjects or trials, but

there were still stibilizing COP shifts by formulating multi-M-mode synergies (Danna-Dos-Santos, Degani, and Latash, 2008; Danna-Dos-Santos et al., 2009). Therefore, we viewed the lack of consistent sets of M-modes as something to be expected.

It is worth noting that the levels of the NIOSH factors that have been used to the factorial experimental design covered a wide range of different lifting and lowering tasks with different risk each. The fact that the levels of the factors affect the multi-M-mode synergy of the related trunk-to-pelvis 3D kinematics angles (i.e., synergy index of θ_{flex} is higher in symmetric as compared to asymmetric lowering and lifting tasks, θ_{tilt} is higher in asymmetric as compared to symmetric lowering tasks, θ_{axial} is higher in symmetric as compared to asymmetric lifting tasks) gives support that the biomechanical rationalization of lifting or lowering objects at work has to take into account the abundance of the DOF at the neuromotor level and lifting tasks have to be treated as a motor control problem since there are M-modes stabilizing trunk-to-pelvis rotations in symmetric tasks, which means that subjects cannot "freeze" intentionally some DOF to constraint movement only in the sagittal plane even though they have been instructed to do so. The differences of the direction and magnitude of GRFs and COP time profile trajectories of the subjects measured by the two force platforms during the symmetric tasks provide evidence that lifting and lowering tasks cannot be considered symmetric. Finally, this was interpreted that motor coordination strategies that subjects were used to solve lifting and lowering motor task problem are based on similar multi-M-mode synergies build with dissimilar M-modes.

The fourth hypothesis was confirmed. M-modes form multi-M-mode synergies stabilizing COP_{AP} simultaneously with trunks' and boxs' PVs. However, synergy indices were not comparable neither across lifting and lowering phases (*Lift, Pull, Push, Deposit*) or across conditions (VD, HD, AM, LD); there was modulation of these indices over lifting and lowering task cycle. In lifting tasks, there was a drop of synergy index mainly after *Lift* phase of the lifting cycle. However, for lowering tasks, there was a drop of synergy indices after the *Lift* phase that was recovered at the *Deposit* phase. Overall, it was found that subjects were used multi-M-mode synergies to stabilize different PVs. For the lifting tasks, synergy indices were significant higher at the beggining of the lifting cycle (*Lift* and partly in *Pull* phases), whereas for the lowering cycle synergy indices were significant higher at the beggining and at the end of the lowering cycle (*Lift* and *Deposit* phases). These results provide support that during lifting and lowering tasks different functions of the the same muscle or muscle group could be required simultaneously in order to stabilize different performance variables related with different control aspects.

Moreover, the study provide support that by manipulating ergonomics stressors related variables – for example the variables that are manipulated during an ergonomic intervention according with the multiplicative models based on the NIOSH lifting equation (EN 1005-2, 2009; Grieco et al., 1997; Hidalgo et al., 1997; ISO 11228-1, 2003; Shoaf et al., 1997; Waters et al., 1993) – trunk M-modes and trunk multi-M-mode synergies were also influenced, which was interpreted as an indication that motor control quality was also influenced. Previous studies postulated that in addition to minimize biomechanical risk factors redundancy in the musculoskeletal system enables the "neural controller" to minimize the influence of external or internal perturbations in lifting or lowering tasks. These studies showed that certain combinations of postural perturbations and

voluntary movements during lifting tasks could require different functions of the same muscle or muscle group simultaneously. If muscle activations patterns that underlying the switching from one task demand to the other are different, this could create a disruption of the ongoing task, and such conflict may lead to motor errors, increasing postural instability and subsequent risk for development of LBD (Ebenbichler et al., 2001; Kollmitzer et al., 2002; Oddsson et al., 1999). Oddsson et al., 1999, postulated that when the hip strategy of the postural control mechanism get into action to correct exogenous postural perturbations during the lift of a load, there is a motor control conflict where different function of the same muscle is required (erector spinae). Therefore, the erector spinae muscle is activated eccentrically after a silence period of postural correction, and the concurrent risk to suffer an acute soft tissue injury is extremely high. Therefore, a general objective of this study was to collect kinematic, stabilometric and EMG data during lifting and lowering tasks and to identify from these data locomotor modules at the neuromuscular level that could help to identify PVs that are controlled by the same M-modes.

Although our study do not provide specific evidence of an underlying injury mechanism related to the motor control of specific PVs, it provides support for a high injury likelihood during the lifting or lowering phases when the underlying control mechanism associated with the trunk muscle activation patterns prioritize the control of different behaviors simultaneously. For example, during the *Lift* phase of the lifting cycle where the COP_{AP}, the θ_{flex} and the a_{ρ} are stabilized by trunk multi-M-mode synergies, the synergy index is high in *asymmetric* tasks when the load is lifted from a position *near* to the body, indicating that a muscle or muscle-group may acts simultaneously to accomplish different tasks. Therefore, the results provide evidence that the incorporation of motor control synergy indices to the ergonomic evaluation of lifting and lowering tasks could reflect better the risk to develop WRLBD. In this sense, *physical neuroergonomics*, although a perceptual-motor branch, may provide the framework to introduce motor control aspects into ergonomics or human factors field.

5.3. Methodological Considerations

When the "neural controller" generates a voluntary movement many muscles are simultaneously activated. Scientific literature agrees that the "neural controller" does not control individually every muscle, rather, it organizes groups of muscles and modulates the activity of the muscles within each group either temporally or spatially by a less number of central variables (Bizzi and Cheung, 2013; Giszter, 2009; Latash, 2008b). These neural coordinative structures have been called muscle synergies or M-modes. Different matrix factorization algorithms have been used to extract the M-modes from the recorded EMG data (Tresch, Cheung, and d'Avella, 2006). An important difference among the algorithms is that in order to perform the UCM analysis the M-modes should be extracted as a set of *orthogonal* vectors in the space of muscle activations. However, not all of the factorization algorithms extract orthogonal factors.

EFA is a statistical multivariate analysis technique that is used to reduce the dimensionality of a dataset of correlated variables by extracting *orthogonal* factors using PCA. Other matrix factorization algorithms like the commonly used non-negative matrix factorization extracts non-

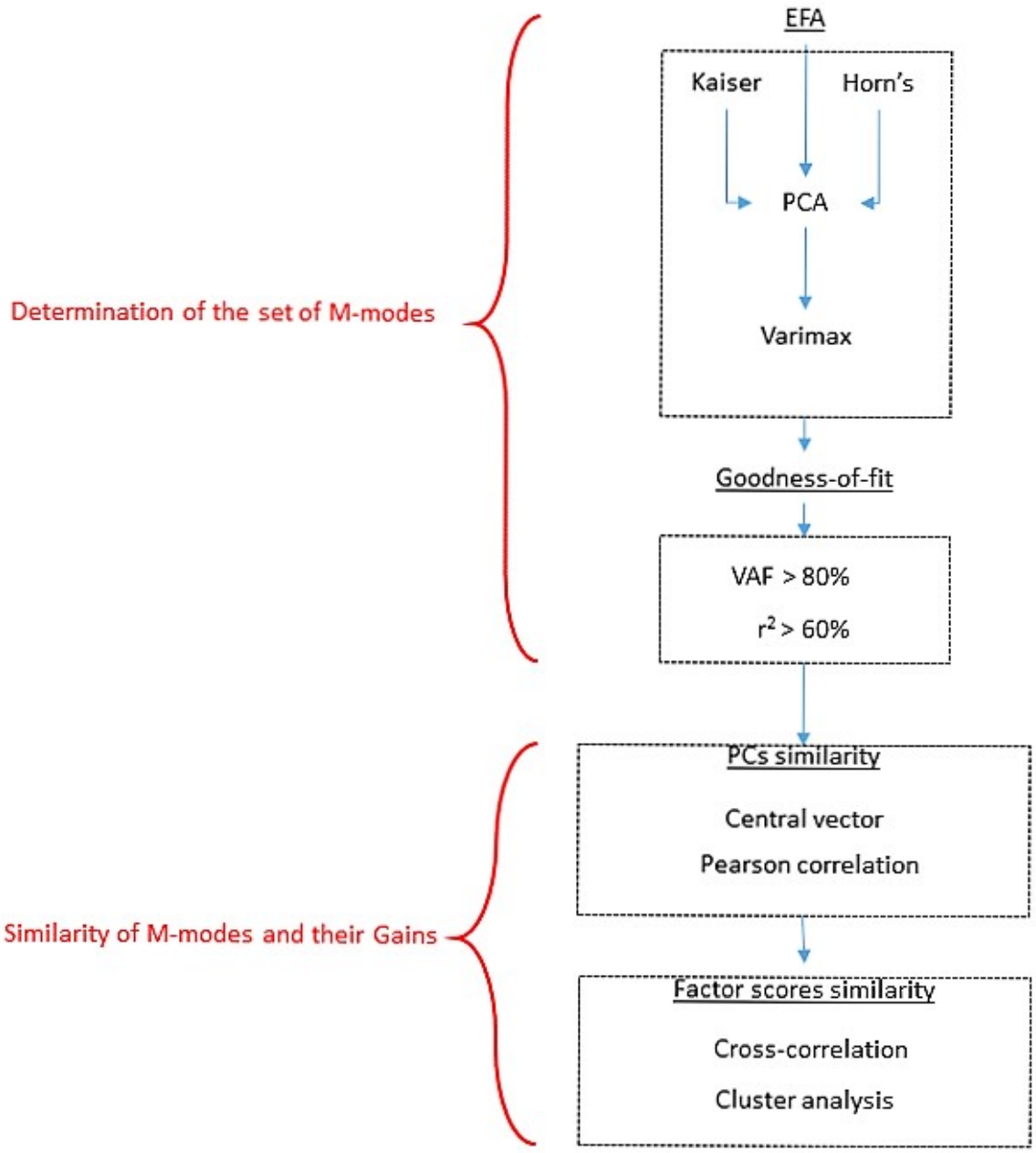

Figure 5.1 Diagram of the procedure used to determine the set of M-modes and their robustness.

orthogonal factors (Ting and Chvatal, 2011) making the computation of the V_{UCM} and V_{ORT} of the UCM procedure impossible since Pythagorean theorem is not valid for non-orthogonal subspaces. Figure 3.4 illustrates how M-modes are related with EFA's output: a multi-muscle activation is represented as a linear combination of the neural gain by each M-modes components magnitude, where the "neural controller" manipulates only three central variables to control 10 different muscles. The dataset was consisted of $m = 10$ EMG time series. The objective was to find n latent common factors ($n \ll m$) that account for as much variance as possible in the observed dataset. EFA does not made any restriction *a priori* about the number of common factors required to represent the data set or which measured variable is related to which latent common factor. Therefore, every variable was linked with the latent common factors.

Either a correlation matrix or a covariance matrix can be used for factor extraction. The correlation between two signals can be obtained by dividing their covariance by the product of their standard deviations. Therefore, a correlation matrix is a "normalized" covariance matrix. If it is known that the studied muscles contribute equally to the tasks the covariance matrix can be used. When muscles contribution is not equal, by using the covariance matrix the variance picture is distored. Therefore, we opted to use the correlation matrix between the dataset of the EMG variables for factor extraction. By using the correlation matrix the PCs have been influenced only by the temporal relationship between the dataset EMG time series. Once the correlation matrix has been estimated, the Horn's Parallel Analysis (PA) (Horn, 1965) and Kaiser's criterion (K1) (Kaiser, 1960) have been used to ensure the robustness of the number of the factors that were retained. Contrary to the *ad-hoc* criterion of VAF or that of r^2 for assessing the number of PCs, the PA and K1 retention criteria offer an automated procedure to select the minimum number of PCs. Other studies were used visual inspection of scree plots ensuring that each muscle was significantly loaded on at least one PC. Retention criteria can be used to retain factors, while VAF and r^2 can be used to assess the adequency of retention factors. The retained PCs were rotated using Varimax procedure to ensure orthogonality.

6

Conclusion

It was found that motor coordination strategies during lifting and lowering tasks are based on similar -M-mode synergies based on dissimilar M-modes. NIOSH factors as well lifting and lowering cycle phases influence motor coordination strategies. These findings have implications in the risk assessment evaluation with multiplicative NIOSH based ergonomics tools. It is suggested the reorganization of NIOSH lifting equation by incorporating a motor control index.

Bibliography

3DSSPP (2012). *3D Static Strength Prediction Program Version 6.0.6. User's Manual*. The University of Michigan, Center for Ergonomics.

Adams MA and Roughley PJ (2006). What is intervertebral disc degeneration, and what causes it? *Spine* **31**(18), pp. 2151–2161.

Alessandro C, Delis I, Nori F, Panzeri S, and Berret B (2013). Muscle synergies in neuroscience and robotics: from input-space to task-space perspectives. *Front Comput Neurosci* **7**.

ANSI (2007). *Reduction of Musculoskeletal Problems in Construction*. American National Standard. (Reference no. ANS A10.40, 2007). Washington.

Arjmand N, Shirazi-Adl A, and Parnianpour M (2008). Trunk biomechanics during maximum isometric axial torque exertions in upright standing. *Clin Biomech* **23**(8), pp. 969 –978.

Armstrong TJ, Buckle P, Fine LJ, Hagberg M, Jonsson B, Kilbom A, Kuorinka IA, Silverstein BA, Sjogaard G, and Viikari-Juntura ER (1993). A conceptual model for work-related neck and upper-limb musculoskeltal disorders. *Scand J Work Environ Health* **19**, pp. 73–84.

Aruin AS and Bernstein NA (2002). The biomechanical foundations of a safe labor environment: Bernstein's vision in 1930. *Motor Control* **6**(1), pp. 3–18.

Asaka T, Wang Y, Fukushima J, and Latash ML (2008). Learning effects on muscle modes and multi-mode postural synergies. *Exp Brain Res* **184**(3), pp. 323–338.

Ayoub M and Woldstad J (1999). «Models in manual material handling». In: *Biomechanics in Ergonomics*. Ed. by K Shrawan. Taylor and Francis. Chap. 15, pp. 267–305.

Balagué F, Mannion AF, Pellisé F, and Cedraschi C (2007). Clinical update: low back pain. *The Lancet* **369**(9563), pp. 726–728.

– (2012). Non-specific low back pain. *The Lancet* **379**(9814), pp. 482–491.

Barbe MF and Barr AE (2006). Inflammation and the pathophysiology of work-related musculoskeletal disorders. *Brain Behav Immun* **20**(5), pp. 423–429.

Barr AE and Barbe MF (2004). Inflammation reduces physiological tissue tolerance in the development of work-related musculoskeletal disorders. *J Electromyogr Kinesiol* **14**(1), pp. 77–85.

Bartlett R (2007). *Introduction to Sports Biomechanics: Analysing Human Movement Patterns*. 2nd Edition. Routledge, Taylor and Francis Group.

Bartlett R, Wheat J, and Robins M (2007). Is movement variability important for sports biomechanists? *Sports Biomech* **6**(2), pp. 224–243.

Basmajian JV and De Luca CJ (1985). *Muscles Alive, their Functions Revelead by Electromyography*. Ed. by J Butler. 5th. Williams & Wilkins.

Beaudette SM, Graham RB, and Brown SH (2014). The effect of unstable loading versus unstable support conditions on spine rotational stiffness and spine stability during repetitive lifting. *J Biomech* **47**(2), pp. 491–496.

Bell A, Pederson D, and Brand R (1989). Prediction of hip joint center location from external landmarks. *Hum Mov Sci* **8**, pp. 3–16.

– (1990). A Comparison of the Accuracy of Several hip Center Location Prediction Methods. *J Biomech* **23**, pp. 617–621.

Benjumea AC (2001). Datos antropométricos de la población laboral española. *Prevención, trabajo y salud* (14), pp. 22–30.

Bergmark A (1989). Stability of the lumbar spine. A study in mechanical engineering. *Acta Orthop Scand Suppl* **230**, pp. 1–54.

Berkinblit M, Feldman A, and Fukson O (1986). Adaptability of innate motor patterns and motor control mechanisms. *Behav Brain Sci* **9**(04), pp. 585–599.

Bernstein NA (1930). Contemporary biomechanics and problems of labor safety. *Hygiene, Safety and Pathology of Labor* **2**, pp. 3–12.

– (1967). *The co-ordination and regulation of movements*. Pergamon Press Ltd., xii, 196 p.

– (1984). «Biodynamics of Locomotion». In: *Human Motor Actions. Bernstein Reassessed*. Ed. by HTA Whiting. Vol. 17. North-Holland. Chap. III, pp. 171–222.

– (1996). «On Dexterity and its Development (Translated by Mark L. Latash)». In: *Dexterity and Its Development Resources for Ecological Psychology*. Ed. by ML Latash and MT Turvey. Lawrence Erlbaum Associates, Inc. Chap. Essay 2: On Motor Control, pp. 25–45.

Bevan S, Quadrello T, McGee R, Mahdon M, Vavrovsky A, and Barham L (2007). *Fit For Work? Musculoskeletal Disorders in the European Workforce*. Tech. rep. London, UK: The Work Foundation.

Bizzi E and Cheung VCK (2013). The neural origin of muscle synergies. *Front Comput Neurosci* **7**, p. 51.

Bizzo G, Ouaknine M, and Gagey PM (2003). *Project of calibration of a stabilometry platform*. Assocation pour le developpement et l'application de la posturologie (ADAP). URL: pierremarie.gagey.perso.sfr.fr/RecetteProtocole-a.htm.

Bloswick D and Hinckley D (2004). «Job Accommodation». In: *Muscle Strength*. Ed. by S Kumar. CRC Press, Boca Raton, FL. Chap. 19, pp. 469–483.

Bobbert MF and Schamhardt HC (1990). Accuracy of determining the point of force application with piezoelectric force plates. *J Biomech* **23**(7), pp. 705–710.

Bogduk N (2005). *Clinical anatomy of the lumbar spine and sacrum*. 4th Edition. Vol. 128. Philadelphia, Pa: Churchill Livingstone.

Bonato P, Boissy P, Croce HD, and Roy SH (2001). Changes in the surface EMG signal and the biomechanics of motion during a repetitive lifting task. *IEEE Trans Neural Syst Rehabil Eng* **10**(1), pp. 38–47.

Boocock MG, Collier JMK, McNair PJ, Simmonds M, Larmer PJ, and Armstrong B (2009). A Framework for the Classification and Diagnosis of Work-Related Upper Extremity Conditions: Systematic Review. *Semin Arthitis Rheum* **38**, pp. 296–311.

Browne J and O'Hare N (2000). A quality control procedure for force platforms. *Physiol Meas* **21**, pp. 515–524.

Buckle P and Devereux J (1999). *Work Related Neck and Upper Limb Musculoskeletal Disorders*. Technical Report 92-828-8174-1. Bilbao: European Agency for Safety and Health at Work.

Burdet E, Franklin DW, and Milner TE (2013). *Human robotics: neuromechanics and motor control*. Cambridge, Massachusetts: MIT Press.

Burdick RK, Borror CM, and Montgomery DC (2005). *Design and analysis of gauge R&R studies: Making decisions with confidence intervals in random and mixed ANOVA models*. Vol. 17. SIAM.

Burgess-Limerick R (2003). Squat, stoop, or something in between? *Int J Ind Ergon* **31**, pp. 143–148.

Burgess-Limerick R and Abernethy B (1997). Toward a quantitative definition of manual lifting postures. *Human Factors: The Journal of the Human Factors and Ergonomics Society* **39**(1), pp. 141–148.

Burgess-Limerick R, Abernethy B, and Neal RJ (1991). «A natural-physical approach to understanding lifting». In: *Ergonomics and human environment proceedings of 27th Conference of the Ergonomics Confederation of Australia*. Ed. by V Popovic and M Walker. Queensland, Coolum: Ergonomics Society of Australia Inc., pp. 295–302.

– (1993). Relative phase quantifies interjoint coordination. *J Biomech* **26**(1), pp. 91–94.

– (1995). Self-selected manual lifting technique: functional consequencees of the interjoint coordination. *Hum Factors* **37**, pp. 395–411.

Burgess-Limerick R, Shemmell J, Barry BK, Carson RG, and Abernethy B (2001). Spontaneous transitions in the coordination of a whole body task. *Hum Mov Sci* **20**, pp. 549–562.

Burton AK (2005). How to prevent low back pain. *Best Practice & Research Clinical Rheumatology* **19**(4). doi: DOI: 10.1016/j.berh.2005.03.001, pp. 541–555.

Burton AK, Balagué F, Cardon G, Eriksen HR, Henrotin Y, Lahad A, Leclerc A, Müller G, and Van Der Beek AJ (2006). Chapter 2 European guidelines for prevention in low back pain. *Eur Spine J* **15**, s136–s168.

Butler D, Andersson G, Trafimow J, Schipplein O, and Andriacchi T (1993). The influence of load knowledge on lifting technique. *Ergonomics* **36**(12), pp. 1489–1493.

Calvo F (1992). *Estadistica aplicada*. 2a Edición. Bilbao: Ediciones Deusto, S.A.

Chaffin DB (1997). Development of computerized human static strength simulation model for job design. *Hum. Factors Man.* **7**(4), pp. 305–322.

– (2009). The evolving role of biomechanics in prevention of overexertion injuries. *Ergonomics* **52**(1), pp. 3–14.

Chaffin DB, Andersson GBJ, and Martin BJ (2006). *Occupational biomechanics*. 4th Edition. Hoboken, New Jersey: John Wiley & Sons, Ltd.

Challis JH (2008). «Data processing and error estimation». In: *Biomechanical evaluation of movement in sport and exercise: the British Association of Sport and Exercise Sciences guidelines*. Ed. by CJ Payton and RM Barlett. Taylor & Francis. Chap. 7, pp. 129–152.

Chiari L, Della Croce U, Leardini A, and Cappozzo A (2005). Human movement analysis using stereophotogrammetry. Part 2: instrumental errors. *Gait Posture* **21**(2), pp. 197–211.

Cholewicki J and McGill SM (1996). Mechanical stability of the in vivo lumbar spine: implications for injury and chronic low back pain. *Clin Biomech* **11**(1), pp. 1 –15.

Cholewicki J, Panjabi MM, and Khachatryan A (1997). Stabilizing function of trunk flexor-extensor muscles around a neutral spine posture. *Spine* **22**(19), pp. 2207–12.

Chvatal SA, Torres-Oviedo G, Safavynia SA, and Ting LH (2011). Common muscle synergies for control of center of mass and force in nonstepping and stepping postural behaviors. *J Neurophysiol* **106**, pp. 999–1015.

Cohen AL, Gjessing CC, Fines LJ, Bernand BP, and McGlothlin JD (1997). *Elements of ergonomics programs. A primer based on workplace evaluations of musculoskeletal disorders*. DHHS (NIOSH) publication. [Atlanta, Ga.] Cincinnati, OH [Springfield, Va.]: U.S. Dept. of Health et al.

Commissaris DACM and Toussaint HM (1997). Load knowledge affects low-back loading and control of balance in lifting tasks. *Ergonomics* **40**(5), pp. 559–575.

Cram JR (2011). *Cram's Introduction to Surface Electromyography*. Ed. by E Criswell. 2nd Edition. Sudbury, MA: Jones and Bartlett Publishers, LLC.

Cresswell AG, Oddsson L, and Thorstensson A (1994). The influence of sudden perturbations on trunk muscle activity and intra-abdominal pressure while standing. *Exp Brain Res* **98**(2), pp. 336–341.

Crisco JJ and Panjabi MM (1992). Euler stability of the human ligamentous lumbar spine. Part I: Theory. *Clin Biomech* **7**(1), pp. 19–26.

Crisco JJ, Panjabi MM, Yamamoto I, and Oxland TR (1992). Euler stability of the human ligamentous lumbar spine. Part II: Experiment. *Clin Biomech* **7**(1), pp. 27–32.

Cutlip RG, Baker BA, Hollander M, and Ensey J (2009). Injury and adaptive mechanisms in skeletal muscle. *J Electromyogr Kinesiol* **19**(3), pp. 358–372.

Dagenais S, Roffey DM, Bishop PB, Wai EK, and Kwon BK (2012). Response to: Low back pain: doesn't work matter at all? *Occup Med* **62**(2), pp. 153–154.

Danna-Dos-Santos A, Slomka K, Zatsiorsky VM, and Latash ML (2007). Muscle modes and synergies during voluntary body sway. *Exp Brain Res* **179**(4), pp. 533–550.

Danna-Dos-Santos A, Degani AM, and Latash ML (2008). Flexible muscle modes and synergies in challenging whole-body tasks. *Exp Brain Res* **189**(2), pp. 171–187.

Danna-Dos-Santos A, Shapkova EY, Shapkova AL, Degani AM, and Latash ML (2009). Postural control during upper body locomotor-like movements: similar synergies based on dissimilar muscle modes. *Exp Brain Res* **193**(4), pp. 565–579.

De Looze M, Boeken-Kruger M, Steenhuizen S, Baten C, Kingma I, and Van Dieën J (2000). Trunk muscle activation and low back loading in lifting in the absence of load knowledge. *Ergonomics* **43**(3), pp. 333–344.

De Luca CJ (1997). The use of surface electromyography in biomechanics. *J Appl Biomech* **13**, pp. 135–163.

De Luca CJ, Gilmore LD, Kuznetsov M, and Roy SH (2010). Filtering the surface EMG signal: Movement artifact and baseline noise contamination. *J Biomech* **43**, pp. 1573–1579.

De Rosario-Martinez H (2015). *phia: Post-Hoc Interaction Analysis*. R package version 0.2-0.

Degallier S and Ijspeert A (2010). Modeling discrete and rhythmic movements through motor primitives: a review. *Biol Cybern* **103**, pp. 319–338.

Delleman NJ (2004). «Motor Behavior». In: *Working Postures and Movements. Tools for Evaluation and Engineering*. Ed. by NJ Delleman, CM Haslegrave, and DB Chaffin. CRC Press. Chap. 3, pp. 51–71.

Dempsey PG and Mathiassen SE (2006). On the evolution of task-based analysis of manual materials handling, and its applicability in contemporary ergonomics. *Appl Ergon* **37**(1), pp. 33–43.

Devleesschauwer B, Havelaar AH, Noordhout C Maertens de, Haagsma JA, Praet N, Dorny P, Duchateau L, Torgerson PR, Van Oyen H, Speybroeck N, et al. (2014). DALY calculation in practice: a stepwise approach. *Int J Public Health* **59**(3), pp. 571–574.

Ebenbichler GR, Oddsson LIE, Kollmitzer J, and Erim Z (2001). Sensory -motor control of the lower back: implications for rehabilitation. *Med Sci Sports Exerc* **33**(11), pp. 1889–1898.

EC Directive 90/629 (1990). Minimun health and safety requirements for the manual handling of loads where the is a risk particularly of ack injury to workers. *Official Journal of the European Communities* **156**(621-90), pp. 9–13.

EN 1005-2 (2009). *Safety of machinery – Human physical performance – Part 2: Manual handling of machinery and component parts of machinery*. British Standard BS EN 1005-2:2003+A1:2008. (Reference no. BS EN 1005-2:2003+A1:2008). London: British Standards Institution (BSI).

Erer KS (2007). Adaptive usage of the Butterworth digital filter. *J Biomech* **40**(13), pp. 2934–2943.

EU-OSHA (2000). *Inventory of socio-economic information about work-related musculoskeletal disorders in the Member States of the European Union*. Technical Report. Luxembourg: European Agency for Safety and Health at Work (EU-OSHA).

Everitt BS (2005). *An R and S-PLUS companion to multivariate analysis*. Ed. by G Casella, S Fienberg, and I Olkin. Springer texts in statistics. London: Springer-Verlag.

Flach P (2012). *Machine Learning: The Art and Science of Algorithms that Make Sense of Data*. New York: Cambridge University Press.

Forde MS, Punnett L, and Wegnar DH (2002). Pathomechanisms of work-related musculoskeletal disorders: conceptual issues. *Ergonomics* **45**(9), pp. 619–630.

Franco G (1999). Ramazinni and worker's health. *The Lancet* **354**, pp. 858–861.

Frère J, Göpfert B, Hug F, Slawinski J, and Tourny-Chollet C (2012). Catapult effect in pole vaulting: Is muscle coordination determinant? *J Electromyogr Kinesiol* **22**(1), pp. 145–152.

Fuchs A and Kelso JAS (1994). A theoretical note on models of interlimb coordination. *J Exp Psychol Hum Percept Perform* **20**(5), pp. 1088–1097.

Furnée EH (1989a). «Advances in TV/computer motion monitoring». In: *Conf Proc IEEE Eng Med Biol Soc*. IEEE, pp. 1053–1054.

– (1989b). «TV/Computer motion analysis systems. The first two decades». PhD thesis. Delf University of Technology.

Gagnon M (2005). Ergonomic identification and biomecanical evaluation of workers' strategies and their validation in a training situation: summary of research. *Clin Biomech* **20**, pp. 569–580.

Gallagher S and Marras WS (2012). Tolerance of the lumbar spine to shear: A review and recommended exposure limits. *Clin Biomech* **27**(10), pp. 973–978.

Gelfand IM and Latash ML (1998). On the problem of adequate language in movement science. *Motor Control* **2**, pp. 306–313.

Gelfand IM and Tsetlin ML (1962). Some methods of control for complex systems. *Russ. Math. Surv.* **17**(95), pp. 95–117.

– (1971). «On mathematical modeling of the mechanisms of the central nervous system». In: *Models of the structural-functional organization of certain biological systems*. Ed. by IM Gelfand, VS Gurfinkel, SV Fomin, and ML Tsetlin. Cambridge, MA: MIT Press. Chap. 1, pp. 1–22.

Gelfand IM, Gurfinkel VS, Tsetlin ML, and Shink ML (1971). «Some problems of the analysis of movements». In: *Models of the structural-functional organization of certain biological systems*. Ed. by IM Gelfand, VS Gurfinkel, SV Fomin, and ML Tsetlin. Cambridge, MA: MIT Press. Chap. 9, pp. 329–345.

Georgakis A, Stergioulas LK, and Giakas G (2002). Wigner filtering with smooth roll-off boundary for differentiation of noisy non-stationary signals. *Signal Process* **82**, pp. 1411–1415.

Giaccone M (2007). *Managing musculoskeletal disorders*. Report TN0611018S. Dublin, Ireland: European Foundation for the Improvement of Living and Working Conditions.

Giakas G, Stergioulas LK, and Vourdas A (2000). Time-frequency analysis and filtering of kinematic signals with impacts using the Wigner function: accurate estimation of the second derivative. *J Biomech* **33**, pp. 567–574.

Giakas G (2004). «Power spectrum analysis and filtering». In: *Innovative analyses of human movement*. Ed. by N Stergiou. Champaign, IL: Human Kinetics. Chap. 9, pp. 223–258.

Gianikellis K, Gálvez A, Bote A, and Moreno A (2008). Relevancia del problema de control motor y reconsideración del protocolo NIOSH en las tareas con manipulación manual de cargas. *Biomecca* **14**(2), pp. 64–71.

Gibson JJ (2014). *The Ecological Approach to Visual Perception: Classic Edition*. Psychology Press.

Gill H and O'Connor J (1997). A new testing rig for force platform calibration and accuracy tests. *Gait Posture* **5**, pp. 228–232.

Giszter SF (2009). «Motor Primitives». In: *Encyclopedia of Neuroscience*. Ed. by LR Squire. Elsevier Academic Press. Chap. 18 (M), pp. 1023–1040.

Gottlieb G, Chen C, and Corcos D (1995). Relations between joint torque, motion, and electromyographic patterns at the human elbow. *Exp Brain Res* **103**(1), pp. 164–167.

Graham RB and Brown SH (2012). A direct comparison of spine rotational stiffness and dynamic spine stability during repetitive lifting tasks. *J Biomech* **45**(9), pp. 1593–1600.

Graham RB, Sadler EM, and Stevenson JM (2012). Local dynamic stability of trunk movements during the repetitive lifting of loads. *Hum Mov Sci* **31**(3), pp. 592–603.

Graham RB, Costigan PA, Sadler EM, and Stevenson JM (2011). Local dynamic stability of the lifting kinematic chain. *Gait Posture* **34**(4), pp. 561–563.

Granat MH, Kirkwood CA, and Andrews BJ (1990). Problem with the use of total distance travelled and average speed as measures of postural sway. *Med Biol Eng Comput* **28**(6), pp. 601–602.

Granata KP, Marras WS, and Davis KG (1999). Variation in spinal load and trunk dynamics during repeated lifting exertions. *Clin Biomech* **14**(6), pp. 367–375.

Grenier SG and McGill SM (2007). Quantification of lumbar stability by using 2 different abdominal activation strategies. *Arch Phys Med Rehabil* **88**(1), pp. 54–62.

Grieco A, Occhipinti E, Colombini D, and Molteni G (1997). Manual handling of loads: the point of view of experts involved in the application of EC Directive 90/269. *Ergonomics* **40**(10), pp. 1035–1056.

Grood ES and Suntay WJ (1983). A joint coordinate system for the clinical description of three-dimensional motions: application to the knee. *J Biomech Eng* **105**(2), pp. 136–44.

Grosse SD, Lollar DJ, Campbell VA, and Chamie M (2009). Disability and disability-adjusted life years: not the same. *Public Health Rep* **124**(2), p. 197.

Gruen A (1997). Fundamentals of videogrammetry?A review. *Hum Mov Sci* **16**(2), pp. 155–187.

Hagberg M, Silverstein BA, Wells RV, Smith MJ, Hendrick HW, Carayon P, and Pérusse M (1995). *Work Related Musculoskeletal Disorders: A reference book for prevention*. Ed. by I Kuorinka and L Forcier. London: Taylor and Francis.

Hagg GM (2000). Human muscle fibre abnormalities related to occupational load. *Eur J Appl Physiol* **83**(2-3), pp. 159–165.

Haken H (1977). *Synergetics. An Introduction*. Berlin: Springer-Verlag.

– (1999). *Information and Self-Organization. A Macroscopic Approach to Complex Systems*. 2nd. Springer.

Haken H, Kelso JAS, and Bunz H (1985). A theoretical model of phase transitions in human hand movements. *Biol Cybern* **51**, pp. 347–356.

Hamill J, Palmer C, and Emmerik REAV (2012). Coordinative variability and overuse Injury. *Sports Medicine, Arthroscopy, Rehabilitation, Therapy and Technology* **4**, p. 45.

Hamrick C (2006). «Overview of ergonomic assessment». In: *The Occupational Ergonomics Handbook. Fundamentals and Assessment Tools for Occupational Ergonomics.* Ed. by WS Marras and W Karwowski. 2nd. Boca Raton, Florida: CRC Press, Taylor and Francis Group. Chap. 34, pp. 34/1–17.

Hebb D (2002). *The Organization of Behavior: A Neuropsychological Theory*. Psychology Press.

Hedrick TL (2008). Software techniques for two-and three-dimensional kinematic measurements of biological and biomimetic systems. *Bioinspiration & biomimetics* **3**(3), 034001 (6pp).

Henneman E, Somjen G, and Carpenter DO (1965). Excitability and inhibitability of motoneurons of different sizes. *J Neurophysiol* **28**(3), pp. 599–620.

Hidalgo J, Genaidy A, Karwowski W, Christensen D, Huston R, and Stambough J (1997). A comprehensive lifting model: beyond the NIOSH lifting equation. *Ergonomics* **40**(9), pp. 916–927.

Hodges P (2004). «Lumbopelvic stability: a functional model of the biomechanics and motor control». In: *Therapeutic Exercise for Lumbopelvic Stabilization. A Motor Control Approach for the Treatment and Prevention of Low Back Pain.* Ed. by C Richardson, P Hodges, and J Hides. 2nd Edition. Churchill Livingstone. Chap. 2, pp. 13–28.

Hof AL (2009). A simple method to remove ECG artifacts from trunk muscle EMG signals. *J Electromyogr Kinesiol* (19), e554–e555.

Hogan N and Sternad D (2007). On rhythmic and discrete movements: reflections, definitions and implications for motor control. *Exp Brain Res* **181**, pp. 13–30.

Horn JL (1965). A rationale and test for the number of factors in factor analysis. *Psychometrika* **30**, pp. 179–185.

Houk J and Henneman E (1967). Feedback control of skeletal muscles. *Brain Res* **5**, pp. 433–451.

Hoy D, March L, Brooks P, Woolf A, Blyth F, Vos T, and Buchbinder R (2010). Measuring the global burden of low back pain. *Best Practice & Research Clinical Rheumatology* **24**(2), pp. 155–165.

Hoy D, Bain C, Williams G, March L, Brooks P, Blyth F, Woolf A, Vos T, and Buchbinder R (2012). A systematic review of the global prevalence of low back pain. *Arthritis Rheum* **64**(6), pp. 2028–2037.

Hunt A (1998). *Guide to the Measurement of Force*. Tech. rep. London: The Institute of Measurement and Control.

Iberall AS (1977). A field and circuit thermodynamics for integrative physiology. I. Introduction to the general notions. *Am J Physiol Regul Integr Comp Physiol* **233**(5), R171–R180.

Institute for Health Metrics and Evaluation (2013a). *The Global Burden of Disease*. IHME. URL: www.healthmetricsandevaluation.org.

– (2013b). *The Global Burden of Disease: Generating Evidence, Guiding Policy*. Tech. rep. Seattle, WA: IHME.

ISO-JCGM 100 (2010). E*valuation of measurement data - Guide to the expression of uncertainty in measurement*. (JCGM 100:2008). JCGP Organizations (BIPM, IEC, IFCC, ILAC, ISO, IUPAC, IUPAP, OIML).

ISO-JCGM 200 (2008). I*nternational vocabulary of metrology – Basic and general concepts and associated terms (*VIM*)*. (JCGM 200:2008). JCGM Organizations (BIPM, IEC, IFCC, ILAC, ISO, IUPAC, IUPAP, OIML).

ISO 11228-1 (2003). *Ergonomics - Manual handling - Part 1: Lifting and carrying*. Tech. rep. International Standard Organization (ISO).

Ivanenko YP, Poppele RE, and Lacquaniti F (2004). Five basic muscle activation patterns account for muscle activity during human locomotion. *J Physiol* **556**(Pt 1), pp. 267–282.

Jarus T and Ratzon NZ (2005). The implementation of motor learning principles in designing prevention programs at work. *Work* **24**(2), pp. 171–182.

Jinha A, Rachid A, and Herzog W (2006). Predictions of co-contraction depend critically on degrees-of-freedom in the musculoskeletal model. *J Biomech* **39**(6), pp. 1145–1152.

Jones T and Kumar S (2004). «Physical demands analysis: a critique of current tools». In: *Muscle Strength*. Ed. by S Kumar. CRC Press, Boca Raton, FL. Chap. 19, pp. 421–467.

Kaiser HF (1960). The application of electronic computers to factor analysis. *Educ Psychol Meas* **20**, pp. 141–151.

Karlsson A and Lanshammar H (1997). Analysis of postural sway strategies using an inverted pendulum model and force plate data. *Gait Posture* **5**, pp. 198–203.

Karwowski W, Sherihiy B, Siemionow W, and Gielo-Perczak K (2007). «Physical Neuroergonomics». In: *Neuroergonomics. The Brain at Work*. Ed. by R Parasuraman and M Rizzo. Human Technology Interaction. New York: Oxford University Press. Chap. 15, pp. 221–235.

Kay BA (1988). The dimensionality of movement trajectories and the degrees of freedom problem: A tutorial. *Hum Mov Sci* **7**, pp. 343–364.

Kee D and Chung MK (1996). Comparison of prediction models for the compression force on the lumbosacral disc. *Ergonomics* **39**(12), pp. 1419–1429.

Kelso JAS (1984). Phase transitions and critical behavior in human bimanual coordination. *Am J Physiol Regul Integr Comp Physiol* **246**(6), R1000–R1004.

Kelso JAS, DelColle JD, and Schöner G (1990). Action-perception as a pattern formation process. *Attention and performance XIII* **5**, pp. 139–169.

Kelso JAS and Engstrøm DA (2006). *The complementary nature*. The MIT Press.

Kelso JAS (1995). *Dynamic patterns: The self-organization of brain and behavior*. MIT press.

Keyserling WM and Chaffin DB (1986). Occupational ergonomics–Methods to evaluate physical stress on the Job. *Ann Rev Public Health* **7**, pp. 77–104.

Khanzode VV, Maiti J, and Ray P (2012). Occupational injury and accident research: A comprehensive review. *Saf Sci* **50**(5), pp. 1355–1367.

Kingma I, Faber GS, Bakker AJM, and Die?n JH van (2006). Can low back loading durin lifting be reduced by placing one leg beside the object to be lifted? *Phys Ther* **86**, pp. 1091–1105.

Klinke S and Wagner C (2008). Visualizing exploratory factor analysis models.

Klous M, Santos A Danna-dos, and Latash M (2010). Multi-muscle synergies in a dual postural task: evidence for the principle of superposition. *Exp Brain Res* **202**(2), pp. 457–471.

Kollmitzer J, Oddsson L, Ebenbichler GR, Giphart JE, and DeLuca CJ (2002). Postural control during lifting. *J Biomech* **35**, pp. 585–594.

Krishnamoorthy V, Latash ML, Scholz JP, and Zatsiorsky VM (2004). Muscle modes during shifts of the center of pressure by standing persons: effect of instability and additional support. *Exp Brain Res* **157**(1), pp. 18–31.

Krishnamoorthy V, Goodman S, Zatsiorsky VM, and Latash ML (2003). Muscle synergies during shifts of the center of pressure by standing persons: identification of muscle modes. *Biol Cybern* **89**(2), pp. 152–161.

Krismer M and Van Tulder M (2007). Low back pain (non-specific). *Best Practice and Research Clinical Rheumatology* **21**(1), pp. 77–91.

Kugler PN, Kelso JAS, and Turvey MT (1980). «On the concept of coordinativce structures as dissipative structures: I. Theoretical lines of convergence». In: *Tutorials in Motor Behavior*. Ed. by GE Stelmach and J Requin. New York: North-Holland Publishing Co., pp. 1–47.

– (1982). On the control and coordination of naturally developing systems. *The development of movement control and coordination* **5**, p. 78.

Kuijer PPF, Takala EP, Burdorf A, Gouttebarge V, Van Dieën JH, Van der Beek AJ, and Frings-Dresen MHW (2012). Low back pain: doesn't work matter at all? *Occup Med* **62**(2), pp. 152–153.

Kumar S (1999). «Selected theories of musculoskeletal injury causation». In: *Biomechanics in ergonomics*. Ed. by S Kumar. Taylor and Francis. Chap. 1, pp. 3–24.

– (2001). Theories of musculoskeletal injury causation. *Ergonomics* **44**(1), pp. 17–47.

Kutch JJ and Valero-Cuevas FJ (2012). Challenges and new approaches to proving the existence of muscle synergies of neural origin. *PLoS Comput Biol* **8**(5), e1002434.

Lancet T (1911). Injury of the spine due to muscular effort. *The Lancet* **178**(4596), pp. 958 –959.

– (2009). Is Europe fit for work? *The Lancet* **374**(9697), p. 1214.

Lanshammar H (1982a). On practical evaluation of differentiation techniques for human gait analysis. *J Biomech* **15**(2), pp. 99–105.

Lanshammar H (1982b). On precision limits for derivatives numerically calculated from noisy data. *J Biomech* **15**(6), pp. 459–470.

Lashley KS (1930). Basic neural mechanisms in behavior. *Psychol Rev* **37**(1), p. 1.

Latash ML (2010). Motor Synergies and the Equilibrium-Point Hypothesis. *Motor Control* **14**, pp. 294–322.

Latash ML, Gorniak SL, and Zatsiorsky VM (2008). Hierarchies of synergies in human movements. *Kinesiology* **40**(1), pp. 29–38.

Latash ML (2008a). *Neurophysiological basis of movement*. 2nd. Human Kinetics.

– (2008b). *Synergy*. Oxford ; New York: Oxford University Press.

– (2009). «Coordination». In: *Encyclopedia of Neuroscience*. Ed. by MD Binder, N Hirokawa, U Windhorst, and MC Hirsch. Berlin: Springer-Verlag, pp. 886–888.

Latash ML (2012). *Fundamentals of motor control*. Access Online via Elsevier.

Latash ML, Scholz JP, and Schöner G (2002). Motor control strategies revealed in the structure of motor variability. *Exerc Sport Sci Rev* **30**(1), pp. 26–31.

Latash ML, Scholz JP, and Schoner G (2007). Toward a new theory of motor synergies. *Motor Control* **11**(3), pp. 276–308.

Latash ML, Krishnamoorthy V, Scholz JP, and Zatsiorsky VM (2005). Postural synergies and their development. *Neural Plast* **12**(2-3), 119–30; discussion 263–72.

Lavender SA (2006). «Training Lifting Techniques». In: *The Occupational Ergonomics Handbook*. Ed. by WS Marras and W Karwowski. 2nd Edition. Taylor and Francis. Chap. 23, pp. 1–14.

Lavender SA, Li YC, Andersson GBJ, and Natarajan RN (1999). The effects of lifting speed on the peak external forward bending, lateral bending, and twisting spinae moments. *Ergonomics* **42**, pp. 111–125.

Lawrence MA (2013). *ez: Easy analysis and visualization of factorial experiments.* R package version 4.2-2.

Lawrence RC, Helmick CG, Arnett F, Deyo R, Felson D, Giannini E, Heyse S, Hirsch R, Hochberg M, Hunder G, Liang M, Pillemer S, Steen V, and Wolfe F (1998). Estimates of the prevalence of arthritis and selected musculoskeletal disorders in the United States. *Arthritis Rheum* **41**(5), pp. 778–799.

Lee J and Nussbaum MA (2013). Experienced workers may sacrifice peak torso kinematics/kinetics for enhanced balance/stability during repetitive lifting. *J Biomech* **46**(6), pp. 1211–1215.

Lees A and Lake M (2008). «Force and pressure measurements». In: *Biomechanical Evaluation of Movement in Sport and Exercise. The British Association of Sport and Exercise Sciences Guidelines*. Ed. by CJ Payton and RM Barlett. Oxon, UK: Routledge, Taylor and Francis Group. Chap. 4, pp. 53–76.

Levin O, Wenderoth N, Steyvers M, and Swinnen SP (2003). Directional invariance during loading-related modulations of muscle activity: evidence for motor equivalence. *Exp Brain Res* **148**(1), pp. 62–76.

Liu Y, Wu C, and Berman MG (2012). Computational neuroergonomics. *Neuroimage* **59**(1), pp. 109–116.

Logan M (2010). *Biostatistical design and analysis using R: a practical guide*. UK: Wiley-Blackwell.

Loo MP van der (2010). *Distribution based outlier detection for univariate data*. Tech. rep. 10003. The Hague/Heerlen: Statistics Netherlands.

Looze M de, Kingma I, Bussmann J, and Toussaint H (1992). Validation of a dynamic linked segment model to calculate joint moments in lifting. *Clin Biomech* **7**(3), pp. 161–169.

Luttmann A, Jager M, Griefahn B, and Caffier G (2003). *Preventing musculoskeletal disorders in the workplace*. Protecting Workers' Health 5. World Health Organization (WHO).

Marras WS (2000). Occupational low back disorder causation and control. *Ergonomics* **43**(7), pp. 880–902.

– (2008). *The working back: a systems View*. John Wiley & Sons, Inc.

Marras WS and Sommerich CM (1991a). A three-dimensional motion model of loads on the lumbar spine: I. Model structure. *Hum Factors* **33**(2), pp. 123–137.

– (1991b). A three-dimensional motion model of loads on the lumbar spine: II. Model validation. *Hum Factors* **33**(2), pp. 139–149.

Marras WS, Lavender SA, Leurgans SE, Rajulu SL, Allread WG, Fathallah FA, and Ferguson SA (1993). The role of dynamic three-dimensional trunk motion in occupationally-related low back disorders. The effects of workplace factors, trunk position, and trunk motion characteristics on risk of injury. *Spine (Phila Pa 1976)* **18**(5), pp. 617–628.

Marras WS, Lavender SA, Leurgans SE, Fathallah FA, Ferguson SA, Allread WG, and Rajulu SL (1995). Biomechanical risk factors for occupationally related low back disorders. *Ergonomics* **38**(2), pp. 377–410.

Marras WS, Fine LJ, Ferguson SA, and Waters TR (1999). The effectiveness of commonly used lifting assessment methods to identify industrial jobs associated with elevated risk of low-back disorders. *Ergonomics* **42**(1), pp. 229–245.

Marras WS, Allread WG, Burr DL, and Fathallah FA (2000). Prospective validation of a low-back disorder risk model and assessment of ergonomic interventions associated with manual materials handling tasks. *Ergonomics* **43**(11), pp. 1866–1886.

Marras WS, Davis KG, Ferguson SA, Lucas BR, and Gupta P (2001). Spine loading characteristics of patients with low back pain compared with asymptomatic individuals. *Spine (Phila Pa 1976)* **26**(23), pp. 2566–2574.

Marras WS, Cutlip RG, Burt SE, and Waters TR (2009). National occupational research agenda (NORA) future directions in occupational musculoskeletal disorder health research. *Appl Ergon* **40**(1), pp. 15–22.

Marras WS (2006). «Biomechanical Basis for Ergonomics». In: *The occupational ergonomics handbook. Fundamentals and assesment tools for occupational ergonomics*. Ed. by WS Marras and W Karwowski. 2nd Edition. Boca Raton, Florida: CRC Press, Taylor and Francis Group. Chap. 11, pp. 11/1–43.

Marras WS and Hamrick C (2006). «The ACGIH TLV for low back risk». In: *The Occupational Ergonomics Handbook. Fundamentals and Assessment Tools for Occupational Ergonomics*. Ed. by WS Marras and W Karwowski. 2nd Edition. Boca Raton, Florida: CRC Press, Taylor and Francis Group. Chap. 50, pp. 50/1–15.

Mathers C, Stevens G, and Mascarenhas M (2009). *Global health risks: mortality and burden of disease attributable to selected major risks*. World Health Organization.

Matthews JD, MacKinnon SN, Albert WJ, Holmes M, and Patterson A (2007). Effects of moving environments on the physical demands of heavy materials handling operators. *Int J Ind Ergon* **37**(1), pp. 43–50.

Mattos D, Kuhl J, Scholz JP, and Latash ML (2013). Motor equivalence (ME) during reaching: is ME observable at the muscle level? *Motor Control* **17**(2), pp. 145–175.

McGill SM (1992). A myoelectrically based dynamic three-dimensional model to predict loads on lumbar spine tissues during lateral bending. *J Biomech* **25**(4), pp. 395–414.

– (1997). The biomechanics of low back injury: Implication on current practice in industry and the clinic. *J Biomech* **30**, pp. 465–475.

– (2007). *Low back disorders: Evidence-Based Prevention and Rehabilitation*. 2nd. Human Kinetics.

McGill SM, Juker D, and Kropf P (1996). Appropriately placed surface EMG electrodes reflect deep muscle activity (psoas, quadratus lumborum, abdominal wall) in the lumbar spine. *J Biomech* **29**(11), pp. 1503–1507.

McGill SM and Norman RW (1986). Partitioning of the L4-L5 dynamic moment into disc, ligamentous, and muscular components during lifting. *Spine* **11**(7), pp. 666–678.

McGlothlin JD (1996). *Ergonomic intervention for the soft drink beverage delivery industry*. Tech. rep. US Department of Health et al.

McKinley MP and O'loughlin VD (2006). *Human anatomy*. McGraw-Hill Higher Education.

Medved V (2001). *Measurement of human locomotion*. CRC Press.

Mehta RK and Parasuraman R (2013). Neuroergonomics: a review of applications to physical and cognitive work. *Front Hum Neurosci* **7**, p. 889.

Mendiburu F de (2015). *agricolae: Statistical Procedures for Agricultural Research*. R package version 1.2-3.

Merskey H and Bogduk N, eds. (1994). *Classification of chronic pain. Descriptions of chronic pain syndromes and definitions of pain terms*. 2nd (Revised 2012). Seattle: IASP Press.

Middleton G and Teacher J (1911). Injury of the spinal cord due to rupture of an intervertebral disk during muscular effort. *Glasg Med J* **76**, pp. 1–6.

Miller MI and Medeiros JM (1987). Recuitment of internal oblique and transversus abdominis during the eccentric phase of the curl-up exercise. *Phys Ther* (8), pp. 1213–1217.

Mirka GA and Marras WS (1993). A stochastic model of trunk muscle coactivation during trunk bending. *Spine* **18**(11), pp. 1396–409.

Mirka G and Baker A (1996). An investigation of the variability in human performance during sagittally symmetric lifting tasks. *IIE Trans* **28**(9), pp. 745–752.

Mirka GA, Kelaher DP, Nay DT, and Lawrence BM (2000). Continuous assessment of back stress (CABS): a new method to quantify low-back stress in jobs with variable biomechanical demands. *Hum Factors* **42**(2), pp. 209–225.

Morowitz HJ (1968). Energy flow in biology; biological organization as a problem in thermal physics.

Nachemson A (2004). «Epidemiology and the economics of low back pain». In: *The Lumbar Spine: Official Publication of the International Society for the Study of the Lumbar Spine*. Ed. by HN Herkowitz, J Dvorak, GR Bell, M Nordin, and D Grob. Lippincott Williams & Wilkins. Chap. 1, pp. 4–10.

National Health Service Centre for Reviews and Dissemination (2001). Stoop or squat. *Database of Abstracts of Reviews of Effectiveness* **3**.

National Institute for Occupational Safety and Health (1981). *Work practices guide for manual lifting*. Technical Report 81–122. Cincinnati, OH: US Department of Health and Human Services and National Institute for Occupational Safety and Health.

– (1994). *Application manual for the revised NIOSH lifting equation*. Technical Report 94-110. Cincinnati, Ohio 45226: US Department of Health and Human Services and National Institute for Occupational Safety and Health.

– (1997). *Musculoskeletal disorders and workplace factors: a critical review of epidemiologic evidence of work-related musculoskeletal disorders of neck, upper extremity, and low back*. Technical Report 97-141. Cincinnati, OH: US Department of Health and Human Services and National Institute for Occupational Safety and Health.

Negrini S, Fusco C, Atanasio S, Romano M, and Zaina F (2008). Low back pain: state of art. *European Journal of Pain Supplements* **2**(1), pp. 52–56.

NIST/SEMATECH (2012). *e-Handbook of Statistical Methods*. National Institute of Standards and Technology.

NRC-IOM (2001). *Musculoskeletal Disorders and the Workplace: Low Back and Upper Extremities*. Ed. by Commission on Behavioral and Social Sciences and Education. Washington, D.C.: National Academy Press.

Oddsson LI, Persson T, Cresswell AG, and Thorstensson A (1999). Interaction between voluntary and postural motor commands during perturbed lifting. *Spine* **24**(6), pp. 545–552.

Op de Beek R and Hermans V (2000). *Research on work related low back disorders*. Technical Report. Luxembourg: European Agency for Safety and Health at Work.

Orfanidis SJ (1996). *Introduction to signal processing*. Prentice-Hall International, Inc.

OSHA (2010). Occupational Injury and Illness Recording and Reporting Requirements (Proposed Rule). *Fed Regist* **75**(19). section 1904.12(b)(1), pp. 4728–4741.

Parasuraman R (2003). Neuroergonomics: research and practice. *Theor Issues Ergon* **4**(1-2), pp. 5–20.

Parasuraman R and Rizzo M (2007). *Neuroergonomics. The Brain at Work*. Ed. by A Kirlik. Oxford series in human-technology interaction. NY: Oxford University Press.

Parent-Thirion A, Fernández Macías E, Hurley J, and Vermeylen G (2007). *Fourth European Working Conditions Survey.* Tech. rep. Dublin: European Foundation for the Improvement of Living and Working Conditions.

Park W, Martin BJ, Choe S, Chaffin DB, and Reed MP (2005). Representing and identifying alternative movement technique for goal-directed manual task. *J Biomech* **38**, pp. 519–527.

Parnianpour M, Wang J, Shirazi-Adl A, Khayatian B, and Lafferriere G (1999). A computational method for simulation of trunk motion: Towards a theoretical based quantitative assessment of trunk performance. *Biomed Eng Appl Basis Comm* **11**, pp. 27–38.

Pećina MM and Bojanić I (2004). *Overuse Injuries of the Musculoskeletal System*. 2nd. CRC Press.

Personick ME and Harthun LA (1992). Profiles in safety and health: the soft drink industry. *Monthly Lab. Rev.* **115**, p. 12.

Pinto VJ, Sheikhzadeh A, Halpern M, and Nordin M (2013). Assessment of engineering controls designed for handling unstable loads: An electromyography assessment. *Int J Ind Ergon* **43**(2), pp. 181–186.

Podniece Z, Pinder A, Yeomans L, Heuvel S van den, Blatter B, Verjans M, Muylaert K, De Broeck V, Eeckelaert L, Buffet MA, Nevala N, Kaukiainen A, Lischka J, Kudasz F, and Kosina M (2007). *Work-related musculoskeletal disorders:* B*ack to work report*. Technical report TE-78-07-300-EN-C. Luxembourg: European Agency for Safety and Health at Work.

Podniece Z, Taylor TN, Takala EP, David G, Woods V, Kudasz F, Heuvel S van den, Blatter B, Roman-Liu D, Eeckelaert L, Op De Beeck R, Willems F, Lomi K, Koukoulaki T, Papale A, Sjogaard G, Lopes Nunes I, Cabecas JM, Reinert D, Ellegast RP, and Ditchen D (2008). *A European campaign on musculoskeletal disorders. Work-related musculoskeletal disorders: Prevention report*. Technical report TE-81-07-132-EN-C. Luxembourg: European Agency for Safety and Health at Work.

Praemer A, Furner S, and Rice DP (1999). *Musculoskeletal Conditions in the United States*. In: National Research Council and Institute of Medicine (2001). Musculoskeletal Disorders and the Workplace: Low Back and Upper Extremities. National Academy Press, pp:40. Rosemont, IL: American Academy of Orthopaedic Surgeons.

Prigogine I and Nicolis G (1971). Biological order, structure and instabilities. *Q Rev Biophys* **4**(2-3), pp. 107–148.

Proakis JG and Manolakis DG (1996). *Digital Signal Processsing. Principles, Algorithms, and Applications*. 3rd Edition. Prentice Hall International, Inc.

Punnett L, Prüss-Ütün A, Nelson DI, Fingerhut MA, Leigh J, Tak S, and Phillips S (2005). Estimating the global burden of low back pain attributable to combined occupational exposures. *Am J Ind Med* **48**(6), pp. 459–469.

Quinn GP and Keough MJ (2002). *Experimental design and data analysis for biologists*. New York: Cambridge University Press.

R Core Team (2013). *R: A Language and Environment for Statistical Computing*. R Foundation for Statistical Computing. Vienna, Austria.

Rabinovich SG (2013). *Evaluating Measurement Accuracy: A Practical Approach*. 2nd Edition. NY, USA: Springer-Verlag.

Radwin RG, Marras WS, and Lavender SA (2002). Biomechanical aspects of work-related musculoskeletal disorders. *Theor Issues Ergon* **2**(2), pp. 153–217.

Revelle W (2015). *psych: Procedures for Psychological, Psychometric, and Personality Research*. R package version 1.5.8.

Robert T, Zatsiorsky VM, and Latash ML (2008). Multi-muscle synergies in an unusual postural task: quick shear force production. *Exp Brain Res* **187**(2), pp. 237–253.

Roffey DM, Wai EK, Bishop P, Kwon BK, and Dagenais S (2010a). Causal assessment of awkward occupational postures and low back pain: results of a systematic review. *The Spine Journal* **10**(1), pp. 89–99.

– (2010b). Causal assessment of occupational pushing or pulling and low back pain: results of a systematic review. *The Spine Journal* **10**(6), pp. 544–553.

– (2010c). Causal assessment of occupational sitting and low back pain: results of a systematic review. *The Spine Journal* **10**(3), pp. 252–261.

– (2010d). Causal assessment of occupational standing or walking and low back pain: results of a systematic review. *The Spine Journal* **10**(3), pp. 262–272.
– (2010e). Causal assessment of workplace manual handling or assisting patients and low back pain: results of a systematic review. *The Spine Journal* **10**(7), pp. 639–651.
Roy SH and DeLuca CJ (1996). «Surface electromyographic assesment of low back pain». In: *Electromyography in Ergonomics*. Ed. by S Kumar and A Mital. London: Taylor and Francis. Chap. 9, pp. 259–295.
Russell SJ, Winnemuller L, Camp JE, and Johnson PW (2007). Comparing the results of five lifting analysis tools. *Appl Ergon* **38**, pp. 91–97.
Salomon JA et al. (2013). Common values in assessing health outcomes from disease and injury: disability weights measurement study for the Global Burden of Disease Study 2010. *The Lancet* **380**(9859), pp. 2129–2143.
Santos BR, Larivière C, Delisle A, McFadden D, Plamondon A, and Imbeau D (2011). Sudden loading perturbation to determine the reflex response of different back muscles: A reliability study. *Muscle & nerve* **43**(3), pp. 348–359.
Schaal S, Sternad D, Osu R, and Kawato M (2004). Rhythmic arm movement is not discrete. *Nat Neurosci* **7**(10), pp. 1136–1143.
Schmid M, Conforto S, Camomilla V, Cappozzo A, and D'Alessio T (2002). The sensitivity of posturographic parameters to acquisition settings. *Med Eng Phys* **24**(9), pp. 623–631.
Schmidt RC and Turvey MT (1995). Models of interlimb coordination–Equilibria, local analyses, and spectral patterning: comment on Fuchs and Kelso (1994). *J Exp Psychol Hum Percept Perform* **21**(2), pp. 432–443.
Schmidt R and Lee T (1998). *Motor control and learning: a behavioural emphasis*. Champaign: Human Kinetics.
Schmiedmayer HB and Kastner J (1999). Parameters influencing the accuracy of the point of force application determined with piezoelectric force plates. *J Biomech* **32**(11), pp. 1237–1242.
Schneider E and Irastorza X (2010). OSH *in figures: Work-related musculoskeletal disorders in the* EU - F*acts and figures.* Technical Report. Luxembourg: European Agency for Safety and Health at Work.
Scholz JP (1993a). Organizational principles for the coordination of lifting. *Hum Mov Sci* **12**(5), pp. 537–576.
– (1993b). The effect of load scaling on the coordination of manual squat lifting. *Hum Mov Sci* **12**, pp. 427–459.
Scholz JP and McMillan AM (1995). Neuromuscular coordination of squat lift,II: Individual differences. *Phys Ther* **75**(2), pp. 58–69.
Scholz JP, Millford JP, and McMillan AM (1995). Neuromuscular coordination of squat lifting, I: Effect of load magnitude. *Phys Ther* **75**(2), pp. 119–132.
Scholz JP and Schöner G (1999). The uncontrolled manifold concept: identifying control variables for a functional task. *Exp Brain Res* **126**(3), pp. 289–306.
Schöner G, Haken H, and Kelso JAS (1986). A stochastic theory of phase transitions in human hand movement. *Biol Cybern* **53**(4), pp. 247–257.

Scoppa F, Capra R, Gallamini M, and Shiffer R (2013). Clinical stabilometry standardization: basic definitions–acquisition interval–sampling frequency. *Gait Posture* **37**(2), pp. 290–292.

Sedgwick AW and Gormley JT (1998). Training for lifting; an unresolved ergonomic issue? *Appl Ergon* **29**, pp. 395–398.

Shekelle P (1997). «The epidemiology of low back pain». In: *Clinical anatomy and management of low back pain*. Ed. by LGF Giles and KP Singer. Vol. I. Clinical Anatomy and Management of back pain. Butterworth-Heinnemann. Chap. 2, pp. 18–31.

Shoaf C, Genaidy A, Karwowski W, Waters T, and Christensen D (1997). Comprehensive manual handling limits for lowering, pushing, pulling and carrying activities. *Ergonomics* **40**(11), pp. 1183–1200.

Sjogaard G (1985). «Intramuscular Changes during Long-term Contraction». In: *Ergonomics of Working Postures: Models, Methods and Cases*. Ed. by JR Wilson, EN Corlett, and I Manenica. Proceedings of the First International Occupational Ergonomics Symposium. Zadar, Yugoslavia: Taylor & Francis Routlege, pp. 136–143.

Sjogaard G and Jensen BR (2006). «Low-Level Static Exertions». In: *The occupational ergonomics handbook. Fundamentals and assesment tools for occupational ergonomics.* Ed. by W Marras and W Karwowski. 2nd Edition. Taylor and Francis. Chap. 14, pp. 14/1–13.

Skiadopoulos A and Gianikellis K (2014). «Random error propagation analysis in center of pressure signal». In: *Biomedical Robotics and Biomechatronics (2014 5th IEEE RAS & EMBS International Conference on*, pp. 632–637.

Slepian D (1976). On bandwidth. *Proc IEEE* **64**(3), pp. 292–300.

Smith TJ, Henning RA, Wade MG, and Fisher T (2014). *Variability in human performance*. CRC Press.

Snook SH and Ciriello VM (1991). The design of manual handling tasks: revised tables of maximum acceptable weights and forces. *Ergonomics* **34**(9), pp. 1197–1213.

Snook SH (2004). Work-related low back pain: secondary intervention. *J Electromyogr Kinesiol* **14**, pp. 153–160.

Solomonow M (2004). Ligaments: a source of work-related musculoskeletal disorders. *J Electromyogr Kinesiol* **14**(1), pp. 49–60.

– (2009). Ligaments: a source of musculoskeletal disorders. *J Bodyw Mov Ther* **13**(2), pp. 136–154.

Srinivasan D and Mathiassen SE (2012). Motor variability in occupational health and performance. *Clin Biomech* **27**, pp. 979–993.

Stergiou N (2004). *Innovative analyses of human movement : Analytical tools for human movement research*. Champaign: Human Kinetics.

Stergiou N and Decker LM (2011). Human movement variability, nonlinear dynamics, and pathology: Is there a connection? *Hum Mov Sci* **30**, pp. 869–888.

Straker L (2003). Evidence to support using squat, semi-squat and stoop techniques to lift low-lying objects. *Int J Ind Ergon* **31**, pp. 149–160.

Suranthiran S and Jayasuriya S (2005). «Conditioning of distorted nonlinear sensor measurements in non-stationary noisy environments». In: *Mechatronic Systems 2004*. Ed. by SOR Moheimani. Vol. 1. Kidlington, Oxford, UK: Elsevier IFAC Publications, pp. 115–119.

Swedish Work Environment Authority (1998). *Ergonomics for the Prevention of Musculoskeletal Disorders. Provisions of the Swedish National Board of Occupational Safety and Health on Ergonomics for the Prevention of Musculoskeletal Disorders, together with the Board's General Recommendations on the implementation of the Provisions*. Tech. rep. AFS 1998:1. SOLNA: National Board of Occupational Safety and Health.

Tafazzol A, Arjmand N, Shirazi-Adl A, and Parnianpour M (2014). Lumbopelvic rhythm during forward and backward sagittal trunk rotations: combined in vivo measurement with inertial tracking device and biomechanical modeling. *Clin Biomech* **29**(1), pp. 7–13.

NASA (2010). *Measuring and Test Equipment Specifications.* NASA *Measurement Quality Assurance Handbook* - ANNEX *3*. Technical Standard NASA-HDBK-8739.19-3. Washington DC: National Aeronautics and Space Administration (NASA).

Thom R (1969). Topological models in biology. *Topology* **8**(3), pp. 313–335.

Ting LH (2007). Dimensional reduction in sensorimotor systems: a framework for understanding muscle coordination of posture. *Prog Brain Res* **165**, pp. 299–321.

Ting LH and Chvatal SA (2011). «Decomposing muscle activity in motor tasks». In: *Motor Control. Theories, Experiments and Applications*. Ed. by F Danion and ML Latash. New York: Oxford University Press, pp. 102–138.

Torres-Oviedo G, Macpherson JM, and Ting LH (2006). Muscle synergy organization is robust across a variety of postural perturbations. *J Neurophysiol* **96**, pp. 1530–1546.

Torres-Oviedo G and Ting LH (2007). Muscle synergies characterizing human postural responses. *J Neurophysiol* **98**(4), pp. 2144–2156.

Tresch M, Cheung V, and d'Avella A (2006). Matrix factorization algorithms for the identification of muscle synergies: evaluation on simulated and experimental data sets. *J Neurophysiol* **95**(4), pp. 2199–2212.

Tunik E, Poizner H, Levin MF, Adamovich SV, Messier J, Lamarre Y, and Feldman AG (2003). Arm-trunk coordination in the absence of proprioception. *Exp Brain Res* **153**(3), pp. 343–355.

Turvey MT (1977). Contrasting orientations to the theory of visual information processing. *Psychol Rev* **84**(1), p. 67.

Van der Burg JCE, Kingma I, and Van Dieën JH (2003). Effects of unexpected lateral mass placement on trunk loading in lifting. *Spine* **28**(8), pp. 764–770.

– (2004). Is the trunk movement more perturbed after an asymmetric than after a symmetric perturbation during lifting? *J Biomech* **37**(7), pp. 1071–1077.

Van der Burg JCE and Van Dieën JH (2001a). The effect of timing of a perturbation on the execution of a lifting movement. *Hum Mov Sci* **20**, pp. 243–255.

– (2001b). Underestimation of object mass in lifting does not increase the load on the low back. *J Biomech* **34**(11), pp. 1447–1453.

Van der Burg JCE, Van Dieën JH, and Toussaint H (2000). Lifting an unexpectedly heavy object: the effects on low-back loading and balance loss. *Clin Biomech* **15**(7), pp. 469–477.

Van Dieën JH and Looze MP de (1999). Directionality of anticipatory activation of trunk muscles in a lifting task depends on load knowledge. *Exp Brain Res* **128**(3), pp. 397–404.

Van Dieën JH, Hoozemans MJM, and Toussaint HM (1999). Stoop or squat: a review of biomechanical studies on lifting technique. *Clin Biomech* **14**, pp. 685–696.

Van Dieën JH, Kingma I, and Van der Burg JCE (2003). Evidence for a role of antagonistic cocontraction in controlling trunk stiffness during lifting. *J Biomech* **36**, pp. 1829–1836.

Van Dieën JH and Van der Beek AJ (2009). «Work-Related Low Back Pain: Biomechanical Factors and Primary Prevention». In: *Ergonomics for Rehabilitation Professionals*. Ed. by S Kumar. CRC Press. Chap. 12.

Verrel J (2010). Distributional properties and variance-stabilizing transformations for measures of uncontrolled manifold effects. *J Neurosci Methods* **191**, pp. 166–170.

Visser B and Van Dieën JH (2006). Pathophysiology of upper extremity muscle disorders. *J Electromyogr Kinesiol* **16**(1), pp. 1–16.

Waddell G (1998). *The Back Pain Revolution*. Edinburgh: Churchill Livingstone.

Wai EK, Roffey DM, Bishop P, Kwon BK, and Dagenais S (2010a). Causal assessment of occupational bending or twisting and low back pain: results of a systematic review. *The Spine Journal* **10**(1), pp. 76–88.

– (2010b). Causal assessment of occupational carrying and low back pain: results of a systematic review. *The Spine Journal* **10**(7), pp. 628–638.

– (2010c). Causal assessment of occupational lifting and low back pain: results of a systematic review. *The Spine Journal* **10**(6), pp. 554–566.

Walker JS (2008). *A Primer On Wavelets And Their Scientific Applications*. 2nd. Chapman And Hall/CRC.

Wang Y, Asaka T, Zatsiorsky VM, and Latash ML (2006). Muscle synergies during voluntary body sway: combining across-trials and within-a-trial analyses. *Exp Brain Res* **174**(4), pp. 679–693.

Waters TR, Putz-Anderson V, Garg A, and Fine LJ (1993). Revised NIOSH equation for the design and evaluation of manual lifting tasks. *Ergonomics* **36**(7), pp. 749–776.

Waters TR, Yeung S, Genaidy A, Callaghan J, Barriera-Viruet H, Abdallah S, and Kumar S (2006). Cumulative spinal loading exposure methods for manual material handling tasks. Part 2: methodological issues and applicability for use in epidemiological studies. *Theor Issues Ergon* **7**(2), pp. 131–148.

Waters TR (2006). «Revised NIOSH Lifting Equation». In: *The Occupational Ergonomics Handbook. Fundamentals and Assessment Tools for Occupational Ergonomics*. Ed. by WS Marras and W Karwowski. 2nd. Boca Raton, Florida: CRC Press, Taylor and Francis Group. Chap. 46, pp. 46/1–28.

Waters TR, Putz-Anderson V, and Garg A (1994). *Application manual for the revised* NIOSH *lifting equation*. Publication No. 94-110. DHHS (NIOSH). Cincinnati, Ohio 45226.

WHO (1985). *Identification and control of work-related diseases*. World Health Organization Technical Report Series 714. Geneva: World Health Organization (WHO).

Wiener N (1985). *Cybernetics: or Control and Communication in the Animal and the Machine*. 2nd. Cambridge, Massachusetts: The M.I.T. Press.

Winter DA, MacKinnon CD, Ruder GK, and Wieman C (1993). An integrated EMG/biomechanical model of upper body balance and posture during human gait. *Prog Brain Res* **97**, pp. 359–367.

Winter DA (2009). *Biomechanics and motor control of human movement*. 4th Edtion. New Jersey, United States of America: John Wiley and Sons,Inc., p. 369.

Winter DA and Patla AE (1997). *Signal Processing and Lineal Systems for the Movement Sciences*. Waterloo, Ontario, Canada: Waterloo Biomechanics.

Wisleder D and McLean B (1992). «Movement artifact in force plate measurement of postural sway». In: *Proceedings of the 2nd North American Congress of Biomechanics*. Chicago, pp. 413–414.

Woltring HJ (1984). «On Methodology in the Study of Human Movement». In: *Human Motor Actions – Bernstein Reassessed*. Ed. by HTA Whiting. Vol. Volume 17. North-Holland. Chap. Ib, pp. 35–73.

– (1986). A Fortran package for generalized, cross-validatory spline smoothing and differentiation. *Adv Eng Software* **8**(2), pp. 104–107.

– (1995). «Smoothing and Differentiation Techniques Applied to 3D Data». In: *Three-Dimensional Analysis of Human Movement*. Ed. by P Allard, IAF Stokes, and JP Blanchi. Selected papers from an invited symposium on three-dimensional analysis held in July, 1991. Human Kinetics. Chap. 5, pp. 79–99.

Woltring HJ, De Lange A, Kauer JMG, and Huiskes R (1987). Instantaneous helical axis estimation via natural cross-validated splines. *Biomechanics: basic and applied research*, pp. 121–128.

Yassi A (1997). Repetitive strain injuries. *The Lancet* **349**, pp. 943–947.

Zernicke R and Whiting W (2000). «Mechanisms of Musculoskeletal Injury». In: *Biomechanics in Sport Performance. Enhancement and Injury Prevention*. Ed. by VM Zatsiorsky. Vol. IX. Encyclopaedia Of Sports Medicine. An IOC Medical Commission Publication in Collaboration with the International Federation of Sports Medicine. Blackwell Science, Ltd. Chap. 24, pp. 507–522.

Zhang X, Nussbaum MA, and Chaffin DB (2000). Back lift versus leg lift: and index and visualization of dynamic lifting strategies. *J Biomech* **33**, pp. 777–782.

Zipp P (1982). Recommendations for the standardization of lead positions in surface electromyography. *Eur J Appl Physiol*, pp. 41–54.

A

Informe de Consentimiento

Yo ..... nombre ..... estoy de acuerdo de participar en el proyecto de investigación con titulo "*Análisis Biomecánico y caracterización de la intervención muscular y la calidad de control motor en el contexto de la manipulación manual de cargas*. Entiendo que esta participación es totalmente voluntaria. Puedo cambiar mi idea en cualquier momento sin ser penalizado y obtener los resultados de mi participación como propiamente míos, borrados de los archivos o destruidos.

Los siguientes puntos del procedimiento han sido explicados a mí:

Se analizarán simulacros de manipulación manual de cargas utilizando técnicas de fotogrametría tridimensional simultáneamente con un sistema de dos plataformas de fuerza. Se usarán marcadores reflectantes pasivos para obtener las coordenadas 3D de diferentes puntos anatómicos del tronco y de la pelvis. Al mismo tiempo un sistema de electromiografía superficial registrará la intervención de los siguientes músculos i) erector spinae ii) dorsal ancho iii) recto mayor del abdomen iv) oblicuos externos e internos del abdomen. Los electrodos de electromiografia y los marcadores se adhieren a la piel del participante mediante una cinta adhesiva hipoalergénica de doble cara.

- No se prevé incomodidad o estrés para los sujetos
- No se prevén riesgos
- El resultado de su participación será confidencial y no serán revelados ningún dato identificativo sin mi propio consentimiento, al menos que sea requerido por la ley.
- El equipo investigador responderá todas las cuestiones sobre la investigación, ahora o durante el curso del proyecto

Cáceres, a ..... de ..... del .....

Fdo.:

B

Additional Methodology

B.1. Gage Linearity and Bias Study for Force Measurements

B.1.1. Background

A Gage Linearity and Bias procedure was used to estimate the accuracy of the force measurement system. The force measurement system is accurate if the bias is small. Bias indicates how close the measurements are to the reference values. Linearity refers to the how much the bias changes throughout the normal operating range of the measurement system. If the bias is consistent, then the linearity is small. The objective of this study was to compute the linearity and bias values of the force measurement system for the uncertainty analysis.

B.1.2. Procedure

Four reference loads ($M_1 = 98\,N$, $M_2 = 196\,N$, $M_3 = 294\,N$, and $M_4 = 392\,N$) were placed on the geometrical center of the top plate of the two force platforms and 50 repeated measurements were recorded for 5 sec each at sampling rate of 30 Hz. The mean value (and standard deviation) was computed for each sample. The study performed by one operator.

B.1.3. Statistical Analysis

The Grubbs' test was used to check for outliers. A regression line was fitted on the bias against the reference values and statistics for the linearity and accuracy of the measurement system computed. It is assumed that biases are corrected by the manufacture's calibration procedure, therefore, only the uncertainties of the correction are presented. The range over which the measurements varies due to normal variation computed by the R&R study (Table B.2).

B.1.4. Results Report

Table B.1 shows the results of the analysis. The maximum absolute value of the bias per part (load) and the linearity values were added to the uncertainty budget for calculating the expanded uncertainty of the measurement system (Table 3.3). Based upon a total of 200 measurements (mean values) on 4 parts ($M_{1\rightarrow4}$), the estimated mean bias of the force platform 1 was -2.92 N

Table B.1 Gage linearity and bias report for force measurements.

Force platform 1				Forcec platform 2			
Gage linearity				Gage linearity			
Predictor	Coef	SE Coef	P	Predictor	Coef	SE Coef	P
Constant	-1.14	0.30	0.000	Constant	-0.70	0.22	0.000
Slope	-0.007	0.001	0.000	Slope	-0.02	0.0008	0.000
S	1.74	R-Sq	17.5%	S	1.25	R-Sq	76%
Linearity	0.10	%Linearity	0.7	Linearity	0.26	%Linearity	2.0
Gage bias				Gage bias			
Reference	Bias	%Bias	P	Reference	Bias	%Bias	P
Average	-2.92	22.5	0.000	Average	-5.62	43.2	0.000
98	-3.33	25.6	0.000	98	-3.66	28.1	0.000
196	-0.24	1.8	0.001	196	-2.68	20.6	0.000
294	-4.45	34.2	0.000	294	-7.53	57.9	0.000
392	-4.14	31.9	0.000	392	-8.61	66.2	0.000

and of the force platform 2 was −5.62 N. They represent the 22.5% and 43.2% of the process variation, respectively, which was specified to be 13.015 N for both force platforms. The linearity (change in bias across the range of product variation) represents 0.7% and 2% of that range for force platform 1 and force platform 2, respectively. These are statistically significant changes in the bias over the range of the reference values at the 5% significance level.

B.2. Gage Repeatability and Reproducibility Study for Force Measurements

B.2.1. Background

A R&R study is a designed experiment to study the variation (Repeatability & Reproducibility) in the measurements results. The Repeatability is an estimation of the variation between measurements made by the same operator on the same part, usually attributed to the gage. The reproducibility is an estimation of the variation between measurements made by different operators on the same part, usually attributed to the operator. Since two force platforms were used in the study, an expanded R&R analysis carried on with additional factor the force platforms (operators and parts are the typical factors). Therefore, the variation between the measurements made by the two force platforms can be added to the total Gage R&R variation. The objective of the current experiment design was to estimate the repeatability and reproducibility of the force measurement system, and to determine if the two force platforms are equally capable for measuring the different parts. The response variable was the $\mathbf{F}_z$ of the ground reaction force.

B.2.2. Design of Gage RR Experiment

A full factorial design of experiment (DOE) with 3 factors (Operators: 2-levels, Force platforms: 2-levels, Parts: 4-levels) and 16 treatment combinations that replicated 50 times in randomized order was run to chart the response of the measurement process (expanded R&R design). The

Table B.2 Contribution of each error source on force measurement system's variation.

Source	Std. Dev (SD)	Study Var (6 × SD)	%Study Var (%SV)	%Tolerance (SV/Toler)
Total Gage R&R	2,169	13,015	1,74	4,43
Repeatability	0,410	2,460	0,33	0,84
Reproducibility	2,130	12,780	1,70	4,35
Operators	0,000	0,000	0,00	0,00
Force platform	1,769	10,613	1,42	3,61
Parts*Operators	0,101	0,605	0,08	0,21
Parts*Force platform	1,182	7,095	0,95	2,41
Part-To-Part	124,970	749,820	99,98	255,04
Parts	124,970	749,820	99,98	255,04
Total Variation	124,989	749,933	100,00	255,08

design of the gage experiment allowed to compare the measurement capability of the two force platforms.

B.2.3. Procedure

A calibrated load was placed by the operator at the geometrical center of the top plate of the force platforms and the $\mathbf{F}_z$ of the GRF was recorded for 5 sec at sampling rate of 30 Hz. This process was repeated for the 16 treatment combinations and their replications. The mean value and standard deviation was computed for each sample. The force measurement system was zeroed before each measurement.

The force measurement system uses a 12-bit precision A/D converter (resolution of $\frac{100}{2^{12}} \approx 0.024\%$). The $\mathbf{F}_z$ range during the measurements was set at 0 - 1250 N. Therefore, the $\mathbf{F}_z$ can be resolved to $\frac{1250\,\mathrm{N}}{2^{12}} = 0.31$ N. As a guideline, the resolution should not be greater than 5% of the process tolerance limits. Hence, the tolerance intervals of the measurement process should not be less than 6.4 N. Manufacturer specified the maximum force error at e = 2% of the applied force, which corresponds to $e_1 = 1.96$ N, $e_2 = 3.92$ N, $e_3 = 5.88$ N, and $e_4 = 7.84$ N. The *conformance zone* is the tolerance interval reduced by the measuring uncertainty at each end. Therefore, if the uncertainty is the 30% of the tolerance and the rest 70% is the conformance zone, the tolerance intervals for each load and for the corresponding errors are $T_1 = 6.53$ N, $T_2 = 13.07$ N, $T_3 = 19.6$ N, and $T_4 = 26.13$ N.

B.2.4. Statistics

Prior to model analysis, the Grubbs' test was used to check for outliers. A three-factor random-effect linear model with 2-order interactions was fitted to the data to analyze the factorial design experiment and hence to quantify the R&R variance component. To compare measurement capability between force platforms, a two-factor random-effect linear model with 2-order interactions was fitted to the data for every part seperately and the R&R variance components were compared. It was supposed that reproducibility is less than repeatability, indicating that most of the variability is accounted for by the inaccuracy of the measurement system and not by operators' variability

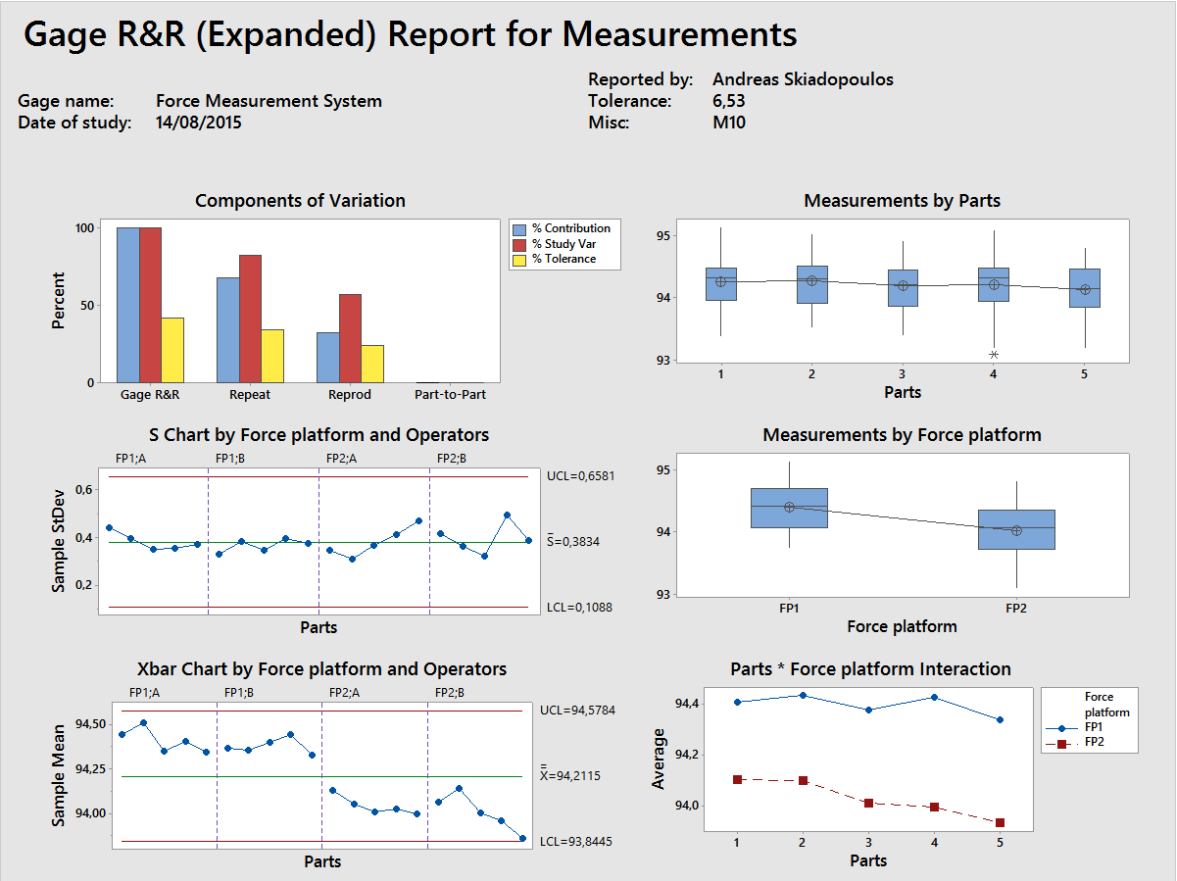

Figure B.1 Gage RR report for $\mathbf{F}_z$ measurements on the M_1 loads.

or difference between the two force platforms. A formal comparison between the measurement capability of the two force platforms was made by comparing the variance of the first force platform with the variance of the second force platform following the procedure of Burdick, Borror, and Montgomery (2005). A two-factor ANOVA was run for every part and force platform combination seperately. In order to compare the capability of the two force platforms, the ratio $\Gamma = \frac{\gamma_1}{\gamma_2}$, where γ_1 represents measurement variance of the first force platform and γ_2 the measurement variance of the second force platform, was computed. Then, 95% confidence interval for $L < \Gamma < U$ was computed as following.

The γ_1 is[1,2]:

$$\gamma = \frac{MS_O^2 + (n_P - 1) \times MS_{O\times P}^2}{n_P}$$

The degrees-of-freedom of the first force platform (DF_1) is[3]:

$$DF_1 = \frac{n_P^2 \times \gamma_1^2}{\frac{MS_O^4}{n_O - 1} + \frac{(n_P - 1)^2 \times MS_{O\times P}^4}{(n_O - 1)(n_P - 1)}}$$

[1]The same for force platform 2 (γ_2).

[2]MS stands for Mean Square, n stands for total number of, O stands for Operator, P for Parts and $O \times P$ for their interaction.

[3]The same for force platform 2 (DF_2).

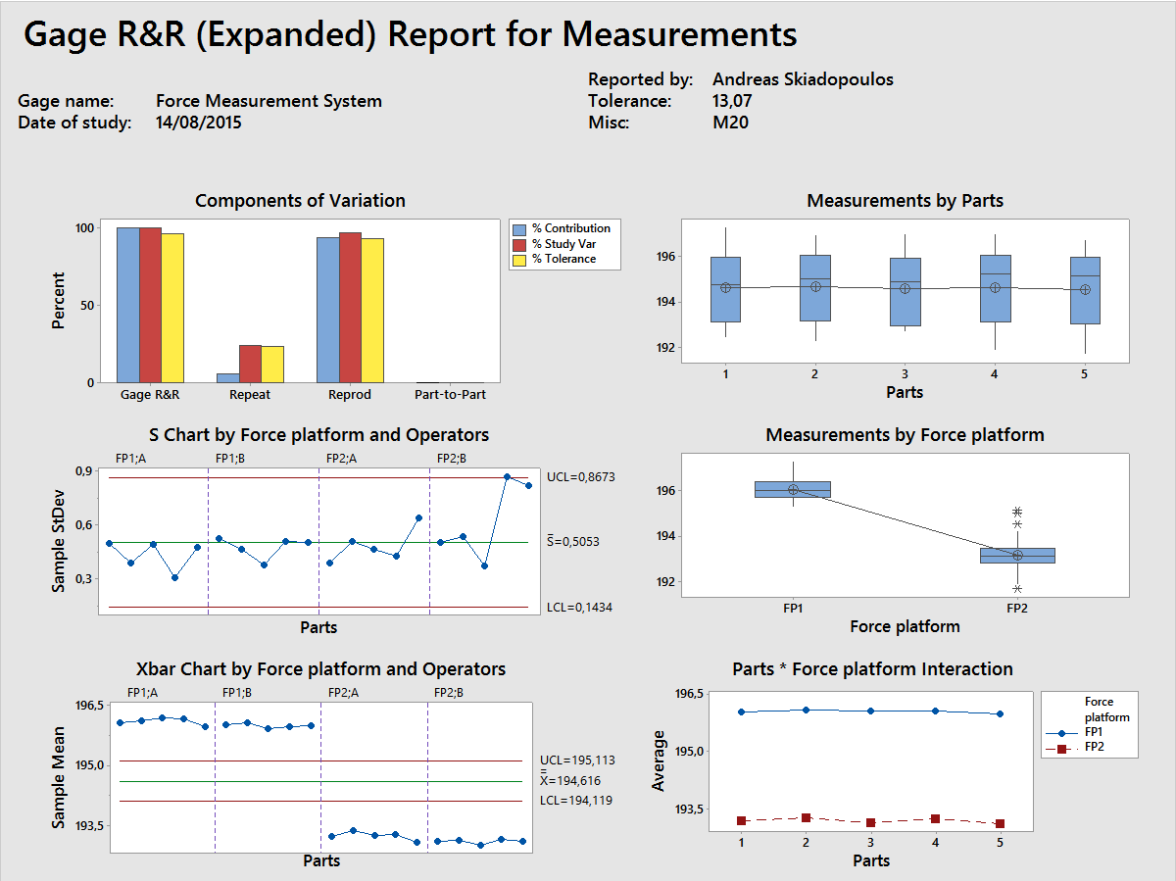

Figure B.2 Gage RR report for $\mathbf{F}_z$ measurements on the M_2 loads.

Using the above values, the 95% confidence interval for Γ ratio is:

$$L = \frac{\Gamma}{F_{0.975;(DF_1,DF_2)}}$$
$$U = \frac{\Gamma}{F_{0.025;(DF_1,DF_2)}}$$

If all values in the confidence interval of this ratio exceed 1, the second force platform has better measurement capability than the first force platform. Conversely, if all values in the confidence interval are less than 1, the first force platform is better. If the confidence interval contains the value 1 there is no difference between the two force platforms (Burdick, Borror, and Montgomery, 2005). Violations of underlying assumptions for the ANOVA models were determined with residual plots. The Minitab 17 statistical software was used for R&R analysis.

B.2.5. Results Report

Table B.2 shows the force measurement system evaluation. The total Gage R&R variation (SD = 2.169 N) was added to the budget uncertainty for calculating the expanded uncertainty of the measurement system (Table 3.3). Figures B.1 to B.4 show the reports of the R&R studies carried on for comparing the two force platforms. Except of M_1 loads, the reproducibility variation is

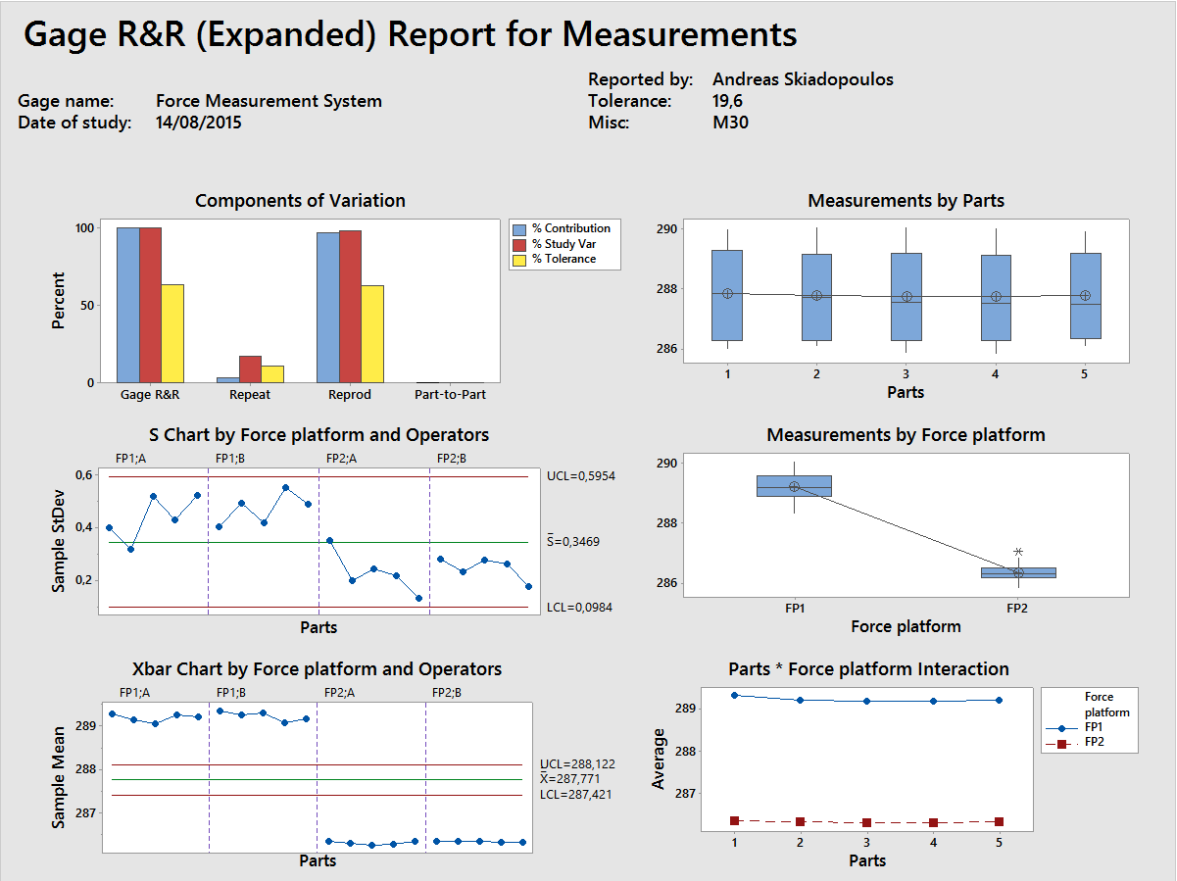

Figure B.3 Gage RR report for $\mathbf{F}_z$ measurements on the M_3 loads.

higher than repeatability, indicating differences in the measurement capability between the two force plaforms (operators' variation is much less than force platforms variation). The ratios with 95% confidence interval (CI) are

- $\Gamma_{M_4} = 0.59$ (0.01, 8.22)
- $\Gamma_{M_3} = 100$ (91, 110)
- $\Gamma_{M_2} = 0.28$ (0.12, 0.52)
- $\Gamma_{M_1} = 0.004$ (3×10^{-4}, 0.0107)

indicating that the measurement capability of force platform 1 is statistically better than that of force platform 2 at the 95% confidence interval.

B.3. Uncertainty Analysis of Center of Pressure Measurements

B.3.1. Background

Ideally, when a static vertical force $\mathbf{F}_z$ is applied on the top plate of the force platform system on a fixed point, the obtained COP coordinates have to be constant in time. Equally, the distance,

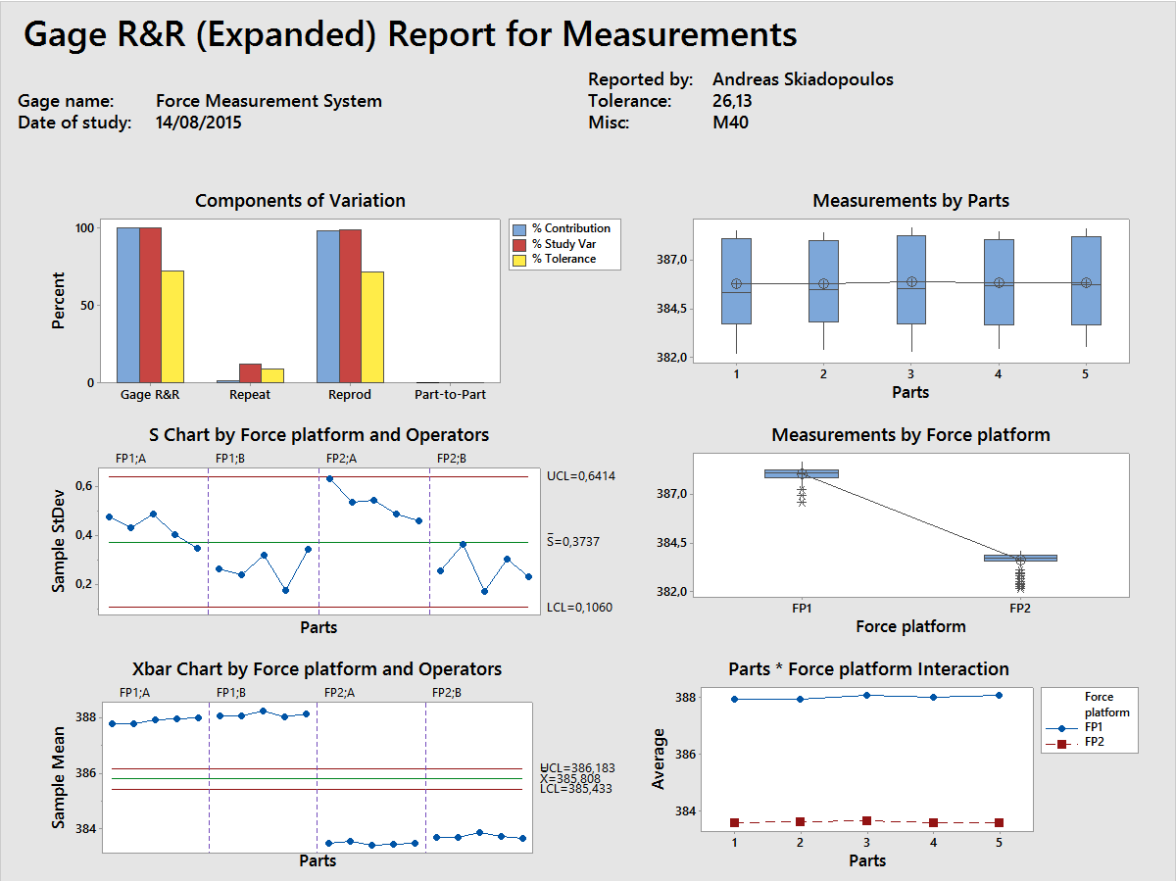

Figure B.4 Gage RR report for $\mathbf{F}_z$ measurements on the M_4 loads.

Δ_{COP}, between two fixed points on the top plate of the force platform that is obtained as the difference between the COP coordinates that the force measurement system registered by applying a static force on the top plate of the force platform on the two fixed points at two different instants, $t_1 and t_2$, and for time period $\tau_1 = \tau_2$ should also be constant—i.e., without any uncertainties in the obtained measurement. Therefore, we can write

$$\Delta_{COP} = COP_{t_1} - COP_{t_2}$$

However, this is not the case as measurement errors affect the COP values obtained by the force measurement system. Uncertainty is a numerical estimate of the dispersion of the error in a measurement resulted of several random and systematic interacting errors inherent to the measurement system, its calibration procedure, the standard used to provide the known values, and the measurement technique. For the purpose of this study, the uncertainty on the COP measurements was quantified based on the procedures described by Bizzo, Ouaknine, and Gagey (2003) and Browne and O'Hare (2000) under the GUM framework (ISO-JCGM 100, 2010; NIST/SEMATECH, 2012; NASA, 2010) in order to provide uncertainty metrics for static loads.

B.3.2. Measurement Process Overview

B.3.2.1. Procedure

The force measurement system was switched on 15 min prior to the measurement process to reach thermal stability and was zeroed at the begin of the procedure. By the help of a millimetre grid that was placed on the top plate of the force platform, the distance between $\xi = 11$ consecutive point was fixed at 10 mm. Therefore, the measurement range was set at 100 mm. Furthermore, all the points were laying on a line which is parallel to the X-axis[4] and crosses the geometrical center of the top plate of the force platform. Moreover, all the points were contained within the area ±50 mm from the geometrical center of the top plate of the force platform in both the X- and Y-axis.

A dead load (M) was displaced on the top plate of the force platform from the point P_0 to the point P_{10} gradually in 10 consecutive stages that corresponded to ξ fixed points and then was returned back from the point P_{10} to the point P_0 in a similar manner. This operation was repeated two times. During the displacements of the dead load M from the point P_0 to the point P_{10} and back to the P_0, at each one of the intermediate points where the load M was placed gradually, the COP was measured for 10 repeated times in an interval of 30 sec between each repetition. Each repeated COP data was collected for a time period of 5 sec at sampling rate of 30 Hz under a set of repeatability conditions of measurement. There are $k = 10$ repeated COP samples comprised of 150 data each, for each one of the ξ fixed points $P_{0\rightarrow10}$, replicated $r = 4$ times. For each point the mean value and standard deviation for each repeated COP sample have been computed, as well as the overall mean value comprised of all the data of the $k = 10$ repeated samples. In total four overall means have been calculated at each point, two in the $P_0 \rightarrow P_{10}$ direction and two in the $P_{10} \rightarrow P_0$. The distance of each point from P_0 was calculated (Fig. B.5a).

To ensure that the dead load was placed accurately on the coordinates indicated by the millimetre grid a point loader was used. The dead load M was placed on a metallic platen that in turns was placed above two parallel adjustable metal bars sustained on the ground away from the force platform being evaluated. A stylus of 5 mm diameter was stuck to the surface of the platen at its geometrical center in order to transmit the load on the top plate of the force platform. This procedure was repeated for the four different reference loads ($M_1 = 98$ N, $M_2 = 196$ N, $M_3 = 294$ N) (Telju, Spain) for the two force platforms used in the study. The same operator conducted the whole procedure.

B.3.3. Definition of the Measurement Model

The measured distance between the two fixed points is

$$D_{COP} = \Delta_{COP} + \varepsilon_{COP}$$

where ε_{COP} is the total error associated with the measurement.

Supposing that we have m output signals (measured distances) that are linearly proportional to the input signal (nominal distances), a regression line can be fitted to the data (Fig. B.5b).

[4] and Y-axis

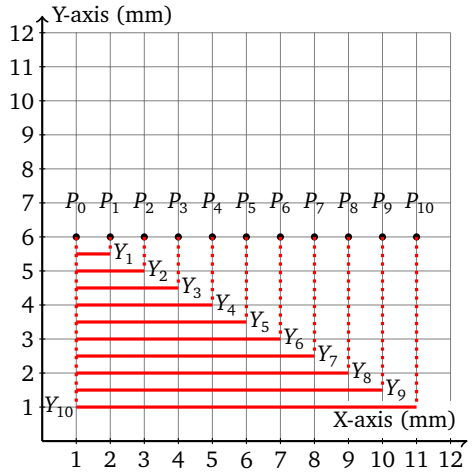

(a) 10 repeated COP measurements at each point P were obtained, averaged and the relative position, Y, with respect to the point P_0 was computed. In total, for each of the points, four average values (distances) were computed, two in the $P_0 \rightarrow P_{10}$ direction and two in the $P_{10} \rightarrow P_0$ one.

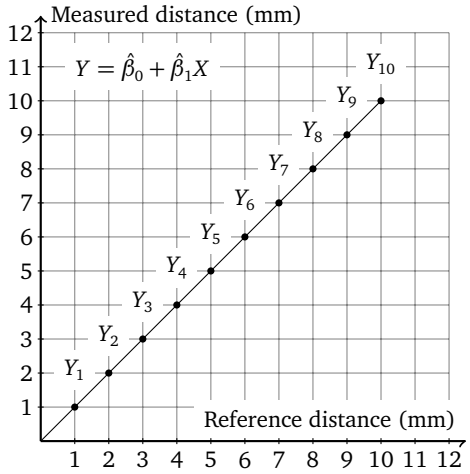

(b) The averaged measured values of the force platform system (Y) are plotted against the quantity values (X) that have been taken by the millimetric grid. Then, a linear regression analysis has been used to maintain the calibrated system in a state of statistical control.

Figure B.5 The static performance characteristics of the force measurement system was studied by plotting the output signal (Y) obtained by the force platform (Fig. B.5a) system against the known input signal (X) in order to generate a scatter plot, wherein a straight-line was fitted with the method of least squares, as it is assumed that the output signal is linearly proportional to the input signal (Fig. B.5b).

It is assumed that biases are corrected by the manufacture's calibration procedure, therefore, only the uncertainties of the correction are presented. In order to estimate the intercept and the slope of the fitted line, the method of least square error is used which minimizes the sum of the squared residuals by taking into consideration that nominal values have no uncertainties and the uncertainty in the measured values is constant over the range of the curve fit. Once the coefficients of the linear model are found, the estimated regression lines for the measured signals can be read. The residuals of the fitted model (Fig. B.6) were analyzed to test the goodness of the fitted linear regression models and to identify possible outliers using the *getOutliers*() function of the package **extremevalues** (Loo, 2010) in R environment (R Core Team, 2013).

B.3.4. Error Model and Sources

The error model for ε_{COP} is the sum of the errors encountered during the measurement process

$$\varepsilon_{\text{COP}} = \varepsilon_{\text{res}} + \varepsilon_{\text{ran}} + \varepsilon_{\text{reg}} + \varepsilon_{\text{lnr}} + \varepsilon_{\text{hys}}$$

where

- ε_{res} is the error associated with the digital resolution of the system display
- ε_{ran} is the error associated with repeated measurements

- ε_{reg} is the uniformity error

- ε_{lnr} is the nonlinearity error

- ε_{hys} is the hysteresis error

Any bias associated with the grid and dead load and the comparison procedure were considered irrelevant to the procedure.

B.3.5. Estimation of Uncertainties

The error uncertainties have been estimated as follows:

Uncertainty of Resolution The resolution error follows a rectangular probability distribution and the uncertainty in resolution is

$$u_{\text{res}} = (\sqrt{\frac{1}{12}})\delta x \tag{B.1}$$

where δx is the smallest significant digit of the indication device.

Uncertainty in Repeatability The repeatability error (precision) follows a normal probability distribution and the uncertainty due to repeatability is estimated by the standard deviation of the sampled mean values ($\bar{y}_i$) relative to the overall mean value ($\bar{y}$). To computed it, the overall standard deviation of all COP samples for one replication at a point P_ξ is decomposed to the between sample sigma (precision), s_b, and the within sample sigma (noise), s_w, as follows (NASA,

2010)

$$
\begin{aligned}
s^2 &= \frac{1}{n-1}\sum_{i=1}^{k}\sum_{j=1}^{n_i}(y_{ij}-\bar{y})^2 \\
&= \frac{1}{n-1}\sum_{i=1}^{k}\sum_{j=1}^{n_i}(y_{ij}-\bar{y}+\bar{y}_i-\bar{y}_i)^2 \\
&= \frac{1}{n-1}\sum_{i=1}^{k}\sum_{j=1}^{n_i}\big((\bar{y}_i-\bar{y})+(y_{ij}-\bar{y}_i)\big)^2 \\
&= \frac{1}{n-1}\sum_{i=1}^{k}\sum_{j=1}^{n_i}\big((\bar{y}_i-\bar{y})^2+(y_{ij}-\bar{y}_i)^2+2(\bar{y}_i-\bar{y})(y_{ij}-\bar{y}_i)\big) \\
&= \overbrace{\frac{1}{n-1}\sum_{i=1}^{k}n_i(\bar{y}_i-\bar{y})^2}^{s_b^2} + \overbrace{\frac{1}{n-1}\sum_{i=1}^{k}(n_i-1)s_i^2}^{s_w^2} + \\
&+ \frac{2}{n-1}\sum_{i=1}^{k}\sum_{j=1}^{n_i}\big((\bar{y}_i-\bar{y})(y_{ij}-\bar{y}_i)\big) \\
&= s_b^2+s_w^2+\frac{2}{n-1}\sum_{i=1}^{k}\Big((\bar{y}_i-\bar{y})\big(\sum_{j=1}^{n_i}y_{ij}-\sum_{j=1}^{n_i}\bar{y}_i\big)\Big) \\
&= s_b^2+s_w^2+\frac{2}{n-1}\sum_{i=1}^{k}\big((\bar{y}_i-\bar{y})(n_i\bar{y}_i-n_i\bar{y}_i)\big) \Rightarrow \\
s &= \sqrt{s_b^2+s_w^2}
\end{aligned}
\tag{B.2}
$$

Therefore, the uncertainty in repeatability (precision) is computed from equation

$$
u_{\text{ran}} = s_b = \sqrt{\frac{1}{n-1}\sum_{i=1}^{k}n_i(\bar{y}_i-\bar{y})^2} \tag{B.3}
$$

The standard deviation within samples is the within sample sigma (noise), s_w, computed from equation

$$
s_w = \sqrt{\frac{1}{n-1}\sum_{i=1}^{k}(n_i-1)s_i^2} \tag{B.4}
$$

and represents the noise in COP measurements. It is used later to obtain the error variance for the smoothing process.

The overall mean ($\bar{y}$) and its standard deviation (s) are computed using the following equations

$$
\bar{y}_i = \frac{1}{n_i}\sum_{j=1}^{n_i}y_{ij}
$$

and

$$
s_i = \sqrt{\frac{1}{n_i-1}\sum_{j=1}^{n_i}(y_{ij}-\bar{y}_i)^2}, \qquad \text{with } i=1,\ldots,k.
$$

where

- n_i = the i^{th} repeated COP sample size
- $\bar{y}_i$ = mean value for the i^{th} repeated COP sample
- s_i = standard deviation of i^{th} repeated COP sample
- y_{ij} = the j datum of the i^{th} repeated COP sample.

The overall mean value for the $k = 10$ repeated samples at each point is computed from equation

$$\bar{y} = \frac{1}{n}\sum_{i=1}^{k}\sum_{j=1}^{n_i} y_{ij} = \frac{1}{n}\sum_{i=1}^{k} n_i \bar{y}_i$$

where $n = \sum_{i=1}^{k} n_i$ is the total number of measurements.

Uncertainty of Uniformity The uniformity error is reported as the estimated changes in the bias over the normal variation process (the same as linearity in R&R studies). Process variation was estimated as 6× the repeatability standard uncertainty. As this error assumed to follow a rectangular probability distribution, the uncertainty on uniformity, u_{unf}, is estimated as

$$u_{\text{unf}} = \frac{|\text{slope}| \times \text{process variation}}{\sqrt{3}} \tag{B.5}$$

Uncertainty of Nonlinearity The nonlinearity error (ε_{lnr}) is assumed to follow a rectangular probability distribution. Therefore, the uncertainty for nonlinearity, u_{lnr}, is the square root of the variance of the rectangular distribution with boundaries the maximum absolute residual of the linear model and is computed as

$$u_{\text{lnr}} = \frac{\max|Y - \hat{Y}|}{\sqrt{3}} \tag{B.6}$$

Uncertainty of Hysteresis The hysteresis error (ε_{hys}) is assumed to follow a rectangular probability distribution. Therefore, the uncertainty due to hysteresis (u_{hys}) is the square root of the variance of the rectangular distribution with boundaries the maximum difference between the upscale and downscale readings among the points $P_{1\to\xi}$ and is computed as

$$u_{\text{hys}} = \frac{\max|Y_{\text{upscale}} - Y_{\text{downscale}}|}{\sqrt{3}} \tag{B.7}$$

B.3.5.1. Combine Uncertainties

Using the variance addition rule to combine statistically independent uncertainties from different sources the uncertainty in the measurement error, u_{COP}, is

$$u_{\text{COP}} = \sqrt{u_{\text{ran}}^2 + u_{\text{res}}^2 + u_{\text{hys}}^2 + u_{\text{lnr}}^2 + u_{\text{unf}}^2}$$

The expanded uncertainty of measurement (U) is reported as the combined uncertainty of measurement multiplied by the coverage factor k = 2 which for a normal distribution corresponds to a coverage probability of 95%

$$U = k \times u_{\text{COP}}$$

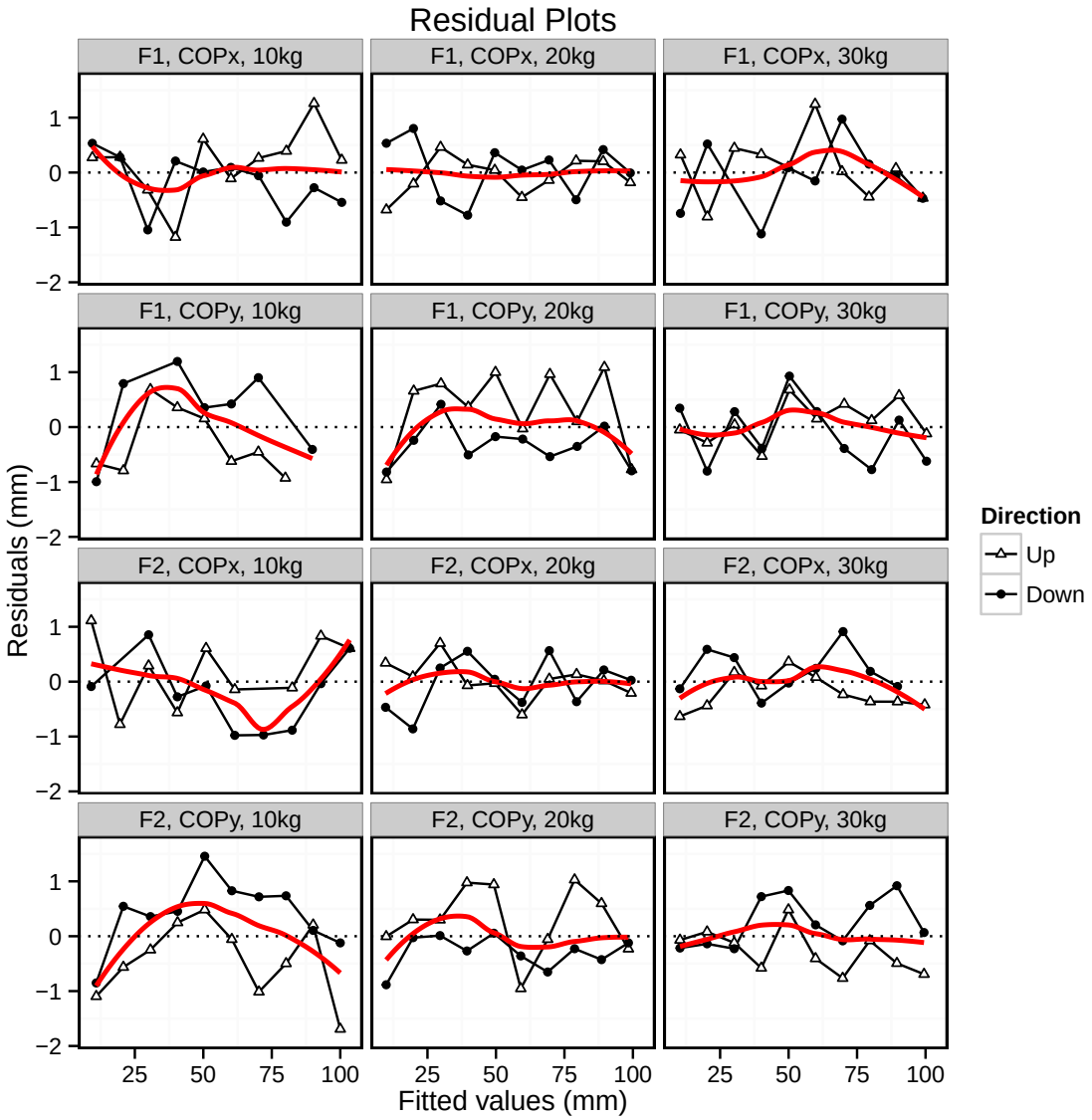

Figure B.6 Residual diagnostic plots for the fitted linear regression model.

B.3.5.2. Results Report

Static performance characteristics provide an indication of how the measuring equipment or device responds to a steady-state input at a particular time. Table 3.4 shows the result of the uncertainty analysis. The uncertainty of measurement associated with the COP is dominated by the combined effect of the hysteresis, uniformity and nonlinearity (Fig. B.7). As the amount of the vertical applied load is lowering the repeatability effect is getting more important.

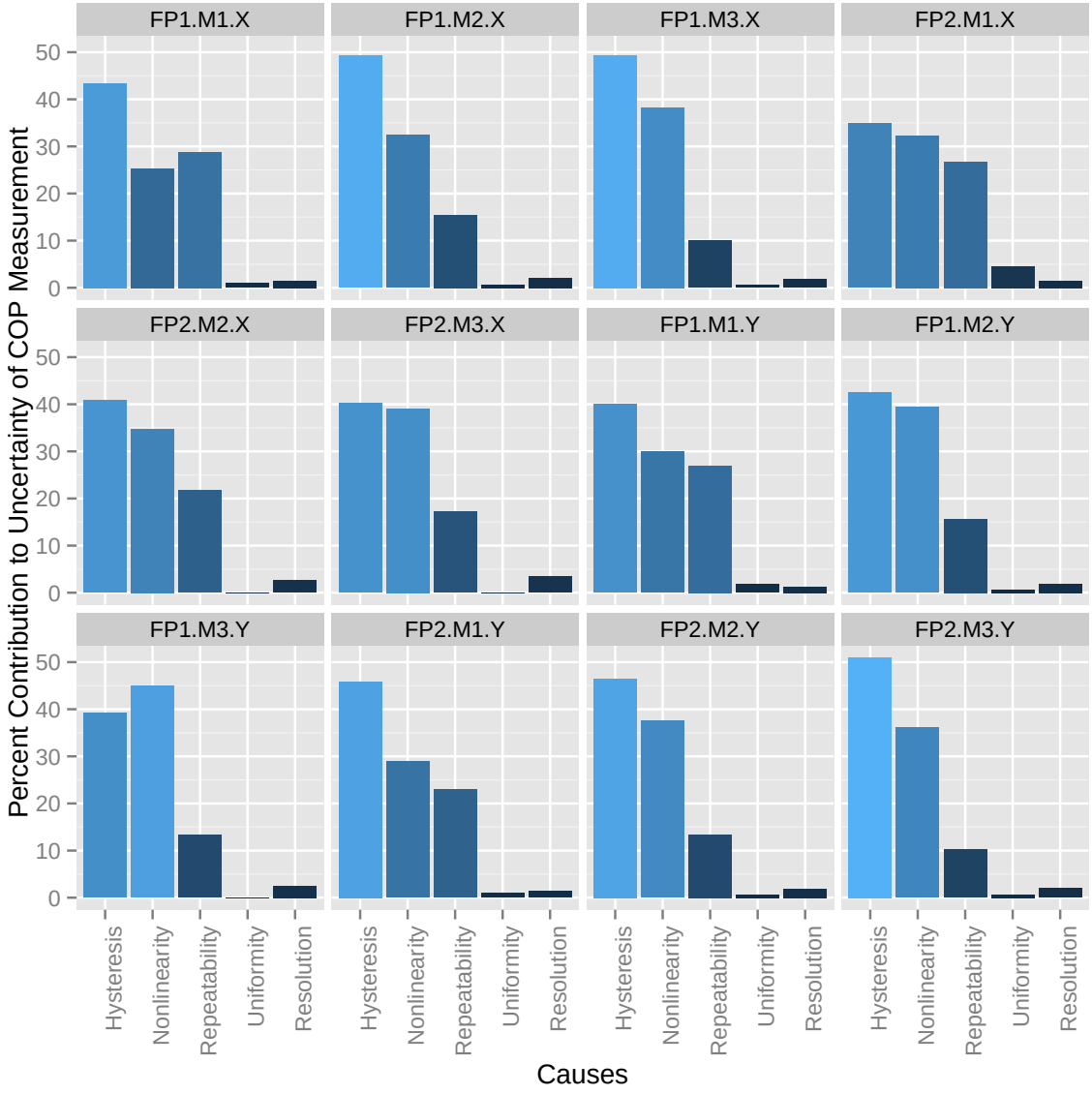

Figure B.7 Pareto chart for COP measurements.

B.4. Gage Study for 3D Kinematics

B.4.1. Background

In this study, a OSS was used to estimate the pose of the musculoskeletal model segments (trunk and pelvis) and box relative to the global reference system (MaxPRO, Innovision Systems, Inc.). The OSS used a system of six charged-couple device (CCD) cameras (Basler-scout, 659×494 px @119 Hz, progressive CCD) with an array of infrared light-emitting diodes mounted around the lens of each camera, to track the 3D position of a set of retroreflective markers affixed to body segments and to the handled box. The OSS detects the reflections of the infrared straboscopic light by the highly retroreflective passive markers. The reflected by the passive markers light is optically registred by the cameras and electronically converted to digital information, i.e.,—3D coordinates. The 3D coordinates are then processed to obtain linear and angular kinematic variables. The

uncertainty in the values of any kinematic variable depends on the error in the 3D coordinates that is propagated in any computed value determined from their combination. The propagated error can be minimized by maximizing the accuracy and precision of the OSS. The accuracy of the 3D coordinates depends on the digitizing procedure and the reconstruction technique, whereas precision depends on the digitizing procedure (Challis, 2008). A 'Gage Linearity and Bias' test was performed to determine the accuracy of the measurement system throughout the expected range of the measurements, and a R&R study to determine system's precision.

B.4.2. Procedure

By placing the cameras on high tripods it was able to capture the surrounding area of the participants ensuring good visibility of the tracking markers, since handling box, adjustable platforms, other equipments, etc., could obstruct the camera's view of the markers. By increasing the angle between the cameras the captured reflections are also diminished. The appropiate set-up of the cameras minimize the dead space in each camera's field of view and maximize system's spatial resolution. Spatial resolution is affected by the capture volume and by camera position in relation to the capture volume. For an $2.0 \times 2.0 \times 2.0\,\mathrm{m}^3$ measurement volume, the diameter of the passive marker needs to cover about $\frac{1}{200}$ of the field of view, i.e.,—for a field of view of 2 m the marker diameter needs to be around 10 mm. In the current study the reflective markers of 20 mm diameter was used.

Inter-marker distance measurement test was performed where four reflective markers attached on a bar on known positions and placed at eight different positions throught the established measurement volume and were recorded for 20 sec at sampling rate of 60 Hz. The motion analysis system was calibrated once at the beginning of the procedure. The 3D coordinates data were introduced to the Visual3D (C-Motion) software. The mean value of each sample was computed. Then, the distance between the markers was computed from their means value coordinate.

B.4.3. Statistical Analysis

The Grubbs' test was used to check for outliers. A regression line was fitted on the bias against the reference values and statistics for the linearity and accuracy of the measurement system computed. It is assumed that biases are corrected by the calibration procedure, therefore, only the uncertainties of the correction are presented. The range over which the measurements varies due to normal variation computed by the R&R study. To determine the repeatability of the measurement system a R&R study carried on. The Minitab 17 statistical software was used for the analysis.

B.4.4. Results Reports

The precision of the measurement system was of 0.0012108 mm. The maximum absolute value of the bias, the linearity value, and the repeatability standard deviation were used for calculating the expanded uncertainty of the measurement system. Due to the anisotropic distribution of the error in the measurement volume, the final measurements took place at the centre of the measurement volume where the error was minimized. Due to the sensitivity of the error to the calibration

procedure, for the smoothing process the precision was computed before each measurement after the corresponding calibration took place.

B.5. Denoise of COP Signal

B.5.1. COP is Distorted with White Noise

The noise in the COP signal is the propagation noise arise from the combination of the components used to compute it with function f. Generally, it is modeled as a wide-band additive, stationary, zero-mean, and uncorrelated noise that contaminates the low-pass COP signal with noise variance σ^2. However, even if the noise of the recorded GRF signals can be modeled as an additive zero-mean "white noise", the nonlinear transformation in COP computation destroys these properties to some extend (Woltring, 1995). The noise in the COP signal becomes non-stationary (i.e., unequal noise variance), except for the case where the $\mathbf{F}_z$ is constant ($\mathbf{F}_z = c$). Therefore, noise stationarity may be true for stabilometric studies and digital low-pass filter or smoothing techniques can be used to remove high frequencies presented in the COP signal (Karlsson and Lanshammar, 1997; Woltring, 1986). The optimal cut-off frequency for the low-pass digital filter can be found by residual analysis (Winter and Patla, 1997) or by using the generalized, crossed-validation natural splines smoothing algorithm (GCVSPL) (Woltring, 1986). Natural splines of m^{th} order behave like an m^{th} order double Butterworth filter, where optimal cut-off frequency is the lowest frequency for which the residual noise is white (Woltring et al., 1987).

Moreover, with sufficient *oversampling* is possible to retain significant signal components avoiding aliasing errors, while reducing noise level (Furnée, 1989a). The noise variance presented in a signal, or in its derivatives, after optimal smoothing depends on the band-limit of the signal and is proportional to the sampling rate and the variance of the inherent band-limited "white noise" presented in the raw data measurement (Lanshammar, 1982b), and is expressed as

$$\sigma_k^2 = \sigma^2 \tau \frac{\omega_b^{2k+1}}{\pi(2k+1)} \tag{B.8}$$

where

- σ_k^2 is the noise variance in the estimate k^{th} order derivative
- σ^2 is the noise variance in the raw measured data (additive "white noise")
- τ is the sampling interval ($\tau = \frac{1}{f_s} = \frac{1}{2\pi\omega_0}$ with $\omega_0 \geq 2\omega_b$)
- ω_b is the band-limit of the signal
- k is the order of the derivative

The term $\sigma^2\tau$ is known as spatiotemporal resolution criterion (Q_{ST}) and together with Shannon sampling theorem can be regarded as sufficient criteria in order to choose the sampling frequency ω_0 (Furnée, 1989a,b; Woltring, 1984, 1995). When a quantizing data acquisition system with

sampling frequency ω_0 introduces sampling "white noise" with variance σ^2, over-sampling would result in its reduction (Furnée, 1989a). Therefore, the sampling rate must not violate Shannon sampling theorem in order to avoid aliasing, but it can be much greater than twice the ω_b in order to reduce the amount of noise mapped into the Nyquist band, as long as the measurement noise above a chosen Nyquist frequency is white (Furnée, 1989a,b; Woltring, 1984, 1995). Since physical signals are not strictly band-limited and therefore ω_b is unknown (Slepian, 1976), the cross-over frequency ($\omega_c = 2\pi f_c$) beyond which the noise level is dominant can be used instead, as long as it is not less than the signal band-limit ($\omega_c \geq \omega_b$) (Lanshammar, 1982a,b; Winter and Patla, 1997; Woltring, 1984, 1995). Once more, sampling frequency greater than twice the ω_c can be used as long as the noise above the Nyquist frequency is white. In any case, the sampling rate should not be more than

$$\tau_{max} = \frac{\sigma_k^2 \pi (2k+1)}{\sigma^2 \omega_b^{(2k+1)}}$$

for a required precision σ_k^2 (Lanshammar, 1982b).

The Q_{ST} has been used as a figure of merit to evaluate motion capture systems (Furnée, 1989a,b; Woltring, 1984, 1995). However, is a figure of merit for any noisy sampled data system (Furnée, 1989a,b; Woltring, 1984) that deals with zero-mean "white noise" introduced by the data acquisition system. Small values of Q_{ST} corresponds to less system's noise. Assuming a perfect input signal, Q_{ST} corresponds with the power spectral density of the quantization error (Orfanidis, 1996, pg. 68). By increasing the sampling rate the quantization noise power spreads over a larger frequency band improving the quality of the signal that is smoothed by a digital low-passed post-filter. Oversampling improves the precision of the measurement by increase the resolution of the quantizer, however, only for a bit for every quadruplicate of the Nyquist frequency. When a differential quantization it is considered, the quantization error added in the reconstructed quantized signal is even less, but the sampling frequency has to be significantly higher than the Nyquist frequency (Orfanidis, 1996; Proakis and Manolakis, 1996; Woltring, 1984). On the other hand, by increasing sampling frequency when a signal is varying slowly the noise will not be any more white (Lanshammar, 1982b; Woltring, 1984). Moreover, by increasing sampling frequency it is also increased the bandwidth of the preceding analog system which may increase the noise superimposed on the input signal to no optimal values. A tradeoff exist between oversampling and signal's noise variance, however, this is equipment related (Woltring, 1995). By increasing the sampling rate of the force measurement system it has been showed that the noise superimposed the COP increases (Granat, Kirkwood, and Andrews, 1990).

B.5.2. COP is Distorted with Non-stationary Noise

In many dynamic studies, there are periods where the applied vertical component of the GRF vector ($\mathbf{F}_z$) changes its magnitude drastically during its evolution in time (Fig. B.8). These fluctuations in $\mathbf{F}_z$ between the "load-unload" phases, result in the COP signal superimposed on a nonstationary variance noise. It has been shown experimentally that a decrease in $\mathbf{F}_z$ magnitude corresponds to an increase in noise variance related by a fractional quadratic function (Wisleder and McLean, 1992). Accordingly, in those experimental situations where $\mathbf{F}_z$ changes drastically,

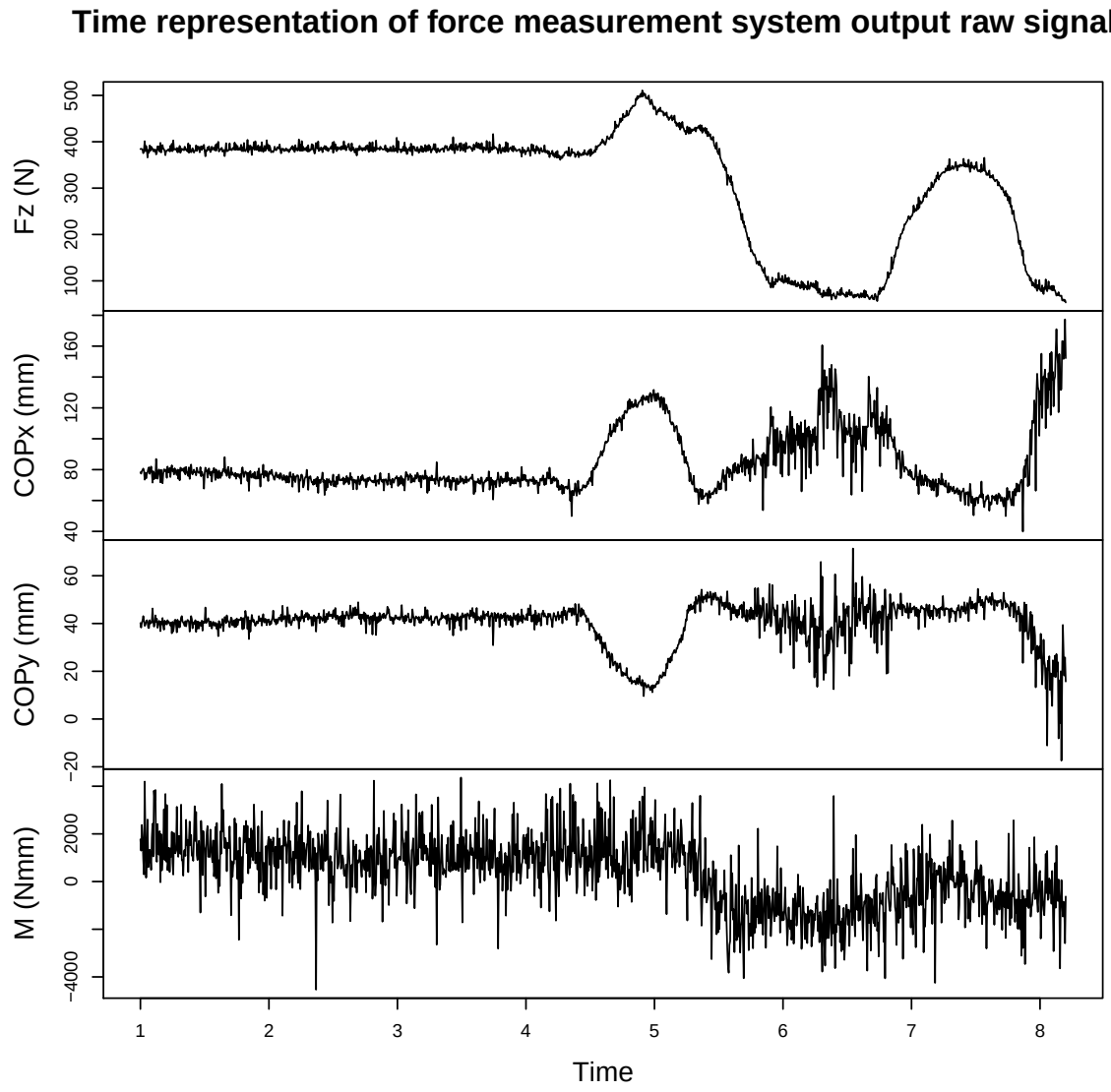

Figure B.8 In asymmetric lifting or lowering tasks in the ergonomics context, there are intervals where the magnitude of the F_z obtained by the force measurement system fluctuates. Clearly, there are intervals where F_z changes its magnitude drastically. These fluctuations result in variations in the variance presented in the raw COP coordinates (COPX: anterioposterior axis; COPy: mediolateral axis).

the noise presented in the raw COP coordinates could be modeled as additive, zero-mean, and nonstationary—i.e., unequal noise variance across COP coordinates and variations in time of the noise power. Weak-correlated noise is also assumed. This renders time-invariant Fourier transform based filtering techniques or GCV-based low pass smoothing suboptimals.

By assuming that the noise is zero-mean "white noise" and additive to the COP signal, the quality of COP signal and of its derivatives after optimal smoothing or filtering depends on the proportion of the noise variance that lies inside the bandlimit of the signal after oversampling rate had spread it evenly over the Nyquist interval (Lanshammar, 1982a,b). However, for nonstationary variance

noise low-pass filtering is not an adequate option as it imposes the same cut-off frequency for the entire signal. Moreover, in dynamic tasks, portions of COP signal may contains high-frequency components. An optimal solution is smoothing or low-pass filtering the raw signals of the components upon COP depends before its computation, however, this is not always possible. Another solution is to use adaptive Fourier transform based or time-frequency filters and wavelets (Erer, 2007; Georgakis, Stergioulas, and Giakas, 2002; Giakas, Stergioulas, and Vourdas, 2000; Giakas, 2004; Suranthiran and Jayasuriya, 2005; Walker, 2008). However, optimal cut-off frequency is difficult to obtain. Another solution is to construct a weighted matrix of the associated noise variance in the COP signal and smooth using the GCVSPL package under mode 1, by using the mean square error at each COP point (Woltring, 1986). However, knowledge of the nonstationary variance of the noise is needed previously.

Therefore, the aim of this study was (i) to quantify the accuracy and precision of the force measurement system, (ii) to analyze the noise in the COP signal under different experimental conditions, and in turns (iii) to construct a weighted variance matrix for the COP noise in conformance with the GUM approach (ISO-JCGM 100, 2010). In Part **??**, the theoretical model for the uncertainty in the measurements of the force platform system and the theoretical model of the propagation error in the COP resulted from the combination of the components used to computed are presented step-by-step, whereas in Part **??** the proposed approach is demonstrated experimentally. Finally in Part § B.5.5 comparisons of the proposed method with different denoise techniques take place.

B.5.3. Noise in the Center of Pressure Signal

B.5.3.1. General Uncertainty Framework

Consider a single real output quantity Y that is related to a vector of real input quantities $\mathbf{X} = (X_1, \ldots, X_N)^T$ by an explicit univariate measurement model $Y = f(\mathbf{X})$. The estimate of the output quantity is $y = f(\mathbf{x})$ with $\mathbf{x} = (x_1, \ldots, x_N)$. Assuming linear or weakly-nonlinear relation and using a first-order Taylor series expansion, the standard uncertainty u_y associated with y is obtained by the "law of propagation of uncertainties" expressed by

$$u_y^2 = S_x \mathbf{U}_x S_x^T \tag{B.9}$$

where S_x is the vector of the sensitivity coefficients expressed by the values of the partial derivatives $\frac{\partial f}{\partial X_j}$ for $j = 1, \ldots, N$, at $\mathbf{X} = \mathbf{x}$ and $\mathbf{U}_x$ is the $N \times N$ uncertainty matrix associated with $\mathbf{x}$ containing the covariances $u(x_i, x_j)$ for $i, j = 1, \ldots, N$ associated with x_i and x_j.

B.5.3.2. Measurement Model

The objective is to estimate the uncertainty in the COP measurand. The estimate of the input quantities upon COP is computed and the associate uncertainty matrix U_x are propagated through a linearization of the measurement model that relates the measurand with the input quantities

$$COP = f(x_1, \ldots, x_N)$$

B.5.3.3. Measurement Function

The COP location in the X axis[5] was calculated using the measurement function

$$COP = \frac{M_x}{F_z} \tag{B.10}$$

where $M_x = (F_z^3 + F_z^4)L$ is the magnitude of the moment of force and L is the constant distance factor (no uncertainty assumption), $F_z = F_z^1 + F_z^2 + F_z^3 + F_z^4$ is the magnitude of the vertical component of the GRF vector, and F_z^1 to F_z^4 are the magnitudes of the vertical components of the GRF vector measured by each of the four load cells. In terms of the GUM annotations

$$COP \equiv f(F_z^1, F_z^2, F_z^3, F_z^2, L)$$

B.5.3.4. Error Model

It is assumed that Eq. (B.10) is continuous and it has also continuous derivatives in the domain of interest. The error model is determined from Eq. (B.10) by applying a first-order Taylor series approximation. The COP error equation is expressed as

$$\varepsilon_y = S_x \varepsilon_x^T$$

where S_x is the sensitivity vector assuming that L has no associated uncertainty

$$S_x = \begin{bmatrix} \frac{\partial COP}{\partial F_z^1} & \frac{\partial COP}{\partial F_z^2} & \frac{\partial COP}{\partial F_z^3} & \frac{\partial COP}{\partial F_z^4} \end{bmatrix}$$

and ε_x is the error vector associated with the inputs quantities

$$\varepsilon_x = \begin{bmatrix} \varepsilon_{F_z^1} & \varepsilon_{F_z^2} & \varepsilon_{F_z^3} & \varepsilon_{F_z^4} \end{bmatrix}$$

B.5.3.5. Uncertainty Model

The associated u_y^2 in the COP measurements is the variance in the propagated error resulted from the combination of the components used to compute COP. Therefore, if $u_{F_z^1}^2$ to $u_{F_z^4}^2$ are the noise variances of the F_z^1 to F_z^2 components respectively, the uncertainty in COP measurement is then expressed by Eq. (B.9) where $\mathbf{U}_x$ is the 4×4 symmetric uncertainty — variance-covariance — matrix associated with $\mathbf{x}$

$$\mathbf{U_x} = \begin{bmatrix} u^2(F_z^1) & u(F_z^1, F_z^2) & u(F_z^1, F_z^3) & u(F_z^1, F_z^4) \\ u(F_z^2, F_z^1) & u^2(F_z^2) & u(F_z^2, F_z^3) & u(F_z^2, F_z^4) \\ u(F_z^3, F_z^1) & u(F_z^3, F_z^2) & u^2(F_z^3) & u(F_z^3, F_z^4) \\ u(F_z^4, F_z^1) & u(F_z^4, F_z^2) & u(F_z^4, F_z^3) & u^2(F_z^4) \end{bmatrix}$$

The diagonal terms of $\mathbf{U}_x$ are the uncertainty (variance) of the input quantities and the off-diagonal terms are their mutual uncertainties (covariance).

[5] The same procedure is used for the Y axis.

B.5.3.6. Measurement Process Errors

Identification It is assumed that the F_z^1 to F_z^4 signals are interfered with zero-mean band-limited "white noise". The assumed error variance sources ($u^2_{F_z^1}, u^2_{F_z^2}, u^2_{F_z^3}, u^2_{F_z^4}$) are the quantization error of the A/D card, the "white noise" inherent to the analog signal input and any additional random error that may be arose while recording and during data analysis originated by degradation of the equipment over time from previous usage (or user abuse), or from influences of installation and operation environment.

Estimation Since the error components were assumed to follow a normal probability distribution, the uncertainty in the input quantities is estimated by the standard deviation of the sample data. It was assumed that the noise variances of the signals registered by each load cell are equals ($u^2_{F_z^1} = u^2_{F_z^2} = u^2_{F_z^3} = u^2_{F_z^4}$) and their sum equals the variance obtained by the force measurements system ($u^2_{F_z^1} + u^2_{F_z^2} + u^2_{F_z^3} + u^2_{F_z^4} = u^2_{F_z}$) for a static registration—i.e., $u_{F_z^{1\to4}} = \frac{u_{F_z}}{2}$. Furthermore, a high negative correlation coefficient was assumed between the errors in the input quantities ($\rho = -0.9$) since $F_z^{1\to4}$ tend to vary in opposite directions when the same F_z is displaced. Hence, the noise standard uncertainty in COP measurement is

$$u_y = \frac{1}{2\sqrt{5}F_z^2} L \Bigg[\Big((F_z^1)^2 + (F_z^2)^2 + 36F_z^2(F_z^3 + F_z^4) + (F_z^3 + F_z^4)^2 + 2F_z^1\Big(F_z^2 + 18(F_z^3 + F_z^4)\Big)\Big) u^2_{F_z} \Bigg]^{-\frac{1}{2}} \tag{B.11}$$

B.5.3.7. Mathematical optimization

The method of Lagrange multipliers was used to find the minimum value of the standard uncertainty u_y subject to the constraint $F_z = F_z^1 + F_z^2 + F_z^3 + F_z^4$ ($F_z^{1\to4}, u_{F_z} \in R_{\geq 0}$). This yields

$$\min\{u_y\} = L\frac{u_{F_z}}{2\sqrt{5}F_z}, \text{ for } F_z^{1\to4} = \frac{F_z}{4} \tag{B.12}$$

B.5.3.8. Noise uncertainty in COP after Optimum Smoothing

According to Eq. (B.8) the noise standard uncertainty of the COP signal after optimal smoothing is

$$u_o \geq \frac{Lu_{F_z}}{F_z}\sqrt{\frac{\tau f_b}{10}} \quad \text{by Eq. (B.12)}$$

B.5.4. Experimental Setup

In addition to the procedure that took place for the uncertainty analysis of the COP measurements (§ B.3), a dead load ($\approx 294N$) was placed on the top plate of the force platform about its geometrical center and the COP was registered at 30, 230 and 500 Hz for 10 sec. A frequency analysis was made on the COP signals to test whether COP noise is "white". To test the influence of the sampling rate another dead load ($\approx 294N$) was placed on the top plate of the force platform about its geometrical center and the COP was registered for 10 sec at an integer sequence of frequencies ($30, 40, 50, \ldots, 300$ Hz).

B.5.5. Comparing Methods to Denoise COP Signals

The source for simulating naturalistic reference signals was the signals obtained by a force platform (Dinascan 600M, IBV, Valencia, Spain) at a sampling rate of 180 Hz, from a population of fourteen subjects, who performed sixteen trials each of manual lifting and lowering tasks in an experiment described in detail in § 3.5. In total 224 were obtained. The first forty harmonics were used to approximate the COP reference signals, ensuring that the reconstructed signals are practically band-limited to $40f_0$ (i.e., Fourier transform is zero outside). Original signals were demeaned before be transformed into Fourier series. Then, the reconstructed signals were decimated by a factor of 6 using an FIR filter of order 30 to match the noise sample rate of 30 Hz. The duration of the new signals is of 30 sec, with resolution $f_o = \frac{1}{30}$, and cut-off frequency = 1.33 Hz. The experimental obtained noise added to the reconstructed signals was generated by measuring different static loads placed at the geometrical center of the top plate of the force platform at sampling rate of 30 Hz for a period of 5 sec. In total 120 noise signals were generated, demeaned, and stored. To check whether the experimental obtained "zero-mean" noise can be characterized as Gaussian white noise (GWN), we examine independence (Box-Pierce and Ljung-Box tests) and normality (Anderson-Darling and Shapiro-Wilks tests) of the time-series. Six noise signals was then pooled randomly, combined in random order, and added to the reconstructed reference signals to simulate COP registrations (Fig. B.9). In total 26880 signals were generated, superimposed with additive non-stationary noise. Three different denoise procedures were compared: low-pass filtering with a fourth-order zero-phase-shift Butterworth filter with cut-off frequency found following the residual analysis procedure (Winter, 2009), by quintic splines using the generalized crossed-validation natural splines smoothing algorithm (GCVSPL) (Woltring, 1986), and by quintic splines according to the "True Predicted Mean-squared Error" of Woltring (1986) following the proposed uncertainty analysis.

B.5.6. Results and Discussion

B.5.6.1. Noise Test

The results showed that for F_z = constant the noise of the COP signal can be modelled as additive, zero-mean "white noise". Different sampling rates influence the COP noise. This is obvious for the COP signals that were registered with different (low - very high) sampling rates (Fig. B.10). For example, the variances of the raw COP data for different sampling rates are ${COP_{ML}}^{RAW}$-30Hz = 0.54 mm^2, ${COP_{ML}}^{RAW}$-230Hz = 0.59 mm^2, ${COP_{ML}}^{RAW}$-500Hz = 0.61 mm^2, and ${COP_{AP}}^{RAW}$-30Hz = 1.10 mm^2, ${COP_{AP}}^{RAW}$-230Hz = 1.20 mm^2, ${COP_{AP}}^{RAW}$-500Hz = 1.30 mm^2. However, for a narrower frequency interval the assumption that the sampling rate do not influence the COP noise can be considered as correct. Notwithstanding, the noise elimination, was higher after oversampling spread the power over higher frequencies. The variance of the COP signals after low-pass filtering is ${COP_{AP}}^{BTW}$-30Hz = 0.24 mm^2, ${COP_{AP}}^{BTW}$-230Hz = 0.05 mm^2, ${COP_{AP}}^{BTW}$-500Hz = 0.03 mm^2 and ${COP_{ML}}^{BTW}$-30Hz = 0.15 mm^2, ${COP_{ML}}^{BTW}$-230Hz = 0.03 mm^2, ${COP_{ML}}^{BTW}$-500Hz = 0.02 mm^2 (Fig. B.11). Other studies have also been shown that cut-off frequency and sampling rate influence stabilometric parameters (Schmid et al., 2002; Scoppa et al., 2013). However, our

study demonstrated that this is dependent also on the magnitude of the vertical force. Moreover, the quality of the COP signal was improved when Q_{ST} decreased (Table 3.4) by increasing F_z magnitude.

B.5.6.2. Noise Curve

There is not a trend among the standard uncertainty of the F_z signal registered with the different dead load weights (Figs. B.1 to B.4), although there are accuracy differences between the two force platforms. Therefore, the highest standard uncertainty of both force platforms ($u_{F_z} = 2.1$ N) was chosen. Therefore, the u_y in the COP measurements is modeled as an hyperbolic function of the F_z magnitude as $u_{F_z} = c$. According to Eq. (B.12) the minimum u_y is obtained when the dead load is placed at the geometrical centre of the top plate of the force platform as in this point the same fraction of the F_z is registered by each load cell. Figure B.12 shows the experimental obtained noise curve together with the minima curve of the model for different cases of statistically correlated error sources, $\rho = -0.9$ to $\rho = -0.1$. The variance explained by the fitted regression models (R^2) are very high. For the Y-axis the experimental obtained COP uncertainty is better modelled with statistically correlated error $\rho = -0.8$, while for the X-axis with $\rho = -0.9$.

B.5.6.3. COP Denoise Procedures Comparison

The results showed that the MSE quintic splines following the proposed procedure with uncertainty analysis provides more smoothed data in comparison with the others procedures.

B.5.6.4. Spatiotemporal resolution criterion

The quality of the COP signal is improved when Q_{ST} decreases (Table 3.4) either by increasing F_z magnitude or by increasing sampling rate.

B.5.7. Conclusion

The implementation of the Metrology "Guide to the Expression of Uncertainty of Measurement" (GUM) approach (ISO-JCGM 100, 2010) to calculate standard uncertainties for specifying the weighted factor for each coordinate of the noisy COP data was introduced. The obtained noise curves can be used (the experimental or the theoretical) in order to obtained the weighted matrix for smoothing purposes. The σ_{COP} in the COP measurements is nonlinearly related to the F_z, with less magnitude when higher F_z is applied onto the plate of the force platform. According to Eq. (B.12) the minimum σ_{COP} is obtained when the dead load is placed at the geometrical centre of the top plate of the force platform as in this point the same fraction of the F_z is registered by each cell. The variance explained by the fitted fractional quadratic models (R^2) is very high. The obtained noise curves can be used (experimental or theoretical) in order to obtained the weighted matrix (W) for the smoothing purposes.

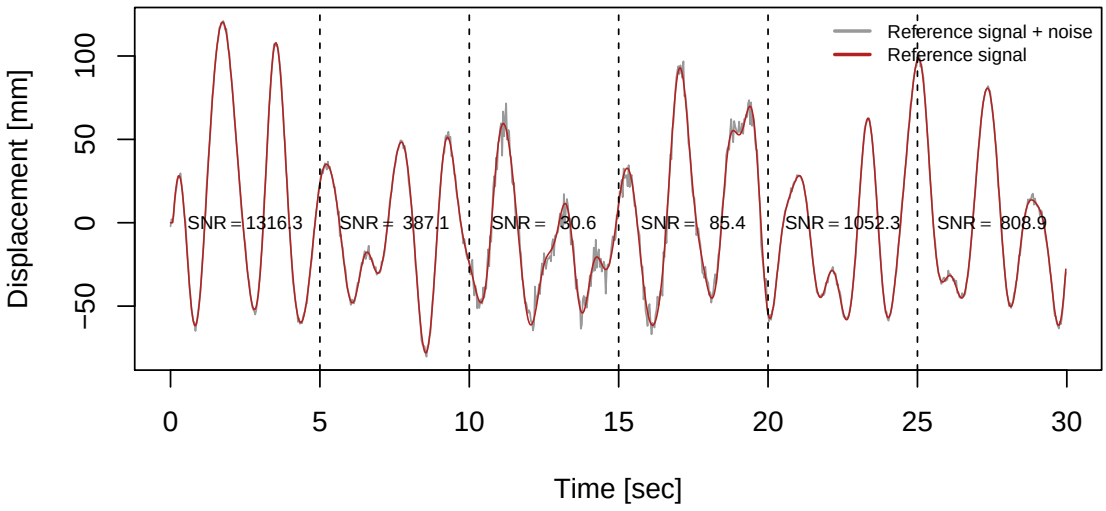

Figure B.9 Representation of a reference signal before and after adding noise. Dot vertical lines indicate when the added random noise is pooled from sources of different variance. Singal-to-noise ratio (SNR) was defined as $SNR = \frac{\sigma^2_{signal}}{\sigma^2_{noise}}$.

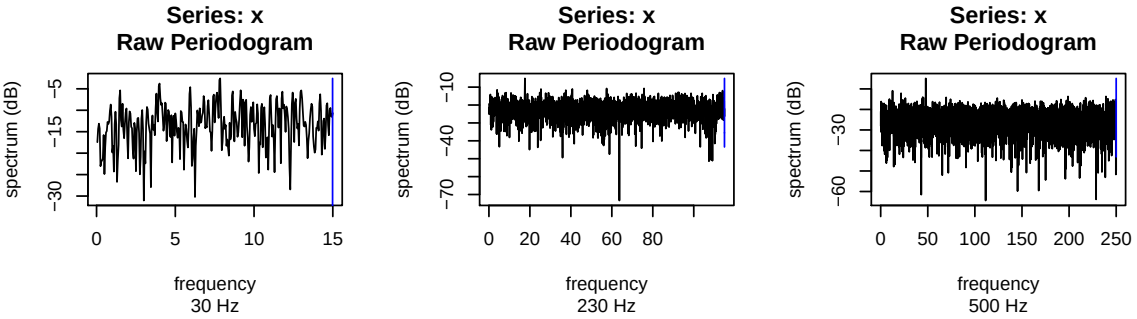

Figure B.10 Power spectral density of the raw COP signals obtained at different sampling rates (only the COP_{AP} is shown).

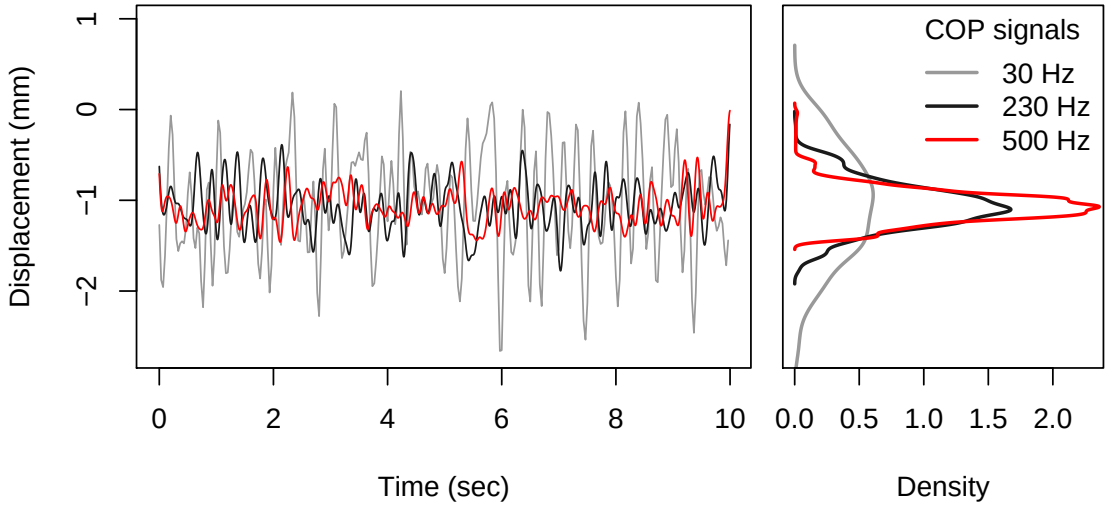

Figure B.11 COP signals with different sampling rates (30, 230 and 500 Hz) after low-pass filtering with a fourth-order zero-phase-shift Butterworth filter (BTW) with cut-off frequency at 5 Hz [1]. The probability function for the distribution is shown for each time series (only the COP_{AP} is shown).

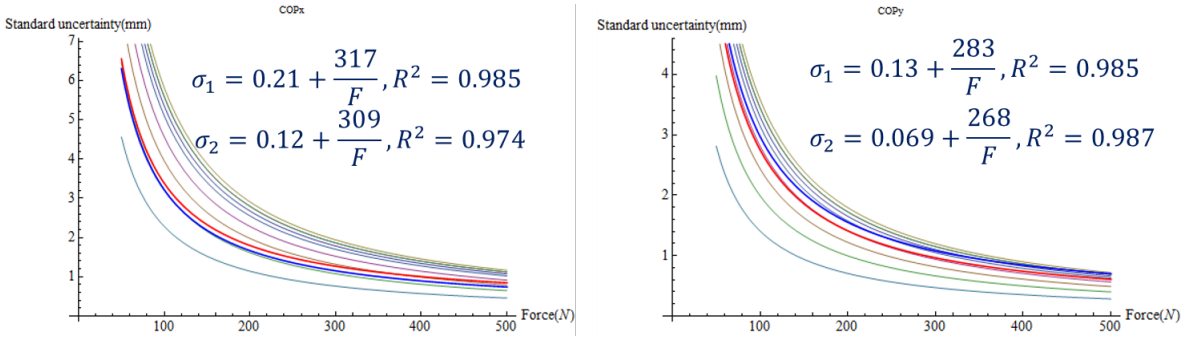

Figure B.12 Values of standard uncertainty obtained for different negative correlations by the propagation law (thin lines) and by experimentaly obtained results (blue - red lines).

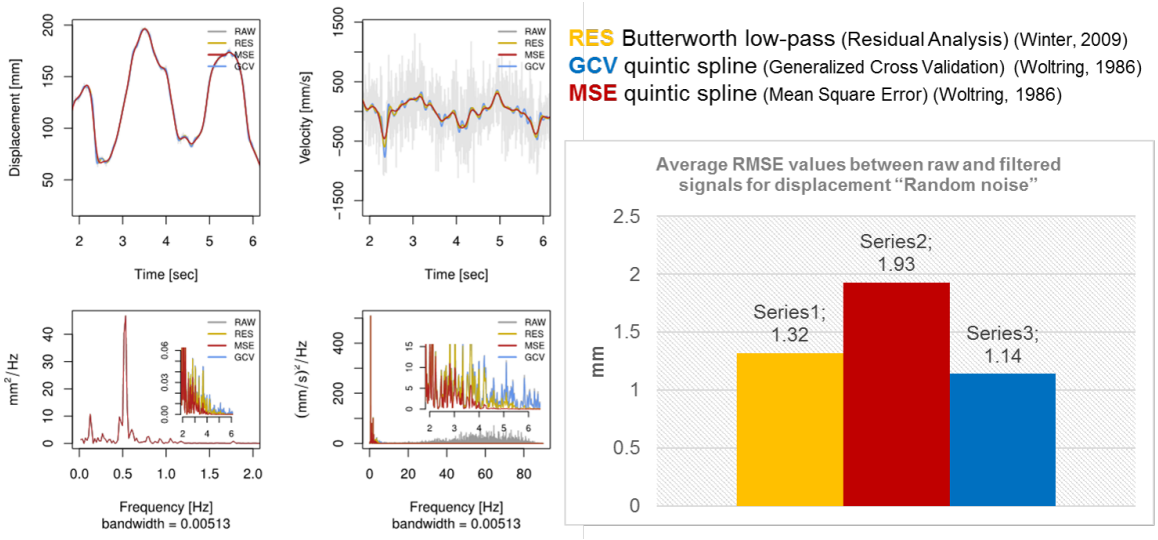

Figure B.13 Comparison of a COP signal after low-pass filtering with a fourth-order zero-phase-shift Butterworth filter with cut-off frequency found following the residual analysis procedure (RES) of Winter (2009), by using quintic splines according to the generalized crossed-validation natural splines smoothing algorithm (GCV) (Woltring, 1986), and by quintic splines according to the "True Predicted Mean-squared Error" of Woltring (1986) following the proposed uncertainty analysis (MSE).